EXPERIMENTAL CHARACTERIZATION OF PU SEPARATION BY PUREX ON A LOW-BURNUP, PSEUDO-FAST-NEUTRON IRRADIATED DUO_2 FOR PRODUCT DECONTAMINATION FACTORS AND NUCLEAR FORENSICS

A Dissertation

by

PAUL MICHAEL MENDOZA

Submitted to the Office of Graduate and Professional Studies of
Texas A&M University
in partial fulfillment of the requirements for the degree of

DOCTOR OF PHILOSOPHY

Chair of Committee,	Sunil S. Chirayath
Committee Members,	Sean M. McDeavitt
	Craig M. Marianno
	Charles M. Folden III
Head of Department,	Yassin A. Hassan

May 2018

Major Subject: Nuclear Engineering

ABSTRACT

Experimental investigations to determine fission product decontamination factors while employing the Plutonium Uranium Recovery by Extraction (PUREX) process were conducted. PUREX process was performed for a depleted UO_2 (DUO_2) sample irradiated in a pseudo-fast neutron environment in the High Flux Isotope Reactor (HFIR). The DUO_2 sample (0.26 wt% ^{235}U) was covered with gadolinium to absorb thermal neutrons and irradiated to a low-burnup (4.43 $\pm$ 0.31 GWd/tHM) and PUREX process was performed 538 days after the neutron irradiation. Decontamination factors (DF), with respect to Pu, for the elements U, Mo, Ru, Ce, Sm, Sr, Pm, Eu, Nd, Pd, and Cd were measured with mass spectrometry. DFs as well as distribution coefficients (DC) were determined with gamma spectroscopy for Cs, Ru, Ce, and Eu. 30 vol.% tri-n-butyl phosphate (TBP) in a kerosene diluent was used for U/Pu extraction and 0.024 M iron(II) sulfamate in HNO_3 with concentrations ranging from 0 to 4 M was used for Pu back-extraction. The Pu in the irradiated fuel was characterized as near-weapons-grade (89.3% ^{239}Pu), with 1.5% of the total fuel mass attributed to Pu, 86% to U, roughly 0.3% attributed to fission products and the rest of the mass attributed to oxygen. Two cycles of a four extraction, three back-extraction process achieved 93% of Pu recovered in a product solution with less than 1% of the original U. The mathematical expression between DCs and DFs was derived for the PUREX experiment and this expression was used to calculate DFs from DCs. The ratio between DFs determined with DCs as opposed to direct measurement was 1.5, 1.0, 0.99, and 0.91 for Cs, Ru, Ce, and Eu, respectively.

Further, a forensic methodology was developed for determining parameters like fuel burnup, scalar neutron flux, neutron irradiation time in reactor, initial ^{235}U enrichment, and time since removal from the reactor. Each parameter was determined in the order listed

because information from earlier calculations was used in later calculations. The above parameters were determined using single group neutron cross sections and fission yields determined by averaging with five different normalized neutron flux spectra. The five reactor flux spectra were: the initial HFIR sample flux spectrum, the Fast Breeder Reactor (FBR) blanket region, an AP1000, a Pressurized Heavy Water Reactor (PHWR), and an average HFIR flux spectrum. Concentrations determined at the end of the PUREX experiment were used with DF values to calculate unprocessed concentrations, which were used as inputs for the forensic calculation. The flux spectra input which most correctly determined sample history among the non-averaged spectra was the AP1000, which indicates that the sample received the majority of its burnup while in a thermal spectrum. Although the sample was covered with gadolinium to remove the thermal flux, investigations with MCNP revealed that the gadolinium burned out some time near the end of irradiation, and consequently the fuel sample was irradiated for an unknown time in a thermal spectrum. This is why the forensic calculations were completed with an average HFIR spectra, which most correctly estimated the sample history. The calculated parameters using the average HFIR flux spectrum estimated the sample to have a burnup of 4.42 GWd/tHM, a scalar flux of 1.62×10^{15} n/cm^{2}s, 45 days of irradiation, an initial uranium enrichment of 0.265 wt.% ^{235}U, and 356 days between removal from reactor and the analysis date. The initial scalar flux for the sample was estimated with MCNP as 1.73×10^{15} n/cm^{2}s, there were 50 days of irradiation, the initial uranium enrichment was 0.26 wt.% ^{235}U, and there were actually 355 days between removal from the reactor and the analysis date. The 6% difference in scalar flux estimates is likely due to the changing flux spectra during irradiation.

DEDICATION

To my mother and father

CONTRIBUTORS AND FUNDING SOURCES

Contributors

This work was supported by a dissertation committee consisting of Professors Sunil Chirayath, Craig Marianno, and Sean McDeavitt of the Department of Nuclear Engineering and Professor Charles M. Folden III of the Cyclotron Institute.

The analyses depicted in Section 5 utilized neutron flux spectra provided by Jeremy Osborn. DUO_2 target irradiation was conducted before the student started on the project and was paid for by the Department of Homeland Security (DHS) Domestic Nuclear Detection Office (DNDO).

All other work conducted for the dissertation was completed by the student independently.

Funding Sources

Graduate study was supported with various teaching assistant positions and with assignments as a research assistant at Texas A&M University.

NOMENCLATURE

U.S	United States
DNDO	Domestic Nuclear Detection Office
SNM	Special Nuclear Material
PUREX	Plutonium Uranium Recovery by Extraction
DF	Decontamination Factors
DC	Distribution Coefficient
IAEA	International Atomic Energy Agency
NPT	treaty on the Non-Proliferation of Nuclear Weapons
MCNP	Monte Carlo N-Particle transport code
PWR	Pressurized Water Reactor
BWR	Boiling Water Reactor
CANDU	Canada Deuterium Uranium
LMFBR	Liquid Metal Fast Breeder Reactor
DUO_2	Depleted Uranium Dioxide
DA	Destructive Analysis
NDA	Non Destructive Analysis
FBR	Fast Breeder Reactors
P5	China, France, Russia, the United Kingdom, and the United States
HPGe	High-Purity Germanium

TABLE OF CONTENTS

Page

LIST OF FIGURES

LIST OF TABLES

1. INTRODUCTION

United States (U.S.) nuclear forensic capabilities have been demonstrated in scenarios of weapons testing, post-detonation exercises, and interdiction[1,2]. Although it is continually hoped that these capabilities are never needed, time has proven their existence is important for national security[1,2]. According to a report from the committee on nuclear forensics released in 2010[1], "the time line for post-detonation analysis and evaluation is longer than desired", and further, in the context of our substantial forensic capabilities, this report notes that these capabilities are "fragile, under resourced, and, in some respects, deteriorating"[1,2]. The committee notes four areas of concern, two of which are the few number of personnel skilled in nuclear forensics, and forensic techniques that are outdated, either technologically or in relation to time-sensitive/environmental standards. Concerns raised by this report will only be remedied if addressed on a government level.

Special Nuclear Material (SNM) origin attribution, in this context, applies to deducing the history of nuclear material, including its production process. This is a large part of nuclear forensics, which has goals rooted in answering key questions surrounding the identity and resources of the actor for an informed response to a nuclear incident, the importance and time sensitivity of which varies widely in different circumstances.

This problem is difficult to solve because of its inverse nature. For example, if chemically purified plutonium were interdicted at a State border, information from a wide variety of sources will be used to arrive at a likely hypothesis for where the material came from. These sources come from radiological inspection, physical characterization, traditional forensic investigations, and isotope/elemental/chemical analyses[3], all of which leads to an informed, studied, and tested hypothesis, which could possibly explain the history of the material.

The point is not to say the exercise is meaningless, but difficult and multi-layered. It is multi-layered because there are many different sources of information and a large number of possible hypotheses. This study presents a nuclear forensics characterization procedure for separated plutonium material, aiding an informed hypothesis for source attribution. Characterization for this project will be limited to determining reactor conditions (reactor type, neutron scalar flux, initial enrichment, and the age of the Pu material). In the example mentioned above, current methods would be hard pressed to determine reactor conditions in which the chemically purified plutonium was produced. This is because purification changes the isotopic composition of the material, making it much more difficult to definitively state the conditions of neutron irradiation. The elemental Decontamination Factors (DFs) herein presented provides a means to remedy this problem by correcting concentrations to what the unpurified material originally was.

Unlike enrichment of ^{235}U, ^{239}Pu "enrichment" involves neutron irradiation, which introduces radioactive fission products that need to be separated by some means. Purification by Plutonium Uranium Recovery by Extraction (PUREX) is most common for irradiated low-enriched uranium fuel[4]– important because ^{238}U, which is very abundant in depleted uranium, converts to ^{239}Pu upon neutron capture and subsequent two β^- decays. Material attribution for separated plutonium is further complicated because the separation process has a substantial amount of variability stemming from the changes in elemental DFs that could be obtained in a given PUREX process.

The measured effectiveness of a PUREX process is described by the DF, and measures the effectiveness with which the concentration, c, of a contaminant, j, is removed from a product. The product of interest in this work is plutonium, and the DF is defined by Equation 1.1,

$$DF_j = \frac{\left.\frac{c_j}{c_{Pu}}\right|_{\text{initial}}}{\left.\frac{c_j}{c_{Pu}}\right|_{\text{final}}} \tag{1.1}$$

where:

initial = initial state of unpurified plutonium

final = final state of purified plutonium.

The problem of attribution for unpurified plutonium material has been previously studied[5–7]. Ideally, if elemental DFs for interdicted plutonium are known, then these previous methodologies could be applied to determine the attributes of purified plutonium. In addition to the determination of elemental DFs for a PUREX process, this work also presents its own unique nuclear forensics attribution methodology. These two steps are visually represented in Figure 1.1, where the initial plutonium impurity levels are estimated through DFs with attribution analysis ensuing. The asterisks in the figure indicate the main areas of study for this project.

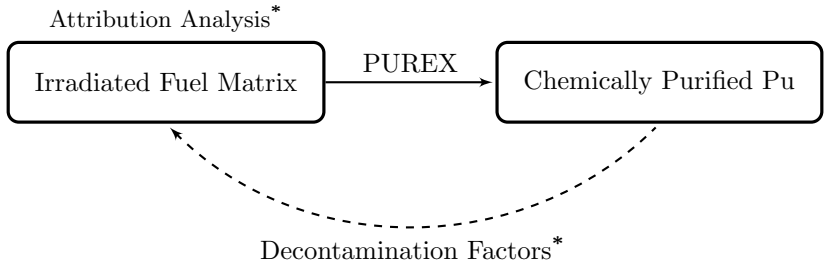

Figure 1.1: Research area for irradiated fuel.

This work starts with the assumption that the specifics of the PUREX process used for plutonium separation are known, so that DFs are applied appropriately. In real world applications, this information would not be readily available, and this same analysis would have to ensue with best estimate PUREX processes and experimentally measured distribution coefficients (DCs, the ratio of concentrations in organic to aqueous phase in the PUREX

process). The above also assumes that all processes in a particular PUREX plant proceed while in equilibrium. This work will not consider process steps after chemical separation which move plutonium from an aqueous solution to a metal. These steps have their own fission product "Decontamination", which should be characterized for this methodology to apply to plutonium which has been processed beyond PUREX. Characterization for these processes is beyond the scope of this project.

1.1. Background

Controlling access to nuclear technology, technical nuclear information, nuclear weapons and weapons usable materials is a simple approach for ensuring that nuclear weapons do not fall into the wrong hands. The main organization that works in this regard is the International Atomic Energy Agency (IAEA)[8]. The IAEA works with countries individually and the international community as a whole to ensure nuclear safeguards and security are in place for states that have signed the treaty on the Non-Proliferation of Nuclear Weapons (NPT).

Depending on the facility type, certain nuclear safeguards measures will be taken to ensure continuity of knowledge for all SNM. For example, reactor type facilities should track fuel assemblies, verify fuel burnup and ensure fuel (either fresh or irradiated) is not diverted by the state for non-peaceful purposes, whereas enrichment facilities track throughput, verify enrichment levels and declared facility layout and design. Reprocessing facilities are of special concern because of the relative ease with which plutonium can be isolated and diverted[9].

The IAEA verifies the peaceful use of nuclear technology through nuclear material accounting and control. Although the IAEA mitigates a large area of proliferation concerns, countries like Iran, India, and North Korea show that their effectiveness is not all encompassing[9]. For example, Iran was able to conceal a nuclear weapons program for several

years and the Khan network provided Pakistan with their weapons[9].

In addition to these core IAEA efforts, another means to limit the use of SNM for illegal activities is to develop a deterrence strategy. Nuclear deterrence, "the credible threat of retaliation"[10], has been the stance of the U.S since the Cold War. Although this stance has been questioned, forensic tools that link nuclear incidents to state or facility actors could be a valuable deterrence[11], but at the very least would quickly provide beneficial insight into a nuclear incident.

Confirmed incidents of interdiction of nuclear material has been an issue since the fall of the former Soviet Union[12]. Although not all cases involve SNM, some do and in order to most effectively qualify nuclear forensics as a deterrence these instances should display the accurate analysis of such samples.

Samples of concern contain SNM, which consists of material that could be used to make a nuclear weapon (^{235}U, ^{233}U, or ^{239}Pu). Although heavier fissile isotopes can be used for weapons purposes, they are not typically discussed in this context as a concern because the relative amounts and accessibility of these materials are much less than for traditional SNM. Each isotope of SNM has its own unique production path.

In order to procure an adequate amount of enriched ^{235}U, natural uranium is required in large quantities, which will be enriched, and because of the large footprint, traditional forensic exercises and safeguards are typically implemented to prevent this route for acquiring a weapon. Production of ^{233}U is similar to ^{239}Pu in that fertile fuel is converted to fissile fuel via irradiation, with large quantities of thorium, a reactor and chemical separation requirements. Unless a large quantity of thorium is on hand, this route is typically more difficult than production of ^{239}Pu through irradiation of natural or depleted uranium, which is utilized in this project.

Plutonium is produced through radiative neutron capture in ^{238}U as shown in Equation 1.2. After two β^- decays, shown below, ^{239}Pu is produced. The probability per target

atom and unit of incident flux for this occurrence, which is summarized in the radiative capture microscopic cross section (σ_γ), depends strongly upon the neutron energy. This is shown in Figure 1.2[13] where the cross section, in units of barns (10^{-24} cm^2), is plotted as a function of energy.

$$^{238}_{92}\mathrm{U} + ^{1}_{0}\mathrm{n} \xrightarrow{(n,\gamma)} ^{239}_{92}\mathrm{U} \xrightarrow[t_{1/2}=23.5\ \mathrm{min}]{\beta^-} ^{239}_{93}\mathrm{Np} \xrightarrow[t_{1/2}=2.4\ \mathrm{d}]{\beta^-} ^{239}_{94}\mathrm{Pu}^{[14]} \tag{1.2}$$

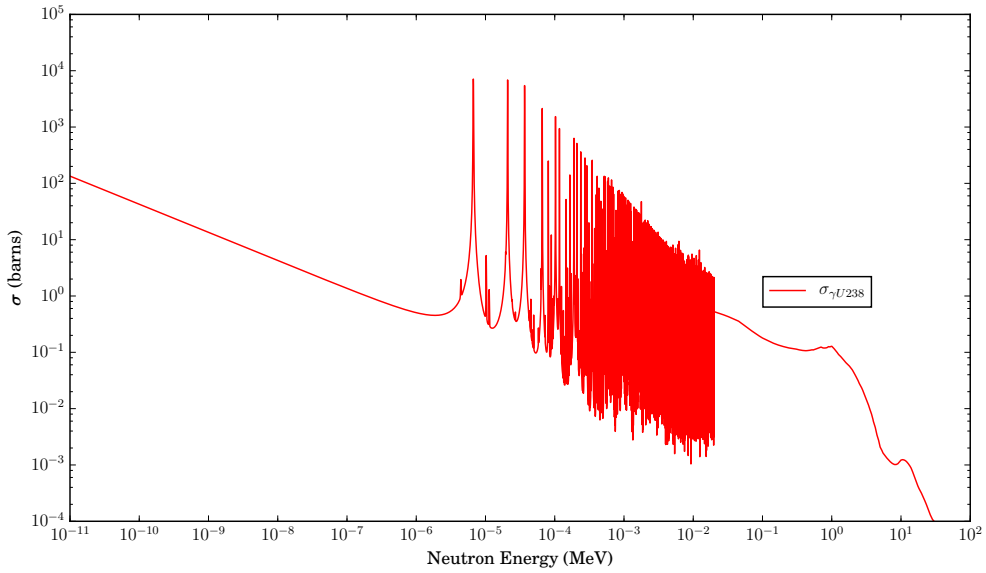

Figure 1.2: ^{238}U radiative capture cross section as a function of energy[13]. Reprinted with open source ENDF/B-VII data.

Typical trends for cross sections are seen in Figure 1.2, where lower energy (<1 eV) interactions have higher probabilities, and large spikes in the cross section (resonances) are seen in the intermediate energy regions (1 eV < E < 0.1 MeV), and unresolved rolling resonances at higher energies. Different reactor systems will have a different intensity of

neutrons (scalar flux ϕ) in various energy regions and the total rate of radiative capture for ^{238}U is determined by integrating the scalar flux and the interaction cross section and multiplying by the number of ^{238}U atoms (N), shown in Equation 1.3.

$$\text{Reaction Rate}(t)\left[\frac{\text{Captures}}{\text{s}}\right] = N(t)\int_0^\infty \phi(t,E)\sigma_\gamma(E)dE \tag{1.3}$$

The irradiated UO_2 contains plutonium isotopes ranging from mass numbers 238 up to 242 from subsequent neutron captures. The amounts of these isotopes depend on how long uranium is irradiated (or on the total burnup of the fuel), the initial ^{235}U enrichment of the fuel, and the neutron flux spectrum[15]. This means an investigation of the composition of the plutonium can provide important information about the reactor type and burnup[16]. Although lower burnup levels (<5000 MWd/MTU) lead to less total mass of plutonium, the plutonium has higher isotopic concentrations of ^{239}Pu (90% or higher), termed as weapons-grade plutonium[17–19], because there is not as much opportunity for heavier plutonium isotopes to absorb a neutron. This is shown in Figure 1.3 where the burnup, a measure of irradiation, is plotted against the ^{239}Pu mass fraction on the left vertical axis and the mass of specific isotopes of plutonium are shown on the right vertical axis for a typical PWR system. The plot shows that lower burnup levels have higher concentrations of ^{239}Pu.

Besides undergoing radiative capture, there is a probability that a neutron absorption will cause a plutonium isotope to fission. These two reactions are competing, and the fraction associated with either is described by the fraction each attributes to the sum of the reactions ($\sigma_\gamma + \sigma_f$). This is the main reason why different reactor types produce different plutonium vector isotopics. In order to highlight this, the average microscopic cross section for radiative capture (σ_γ) and fission (σ_f) of the heavier plutonium isotopes were calculated for the thermal, resonance, and fission energy regions, where averaging schemes were determined as described in Appendix A. The cross sections along with as-

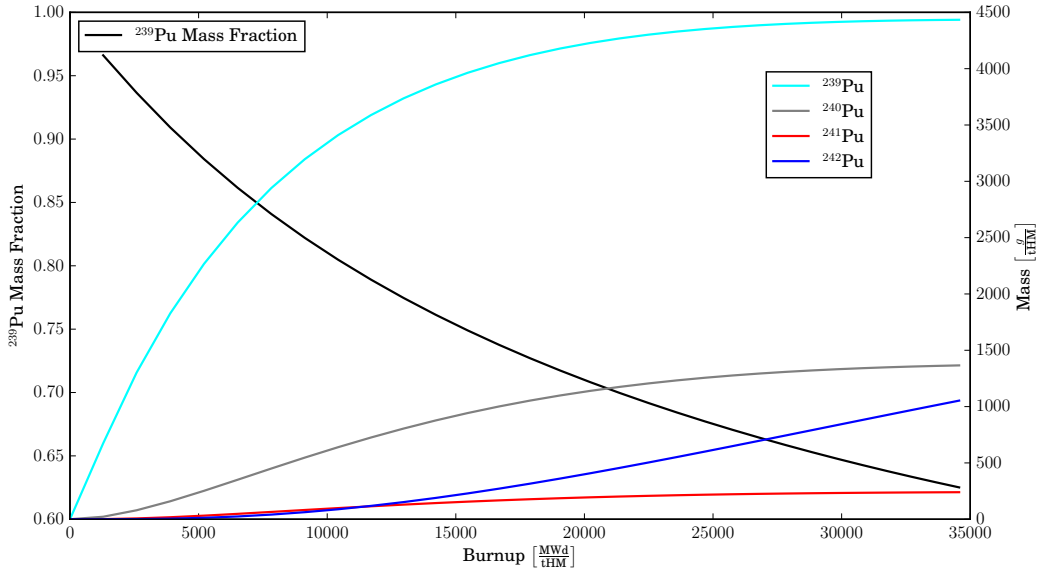

Figure 1.3: PWR example of plutonium isotopics. Burnup is plotted against the ^{239}Pu mass fraction of the left vertical axis and the mass of the specific isotopes of plutonium are shown on the right vertical axis

sociated fraction of fission and absorption are shown in Table 1.1, where the cross section is listed in units of barns and in parenthesis the fraction of fission or absorption are given. For example, in the energy range between 10^{-5} to 10 ev, ^{239}Pu would have a 28% chance of absorption and a 72% chance of fission if those where the only two avaiable neutron reactions. At lower to intermediate energies the probability of radiative capture for these listed isotopes represents 20 to 100 percent of the absorption cross section, whereas in the high energy region, this fraction is less than 8 for all isotopes. This shows that systems with softer neutron spectra have more production of the heavier isotopes[15]. Heavier isotopes of Pu are not ideal for making a weapon because both ^{240}Pu and ^{242}Pu fission spontaneously.

It might seem counterintuitive, but a method to help limit the illegal production or use of plutonium is to study how it is optimally produced and to study the production

Table 1.1: Plutonium radiative capture and fission cross section for different energy groups. The cross section is listed in units of barns and the fraction of fission or absorption is given in parenthesis. For example, in the energy range between 10^{-5} to 10 ev, ^{239}Pu would have a 28% chance of absorption and a 72% chance of fission if those where the only two avaiable neutron reactions.

Isotope	Reaction (barns)	Energy Range (eV)		
		10^{-5}-10	0.5-10^{5}	10^{5}-10^{7}
^{239}Pu	σ_γ (%)	275.(28)	181.(38)	0.04(2)
	σ_f (%)	699.(72)	293.(62)	2.(98)
^{240}Pu	σ_γ (%)	262.(99.9)	8497.(100)	0.1(7)
	σ_f (%)	0.06(0.1)	2.7(0)	1.3(93)
^{241}Pu	σ_γ (%)	331.(26)	179.(24)	0.1(6)
	σ_f (%)	939.(74)	561.(76)	1.6(94)
^{242}Pu	σ_γ (%)	19.(99.9)	1123.(100)	0.1(8)
	σ_f (%)	0.01(0.1)	0.23(0)	1.14(92)

path for indicators or characteristics that provide useful information. A fast neutron environment was just established as more effective so that heavier plutonium isotopes are less likely. Another means of limiting the production of heavier plutonium isotopes was through limiting the burnup of the fuel. Also, ^{239}Pu is a product of ^{238}U, and therefore uranium depleted in ^{235}U is also beneficial for transmuting uranium into plutonium. These three conditions are true for the depleted UO_2 (DUO_2) assemblies present in the radial blanket region of Fast Breeder Reactors (FBR)[20–22]. This is the reason plutonium was produced for this project in minute quantities (microgram level) through the irradiation of DUO_2 in a pseudo-fast-neutron environment to a low burnup.

The next step in producing ^{239}Pu would be to chemically isolate plutonium from the irradiated uranium. The most common method for this is the PUREX process[4,23]. PUREX takes advantage of the large relative difference between the extractability of Pu(IV) and Pu(III) into tri-n-butyl phosphate (TBP) from nitric acid. The PUREX process was devel-

oped as part of the Manhattan Project in 1947 and focuses on isolating plutonium from fission products and uranium[24,25].

An important goal of this project is to determine the level of decontamination of specific fission product elements in the product Pu, previously defined as the DF. These elemental DF values are strong functions of the specifics of the PUREX process utilized for purification and therefore should be strongly correlated to process step elemental DCs. Another significant contribution of the project comes from the methodology development that will aid in identifying the origins of chemically processed plutonium, which is a valuable deterrence capability.

1.2. Objectives

In the event of interdiction of SNM at the U.S boarder, the material would first be subject to Non-Destructive Analysis (NDA). If any signatures suggest the presence of plutonium, analysis would proceed with Destructive Analysis (DA). Through DA, DFs of fission products compared to the plutonium can be determined so that an informed source attribution methodology can be applied.

Previously, computational studies have indicated that analysis of contaminants in PUREX processed plutonium could give indications of material origins[5].

The main objective of this research is to determine DFs and DCs for a bench-top scale PUREX process for important forensics attribution elements noted in previous research (Cs, Eu, Rb, Sr, Nd, Pm, Sm, U, and Pu)[5]. Both DCs and DFs will be determined for this process so that the two parameters will be experimentally connected to the specific PUREX process utilized. This establishment is important because the nuances for a particular PUREX process vary widely and result in different DFs from process to process[26]. Mathematically, DC values, coupled with process information, can be used to calculate a reasonable estimate of a DF[27–30], leading to original concentrations of impurities in puri-

fied plutonium, which in turn allows for use of more traditional forensic analysis.

A second objective is to develop a forensic methodology to determine fuel burnup, reactor neutron scalar flux (assumed constant), irradiation time in reactor, initial enrichment, and fuel age associated with the plutonium production.

The above points are summarized in the list below:

1. Characterize a 4 extraction, 3 back-extraction PUREX process
    - ❖ Collect DC-values for each step
    - ❖ Collect DF-values for the process (and the two steps)
    - ❖ Mathematically connect DC-values to DFs
2. Determine attribution indicators:
    - ❖ Derive equations for indicators listed below
        - – Burnup
        - – Scalar Flux
        - – Time in Reactor
        - – Initial Enrichment
        - – Decay Time
    - ❖ Develop an algorithm and code to solve for the above parameters given the heavy metal uranium concentration ratios
3. Perform the above calculations using several different flux spectra as inputs

1.3. Literature Review

The literature review was separated into two parts, the first part reviewed previously developed attribution or forensic tools/methodologies for SNM. The second part reviewed

the PUREX process in general, and specifically reviewed DF values for given processes, and DC values for specific elements for the extraction and back-extraction PUREX steps.

1.3.1. Forensic Tools/Methodologies

There are many studies that present procedures to differentiate *unpurified* spent fuel[31]. These studies are useful for the differentiation that can be done based on reactor type, final burnup, or initial fuel type. Data utilized for differentiation could be isotope ratios of the heavy metals or of the fission products[32].

A method for distinguishing reactor types utilizes statistical techniques known as factor analysis[31], which reduces high dimensional data to several components. These studies utilize ORIGEN-2[33] calculations to model the time-varied isotopic inventory for several reactors (PWR, BWR, CANDU, and LMFBR). Isotope ratio results from simulations are used in the factor analysis and 3-dimensional plots showed that there is a clear distinction among reactor types. It is uncertain whether or not this methodology will work if certain ratios were removed from the factor analysis. This is important because when plutonium is chemically processed the concentrations of all species in the material is changed. Therefore only plutonium ratios would be available in this analysis, and it is unclear how well the methodology would work. Some research seems to indicate that this might not be as promising[7].

Previous studies have utilized isotope ratios $^{242}Pu/^{240}Pu$ and $^{238}Pu/^{tot}Pu$ to try and mark a distinction between reactor types that produced the plutonium[15,16]. This methodology seems to work well for very different reactor types such as a PWR and a FBR, but some samples, such as ours, did not conform to the pattern of the plots presented in[16]. These isotope ratios also fail to distinguish between plutonium producing reactors such as a CANDU and a Hanford-type graphite moderated reactor.

The use of chronometers is another widely accepted method for determining the time

since last chemical purification[15,16]. This utilizes the parent/daughter relations of plutonium isotopes with its daughters. This provides useful information for last chemical processing date, but typically has the issue of assuming perfect separations.

Isotopic compositions and ratios in spent reactor fuel have been used for fuel burnup verification. One study utilized measurement of isotopic ratios of stable noble fission gases during reprocessing in order to verify fuel burnup[34]. They used data analysis methods to determine specific fuel parameters and then compared them with the measured values of stable noble gases. Fuel burnup is important to verify for reasons described above. If a fuel assembly was burned to a lower level than reported, then further investigation is necessary to either alleviate or confirm suspicions of nefarious activities.

Others have analyzed later stages of processing used nuclear fuel. Given the spent fuel from a reactor that is used for a radiological dispersal device (RDD), a study sought to determine the burnup, enrichment, and age for the fuel[6]. These combined data would then be subsequently used for reactor attribution purposes. This study is similar to our scenario in that it looks at fission products in the matrix of the fuel itself and deduces reactor type and information about the history of the fuel, but this method does not consider any chemical processing.

A study from Los Alamos forensically analyzed two plutonium foils[35] and determined which reactor they came from. The approach for their analysis was to use the high ^{239}Pu content (>98%) to narrow in on a heavy-water and graphite moderated reactor, not entirely because of its spectrum, but because of its low burnup[i]. This combined with last known processing dates of 1948 and 1955 were used with reactor simulation to verify that the fuel was 60 years old. The initial enrichment was not explicitly stated but could be inferred from the known reactor type. This analysis used similar forensic methodolo-

[i]Softer spectra, as discussed previously, produce more heavier isotopes of plutonium that fast spectra but less heavier isotopes than intermediate spectra, see Table 1.1.

gies as described in the previous papers. Mass spectrometry results were analyzed but not connected to fission products, which is something this project proposes to do.

Studies have been done to investigate a core assumption in the age calculation for chemically separated plutonium[36], the assumption being that the daughter isotopes used for age determination are not initially present in the matrix, and build into the system as a function of time. The study showed that weapons-grade plutonium is more sensitive to biases at lower decay times, even with 0.1 ppm residual uranium. Relative bias can reach up to 70% for systems that had undergone short decay times. This is a reason for developing another means for determining an age for the fuel.

A forensic case study analyzed plutonium metal for reactor source, time since irradiation, time since purification, and plutonium reprocessing scheme[37]. Several quotes from this source are noteworthy: "relatively few ... validation studies focus on plutonium samples", "... studies demonstrate the limited utility of individual attributes for forensic determination of process history, and highlight the need for a multi-faceted analytical approach for attribution of unknown Pu materials", "at low burnup many ... signatures are more difficult to differentiate among reactor types."

The method used to determine the reactor type displayed in this study assumed a graphite reactor because the age of plutonium reflected a time when graphite reactors dominated the plutonium production "market". This assumption may not be warranted, because the time of reprocessing was determined to be in the 1980s. From this assumption, the time since being removed from a reactor utilized burnup simulations from this assumption, and found that by comparing the present $^{241}Pu/^{239}Pu$ with the "irradiated" $^{241}Pu/^{239}Pu$ concentration, the irradiation date was around 57 years ago. It should be noted that this method started with an assumed reactor, and utilized simulation data to determine the end of irradiation time. A more rigorous analysis would compare this result from other assumed reactors.

In Moody's, "Determination of Plutonium Metal Origins"[38] he states that plutonium isotopics clearly define the reactor type, which the above reference slightly disagreed with. Moody also states that neodymium contamination can be used to determine process history. He lists ^{242,244}Cm as a reactor flux parameter and for determining the reactor discharge time, which is not particularly useful for a lower burnup.

Post-detonation forensic activities are a different branch of nuclear forensics. There have been many studies in this arena, some of which can even determine weapons design. Two studies analyzed nuclear debris including trinitite for forensic signatures[39,40].

The current work expands upon previous work because many more parameters, beyond reactor type and time since last chemical purification are being determined for *chemically separated* plutonium. Among these are the burnup, the fuel age, defined as the time since being removed from the reactor, the initial enrichment of the fuel that produced the plutonium as well as the neutron scalar flux.

1.3.2. PUREX Processes with DFs and DCs

There are many different processes which can be used to chemically purify plutonium contained in irradiated UO_2[41]. Several aqueous and non-aqueous methods are available. Examples of aqueous methods include liquid-liquid extraction, ion exchange, and precipitation. Two non-aqueous methods for separation are electro-refining, and fluoride volatility[42]. Most methods utilize the behavior changes that different oxidation states of plutonium exhibit.

Chemical separation of plutonium focuses mostly on separating plutonium from fission products, and because the fission products span all groups in the periodic table, the chemistry can be quite complex. This means proven methods are much more likely to be used on a production scale. Among the common purification schemes, PUREX, which utilizes a liquid-liquid extraction, is by far the most widely accepted and used[4].

This is why the chemistry aspect of this project spent time investigating DCs for specific elements for the extraction and back-extraction steps of the PUREX process as well as DF values for production scale PUREX plants. These values have wide variability depending on the conditions in which the extractions took place. Numbers in literature are provided for certain elements in specific conditions, but elements noted as forensically important[5] have largely been ignored in these studies. Although there are several complicated steps in the PUREX process, such as counter-current centrifugal contacts, pulsed columns, or mixer settlers, the two main separation steps for PUREX were reviewed because they are the main decontamination and separation steps for the whole process.

After chemical purification, plutonium is typically processed further to either an oxide or a metal. Comprehensive forensic analysis would need to include the decontamination, and in some instances, the contamination associated with these steps. This is beyond the scope of this project and DF values will be determined for PUREX processed material only.

Previous literature has explored DCs for the three different oxidation states of Pu, (III), (IV), and (VI), in nitric acid or sodium nitrate, with TBP diluted in kerosene[43]. These experiments varied nitric acid, TBP, Pu, and uranyl concentrations to determine DCs under many conditions. These dependencies can be related to the power of the number of molecules needed for reactions (equilibrium constant). Errors for previous work for Pu DC values are due to residual Pu(IV) during Pu(VI) experiments (up to 9%) and the reproducibility of final results was $\pm 10\%$.

Pu(IV) is most readily extracted by TBP in kerosene, followed by Pu(VI), and Pu(III), each with a DC value less than the previous by an order, and two orders of magnitude, respectively. Studies have also shown that increasing nitric acid concentrations increased extractability due to increased availability of nitrate ions[43].

Increasing TBP concentration for Pu(IV) has showed a square law increase in DC-

values with constant nitric acid concentration because two TBP molecules are needed to form the extractable complex[43]. Sodium nitrate has also been tested as the salting solution for Pu extraction and found that, mole for mole, sodium nitrate was more effective at extracting across the board. This was compared with $Al(NO_3)_3$, which is even more effective than sodium nitrate.

Uranyl nitrate has been shown to decrease DC values for Pu, simply because uranyl loads the organic phase, reducing the amount of free TBP, which lowers DC-values for all other dissolved species[43]. Plutonyl nitrate has been shown[43] to be less extractable than uranyl nitrate by a factor of approximately 10.

The coefficient of change in DC value with respect to temperature for Pu has been measured as well[?]. The dependency is complex, but for small temperature changes (15°C), the DC value does not change by a large amount (<50%).

Previous literature has shown that the shape of the DC-value versus nitric acid concentration curve is the same for different concentrations of TBP[43]. This is useful because the results could be extrapolated to different TBP loadings[43].

Descriptions of various PUREX processes are provided in many sources with explanations of chemistry including flow sheets and gross gamma DFs[4,44–48]. These sources generally report overall beta or gamma radiation DFs of up to 10^8 with Pu recoveries of 99.7% for industrial scale reprocessing facilities. While DCs for the various process steps of PUREX have been previously reported, details about elemental DFs for PUREX cycles have been largely limited to the major activity contributors, such as ^{106}Ru and ^{95}Zr[48]. A compilation of distribution data for PUREX extraction processes provides data for U, Th, and Pu in a variety of concentrations[49]. DCs for Zr, rare earth metals, Pu, and Th have also been studied in a series and are available[43,50–54]. The conditions for extraction in this series are similar to the conditions used in this experiment, and will be useful for comparison of DC values. Additionally, Ga has been studied for separation[55] because it

is a common contaminant in weapons-grade plutonium.

PUREX co-processing, where uranium and plutonium are not separated during reprocessing, of spent LWR fuels has also been studied[26]. Several DFs and production yields for uranium and plutonium were determined. The specific goal of this paper was to demonstrate that uranium and plutonium could be co-extracted for reprocessing. This study was also limited in determining DFs for a wide array of isotopes, which may not be important in terms of reprocessing, because higher levels of contamination are acceptable for fuel, but it is important in nuclear forensic analysis, because trace isotopes, whether radioactive or not, could give an indication of the origin of plutonium[25].

There also have been various studies about overall DFs that result from the overall PUREX process[48]. This is important because there are variations implementing the PUREX process and understanding the intermediate steps is helpful because they produce different distribution ratios and potentially different DFs.

Useful partition coefficient constants for plutonium, uranium, and some fission products have been provided in previous literature. These values help by providing a basis for our measurements, but ultimately will not be the same as for our experiments because the concentrations of dissolved species in our experiments are different. Most previous measurements of DC values for fission products Pu and U are in “isolated” scenarios, where a single species is dissolved in solution and extracted. In the case at hand, an entire irradiated pellet, fission products, uranium, and plutonium were dissolved. This will provide values that are closer to reality.

2. EXPERIMENTAL CONTEXT, OVERVIEW AND PROCEDURES

The project work was split into two distinct parts, chemical separations/analysis, and nuclear forensic analysis. The description and procedure will also be broken up along these same lines. Although both parts require some element of experimental procedure, the first requires more and will be discussed in greater detail below, while the other will be more analytical in nature with discussion starting in Section 4. The initial portion of this chapter discusses the PUREX process, which includes discussion of co-decontamination (extraction) and uranium/plutonium partition (back-extraction) as well as derivations for mathematical correlations between DCs and DFs for these two steps. The mathematical derivation for the process employed in this work will build upon the concepts presented in this section, but will be fully expressed in sections 3.5 and 3.5.2. After the mathematical correlations between DCs and DFs are discussed, the final sections describe the experimental setup and procedure followed to quantify the separated material of interest, plutonium.

2.1. The PUREX Process

The PUREX process was developed in the 1940s in order to recover and separate plutonium from used uranium fuel. Depending on the fuel burnup, the fuel composition will consist of different fractions of uranium, plutonium, other transuranics, and fission products. The largest fraction of the fuel composition is (>90%) uranium, which is usually followed by fission products and then transuranics. Used fuel can contain many elements in the periodic table[56]. Separation of elements in this broad range of possibilities is achieved in PUREX with the TBP ($(C_4H_9)_3PO_4$) solvent. This solvent is excellent for the following reasons[4,48]:

1. The ratio of DCs between extracted (even oxidation states) and non-extracted (odd oxidation states) species is high (alkali metals, such as ^{137}Cs generally have an odd oxidation state of +1)

2. Both uranium (VI) and plutonium (IV) have DC values greater than unity at concentrations used in extraction

3. Pu(III) is readily stripped from TBP phase during back-extraction

4. The physical properties of immiscibility with water, low viscosity, and high interfacial tension are acceptable. TBP has a density comparable with water and is fairly viscous, but dilution with kerosene mitigates these problems.

5. "For safety reasons it is relatively nonvolatile, nonflammable, and nontoxic."[4]

6. It can be purified and recycled[4]

7. "It is stable in the presence of chemical agents used in the process, such as nitric acid. It also has a good radiation stability."[4]

The first step for the whole process is to prepare the used fuel for dissolution by opening the cladding and capturing radioactive fission gases. The fuel is then dissolved in hot nitric acid (6-8 M) where most of the heavy metal and fission products are dissolved. The temperature is usually limited to below boiling, where higher temperatures increase the rate of dissolution. The concentration of the nitric acid is usually changed (~ 4 M) after dissolution for optimal conditions. Plutonium extraction into TBP is strongly dependent on oxidation state. Pu(IV) and Pu(VI) are extracted by TBP, while Pu(III) is not. This is shown in Table 2.1[23] where the DC, the ratio of concentration between organic and aqueous phases in the PUREX process, for liquid-liquid contact between 30 vol.% TBP diluted in kerosene at room temperature and 3 M HNO_3 are given.

Table 2.1: Distribution ratios reprinted from[47] for uranium and plutonium and some fission products.

	U(VI)	Pu(VI)	Pu(IV)	Pu(III)	Fission Products
Distribution Coefficient	8.1	0.62	1.55	0.008	0.001

Plutonium will be present as Pu(III), Pu(IV), Pu(V), and Pu(VI) in dissolved nitric acid solution[4,42]. Pu(V) is transitory at high acidities but any trivalent or hexavalent species in solution should either be oxidized or reduced to the tetravalent state. Both reactions are shown in Reactions R.2.1 and R.2.2 with the nitrite ion, which was introduced into the system with sodium nitrite[47]. It should be noted that there are other paths for reduction and oxidation as the two listed below are from the same reference[i].

$$6Pu^{+3}_{(aq)} + 2NO^{-}_{2(aq)} + 8H^{+}_{(aq)} \rightleftharpoons 6Pu^{+4}_{(aq)} + N_{2,(g)} + 4H_2O_{(aq)} \tag{R.2.1}$$

$$PuO^{+2}_{2,(aq)} + NO^{-}_{2,(aq)} + 2H^{+}_{(aq)} \rightleftharpoons Pu^{+4}_{(aq)} + NO^{-}_{3,(aq)} + H_2O_{(aq)} \tag{R.2.2}$$

where:

aq = aqueous phase

o = organic phase

g = gas phase

Initial co-decontamination, here also called extraction, refers to separation of uranium and plutonium from the fission products into the organic TBP phase. This occurs when the nitric acid solution comes into physical contact with TBP so that uranium and plutonium

[i] Another example: $2Pu^{+3} + 3H^{+} + NO^{-}_{3} \rightleftharpoons 2Pu^{+4} + HNO_2 + H_2O$ [42]

form complexes with nitrate ions and TBP where their extraction utilizes covalent bonds with TBP as described by the equilibrium formula shown in Reactions R.2.3 and R.2.4[4].

$$UO^{2+}_{2,(aq)} + 2NO^{-}_{3,(aq)} + 2\text{TBP}_{(o)} \rightleftharpoons UO_2(NO_3)_2 \cdot 2\text{TBP}_{(o)} \tag{R.2.3}$$

$$Pu^{4+}_{(aq)} + 4NO^{-}_{3,(aq)} + 2\text{TBP}_{(o)} \rightleftharpoons Pu(NO_3)_4 \cdot 2\text{TBP}_{(o)} \tag{R.2.4}$$

Most of the fission products are left in the aqueous solution at valence III and V states[57], with a couple of exceptions. Ruthenium is an example, with multiple valence state possibilities, including extractable Ru(IV)[4] – which emphasizes the importance of preconditioning the feed solution. Odd oxidation states are not extracted as readily as even oxidation states because even oxidation states more readily form neutral complexes, as the odd oxidation states do not have sufficient charge density to pick up enough nitrates for neutrality.

U and Pu extraction trends can be described by additionally analyzing equilibrium extraction from nitric acid with TBP and determining the distribution ratio in terms of the equilibrium constant[4]. This is given for uranium in Equation 2.1, where K_U is the equilibrium constant for the uranium equilibria equation above, and M corresponds to the molar concentrations of the subscripted species.

$$D_U = K_U \left[M_{NO_3^-(aq)}\right]^2 \left[M_{\text{TBP(o)}}\right]^2 \tag{2.1}$$

Equation 2.1 shows that as the molar concentration of either species increases, the distribution coefficient increases. This does not indefinitely occur because nitric acid complexes with TBP, as shown in the extraction equilibrium below, and reduces the total free TBP in the system[58,59], which decreases distribution coefficients[48]. Also if the concen-

tration of uranium in the system increases, then the available uncombined TBP decreases, thereby decreasing the distribution coefficient. These formulations can be further carried out and written in terms of initial concentration of TBP and aqueous concentrations[4].

$$H^{+}_{(aq)} + (NO^{-}_{3})_{(aq)} + \text{TBP}_{(o)} \rightleftharpoons \text{TBP} \cdot HNO_{3,(o)} \tag{R.2.5}$$

$$H^{+}_{(aq)} + (NO^{-}_{3})_{(aq)} + 2\text{TBP}_{(o)} \rightleftharpoons \text{TBP}_2 \cdot HNO_{3,(o)} \tag{R.2.6}$$

To separate U and Pu, another liquid-liquid contact occurs between the extracted U and Pu in TBP with a separate aqueous phase; in this scenario Pu(IV) is reduced to Pu(III). Table 2.1 shows that Pu(III) preferentially favors the aqueous phase, as do the fission products. This means that the FP that were extracted into the organic phase will follow the Pu(III) as it is back-extracted. The reduction agent used is Fe(II), which is introduced into the aqueous phase with ferrous sulfamate. The addition of sulfamate helps increase the stability Fe(II) in the nitric acid solution[48]. Sulfamate removes trace nitrite from the system, which oxidizes and removes Fe(II) from the system, by reacting with it to create nitrogen gas and a sulfate ion[47],[ii]. The reduction of Pu(IV) to Pu(III) is shown below[23].

$$\begin{aligned} Pu(NO_3)_4(\text{TBP})_{2,(o)} + Fe^{+2}(aq) + (NH_2SO^{-}_{3})_{(aq)} \rightleftharpoons \\ Pu^{+3}_{(aq)} + 4NO^{-}_{3,(aq)} + 2\text{TBP}_{(o)} + Fe^{+3}_{(aq)} + (NH_2SO^{-}_{3})_{(aq)} \end{aligned} \tag{R.2.7}$$

The reason Pu(IV) is selectively reduced can be generically explained through standard reduction potentials. The system in PUREX processing will not be in standard conditions,

[ii] see R.2.8

and precise analyses could be conducted to determine the electromotive force produced by the system, but to highlight why Pu(IV) is more prone to reduce in the conditions of PUREX than U(IV) the relative differences between their standard reduction potentials with respect to the standard reduction potential of Fe(II) is given below. The standard reduction potential for Fe(II) is 0.77 V. The most direct route for reduction of Pu(IV) to Pu(III) has a standard reduction potential of 0.9821 V, which means, under standard conditions, this reaction will spontaneously occur [iii]. Conversely, the maximum potential for U(VI) reduction to U(IV) is 0.338 V. This reaction will not spontaneously occur in standard conditions because the overall potential associated with this reaction is negative[iv].

After Pu(III) back-extraction, oxidation of Pu(III) is accomplished with the addition of $NaNO_2$ to the solution in order start the process over with the first reaction listed in this section. This brings all plutonium to the most extractable tetravalent state. Excess sulfamate, which removes nitrite from the system is reacted away with the excess nitrite[47]. This allows for the removal of excess Fe(II) so the plutonium can be re-oxidized.

$$NH_2SO^-_{3,(aq)} + NO_{2,(aq)} \rightarrow N_{2,(aq)} + SO^{-2}_{4,(aq)} + H_2O_{(aq)} \quad \text{(R.2.8)}$$

$$NO_{2,(g)} + 2Fe^{2+}_{(aq)} + 2H^+ \rightarrow 2Fe^{3+}_{(aq)} + NO_{(g)} + H_2O_{(aq)} \text{ [60]} \quad \text{(R.2.9)}$$

The fission products that contribute mostly to the radioactive contamination of product in PUREX are zirconium, niobium, and ruthenium[4]. The DCs for these elements vary from 0.3 to 0.0001 depending on solution fuel saturation and nitric acid concentration. These transition metals have multiple oxidation states this leads to these elements being the limiting fission products in the decontamination of plutonium.

Several relevant phenomena, which could reduce extraction of plutonium are briefly

[iii] 0.9821 V - 0.77 V = 0.212 V
[iv] 0.338 V - 0.77 V = -0.432 V

listed below:

1. Degradation of TBP in high radiation fields, which contributes towards the production of monobutyl phosphate, which strongly complexes with U and Pu[48].

2. As mentioned before the catalytic oxidation of Fe(II), which has, even in the presence of sulfamate, has a varying chemical half-life from 0.1 to 130 hours[v].

3. The formation of unextractable polymeric species of plutonium in low acidities[47] at certain concentrations of plutonium and nitrate.

4. The formation of unextractable plutonium sulfate in the presence of excess sulfate ion – which comes from removing sulfamate.

5. Disproportionation of Pu(IV) and Pu(V) coupled with hydrolysis[vi] can shift oxidation towards the trivalent states[42].

6. Certain concentrations of nitrite, and nitrate, when added to the system, can actually shift plutonium oxidation towards the trivalent state[61,62].

2.1.1. DCs and trends for Co-Decontamination

The PUREX process includes an initial uranium/plutonium co-decontamination step as well as a plutonium partition step. These two steps are referred to as extraction and back-extraction, respectively. Each contact of TBP solution with nitric aqueous solution relocates dissolved materials in each solution based on DCs. DC, here defined as the ratio of grams per liter of solute in the organic solution over grams per liter of solute in the aqueous solution, as shown in Equation 2.2, where m is the mass of solute in a phase and V is the corresponding volume of the phase. DCs describe the steady state location of

[v] A strong function of nitric acid concentration

[vi] The time for equilibrium to be established between Pu(III), (IV), (V), and (VI) can vary widely depending on plutonium and nitrate concentrations[48]

any species in the system[4]. DCs have been reported per unit mass instead of volume, for simplification in calculations[48], but the general trend is to report per unit volume and therefore the current work will as well. To be expected, DCs are different from element to element, and vary widely with concentration and temperature of either phase. DCs represent the ratio of solubility of a species in either phase and are drastically affected by saturation of the major species, uranium and plutonium, in the system[24,48].

$$DC = \frac{\text{concentration of solute in organic phase}}{\text{concentration of solute in aqueous phase}} = \frac{m_{\text{o}}}{V_{\text{o}}} \cdot \frac{V_{\text{aq}}}{m_{\text{aq}}}, \tag{2.2}$$

A single extraction or co-decontamination is visually represented in Figure 2.1. The dissolved fuel in the aqueous solution comes into contact with TBP and U(VI) and Pu(IV) preferentially transfer to the organic phase while the majority of the fission products stay in the aqueous phase. The fraction, f, of a species, j, that transfers to the organic phase is given in Equation 2.3.

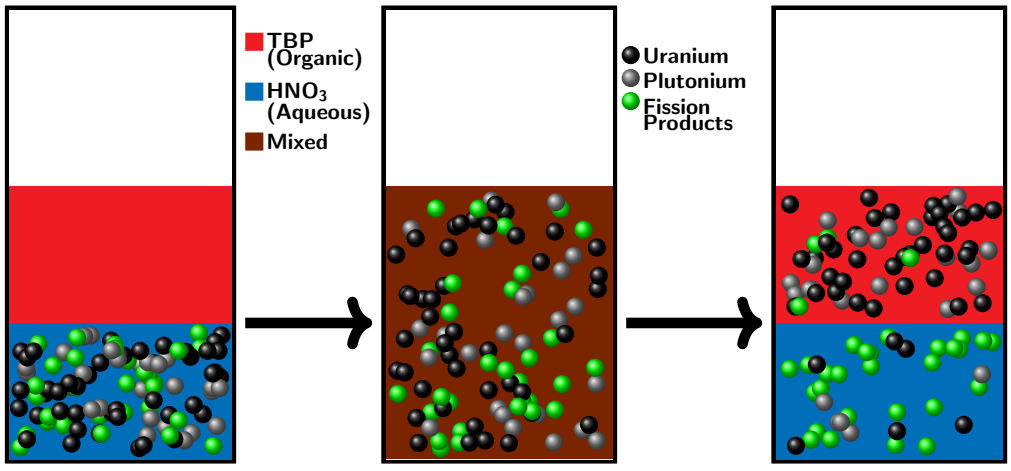

Figure 2.1: Co-decontamination of uranium and plutonium from fission products diagram.

$$f_{org,j} = (1 + DC_j^{-1} V_R^{-1})^{-1} \tag{2.3}$$

where:

$$V_R = V_o / V_{aq}$$

The mass fraction deposition in the organic phase as a function of volume ratio shown in Equation 2.3 was derived with the assumptions that mass is conserved in the process, the total volume of each phase is constant, and the system is in equilibrium. The second assumption is an approximation, as the density of at least the TBP can change appreciably[48] and there is also some solubility of the two phases in each other. In order to highlight certain trends, literature values for DCs at different experimental conditions[vii] were used with Equation 2.3 to produce Figure 2.2[48]. This shows the extraction as a function of volume ratio between the phases[viii]. The sharp increase of uranium and plutonium in TBP at low volume ratios is due to the DC being greater than one. Although the DC does not depend on volume, the volume of the two species being mixed will determine the mass of solute in each phase, which Figure 2.2 shows that as the volume of TBP in each contact increases, the mass extraction increases for all species.

Although Figure 2.2 was determined for a single contact of TBP, the trend generally follows for multiple contacts. Namely, as the volume of total TBP that contacts the stock solution increases, the distribution of mass extracted will continue to increase as well. It probably will not follow the exact lines as shown in Figure 2.2, because subsequent contacts change the form of the mathematical representation in an increasingly complicated way, but trends are still maintained.

To illustrate, Figure 2.3 is a plot showing the total mass fraction extracted into TBP as a function of distribution ratio. From the lower right of the plot to the upper right, the

[vii] 2 M HNO_3 at 0 % uranium sat and 30 vol.% TBP

[viii] as explained in the literature review, this work will provide more DCs than provided in literature and at different conditions. This work also determines DFs

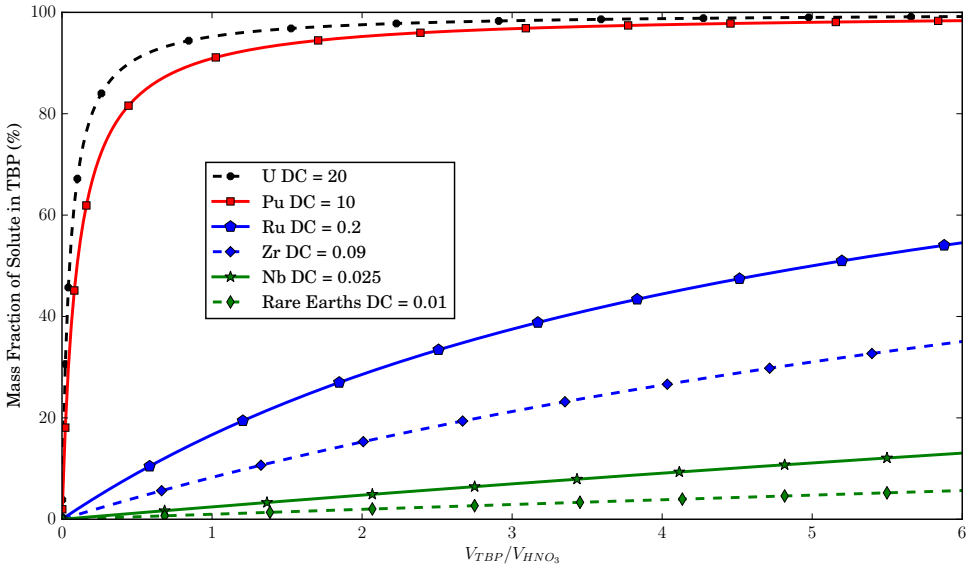

Figure 2.2: Mass fraction of solute in TBP as a function of volume ratio.

thickness of each plotted line increases. The lines' increasing thickness indicates an increasing volume ratio: the black/green solid lines correspond to a single contact of TBP and the red/green dashed lines correspond to two combined contacts of TBP. Both single and double contacts correspond to the same sum total volume of TBP contacting the aqueous phase. This means that the V_R for the single contact is twice that of the twice contacted because the sum total volume of organic is the same. The green sets of lines corresponds to a volume ratio of one. Figure 2.3 shows that multiple contacts remove more solute than otherwise and that the trend of increasing volume leading to increasing solute extraction is maintained.

If product yield were not a major concern, large DFs could be accomplished relatively simply by using a very small amount of TBP. This is highlighted in the bottom-most curves with the smallest volume ratios in Figure 2.3, where less than 10% of plutonium is extracted, but with very minimal fission products. This might not be practical because as

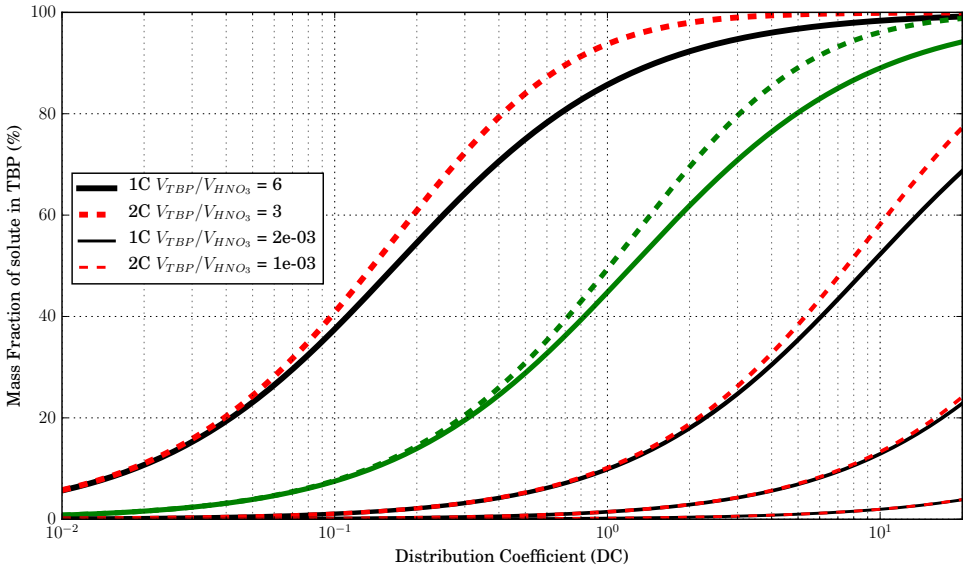

Figure 2.3: Concentration of solute in TBP as a function of distribution ratio and volume fractions.

the volume of TBP decreases, the level of saturation in TBP will increase, which usually decreases DC values across the board. The relative difference between uranium/plutonium and the fission products would still probably be sizable, but the uranium/plutonium DC values might be less than unity[48].

The green line in Figure 2.3 shows the approximate situation for the experimental procedure followed. Due to laboratory limitations, the most feasible method for liquid-liquid extraction and back-extraction were with comparable volumes of TBP and HNO_3. Given this limitation, the green lines in Figure 2.3 shows that multiple contacts – as opposed to a single large contact, is more beneficial for extracting the maximum amount of plutonium while maintaining that the fission products are left in the waste stream. This is highlighted by recalling that plutonium and uranium have larger DC values and are on the right side of Figure 2.3, while the fission products have lower DC values and are on the right side of

Figure 2.3.

It should be noted that even though the values for the distribution ratio are calculated at steady state conditions, PUREX cycles that utilize counter-current and/or continuous flow can utilize these numbers to determine reasonable estimates of elemental DFs[4,48].

Figure 2.4 shows the mass fraction extracted in the second contact *only*, assuming that a first contact occurred which had the same volume ratio as the second contact. It is obvious that at the standard V_R of one, the fraction of fission products being removed is greater than for uranium/plutonium. This is because the first contact removed a large fraction of the uranium and plutonium because of their high DC values. This means that a linear multi-contact system near a volume ratio of unity will have DF values that are getting worse with each subsequent extraction because more FPs are extracted with each contact.

The DCs used in this example were from a 0% saturation of U. Assuming the temperature and concentrations of nitric acid and TBP remain the same, the second contact will have similar DC values for all species because the saturation of uranium in either phase has not changed much. In instances where this is not the case, the fact that a large fraction of uranium was removed from the system would change the saturation of uranium in TBP. This would increase the amount of free TBP and increase DCs across the board.

2.1.2. DCs and trends for U/Pu Partition

Uranium and plutonium partitioning occurs when the extracted organic phase comes into contact with a reducing aqueous phase that selectively reduces the Pu(IV) complex to Pu(III). This process is visually represented in Figure 2.5. The fraction back-extracted into the aqueous phase from the organic phase is described in Equation 2.4 and has a similar form to Equation 2.3. The same trends that were described for extraction also apply for back-extraction: increased recovery will occur with increased contact volume,

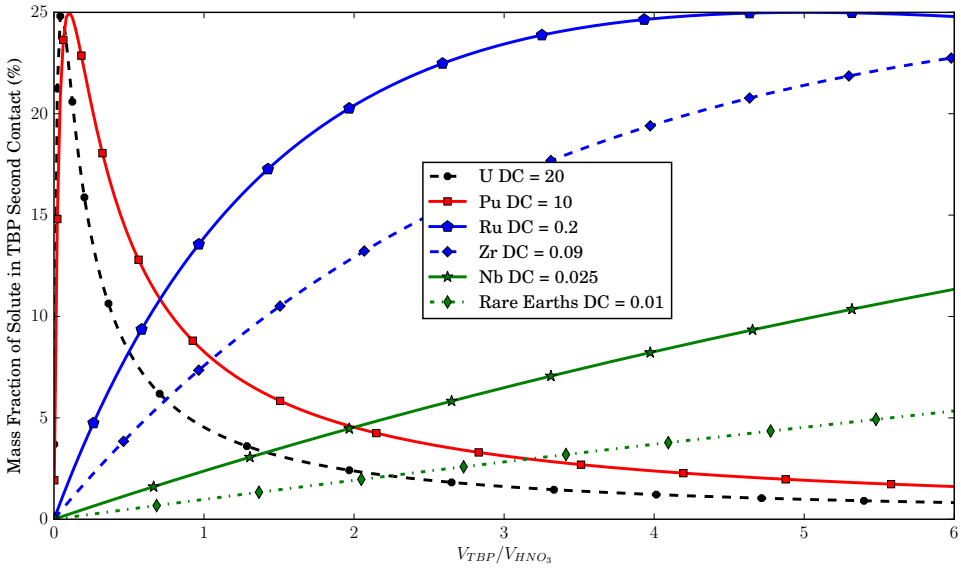

Figure 2.4: Fraction of original mass removed in second contact for different species.

and multiple contacts increase product recovery, but reduce DFs near volume ratios near unity.

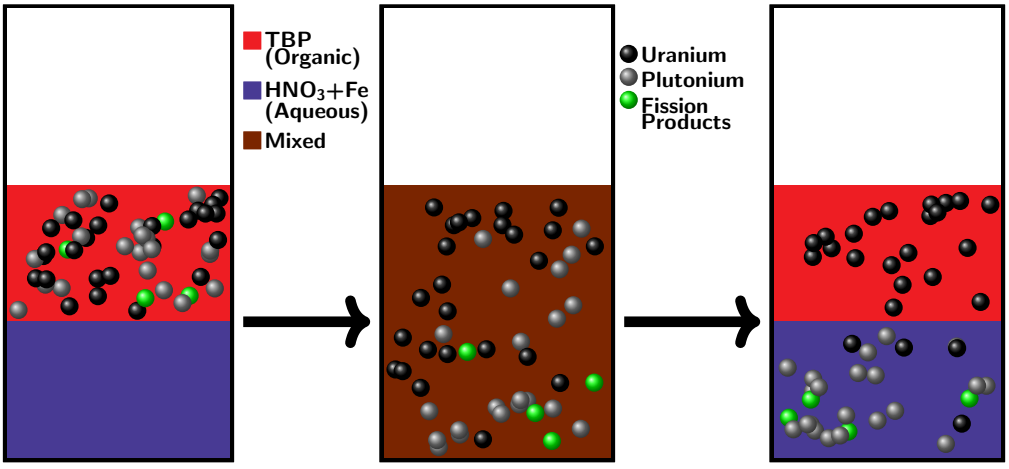

Figure 2.5: Partition of uranium and plutonium.

$$f_{aq} = (1 + DC_iV_R)^{-1} \tag{2.4}$$

2.1.3. DFs for Co-Decontamination and Pu Partition

A plant which reprocesses by the principles of PUREX are large and complex. From dissolution to conversion to oxide, the equipment used in the facility are specifically designed for each step. The extraction and back-extraction steps described above are usually intermediately coupled with a scrubbing section at low acid concentrations to remove accompanying fission products. Counter current centrifugal contactors, pulsed columns, and mixer settlers can be used for these different steps. In practice, after plutonium is back-extracted, the process can be reset and repeated with the addition of sodium nitrite to oxidize Pu(III). The process from first extraction, to making the solution just ready for this oxidation, will be referred to as a cycle.

After cycles of plutonium extraction/scrubbing/back-extraction are complete, the measured effectiveness of the PUREX process is described by the DF, which was was described before to measure the effectiveness with which a contaminant is removed from a product. The equation for the DF is reproduced in Equation 2.5, where C represents concentration either at an initial or final state. It should be noted that as long as the concentrations are of the same kind, then it does not matter whether they are reported in mass per unit volume or atoms per unit volume.

$$DF = \frac{\left.\frac{C_j}{C_{\text{Pu}}}\right|_{\text{initial}}}{\left.\frac{C_j}{C_{\text{Pu}}}\right|_{\text{final}}} = \frac{C_{j,\text{Initial}}}{C_{j,\text{Final}}} \cdot \frac{C_{\text{Pu,Final}}}{C_{\text{Pu,Initial}}} \tag{2.5}$$

DFs are characteristic of different PUREX process cycles[ix]. Most industrial processes report DFs on the order of 10^7 for an *over-all* DF[4,57]. An over-all DF, by definition, would be described with Equation 2.6, where j is summed over all contaminates. There-

[ix] There is also some dependence on the composition of the used fuel

fore industrial processes usually report DF with regard to total gamma or total beta counts, where an "over-all" amount is more easily determined. Otherwise, each individual contaminant should be measured and quantified. The over-all beta or gamma decontamination factor, $DF_{\text{overall,activity}}$, can be represented with Equation 2.7, where $\text{cps}_{\text{total}}$ is the total registered efficiency corrected counts per second for a given radiation detector. Of course $DF_{\text{overall}} \neq DF_{\text{overall,activity}}$ because all contaminants are not radioactive. It also follows that the DF associated with beta counts will not equal the DF associated with gamma counts for a similar reason.

$$DF_{\text{overall}} = \frac{\left.\frac{\sum_{j=1}^{J} C_j}{C_{\text{Pu}}}\right|_{\text{initial}}}{\left.\frac{\sum_{j=1}^{J} C_j}{C_{\text{Pu}}}\right|_{\text{final}}} \tag{2.6}$$

$$DF_{\text{overall,activity}} = \left.\frac{\text{cps}_{\text{total}}}{\text{cps}_{\text{total}}}\right|_{\text{Final}}^{\text{Initial}} \cdot \left.\frac{C_{\text{Pu}}}{C_{\text{Pu}}}\right|_{\text{Initial}}^{\text{Final}} \tag{2.7}$$

For example, the overall DF, given in terms of individual DFs, is shown in Equation 2.8, where both i and j loop over all contaminants. Two factors are competing for influence in this equation. First, the elements with the largest individual DFs will contribute most towards this sum and secondly, the species contributing most towards the final concentration of contaminants will also weight its DF more heavily than others. This equation was derived from Equation 2.6, which uses concentrations, but the concept still applies for the gamma or beta forms of the DF. These two competing factors make it difficult to derive concrete information about a particular element's level of decontamination based on a reported over-all decontamination.

$$DF_{\text{overall}} = \sum_{j=1}^{J} DF_j \left(1 + \sum_{i=1, i\neq j}^{I} \left.\frac{c_i}{c_j}\right|_{\text{final}}\right)^{-1} \tag{2.8}$$

Coupling Equation 2.5 with the section 2.1.1 analysis for mass fraction passing to the

organic phase, Figure 2.6 can be produced, which shows the decontamination factors for various elements at 0% uranium saturation and 30 vol.% TBP for an extraction into TBP.

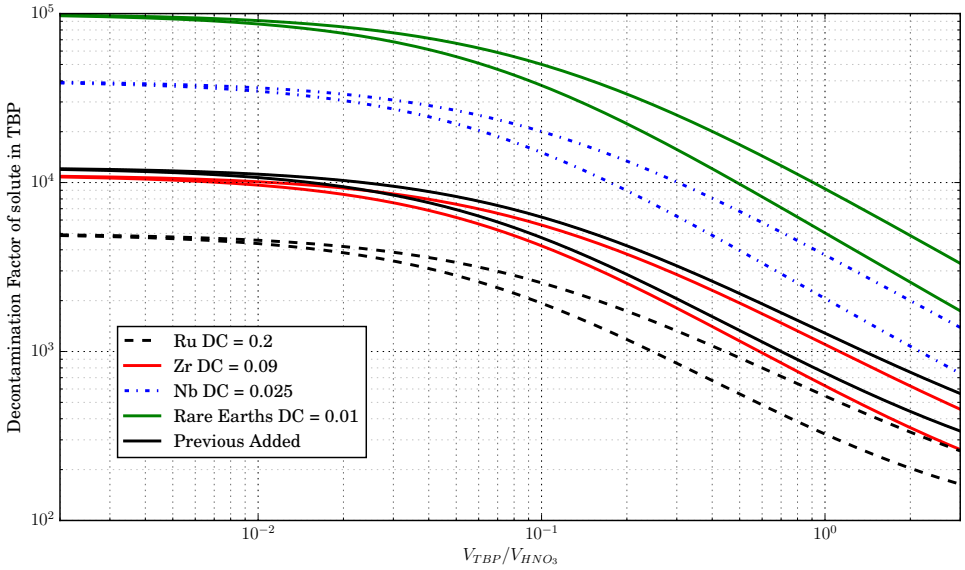

Figure 2.6: Decontamination factors as a function of volume ratios for first and second contact.

Figure 2.6 shows the decontamination factors for one and two contacts of TBP with the same volume ratio between both contacts. This plot assumes that the second contact of TBP is combined with the first contact. Different elements were plotted with their DCs and the sum of all four elements is given in the solid black lines. The lower line in each case is the second contact. This figure shows that extremely large decontamination factors can be achieved with minimal TBP solution. The caveat is that a small amount of plutonium is removed from the stock solution as well as potential for TBP saturation. This plot also shows that in this system, the DF values drop dramatically above a volume ratio of around 0.1.

The summed line assumed that each of the elements had equal mass in the stock solution, which is why the summed line acts like a line with a decontamination factor of 0.08125 which is an average of the four elements. This is the condition in order to say that decontamination factor is precisely an average of all the decontamination factors in the system. Elements with larger mass fractions in the solution will contribute most towards the overall decontamination factor in the product solution. This also highlights how overall decontamination factors can be approximated.

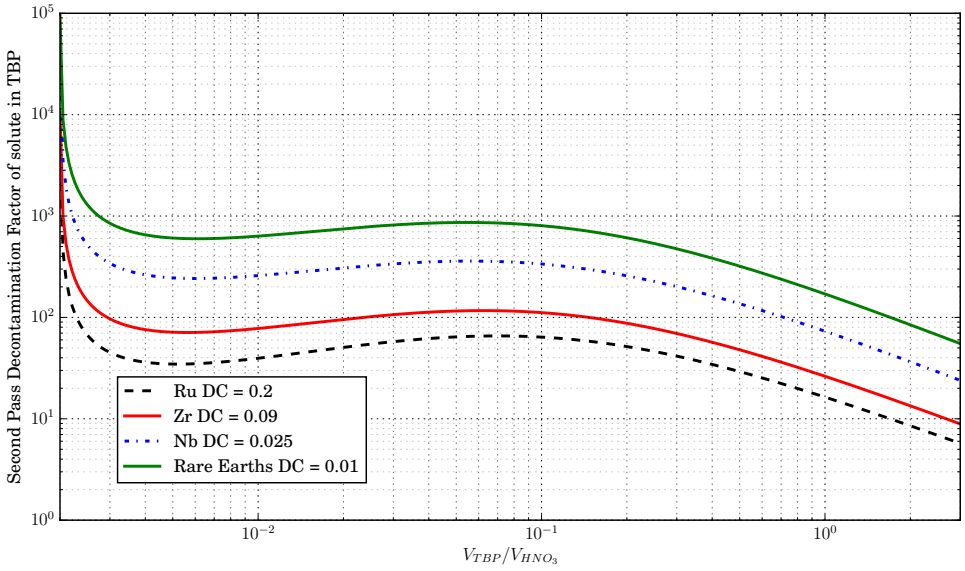

Figure 2.7: Second contact of TBP decontamination factors.

The isolated second contact DFs for TBP are shown in Figure 2.7. This calculation assumed that the volume ratios for both passes were equal, and that the TBP was not combined with the first pass. These numbers are two orders of magnitude lower in DF than the initial contact. The reason for the left most peak is due to the small amount of plutonium removed in the first contact, and the middle peak around 0.1 volume fraction

is due to the turnover in the previous plot, namely that around 0.1 volume fraction, the largest amount of Pu(IV) is extracted for the smallest amount of fission product. This is emphasized by plotting the mass fraction of solute in TBP for the first and second contacts on a logarithmic scale, shown in Figure 2.8.

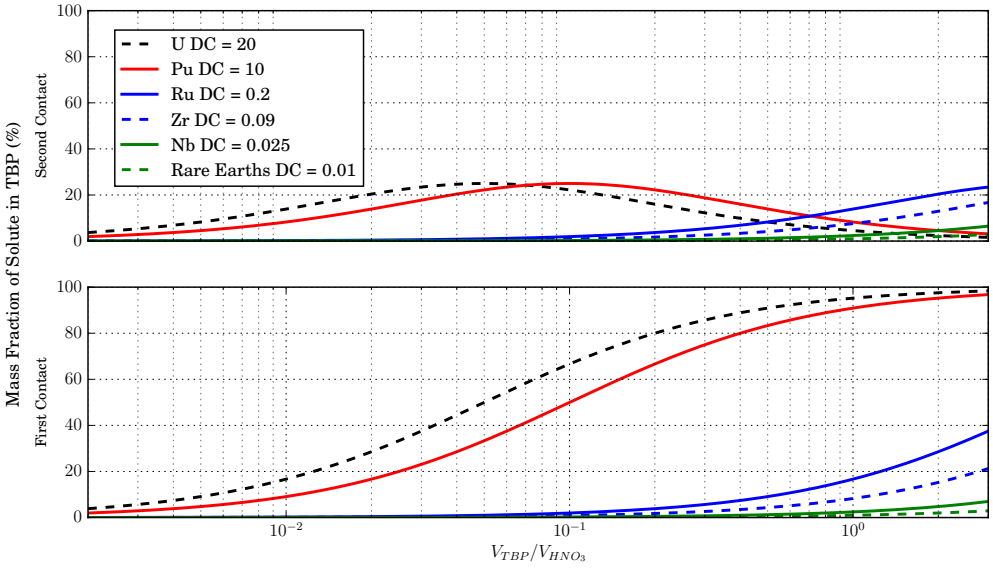

Figure 2.8: Mass fraction of solute deposited in TBP for first and second contacts.

The optimal volume ratio for plutonium extraction is 0.1 because the distribution ratio used for these calculations was 10, and the optimum volume ratio occurs at its inverse. This is verified with the uranium peak at a 0.05 optimum volume ratio. Notice in Figure 2.8 and Figure 2.6 how the first contact removes about 50% of the plutonium and gives a certain decontamination factor, while the second contact removes about 25% of the plutonium and decreases the decontamination factor by a factor of approximately two. In order to utilize this information for our experiment, three things should be considered.

1. After decontamination, a certain minimum activity should be detectable in the gamma detector

2. More concentrated samples use more of the irradiated pellet, and reduce the total number of PUREX experiments that could be done

3. Laboratory-scale liquid-liquid extractions compound volumes to fill vials quickly, so the final volume of the solution should be no more than 15 ml, which is the size of the centrifuge tubes used

With these considerations, and assuming that 0.5 ml is the starting volume, the optimum volume to remove 75% of the plutonium without increasing the DF by a large portion would be around 50 μl. Pipetting 50 μl by hand is possible, but when in the context of 0.5 ml, cross contamination would be a huge concern. Due to the fact that the project's goal was to extract as much plutonium as possible, the previous was not optimized on, just used for reference, as the distribution ratios for this experiment were expected to be different.

2.2. Experimental Setup and Procedure

2.2.1. Overview

The focus of the experiments was to experimentally characterize DCs for extraction and back-extraction, and connect these values to process DFs. Experiments determining DC values in scrubbing scenarios would be similar to studying DC values at lower nitric acid concentrations and are available for future experiments. This experiment did not focus on excessive scrubbing for marginal increase of decontamination factors.

12.9 mg of irradiated DUO_2 was dissolved in 5.17 $\pm$ 0.05 ml of 69% nitric acid and termed the closet solution because it was stored in a closet. Experiments were conducted with solutions diluted by a factor of either 10 or 5 from the closet solution. Each of these dilutions were conducted with 0.5 ml of the closet solution, which is about 10% of the

total sample, and termed the stock solution. The stock solution was approximately 4 M HNO_3 and PUREX ensued with aliquots ranging from 0.3 ml to 0.5 ml, which ranged from 0.6% to 2.4%[x] of the pellet. The plutonium oxidation state for this aliquot was adjusted to Pu(IV) by adding < 0.1 grams of sodium nitrite. U(VI) and Pu(IV) were extracted and decontaminated by contacting the solution with a solution of 30 vol.% TBP with a kerosene diluent. Plutonium was then reduced to Pu(III) and back-extracted and separated from uranium by contacting the TBP solution with a HNO_3/0.024 M ferrous sulfamate solution via oxidation of Fe(II). The HNO_3 solution varied in concentration, but the ferrous sulfamate generally stayed at 0.024 M. The experiments that studied multiple cycles converted the final solution Pu(III) to Pu(IV) with sodium nitrite and further decontamination/extraction ensued. The chemistry for these experiments was discussed in section 2.1.

2.2.2. Materials

The closet solution and the stock solution were stored in 20 ml glass disposable scintillation vials with urea caps from Fisher Scientific. Some experiments used VWR ultra high performance centrifuge conical-bottom tubes made of ultra-clear polypropylene copolymer with caps made of high density polyethylene. 50 ml centrifuge tubes were used for prepared reused solutions and 15 ml centrifuge tubes were used to hold samples from the stock solution. Other experiments used 5 ml polypropylene round-bottom tubes reference number 352063 from FALCON for extractions and back-extractions. These experiments used 1.5 ml disposable snap cap conical bottom tubes from VWR for precise phase separations. Axygen 5 ml self standing screw cap transport tubes were used for dilutions for alpha samples. These centrifuge tubes were parafilm wrapped while samples were not in use to reduce evaporation losses, and marked with fine point sharpie permanent marker to distinguish vials. The Champion F-33D fixed angle digital variable speed centrifuge from

[x] $\left(\frac{1}{10} \cdot \frac{0.3}{5} = 0.006\right)$ and $\left(\frac{1}{5} \cdot \frac{0.3}{2.5} = 0.024\right)$

Ample Scientific was used for centrifuging samples after mixing in a Fisher Scientifics Digital Vortex Mixer.

Most operations were conducted in a mBraun LABmaster Pro Glove Box Workstation with four glove stations and an approximate volume of 1.4 m^3. The glove box was equipped with a mBraun HEPA filter, a 29 kg Edwards Pump model number RV12, 0.4 mm gloves, and two antechambers. All of which are shown in Figure 2.9. Both the glove box gloves and the 15 ml centrifuge tubes were cleaned periodically with Radiacwash Towelettes from BioDex Medical Systems Incorporation to minimize contamination. Pure argon and a hydrogen/argon fill gases was acquired from Praxair. Argon was used for normal operation while the combination gas was used to regenerate the filter.

Figure 2.9: Glove box workstation.

Shielding was provided in the glove box by a lead shielded viewing workstation, lead

bricks, and a lead pig for the glass scintillation vial containing the stock solution. The lead shielding, along with the vortex mixer and centrifuge can be seen in Figure 2.10. The lead pig for shielding the scintillation vial is shown in Figure 2.11.

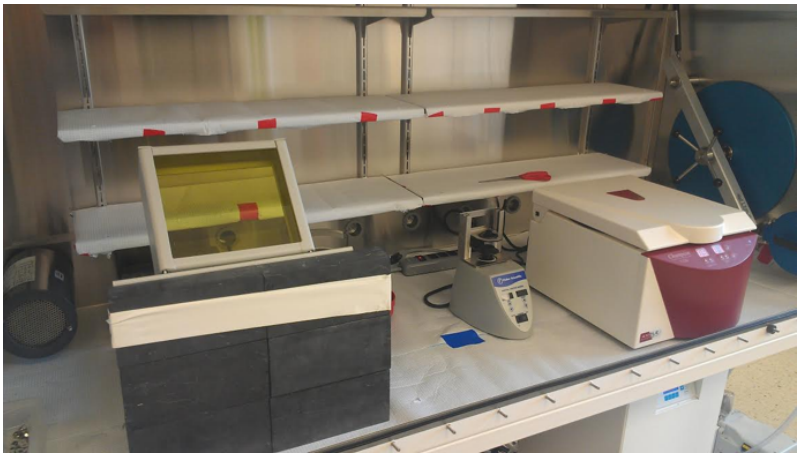

Figure 2.10: Glove box workstation showing the centrifuge, vortex mixer, and the lead shielding.

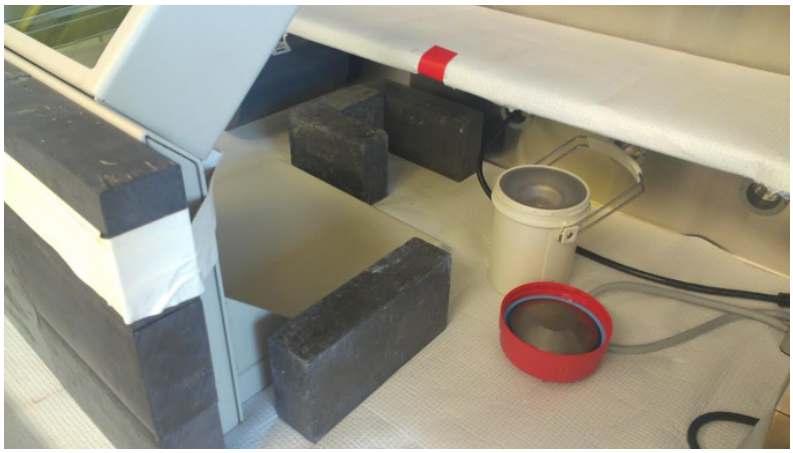

Figure 2.11: Glove box workstation showing the lead pig and the back of the lead shielding.

Laboratory procedures were conducted with standard personal protective equipment, including stretch ease powder-free nitrile examination gloves from Denville Scientific Incorporation. Pipetting was done with an Eppendorf 1000 μl adjustable pipette with dual filter 1250 μl, certified clean and sterile purity-grade tips. Fine tip transfer disposable pipettes were also used from Globe Scientific.

The distilled water used for dilutions was acquired from a 03/08/2011 manufactured Purelab flex water purification system with a model number PF3XXXXM1 to purify College Station tap water. The kerosene (100%), sodium nitrite (100%), and hydrofluoric acid (48%) were acquired from sciencelab.com, 69% nitric acid was acquired from Mallinckrodt Chemicals, Tri-n-butyl phosphate (>99%) was acquired from Fisher Scientific, iron sulfamate (40.26%) was acquired from Strem Chemicals Incorporation, and neodymium fluoride (99.95%) was acquired from GuideChem.

The pellet, both prior to dissolution and after, was counted with two Canberra Ge detectors. The first was a portable, mechanically cooled Falcon 5000 shown in Figure

2.12, and the second was a Canberra electrode coaxial Ge detector model number CC4018 which was connected to a Canberra Lynx multichannel analyzer (MCA). The second was cooled with liquid nitrogen supplied from Praxair and is shown, with liquid nitrogen dewar, detector face and brick set up in Figure 2.13. GENIE software was used to analyze spectrum and samples were typically encased in a lead tomb shown in Figure 2.14. Inductively coupled plasma mass spectrometry (ICP-MS) was also conducted for some samples with use of the University of Missouris PerkinElmer NexION 300X quadrupole ICP-MS operated in standard mode by Dr. James McKamey.

Figure 2.12: Falcon 5000 HPGe detector.

Figure 2.13: HPGe detector system with geometry and dewar shown.

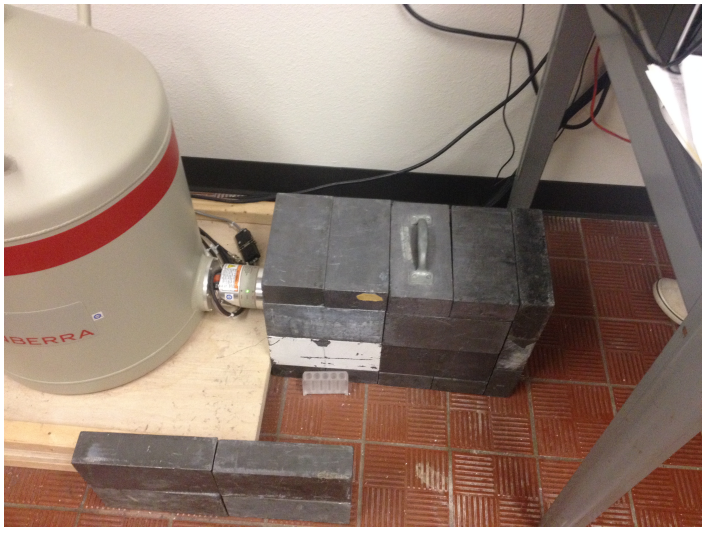

Figure 2.14: HPGe detector system showing lead tomb.

A Canberra semiconductor PIPS detector was used to collect alpha spectrum data for

the experiment. The detector is shown in Figure 2.15. A Welch model 8905B-24 vacuum pump was used to evacuate the atmosphere so that alpha attenuation would be negligible. A Canberra multiport II MCA was used to process pulse information. The entire system was held in a Canberra NIM Bin model 2100.

Figure 2.15: Alpha detector system with geometry shown.

2.2.3. Procedure

The irradiated DUO_2 pellet was weighed in a weighing boat on an electronic balance and transferred to a round bottom flask. 5.17 $\pm$ 0.05 ml of 15.35 $\pm$ 0.13 M HNO_3 was added to the round bottom flask and the flask was heated at 50^{o}C with constant 100 rpm stirring for two hours. The dissolution apparatus is shown in Figure 2.16.

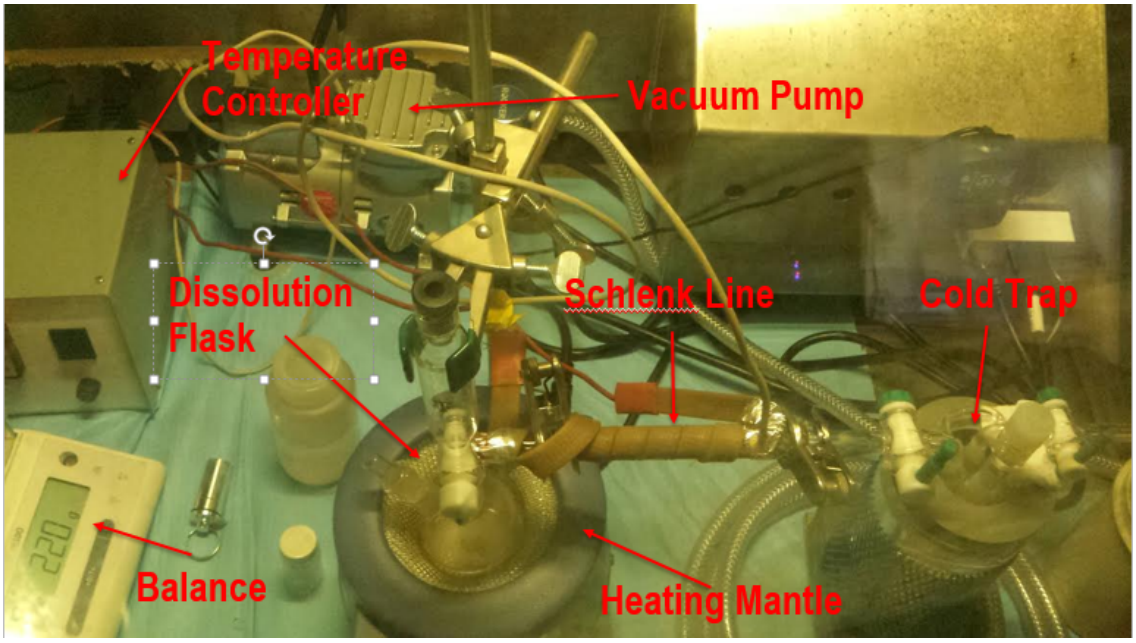

Figure 2.16: Dissolution of the irradiated DUO_2 pellet.

The round bottom flask was connected to a cold trap with the help of a schlenk line. The fission product gases such as H_2, CO_2, Kr, Br, I and N_2O were captured in the cold trap inside the molecular sieves which were surrounded by liquid nitrogen. The 5.17 $\pm$ 0.05 ml of 15.35 $\pm$ 0.13 M HNO_3 concentrated solution was transferred from the round bottom flask to a 20 ml glass scintillation vial and kept heavily shielded. This solution is the "closet solution" described above.

In order to reduce the amount of activity per sample, 500 μl from the closet solution, which corresponds to 9.7% of the pellet, was diluted. Initial steps diluted the closet solution by a factor of 10 and later experiments diluted this same amount by a factor of 5. This solution is referred to as the "stock solution". The concentration of the stock solution was intended to be 4 M HNO_3, which was different from the closet 15.46 M HNO_3. Initial experiments did not account for the change in density between these two concen-

trations, which is around 20%, and therefore volume/molarity calculations were slightly off. Results are reported with the proper concentrations. A python program was written to perform the dilution calculations and is reproduced in Appendix E. The gamma activity concentration of the stock solution that was diluted by a factor of 10 was about 80 mCi/L while performing the experiments. The stock solution was stored in its own 20 ml glass scintillation vial in a lead pig inside the glovebox.

The flow chart for a PUREX cycle for the experiments is shown in Figure 2.17. Procedures up to the step titled, "Stock solution" has been described in the begining of this section. Each PUREX experiment started by transferring 200 to 500 μl of stock solution to a new vial along with approximately 0.5 mg of $NaNO_2$. This aliquot was then contacted by TBP of comparable volume to the aqueous phase, at room temperature. The volume of TBP, with relation to the aqueous phase, also varied with experiment, but the concentration remained the same with 30% by volume TBP diluted with kerosene. The volume of TBP was either equal to the volume of the aqueous phase or had excess up to 0.2 ml. When a larger volume of TBP was contacted with stock solution the extra was added to so that cross contamination of phases would be less likely during pipetting. Similarly, equal or slightly excess contact volumes of iron sulfamate solution were used during the plutonium and uranium separation. Later experiments utilized smaller vials with conical bottoms and finer tip pipettes for better separation so that equal volumes were used. Despite these improvements in the experimental procedure, about 80 μl of a mixture of both phases remained unseparated at the end of each liquid-liquid extraction. Both types of extractions had the aqueous and organic phases mixed on a vortex mixer for 15 minutes at 1500 rpm, and then separated via careful pipetting. Multiple extraction and back-extraction contacts occurred to ensure the quantitative recovery of heavy metal from the stock solution.

Three concentrations of HNO_3 were used in the ferrous sulfamate that helped process solutions from the closet solution. Other concentrations of ferrous sulfamate were used

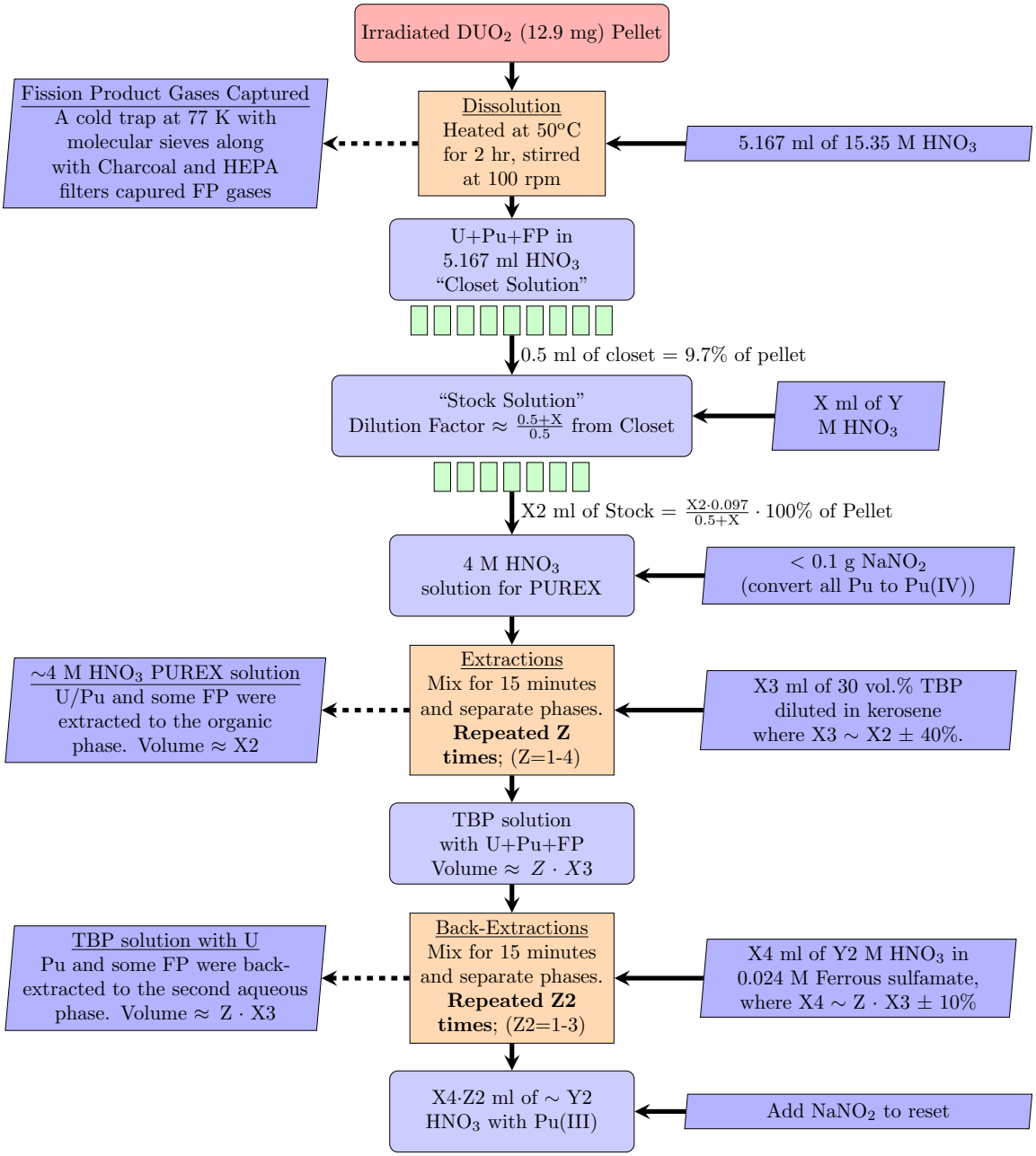

Figure 2.17: Flow chart for experiment.

with a different DUO_2 solution and are discussed in section 3.1.3. The concentration range of HNO_3 was from ~ 0 M - 8 M. These different concentrations were used to determine

differences in uranium stripping (back-extraction). Further, an experiment was conducted without the addition of sodium nitrite. As was mentioned previously, the half-life of Fe(II) in a solution of nitrite is a concern and therefore the solution was prepped beforehand.

After the back-extraction of Pu(III) the solution was either prepped for another cycle of Pu decontamination with the addition of $NaNO_2$ or precipitated with NdF_3 and HF for alpha spectrometric measurements. Dry runs of the above described experiment were conducted with depleted uranium to ensure that uranium is removed from the stock solution and does not make its way to the product solution. Dry runs were also done without uranium to analyze the background contamination in stock solutions for mass spectrometry.

Excerpts from the laboratory notebook used for these experiments is included in Appendix D. Also a table summarizing the experiments will be provided in section 3.1.4.

2.3. Methods of Measurement

The DCs were determined for each liquid contact by analyzing the stock solution before and after contact with TBP. Analysis utilized gamma spectroscopy with a HPGe on the whole sample and mass spectrometry on small ($\sim$ 50 μL) aliquots of the sample. Decontamination factors were determined with the same equipment and analyzed the end ferrous sulfamate solutions along with the waste stream and comparing with these to the initial. Quantification of plutonium recovery utilized alpha spectrometry on small evaporated samples of aqueous solutions. Organic solutions left visible residue on the plated surface and presumably attenuated alpha particles so that the TBP solutions were not quantified by alpha spectroscopy.

2.3.1. Mass Spectrometry

The NexION 300X quadrupole ICP-MS was utilized for gathering mass spectrometric data. This machine works by drying, atomizing, and ionizing liquid samples. These samples are then passed through cone filters, curved in a quadrupole ion deflector, purified

in a universal cell, refined in another quadrupole with a final mass-to-charge filtration and focused on a dual mode detector. The detector registered counts per second for particular isotope masses. Calibration occurred for a broad range of isotopes with seven different standards, listed in Table 2.2, each having multiple elements at various concentrations. These standards were used to determine instrument responses, with units of parts per billion (ng/g)[xi] per count per second (ppb/cps).

Table 2.2: List of ICP-MS standards used for experiments.

Name	Elements	Concentrations (ppb)
MS-B	Sc, Y, La, Ce, Pr, Nd, Sm, Eu, Gd Tb, Dy, Ho, Er, Tm, Yb, Lu, Th	10.19
MSCS-M	Li, Be, B, Na, Mg, Al, Ca, V, Cr, Mn, Fe, Co, Ni, Cu, Zn, As, Se, Sr, Mo, Ag, Cd, Sb, Ba, La, Eu, Ho, Yb, Tl, Pb, Bi, Th, U, Sc[b], In[c]	11.48 20.61[b] 40.99[c]
MS-C	Ru, Rh, Pd, Sn, Sb, Te, Hf, Ir, Pt, Au	10.00
MS-D	B, Si, P, S, Ti, Ge, Zr, Nb, Mo, Ta, W, Re	9.60
Custom Mix	Na, Mg, Al, K, Ca, Mn, Fe Ga, Rb, Sr, Y, Ba, Cs	504, 501, 501, 501, 1996, 255, 253 2.1, 2.1, 8.5, 1.1, 8.5, 1.1
Plutonium Standard	^{238}Pu, ^{239}Pu, ^{240}Pu, ^{241}Pu, ^{241}Am, ^{242}Pu	8E-5, 6.1, 0.13 2.4E-4, 1.1E-4, 6.3E-5
U & Th Standard	^{232}Th, ^{234}U, ^{235}U, ^{238}U	2.3, 2.9E-4 3.8E-2, 5.3

The instrument response as a function of mass for molybdenum is shown in Figure 2.18 with the detector response and error graphically represented. Instrument responses were

[xi] as reported by the operator

determined by multiplying the concentration for an individual isotope by its natural *mass* abundance and dividing by the counts per second for that particular mass bin. Instances of multiple isobars were avoided when determining instrument response from the standards. Isotopes of interest in the samples that had other isobars present were approached by assuming the superposition principle, meaning the detector response was the sum of the responses that would have been caused by each isobar individually. For low concentrations, this may be appropriate, but interferences between the isobars would be an issue at higher concentrations. Because the errors for these particular calculations were much higher, these calculations were avoided as well, and results that do employ this method are present mostly for rough estimates and clearly stated as such. Also extrapolation, when necessary for radioactive species, of instrument response used extrapolation from the same element.

Interferences from molecular species like UH were measured and corrected for by the MS operator.

Each calibration standard was run at different times during mass spectrometry measurements. For any given sample concentration calculation, the instrument response which most closely correlated with the time the sample was run was used. Figure 2.18 shows a downward sloped trend for increasing atomic mass. This was typical for most of the isotopes because the detector probably had some residue from previous samples, even though a rinsing solution was used between measurements. Some calculations utilized this as an assumption to either extrapolate or solve a system of equations for instrument responses for standards that had isotopes with overlapping mass numbers. In Figure 2.18 the MS-D standard had zirconium background in mass bins 92, 94, and 96. The instrument response was determined by subtracting out the zirconium response, which is why those particular instrument responses have larger error, because of propagation.

It should also be noted that the trends in Figure 2.18 should not be correlated with

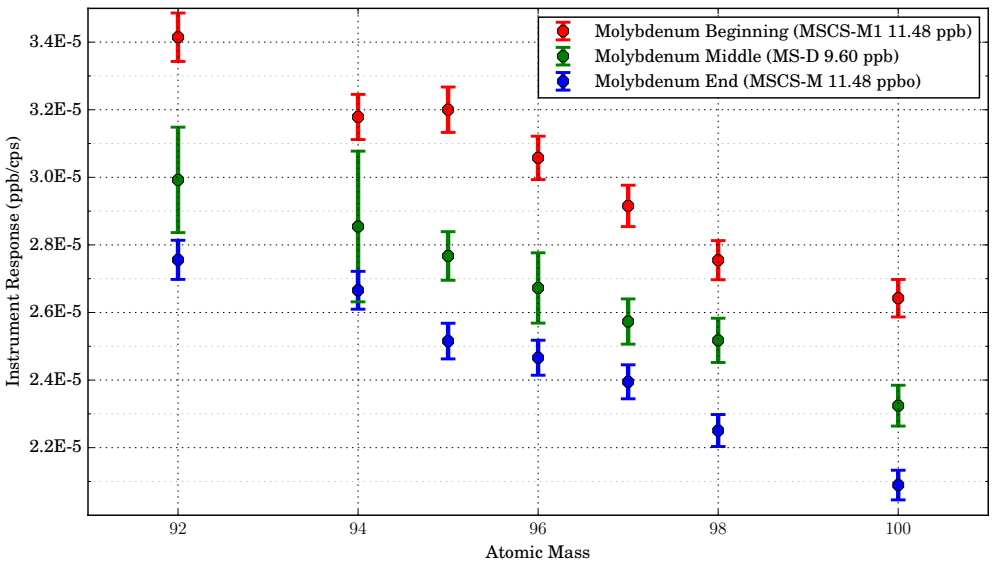

Figure 2.18: Molybdenum calibration curve from three different standards.

the natural abundances of molybdenum isotpes because the instrument response calculation incorporates this value when determining the concentration of an isotope from the standards.

The elements and corresponding isotopes for which instrument responses were determined are shown in Table 2.3. The atomic number is shown next to the element symbol in the first and third columns. Only the stable isotopes with natural mass abundances were determined for all samples except the plutonium sample. Extrapolations from the isotopes listed were utilized to determine response functions for radioactive isotopes.

Mass spectrometry is very sensitive, and therefore sample contamination was quantified for the experiment. This was done by conducting a dry run of the experiment, sampling stock solutions, and leeching the vials used in the experiment. The main background contaminants are listed in Table 2.4 with the average contaminant concentration for the element as a whole listed. To account for contamination for a particular isotope, an av-

Table 2.3: List of determined instrument responses.

Element	Isotopes	Element	Isotopes
$_{37}$Rb	85, 87	$_{51}$Sb	121, 123
$_{38}$Sr	86, 87, 88	$_{52}$Te	120, 122, 123, 124
$_{39}$Y	89		125, 126, 128, 130
$_{40}$Zr	90, 91, 92, 94	$_{56}$Ba	130, 132, 134, 135
	96		136, 137, 138
$_{41}$Nb	93	$_{55}$Cs	133
$_{42}$Mo	92, 94, 95, 96	$_{57}$La	138, 139
	97, 97, 100	$_{58}$Ce	136, 138, 140, 142
$_{44}$Ru	96, 98, 99, 100	$_{60}$Nd	142, 143, 144, 145
	101, 102, 104		146, 148, 150
$_{45}$Rh	103	$_{59}$Pr	141
$_{46}$Pd	102, 104, 105, 106	$_{62}$Sm	144, 147, 148, 149
	108, 110, 104		150, 152, 154
$_{47}$Ag	107, 109	$_{63}$Eu	151, 153
$_{48}$Cd	106, 108, 110, 111	$_{64}$Gd	152, 154, 155, 156
	112, 113, 114, 116		157, 158, 160
$_{49}$In	113, 115	$_{66}$Dy	156, 158, 160
$_{50}$Sn	112, 114-120	$_{94}$Pu	239, 240, 241, 242
	122, 124, 126	$_{92}$U	234, 235, 238

erage contamination was multiplied by a corresponding natural abundance mass fraction and subtracted from the total response for that isotope. Barium had very large and widely varying background contamination which seemed to correlate with the concentrations of nitric acid used and sitting time. Mass bins 136 and 132 should mostly be ^{136}Ba and ^{132}Ba from contamination and not from fission because both isotopes are blocked by stable isotopes of Xe, which was removed from the system. This information was used to make some estimates on barium contamination for a particular sample. Results presented

using this assumption were limited to unprocessed samples due to large potential for errors in samples with lower concentrations. This is will be discussed in later results, but proved to make DC and DF calculations for some isotopes of cesium impossible with mass spectrometry. Some of these isotopes, like ^{134}Cs and ^{137}Cs were determined with gamma spectrometry.

Table 2.4: Contamination concerns for experiment.

	Zn	Sr	Y	Mo	Sn	Ba	Nd
Parts Per Billion	536.0	22.8	1.3	6.2	1.5	392.9	2.3

Evaporation, which leads to a concentration change in the sample during transfer was estimated. Mass transfer as a result of radiolysis was assumed to be negligible because of the low specific activity of the solution (max ~ 80 mCi/L). Each sample was approximately 50 μl encapsulated in a 15 ml volume with an estimated ideal gas equilibrium vapor mass of 177 μg. From these estimates, assuming vials were fully sealed in a dry environment, concentration changes due to evaporation were quantified using the ideal gas law to be an estimated 0.45% loss in volume.

Quantification on sample heating while changing molar concentrations of nitric acid was estimated as well. Density changes were estimated to have a maximum range of 5% for a temperature swing of 80 degrees kelvin. As such, it was assumed that these effects were negligible.

2.3.1.1. Mass spectroscopy Measurements and Analysis

Samples prepared for mass spectrometry measurements were sent to the University of Missouri to be measured by Dr. James McKamey with the PerkinElmer NexION 300X quadruple ICP-MS. Samples included aqueous phases for the stock solution, waste after

extraction, and product solutions. Organic phases were not measured by mass spectrometry because the machine was not designed for organic material. Samples were centrifuged and carefully weighed in preparation for measurements. Some samples were diluted. All samples were measured on the machine five times, and data was averaged over all the measurements. Dr. McKamey provided raw count rate data for the mass bins 66-160, and 231-243 as well as concentration estimates for the actinides.

In order to determine the concentration of a particular isotope, i, in a solution measured by mass spectrometry the count rate was multiplied by the appropriate instrument response, as shown in Equation 2.9.

$$\text{Concentration}\left[\frac{\text{ng}_i}{\text{g of solution}}\right] = \text{CPS}_\text{i} \cdot \text{Instrument response}\left[\frac{\frac{\text{ng}_\text{i}}{\text{g of solution}}}{cps}\right] \tag{2.9}$$

Errors in the initial count rate were determined as described in Appendix B. This appendix also describes generally how errors were propagated through the calculations. Dr. McKamey analyzed the first sample sent on a volume basis because the sample density was very near 1 g/cm^3. All later samples were analyzed on a per gram of solution basis.

All presented results were given in terms of the concentration and total amount of determined species in the original solution of the sample that was sent. For example, if the final back-extraction solution had a volume of 8 ml and 50 μl of this solution was used in mass spectrometry, then the concentration of the back-extraction solution - determined with the 50 μl - would be multiplied by the total mass of the back-extraction solution ($8 \cdot \rho$) for the total mass of species in the back-extraction solution. Further, results were also presented in terms of the total amount in the entire pellet itself (i.e. as if the entire pellet were used). This later calculation was done by dividing the total mass just determined by the fraction of the pellet that the solution represented. This fraction, F, for 0.5 ml of stock

solution is given with Equation 2.10.

$$F = \frac{0.5 \text{ ml of stock processed}}{\text{Initial Volume of Stock (ml)}} \cdot \frac{0.5 \text{ ml of closet diluted}}{\text{Initial Volume of Closet (ml)}} \tag{2.10}$$

F would be the same for 0.5 ml of stock solution as well as the the final product solution that started with 0.5 ml of stock solution because F represents the fraction of the pellet that was processed. The reason results are presented in this manner is to provide a basis for the masses presented in the results. The fraction of error increases from the concentration of a particular isotope to the result which references the total of the closet solution because error propagation includes errors associated with pipetting.

2.3.2. Gamma Spectroscopy

A standard stationary Canberra electrode coaxial High Purity Ge (HPGe) detector as well as a portable Falcon 5000 Canberra detector were used to collect gamma spectra data for the experiment. The HPGe is a semiconductor detector which has the advantage of distinguishing gamma ray peaks at resolutions of ~ 1-3 keV[63]. This ability arises from Ge having a small band gap (0.7 eV) for electrons leaving the valence band to enter the conduction band which leads to a sharper energy resolution, shown by a narrower Full Width at Half Maximum (FWHM) for an energy peak. The small band gap also necessitates the detector being cooled to liquid nitrogen temperatures (77 K) to prevent thermal leakage. High resolution was needed for this project due to the many different gamma energies emitted by irradiated fuel.

A ^{152}Eu source was utilized for energy and efficiency calibrations because this isotope emits a number of gamma rays across a broad range of energies. Table 2.5 shows that ^{152}Eu gamma energies span energies from 46.03 keV to 1408 keV. Calibration across this range of energies is important because the fission products gamma energies of interest are mostly in this range.

Table 2.5: ^{152}Eu gamma energies with yields.

Energy (keV)	Yield (%)
46.03	14.2
121.78	28.6
244.70	7.6
344.28	26.5
367.79	0.9
411.12	2.2
443.97	3.2
688.67	0.9
778.90	12.9
867.38	4.2
964.08	14.6
1005.27	0.6
1085.87	10.2
1089.74	1.7
1112.07	13.6
1212.95	1.4
1299.14	1.6
1408.01	21.0

Energy calibration was done by adjusting the energy scale on the GENIE software to line up with ^{152}Eu gamma energies, and energy-dependent efficiency calibration utilized information about the current activity of the ^{152}Eu source, gamma yields, total number of background corrected registered radiation events at a particular energy and count times. The second was calculated with Equation 2.11, where dead-time corrected counts and yield are for a particular gamma energy, the activity is the decay rate of the ^{152}Eu source at the time of counting, the time corresponds to the total time of data collection, and yield is the absolute yield for the gamma energy of interest. Different methods exist for determining gamma energy peak areas but the non-linear least squares fit built into GENIE's software was utilized to fit the peak and subsequently determine the peak area, which cuts off the

Compton continuum and background.

$$\epsilon(E) = \frac{\text{Counts}(E)}{\text{time} \cdot \text{activity} \cdot \text{yield}(E)} \tag{2.11}$$

In order to ensure the efficiency calibration is useful, the geometry for the calibration standard and sample should be consistent and background radiation levels should be the same. To maintain geometry, a liquid ^{152}Eu source of 1.00568 g, which corresponds to 497.0 nCi, assayed February 15, 2012 was was used and placed in the same centrifuge vial as the samples. This is shown in Figure 2.19. It should be noted that the liquid source does not fill the entire geometry of the vial, introducing some geometric counting error, which is why samples were counted 26 cm away from the detector face. Background radiation levels were minimized by not counting samples when large sources were nearby.

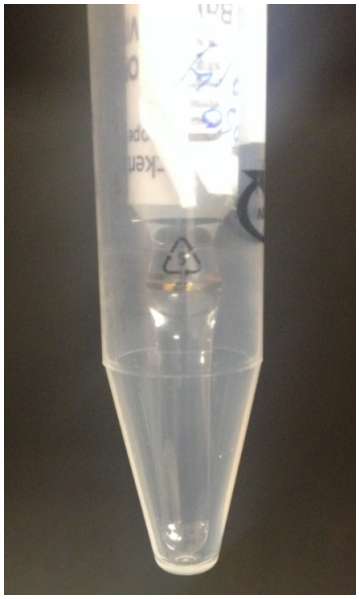

Figure 2.19: ^{152}Eu liquid calibration source in centrifuge tube.

Efficiency calibration utilizes interpolation for energies between those listed for the en-

ergy curve calibration. The interpolation function is a polynomial of the natural logarithm of both efficiency and energy as shown in Equation 2.12,

$$ln(\epsilon) = \sum_{i=1}^{N} a_i (ln(E))^{i-1} \tag{2.12}$$

where a_i are coefficients for the polynomial and N is the order of the polynomial, the value of which is typically set to 4 or 5. There are different methods for determining this fitting function, and a non-penalized least squares method was used in the present work. Excel's and Python's polynomial fitting functions, which yielded similar coefficients, were used for calculations. An example of an efficiency curve utilized is shown in Figure 2.20, with the right most y-axis corresponding to efficiency. Two different polynomial orders are shown on the plot to indicate that the 4^{th} order was preferential because of its better fit and used to determine gamma efficiency.

Two important gamma interactions in an HPGe are Compton scattering and photo-electric absorption. Photo-peaks are resultant from photoelectric absorption, the mass attenuation coefficient, μ/ρ, of which for germanium was plotted with the efficiency curve in Figure 2.20, with its y-axis on the left, to show that the efficiency increases as photon energy decreases due to an increase in photoelectric cross section. The decrease in detector efficiency in energies below 180 keV is not the trend seen in the photoelectric curve in Figure 2.20. The decrease is due to attenuation between the source and the detector volume. Photo-peaks in this area were suspect to some skepticism because few calibration points were recorded in this area.

Error estimates for the gamma spectroscopy assumed Gaussian distributions, and standard error propagation through calculations, as described in Appendix B. The experimental procedure called for numerous gamma spectra to be taken. A program was written to pull and organize peak fitted data for much faster processing of the data. The programs utilized

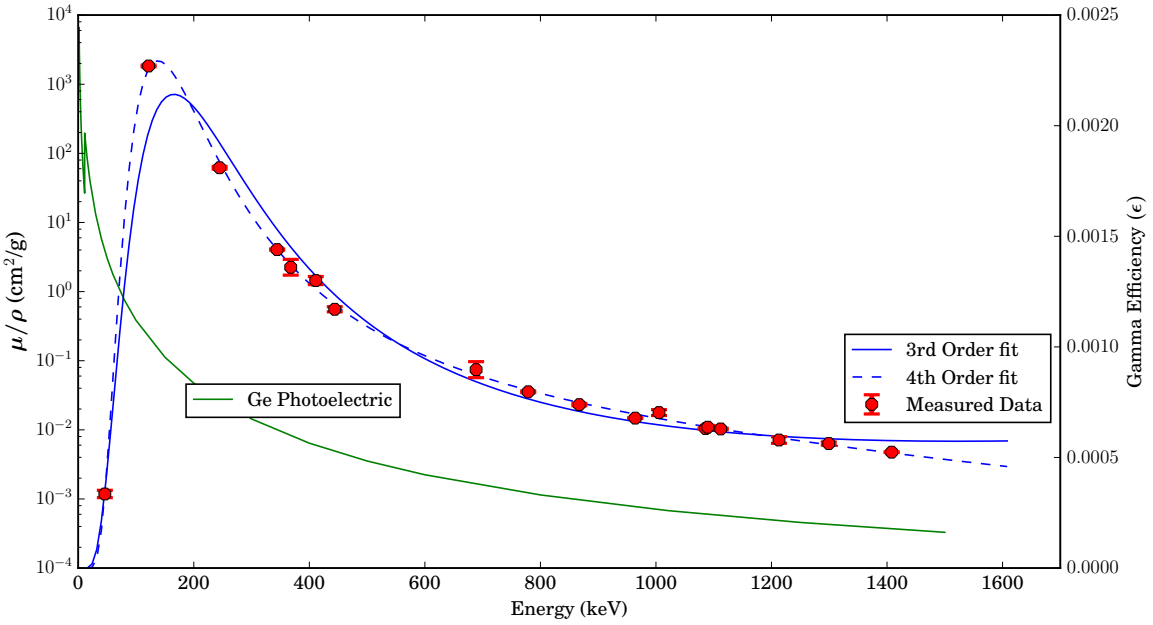

Figure 2.20: HPGe efficiency curve coupled with photoelectric absorption coefficient.

for this are in Appendix E.

2.3.3. Alpha Spectroscopy

A four-peak alpha standard was utilized for energy and efficiency and energy calibration. Energy calibrations have a linear correlation with channel number, and efficiency calibrations should be flat with respect to energy because the alpha efficiency depends on geometry only, and not probability of interaction which is effectively 100%. This is because any alpha particle impacting a detector volume will cause ionizations because of its large charge. The four main alpha emitting nuclides for the calibration source were ^{239}Pu, ^{241}Am, ^{244}Cm, and ^{148}Gd. The calibration source had other alpha emitting nuclides from impurities, and although their effect was small, corrections were made to account for this. Table 2.6 shows the principle alpha decays for each the above listed nuclides.

Energy calibration was done by adjusting the energy scale on the GENIE software

Table 2.6: Four Peak alpha calibration source principle alpha energies.

Isotope	Energy (keV)	Yield (%)
^{148}Gd	3182.787	100.
^{239}Pu	5156.59	73.3
	5144.3	15.1
	5105.5	11.5
^{241}Am	5485.56	84.5
	5442.80	13.0
	5388.23	1.6
^{241}Cm	5804.82	76.4
	5762.70	23.6
	5664	0.022

to line up with above listed energies, and the efficiency calibration utilized information about the current activity of a particular peak, alpha yields, total number of background corrected registered radiation events at a particular energy and count times. The second was calculated with Equation 2.11, which was discussed above.

Figure 2.21 shows the calibration source spectrum. As expected, there are four peaks. The lower energy shoulders for each peak are due to the lower energy, lower yield alphas that most of the radioisotopes emit. Straggling in the source was not an issue because the standard used had a very thin electroplated surface whereby alphas emitted were not attenuated. The vacuum also ensured the alpha particles did not lose energy before they reached the detector. The efficiency was calculated to be around 20.5%, and was used in all calculations.

Alpha samples were initially prepared by filtering precipitated plutonium. The samples had energy smearing such that the energy peaks were unrecognizable. Later alpha samples were prepared by diluting solutions so that the detector received around 3 cps for the most concentrated samples. The detector could resolve a higher count rate, but sample self-

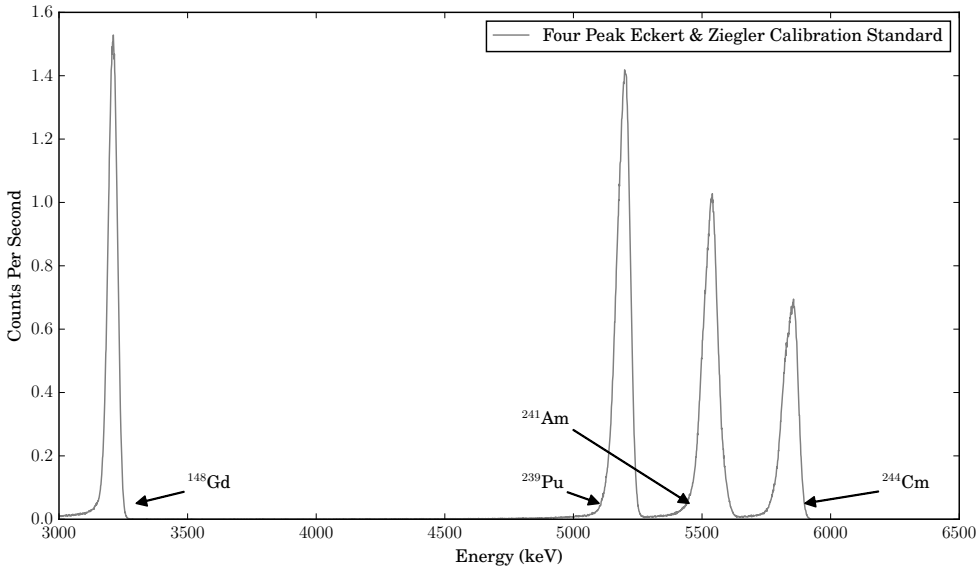

Figure 2.21: Four peak calibration standard.

attenuation became a concern beyond 3 cps. An example spectrum from the later series of experiments is shown in Figure 2.22.

Error estimates for the alpha spectroscopy assumed Gaussian distributions, and standard error propagation through calculations, as described in Appendix B. Some of the alpha calculations had difficult forms of the error propagation and and therefore python's error propagation package 'uncertainties' was utilized in a program that calculated mass. The code is reproduced in Appendix E.

Calibration measurements were shown in this section for alpha and gamma spectroscopy as well as for mass spectrometry as preliminary measurements were needed for the experiments. Preliminary results were also shown for alpha spectroscopy in this chapter to highlight issues with higher count rates for samples that were prepared. This also was a type of calibration for preparing alpha samples. The results for DCs and DFs are presented in Section 3.

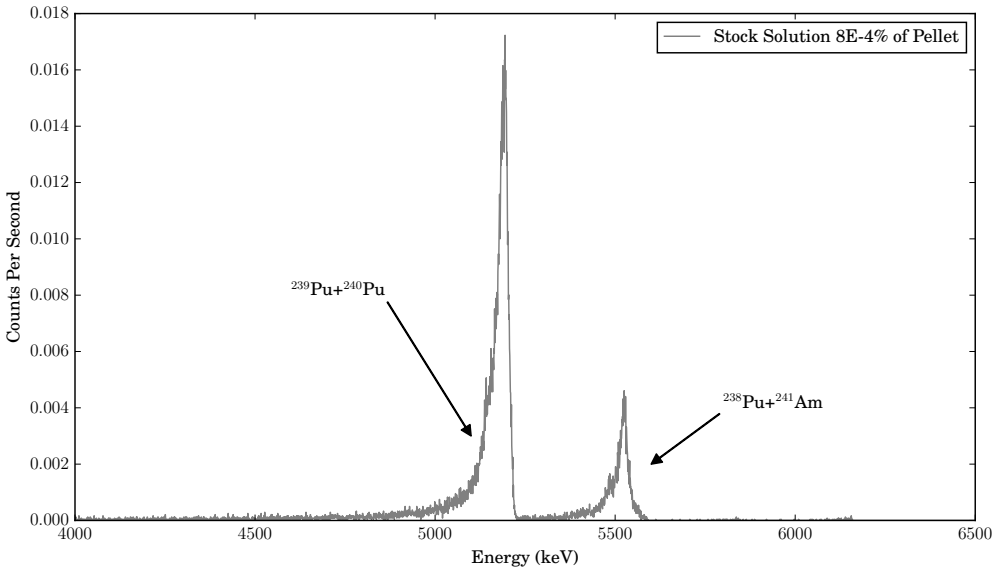

Figure 2.22: Example alpha spectrum from experiment.

3. EXPERIMENTAL DETERMINATION OF FISSION PRODUCT AND ACTINIDE DISTRIBUTION COEFFICIENTS AND DECONTAMINATION FACTORS*

The PUREX experimental procedure followed the general procedures described in section 2.1 and section 2.2. This section will cover 7 different experiments with results and discussion. Results include DC information for extraction/back-extraction, DF values for a specific PUREX process, and characterization of the pellet. Afterwards a mathematical derivation relating DCs to DFs for a 4 extraction 3 back-extraction process will be shown. This relation will be used to determine how well DC values can be used to determine a process DF. Section 5 will use these results in a plutonium source attribution analysis.

3.1. Experiments

Experiments were completed to ensure the PUREX process was conducted correctly. The experiments were designed to answer specific inquiries and the results will reflect the progression towards the final goal of determining elemental DCs and DFs for a PUREX process performed on a neutron irradiated DUO_2 pellet. The description will be ordered as such, with inquiry stated, conditions listed, and results presented.

Each aliquot of stock solution (0.3 - 0.5 ml) was contacted one to four times with TBP and mixed on a vortex mixer for 15 minutes. The two phases of HNO_3 and TBP were allowed to settle and separate either through gravity or with a centrifuge. An example of the settled phases are shown in Figure 3.1.

Pipetting was used to physically separate the two phases into different vials. Although care was taken to keep the two phases separate in the pipetting process, initial experiments had a small carry over of HNO_3 with the TBP. This manifested itself as a small bubble

*Sections 3.2 and 3.3 contain information reprinted with permission from "Fission product decontamination factors for Pu separated by PUREX from low-burnup, fast-neutron irradiated depleted UO_2" by Paul Mendoza, 2016. Applied Radiation and Isotopes, 118, 38 - 42, Copyright 2016 by Elsevier.

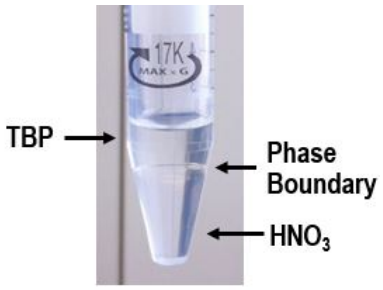

Figure 3.1: HNO_3 and TBP phase separation

(< 50 μl) at the bottom of the TBP collection vial. The next set of experiments used an excess of TBP so that an intermediary between the phases would exist during physical separation. For example, if an aliquot of HNO_3 stock solution was 0.5 ml (~ 1 % of the pellet), and if an excess of 0.2 ml TBP was used as an intermediary, then 0.7 ml of TBP would be initially added to the stock solution and 0.5 ml would be removed for the TBP collection vial. Subsequent contacts would proceed with the addition of 0.5 ml of TBP to keep the overall volume of TBP at 0.7 ml in the mixing solution. In these instances where a process DF value was estimated, it was corrected so that it would be the value for equal contact volumes. The final series of experiments used equal contact volumes with a more detailed separation procedure, which is covered in the laboratory notebook pages provided in Appendix D.

3.1.1. Experiment 1: Plutonium Precipitation

3.1.1.1. Inquiry

In order to verify the existence of plutonium in the sample, plutonium was co-precipitated with NdF_3 and HF and captured on filter paper to be counted via alpha spectroscopy. The mechanism of co-precipitation utilized the low solubility of NdF_3 and PuF_3 in solution.

3.1.1.2. Conditions

Plutonium was first extracted from the 4 M HNO_3 stock solution in order to reduce the presence of fission products in solution. This was done by contacting the HNO_3 with an equal volume of TBP and physically separating the two phases. Fission products are usually in the trivalent state and could therefore co-precipitate with Pu(III), which was not desired. Although alpha particles are much higher energy than the gammas and betas from the fission products and are easily distinguishable, fission products were removed so that while the filter paper dried, less fission products were aerosolized, and less fission products would be subject to vacuum for alpha counting. Less fission products also helps with detector dead time as well as reduced chance of pileup pulses reaching the alpha energy regions.

Back-extraction occurred into an iron sulfamate solution of low acid concentration for the precipitation. About 0.2 μg of $NdCl_3$ was added to solution, which readily disassociated in the aqueous solution. The acid concentration was increased and excess fluorine was added with 1 ml of 2.2 M HF. This caused NdF_3 and PuF_3 to precipitate out of solution. Because HF is a weak acid, mostly staying as HF in solution (K_a=$3.5 \cdot 10^{-4}$). Filtering of the precipitate occurred after 2-3 minutes. The conditions for the experiment are listed in Table 3.1 below.

This co-precipitation experiment included the steps for PUREX, but was conducted before analyzing the steps of PUREX in order to verify the existence of plutonium in the system.

3.1.1.3. Results

A gamma spectrum of the 0.5 $\pm$ 0.05 ml of stock solution was taken and shown in Figure 3.2 with several gamma radiation photo-peaks labeled. The photo-peaks are labeled with the radionuclide as well as the gamma yield for that particular energy peak. Keeping

Table 3.1: Conditions for Experiment 1.

Concentration of Stock	$1.98 \frac{\%\text{ of Pellet}}{\text{ml}} \pm 0.02$ in 3.95 ± 0.13 M HNO_3
Volume of Stock Used	0.5 ± 0.05 ml
Sodium Nitrite Addition	Yes
Extraction Solution	30 ± 0.2 %vol. TBP diluted in kerosene
Times Extracted	4 Extractions collected in a single vial
V_R (Extraction)	1.00 ± 0.01
Volume Back-Extracted	1.5 ± 0.1 ml TBP
Back Extraction Solution	0.134 ± 0.001 M $Fe(NH_2SO_3)_2$
Times Back Extracted	3 Back-Extractions collected in a single vial
V_R (Back-Extraction)	1.00 ± 0.01
Volume Final	4.5 ± 0.045 ml 0.134 M $Fe(NH_2SO_3)_2$
Further Processing	Precipitation with $NdCl_3$ and HF

in mind the fact that the detector efficiency decreases with increasing energy, it should be noted that there should be some correspondence with the height of the peak and the yield. An exception is the ^{154}Eu 723 keV and 756 keV peaks, where the lower yield 756 keV peak is larger than the 723 peak. This particular instance is due to the fact that the much higher specific activity ^{95}Zr also emits gammas at these same two energies[i], but with swapped yield intensities. Later gamma spectra will show these two peaks lining up with their expected relative count rates.

Final precipitated PuF_3 was filtered through filtered paper, dried, and glued to a US penny. An alpha spectra was collected of the sample and is shown in Figure 3.3. Peaks of Pu and Am are clearly seen at slightly depressed energies from their peaks. This spectra has very broad smearing of energies because of attenuation through NdF_3 and through the filter paper. This qualitative analysis proved that plutonium existed in our sample and that it was back-extracted into the product solution.

[i] ^{95}Zr is identified in Figure 3.2 by its lower energy and yield peak 220 keV

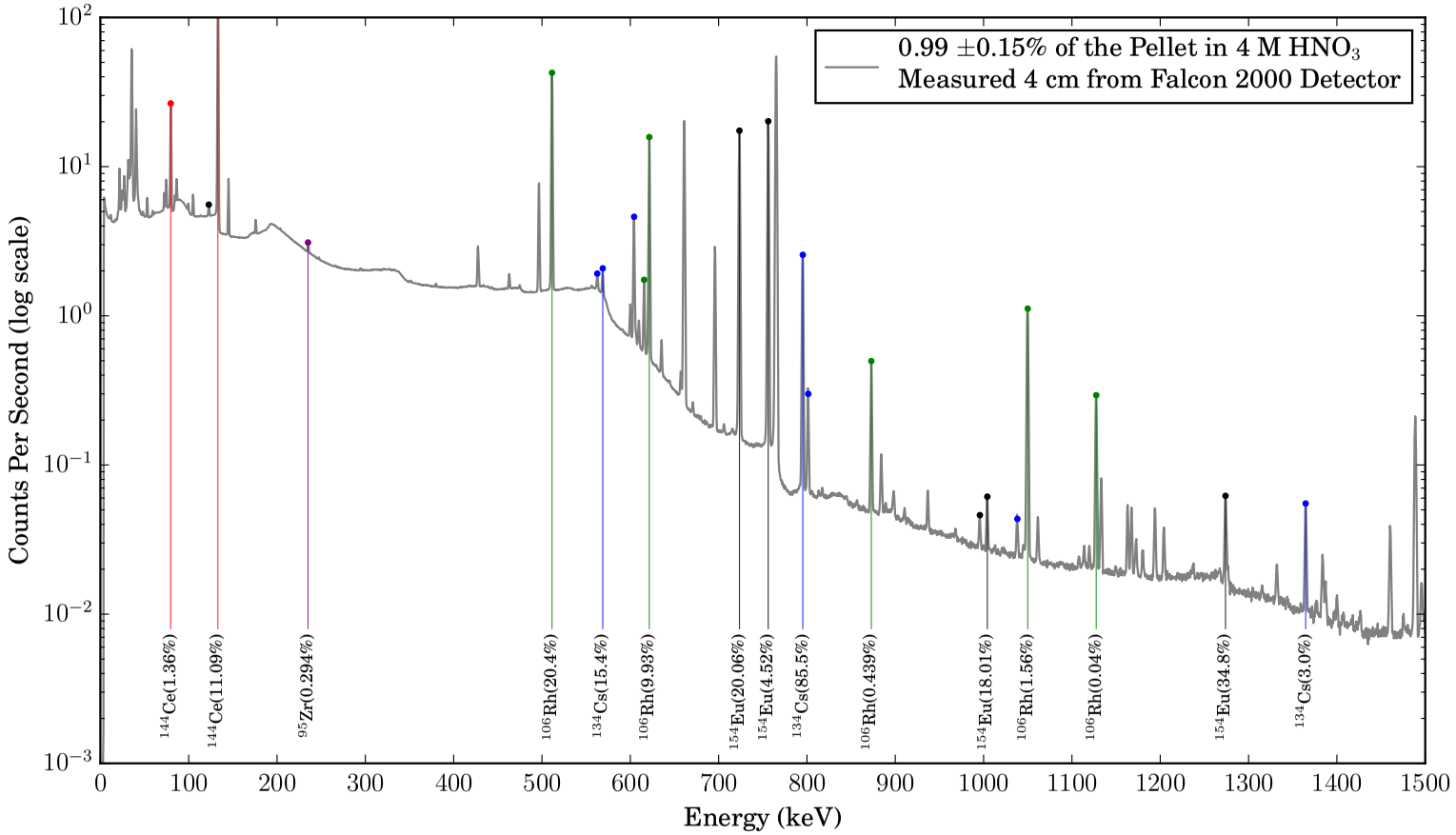

Figure 3.2: Gamma spectrum of stock solution with several peaks identified.

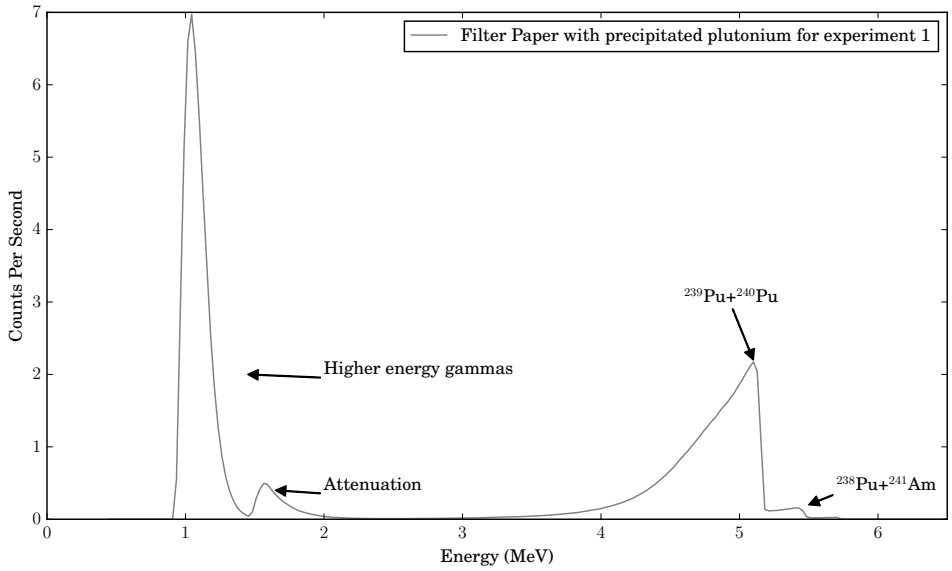

Figure 3.3: Alpha spectrum for precipitation experiment.

3.1.2. Experiment 2: Uranium Plutonium Partition

3.1.2.1. Inquiry

After plutonium was verified as being present and traversing both the extraction and back-extraction steps, partition of uranium and plutonium during the back extraction phase was tested. This was done by analyzing the final combined iron sulfamate solution used for back-extraction. Initial studies did not give indication that the nitric acid concentration of the back-extraction solution should be of any particular value. Therefore the previous experimental conditions were repeated, without precipitating plutonium and the resulting solutions were analyzed using mass spectrometry.

3.1.2.2. Conditions and Results

The concentrations of solutions as well as the procedure for experiment 2 were similar to experiment 1. The two differences were first, an additional back-extraction (4 total)

was completed, and second, Pu was not precipitated out of solution. The final volume of solution sent for ICP-MS was 8.0 $\pm$ 0.08 ml. The final sample was prepared for shipping to the University of Missouri and mass spectrometry analysis was done in the mass range of 234-242 to quantify plutonium and uranium amounts in the final solution. The mass spectrometry procedure as well as how the analysis was completed are described in section 2.3.1. The results for this experiment are shown in Table 3.2, in terms of the concentration of the solution sent, the total nanograms of isotope in the final back-extracted solution and the total mass (mg) that would have been found if the entire pellet solution underwent the same process.

Table 3.2: Mass Spectrometry results for experiment 2.

Isotope	Sample (ng/ml)	Tot mass in Vial Sent (ng)	Total mass if entire solution processed (mg)
^{234}U	$(2.08 \pm 0.31)\times10^{-1}$	$(1.66 \pm 0.25)\times10^{0}$	$(1.68 \pm 0.26)\times10^{-4}$
^{235}U	$(3.72 \pm 0.09)\times10^{1}$	$(2.98 \pm 0.08)\times10^{2}$	$(3.00 \pm 0.20)\times10^{-2}$
^{236}U	$(1.83 \pm 0.27)\times10^{0}$	$(1.46 \pm 0.22)\times10^{1}$	$(1.48 \pm 0.23)\times10^{-3}$
^{237}Np	$(4.39 \pm 0.66)\times10^{-1}$	$(3.51 \pm 0.53)\times10^{0}$	$(3.54 \pm 0.56)\times10^{-4}$
^{238}U	$(1.30 \pm 0.03)\times10^{4}$	$(1.04 \pm 0.03)\times10^{5}$	$(1.05 \pm 0.06)\times10^{1}$
^{239}Pu	$(2.17 \pm 0.06)\times10^{2}$	$(1.74 \pm 0.06)\times10^{3}$	$(1.75 \pm 0.10)\times10^{-1}$
^{240}Pu	$(1.83 \pm 0.06)\times10^{1}$	$(1.46 \pm 0.05)\times10^{2}$	$(1.48 \pm 0.08)\times10^{-2}$
^{241}Pu+^{241}Am	$(6.89 \pm 0.95)\times10^{0}$	$(5.51 \pm 0.76)\times10^{1}$	$(5.60 \pm 0.80)\times10^{-3}$
^{242}Pu	$(3.94 \pm 1.27)\times10^{-1}$	$(3.15 \pm 1.02)\times10^{0}$	$(3.18 \pm 1.00)\times10^{-4}$
^{235}U Part (%)	0.285 ± 0.009	U Total	10.52 ± 0.60
^{239}Pu Part (%)	89.5 ± 3.5	Pu Total	0.196 ± 0.012

Table 3.2 shows that the final combined back-extraction solution contained a large portion of the original uranium present from when the experiment started. This is highlighted at the bottom of the fourth column, where 10.52 mg of uranium would have existed in the

final product if the entire pellet were processed. The macroscopic mass of the pellet was measured to be 12.9 mg, and if 86% of this mass were uranium, then the entire mass of uranium should be around 11.1 mg. This shows that uranium and plutonium were not separated in the uranium/plutonium partition step. Another interesting feature of these results is that the enrichment of uranium is much higher than expected for this sample (0.285% as opposed to 0.22%) and highlighted the need to examine further results to determine how accurate and consistent the reported enrichment of ^{235}U was. This does not affect DC or DFs values for the process employed, but needs to be taken into consideration in the forensic analysis. These results also show that the plutonium enrichment is near weapons-grade at 89.5% ^{239}Pu, which was expected because of the low burn-up irradiation. The total mass of the pellet was 12.9 mg, which means the Pu that would have been back-extracted if the entire pellet was processed would represent around 1.5% of the total mass of the pellet. Given the fact that Pu usually does not constitute more than 1.5% of an irradiated uranium pellet[ii], it can be deduced that a large fraction of the expected plutonium was back-extracted.

A literature review indicated that the nitric acid concentration of the back-extraction solution plays a significant role in the partition between uranium and plutonium during the second step of the process. This is due to the fact that less free NO_3^- in the system during back-extraction pushes uranium equilibrium towards being uncomplexed with TBP. This is why this experiment had a large fraction of uranium in the product solution. This mechanism would also remove plutonium from TBP, which is why there is a larger fraction of Pu in this product solution than in future experiments.

[ii] under low burnup fast neutron irradiations

3.1.3. Experiment 3: Uranium Dry Run

3.1.3.1. Inquiry

In order to increase the partition between uranium and plutonium an experiment was conducted to determine the nitric acid concentration in the iron sulfamate solution necessary to ensure that uranium stays in the organic phase during back extraction. This experiment did not use the closet solution but rather 25 mg of non-irradiated DUO_2 with ^{235}U enrichment of 0.45 $\pm$ 0.05% dissolved in 15 ml of 4 M HNO_3. This solution will be called "Kirrah's solution". The total concentration of uranium in the solution was 1.30E6 $\pm$ 0.03E6 nanograms of uranium per gram of solution. The enrichment and concentration were determined from mass spectrometry.

3.1.3.2. Conditions

The dry run experimental procedure was very similar to Experiments 1 and 2. Two different cases of this experiment were conducted where conditions for both are listed in Table 3.3 on the next page. Both cases started with 0.5 $\pm$ 0.05 ml of Kirrah's solution which was contacted 4 separate times with TBP. The organic to aqueous volume ratio, V_R, for this extraction was 1.00 $\pm$ 0.01 for Case 1 and 1.4 $\pm$ 0.02 for Case 2. The total volume used for extraction was collected in a single vial and was approximately 2.0 ml of TBP for both cases. In Case 1 this vial was partitioned into four different vials each containing 0.5 ml of TBP with the same concentration of uranium, and in Case 2 this vial was used as a whole. Case 1 back-extraction of the four separate equal uranium concentration vials were completed with four different iron sulfamate solutions shown in Table 3.4, one for each vial. Case 2 back-extraction of the single TBP vial was conducted with 0.75 $\pm$ 0.019 M HNO_3 in a 0.0241 $\pm$ 0.0007 Fe(II) solution. The organic to aqueous volume ratio for the back-extraction was 1.00 $\pm$ 0.01 for Case 1 and 0.91 $\pm$ 0.01 for Case 2.

Table 3.3: Conditions for Experiment 3.

Condition	Case 1	Case 2
Concentration of Stock	1.30E6 $\pm$ 0.03E6 ng/g U in 4 M HNO_3	Same
Volume of Stock Used	0.5 $\pm$ 0.05 ml	Same
Sodium Nitrite Addition	Yes	Same
Extraction Solution	30$\pm$ 0.2 %vol. TBP diluted in kerosene	Same
Times Extracted	4 Extractions collected in a single vial	Same
V_R (Extraction)	1.00 $\pm$ 0.01	1.4 $\pm$ 0.02
Volume Back-Extracted	2 ml TBP (in four vials)	2 ml TBP (in one vial)
Back Extraction Solution	**Varied** M HNO_3 in 0.027 $\pm$ 0.004 M $Fe(NH_2SO_3)_2$	0.75 M HNO_3 in 0.0241 M Fe(II) Sol.
Times Back Extracted	4 Separate Back-Extractions collected in different vials	1 Back-Extraction
V_R (Back-Extraction)	1.00 $\pm$ 0.01	0.91 $\pm$ 0.01
Volume Final	2 $\pm$ 0.02 ml Fe solution (Separate Vials)	Same
Further Processing	Mass Spectrometry analysis TAMU campus	Same

3.1.3.3. Results

Results for Experiment 3 utilized mass spectrometry information from the aqueous phases in the experiment. Dilution occurred in 1% HNO_3 with dilution factors ranging from 45 to 2500, with differences due to different expected concentrations of each solution. The uranium standard used for calibration was 1 ppm natural uranium. The results were determined in terms of the fraction of the initial uranium found in the final solution, which is plotted in Figure 3.4, as well as an estimate of the DC value between 30 vol.% TBP and the back-extraction solution. These values are shown in Table 3.4.

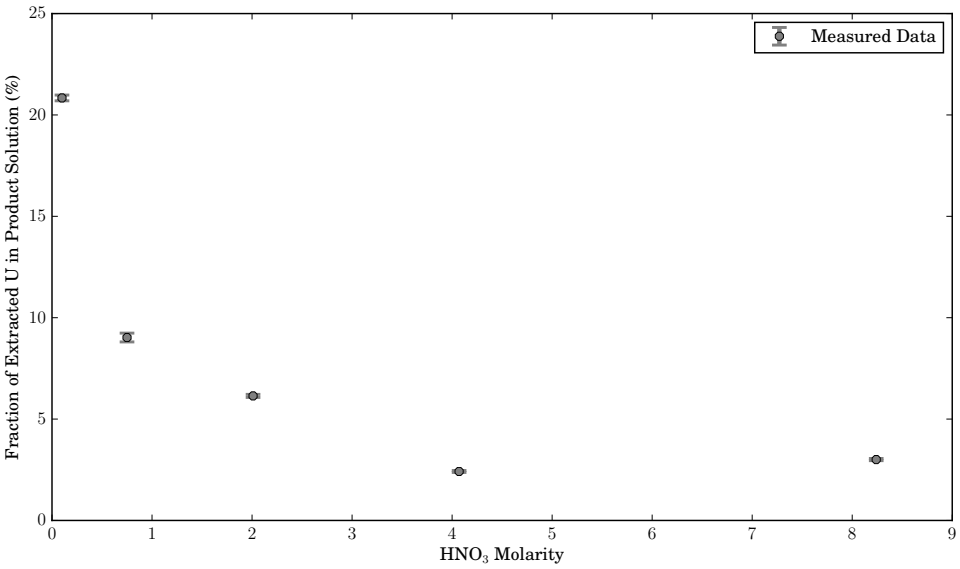

Figure 3.4: Fraction of extracted uranium in back-extracted solution.

Figure 3.4 shows that a minimum of uranium in the product solution occurs when the HNO_3 concentration is approximately 4 M. After this point the excess nitrate reaction with TBP starts to appreciably reduce the free TBP in the system. Based on these results, the

Table 3.4: HNO_3 concentrations for uranium dry run experiment as well DC values for the back-extraction.

Concentration	DC between 30 vol.% TBP and listed solution
8.24 ± 0.13 HNO_3 with 0.0251 ± 0.0013 Fe(II)	32.30 ± 0.12
4.07 ± 0.08 HNO_3 with 0.0248 ± 0.0012 Fe(II)	40.39 ± 0.17
2.01 ± 0.04 HNO_3 with 0.0245 ± 0.0012 Fe(II)	15.28 ± 0.04
0.75 ± 0.02 HNO_3 with 0.0241 ± 0.0010 Fe(II)	10.08 ± 0.05
0.100 ± 0.002 HNO_3 with 0.0242 ± 0.0012 Fe(II)	3.80 ± 0.01

concentration of 4 M HNO_3 was be utilized for the majority of experiments described here because here is where an expected maximum partition between uranium and plutonium would occur. The previous experiment ran into the problem that both uranium and plutonium were in the product solution because less HNO_3 in the system pushes equilibrium towards uncomplexed heavy metals. At this higher concentration of nitric acid, less plutonium would be back-extracted, but the partition between uranium and plutonium would be significantly greater. It should also be noted that the DC values listed in Table 3.4 are higher than the DC for extraction values determined in later experiments. This is due to the fact that there are no other species in solution, the nitric acid is at a higher concentration than later experiments.

3.1.4. Further Experiments

The rest of the experiments were conducted under various conditions and/or procedures. These experiments were focused on determining DC values for extraction/back-extraction and DF values for the process of 4 extractions and 3 back-extractions. A summary of the different experiments is given in the section directly below. This section will comment on why certain experiments were conducted in a specific manner, will provide description on specifics of chemical processing for each experiment, and will detail which

methods of measurement were used (alpha, gamma, or MS). Sections 3.2 and 3.3 will present the DC and DF results and discussions.

3.1.4.1. Summary

Table 3.5 contains a summary of the chemical experiments that were conducted to determine DCs and DFs. The limited processing information available in Table 3.5 specifically highlights volume and stable background contamination corrections for the DF values associated with the process chosen for analysis. The process for which DF values were determined in these experiments was an equal volume 4 extraction, 3 back-extraction experiment, where all extraction and back-extraction volumes are collected in a single vial. This procedure will be called a "mega cycle".

Table 3.5: Table of Experiments conducted.

Experiment	Brief Description	Measurements
Experiment 1	Plutonium Precipitation	Alpha
Experiment 2	Uranium Plutonium Partition	MS, Gamma
Experiment 3	Uranium Dry Run	MS
Experiment 4	Nitrite Test	MS, Gamma
Experiment 5a	Round x3 (volume corrected)	MS, Gamma
Experiment 5b	Round x1 (dry run)	MS
Experiment 5c	Round x3 (separate vials)	MS
Experiment 6	Cs DC characterization	Gamma
Experiment 7	Round x1 (equal volume)	Gamma, Alpha

Experiments 5 and 7 were both used for DF estimates for a mega cycle. Experiment 4 tested the effect of not adding nitrite to the system and provided information about the oxidation state of the plutonium in the stock solution. Experiment 6 was specifically focused on determining the DC value for Cs because Cs has a very high preference for the aqueous phase. All the experiments after Experiment 4 were used to determine DC values.

Several of these experiments were performed in triplicate and values presented from these are averaged over three trials of the same experiment.

To clarify the processing for the mega cycle chosen for DF analysis, Figure 3.5 is provided. In the figure, "Vial A" starts with the aqueous stock solution containing uranium, plutonium and fission products. In this example, an equal volume of organic phase is added to "Vial A". After aqueous and organic phases are mixed and allowed to settle they are physically separated into two separate vials, this can be seen in the second row of Figure 3.5, where the organic phase from "Vial A" is transferred to "Vial B". After this, additional organic phase is added to "Vial A", which starts the second extraction. This organic phase is also transferred to "Vial B", and the third and fourth extraction contacts proceed in a like manner. Figure 3.5 shows the vial situation after three extractions where "Vial B" has three times the volume of "Vial A". The back-extraction procedure is very similar to the extraction procedure and would begin with the final state of "Vial B".

It should be noted that each extraction removes a large fraction of the uranium and plutonium in the aqueous phase and a small portion of the fission products. If the first extraction removed approximately 90% of the heavy metals, and less than 1% of the fission products, then the second extraction would remove approximately 9% of the heavy metals and 1% of the fission products. Thus, each extraction worsens the DF value while more Pu is extracted.

3.1.4.2. Conditions

The conditions for Experiment 4 are shown in Table 3.6. Sodium nitrite was not added to see how much of the plutonium was in the tetravalent oxidation state. According to literature, plutonium most likely existed in our solution as unextractable Pu(III) and extractable Pu(IV). The amount of plutonium that was extracted in this experiment, without the addition of nitrite to increase the oxidation state of Pu(III), showed how much of the

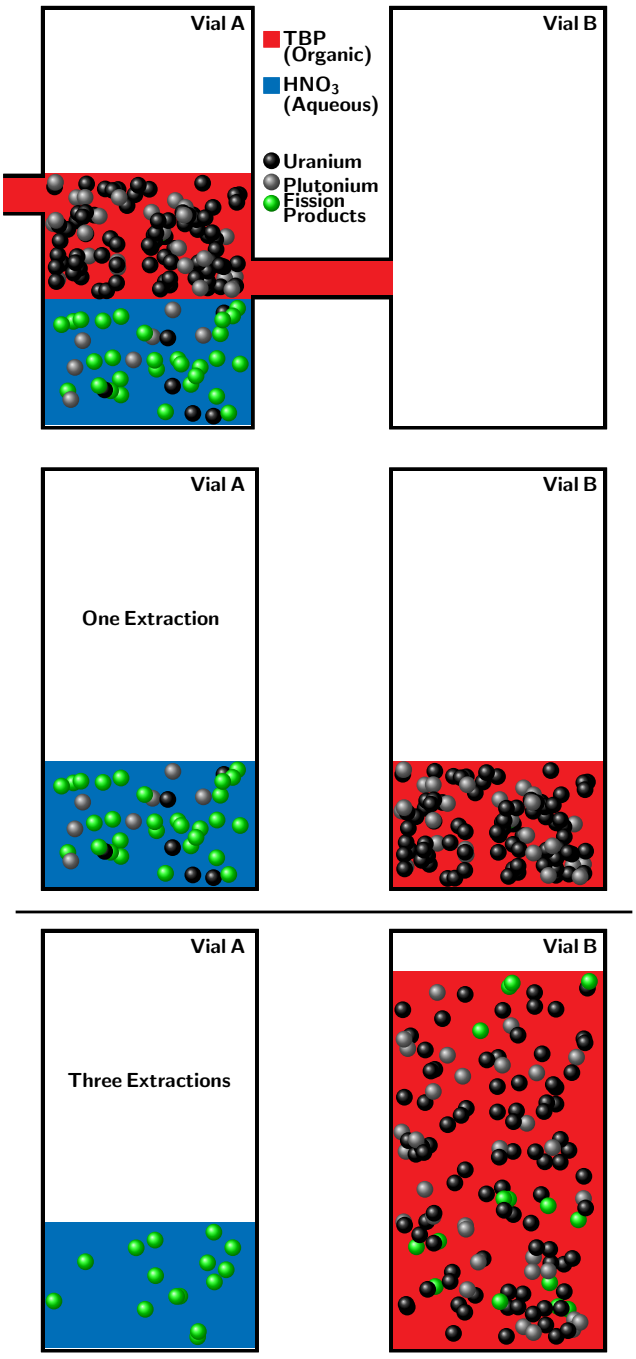

Figure 3.5: Example figure showing three extractions of stock solution

plutonium was Pu(IV).

Table 3.6: Conditions for Experiment 4.

Concentration of Stock	$1.98 \frac{\%\text{ of Pellet}}{\text{ml}} \pm 0.02$ in 3.95 ± 0.13 M HNO_3
Volume of Stock Used	0.50 ± 0.05 ml
Sodium Nitrite Addition	No
Extraction Solution	30 ± 0.2 %vol. TBP diluted in kerosene
Times Extracted	1 Extraction
V_R (Extraction)	1.40 ± 0.02
Volume Back-Extracted	0.50 ± 0.01 ml TBP
Back Extraction Solution	0.75 ± 0.02 M HNO_3 in 0.0241 ± 0.002 M $Fe(NH_2SO_3)_2$
Times Back Extracted	1 Back-Extraction
V_R (Back-Extraction)	1.20 ± 0.02
Volume Final	0.500 ± 0.005 ml
Further Processing	Analysis with MS

Experiment 5 consisted of three different experiments. Table 3.7 has the conditions for Experiment 5a. This experiment was unique in that after an initial mega cycle, the plutonium in the product solution was changed to the tetravalent oxidation state, and another mega cycle ensued. A total of three mega cycle were completed for Experiment 5a. Experiment 5b conditions were very nearly the same except that 4 M HNO_3 was used instead of a pellet solution derivative. This "dry run" was analyzed in the same way as Experiment 5a, and contamination in the system was determined with the results; only a single round was completed for this experiment. Experiment 5c had a very similar procedure as Experiment 5a, even with three separate mega cycles, the major difference was that each solution after extraction was processed separately. This led to many different vials, most of which had very low concentrations, leading to non-reliable results for these experiments.

An exception was uranium, which was the most abundant species in the system. Uranium readings for most of these experiments were provided, and gave many measurements of the enrichment of ^{235}U in the pellet.

Table 3.7: Conditions for Experiment 5.

Concentration of Stock	$2.15 \frac{\%\text{ of Pellet}}{\text{ml}} \pm 0.02$ in 3.95 ± 0.13 M HNO_3
Volume of Stock Used	0.50 ± 0.05 ml
Sodium Nitrite Addition	Yes
Extraction Solution	30 ± 0.2 %vol. TBP diluted in kerosene
Times Extracted	4 Extractions collected in a single vial
V_R (Extraction)	1.40 ± 0.02
Volume Back-Extracted	2.0 ± 0.1 ml TBP
Back Extraction Solution	4.00 ± 0.08 M HNO_3 in 0.0248 ± 0.0012 M $Fe(NH_2SO_3)_2$
Times Back Extracted	3 Back-Extractions collected in a single vial
V_R (Back-Extraction)	0.95 ± 0.013
Volume Final	6 ± 0.03 ml
Further Processing	MS & addition of $NaNO_2$ for next Round

Determining the DC value for Cs was more difficult than for other isotopes. Cesium, which exists as an ion in aqueous solutions, very strongly stays in nitric acid. The DC values for caesium were very low, and therefore Experiment 6 used larger fractions of pellet solution as well as larger fractions of extracting solution to determine more precisely the DC value for this element. There were two different cases for experiment 6, the second of which is described in Table 3.8. The first case had a fourfold increase in volume while the second case had a ten-fold increase in volume.

Experiment 7 had five different cases. Three of which were carried through a full mega cycle with alpha and gamma measurements at every step of the process. Two other cases

Table 3.8: Conditions for Experiment 6.

Concentration of Stock	$6.81 \frac{\%\text{ of Pellet}}{\text{ml}} \pm 0.09$ in 4.00 ± 0.05 M HNO_3
Volume of Stock Used	0.800 ± 0.008 ml
Sodium Nitrite Addition	Yes
Extraction Solution	30$\pm$ 0.2 %vol. TBP diluted in kerosene
Times Extracted	3 Extractions collected in separate vials
V_R (Extraction)	10.00 ± 0.14

were utilized to further measure DC values, but did not complete a full mega cycle. Table 3.9 shows the conditions for three samples of stock solution which were processed through a full mega cycle. Equal volume contacts were utilized in these experiments and results for DC values were fairly straightforward to determine. Small volume losses throughout the experiment were corrected for in the final DF values for the gamma emitting nuclides.

Table 3.9: Conditions for Experiment 7.

Concentration of Stock	$7.15 \frac{\%\text{ of Pellet}}{\text{ml}} \pm 0.10$ in 4.00 ± 0.05 M HNO_3
Volume of Stock Used	0.400 ± 0.008 ml
Sodium Nitrite Addition	Yes
Extraction Solution	30$\pm$ 0.2 %vol. TBP diluted in kerosene
Times Extracted	4 Extractions collected in a single vial
V_R (Extraction)	1.00 ± 0.01
Volume Back-Extracted	~ 900 ml TBP
Back Extraction Solution	4.00 ± 0.05 M HNO_3 in 0.024 ± 0.001 M $Fe(NH_2SO_3)_2$
Times Back Extracted	3 Back-Extractions collected in a single vial
V_R (Back-Extraction)	1.00 ± 0.01
Volume Final	~ 0.600 ml
Further Processing	Alpha and gamma spectroscopy

3.2. Distribution Coefficient Results and Discussion

The DC for the above described experiments were calculated with two different methods. In the first method, which is more straightforward and less prone to experimental error, a ratio of concentrations between the two phases was taken. This was represented in Equation 2.2. For the samples measured by gamma spectroscopy the mass term from Equation 2.2 can be replaced with the radioactivity, A, in each phase. This is shown in Equation 3.1, where the volume is not the total volume used in the extraction, but the volume used to measure the activity.

$$DC = \frac{A_o}{V_o} \cdot \frac{V_{aq}}{A_{aq}} = \frac{V_{aq}}{V_o} \cdot \frac{A_o}{A_{aq}} \tag{3.1}$$

If the counting geometry is the same, and attenuation differences between the two phases are negligible, then the activity in the above equation could be replaced with the count rate in each phase. This was the second method used to determine DC values for the majority of the samples measured by gamma spectroscopy. The cases where this was not done were when the samples were counted in different geometries.

For the samples measured with mass spectrometry and alpha spectrometry, Equation 3.1 will not work because the organic phases could not be adequately measured for either of these methods. For these two methods of measurement Equation 3.2 was used, where f_{aq} is the fraction of the concerned species in the aqueous phase.

$$DC = \frac{V_{aq}}{V_o} \cdot \left(\frac{1}{f_{aq}} - 1 \right) \tag{3.2}$$

Equation 3.2 was derived from Equation 2.2 by conserving mass and by relating the volume-weighted concentration to the mass-weighted concentration by the density of the solution (i.e. $C_{\text{vol}} = \rho C_{\text{mass}}$). The fraction of mass in the aqueous phase after an extraction

can be determined with either concentration type, and because mass spectrometry provides results in terms of the mass ratio, this type was used. The fraction of species in the aqueous phase was determined with the concentration of the species in the aqueous phase initially and the concentration of species in the aqueous phase after extraction, which is shown in Equation 3.3.

$$f_{aq} = \frac{C_{\text{final,aq}}}{C_{\text{initial,aq}}} \tag{3.3}$$

Both methods assume that no mass is lost from the system. This can be easily verified for the gamma measurements, where the initial activity of the aqueous solution before extraction is compared to the activity of both the aqueous and organic solutions after extraction. This relationship is shown in Equation 3.4.

$$A_{\text{initial,aq}} = A_{\text{measured,final,aq}} \cdot \frac{V_{\text{total,aq}}}{V_{\text{measured,aq}}} + A_{\text{measured,final,o}} \cdot \frac{V_{\text{total,o}}}{V_{\text{measured,o}}} \tag{3.4}$$

The relationship is not as straightforward for the mass spectrometric and alpha spectroscopy measurements. A handful of organic alpha samples were prepared for mass balance. This was accomplished by diluting 10 μl of organic phase in 990 μl of very low acidity HNO_3. The fraction of mass in the aqueous phase is given in Equation 3.5 and with the ratio of organic to aqueous volumes just described, 99% of the mass of a species with DC of unity would be transferred to the aqueous phase. If the DC value was 0.1 then 99.9%[iii] of the species would be in the aqueous phase. Alpha spectroscopy was used to analyze plutonium content, and at lower acidities plutonium will not complex with TBP and preferentially stays in the aqueous phase. This means that the DC value for plutonium at a low HNO_3 concentration is much less than unity, and therefore it will be assumed that

[iii] $\frac{1}{1+0.1\cdot\frac{10}{1000}} = 0.999$

all the mass transferred into the aqueous phase.

$$f_{aq} = \frac{1}{1 + DC\frac{V_o}{V_{aq}}} \tag{3.5}$$

3.2.1. Mass Balance

The gamma photo-peaks characterized for these experiments are shown in Figure 3.6. The labeled peaks dictate which gamma energy lines were followed for specific radionuclides. These were used to determine gamma activity which was used for activity balance as well as for determining DC and DF values. Each peak is labeled with a corresponding radionuclide with yields provided. In section 3.1.1 it was mentioned with regard to Figure 3.2 that the ^{154}Eu 723 keV and 756 keV relative peak heights were swapped due to contributions from the short lived ^{95}Zr in both peaks. The spectrum shown in Figure 3.6 was taken after ^{95}Zr had more opportunity to decay and now the ^{154}Eu peaks in the 700 keV region have a more appropriate ratio with respect to their yields. For radionuclides with multiple gamma lines, an average activity was determined.

In order to ensure mass is conserved for a particular extraction or back-extraction, gamma spectra were collected of: the initial aqueous solution, the final aqueous solution, and the final organic solution. The final activity of the system was determined with Equation 3.4 and compared with the initial activity. An example showing the data for this is given in Table 3.10. This table includes decay corrected activities to the date when the sample was first dissolved (5/5/2014). This date was chosen because it was the first day the author started this project. The final activity for most of the radionuclides are fairly close to the initial activity. This is even the case for ^{106}Rh, which is a daughter of ^{106}Ru, because the maximum time to reach secular equilibrium was about 7 minutes. Due to the large number of extraction experiments, the rest of the activity balance tables are provided

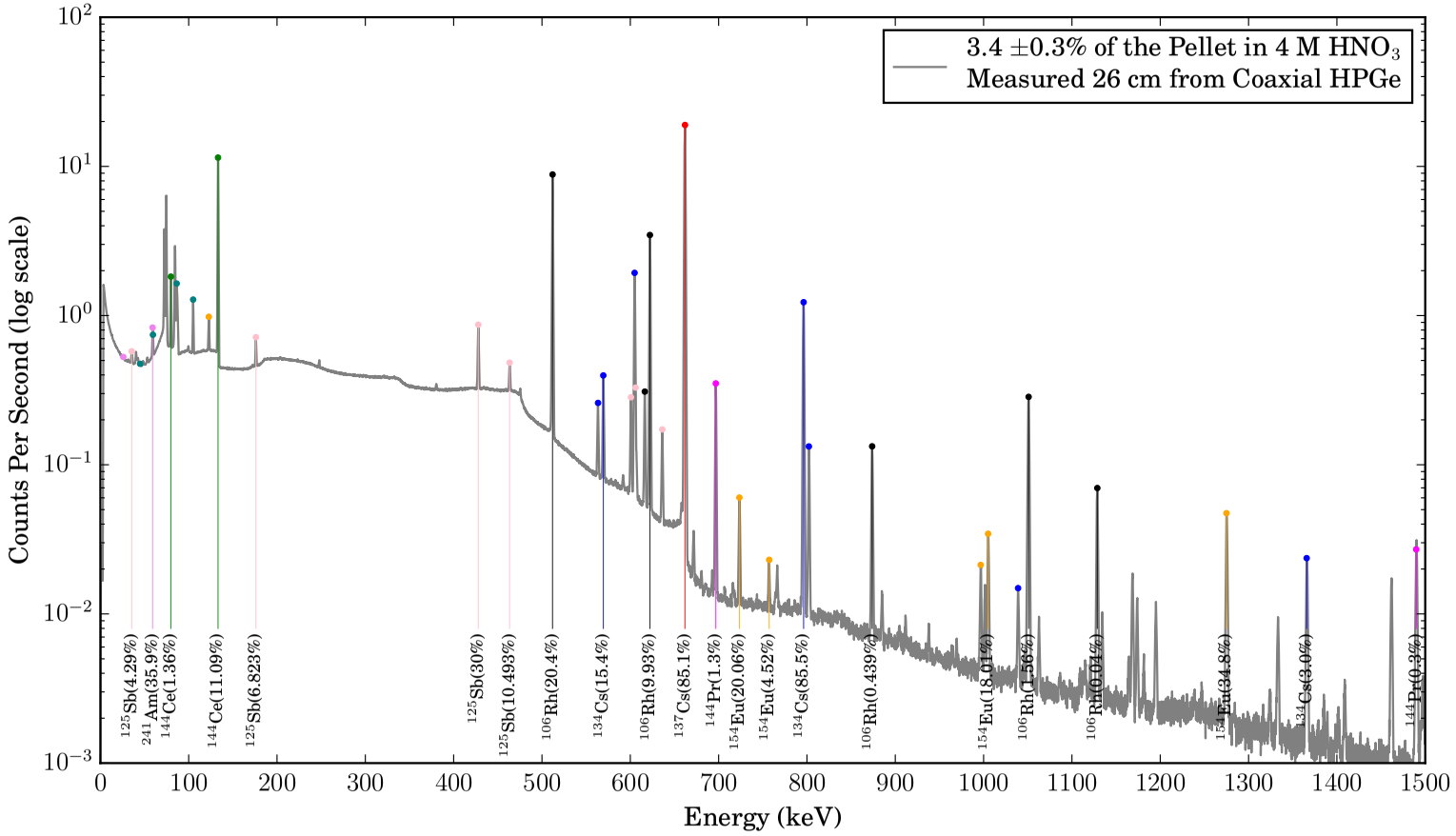

Figure 3.6: Gamma Spectra for Vial 5 with peaks characterized. ^{95}Zr is not labeled because it decayed away by the time these experiments were conducted.

in Appendix F.

Table 3.10: Vial 56 Extraction I Activity Balance

Vial 56 Extraction I	A_{initial} $[\mu Ci]$	$A_{\text{final,aq,m}}$ $[\mu Ci]$	$A_{\text{final,or,m}}$ $[\mu Ci]$
^{155}Eu (105 keV)	0.509 ± 0.013	0.256 ± 0.007	0.2377 ± 0.0058
^{154}Eu	0.121 ± 0.002	0.061 ± 0.001	0.0576 ± 0.0004
^{144}Ce (133 keV)	89.426 ± 1.615	54.424 ± 0.981	32.6828 ± 0.5891
^{125}Sb	0.764 ± 0.007	0.749 ± 0.006	0.0101 ± 0.0008
^{106}Rh	57.071 ± 0.856	41.867 ± 0.613	13.2734 ± 0.2061
^{134}Cs	1.485 ± 0.007	1.477 ± 0.005	0.0010 ± 0.0001
^{137}Cs	9.031 ± 0.050	8.919 ± 0.049	0.0028 ± 0.0002
Activity Units $[\mu Ci]$	$A_{\text{final,tot}}$ $[\mu Ci]$	$\frac{A_{\text{initial}} - A_{\text{final,tot}}}{A_{\text{initial}}}$	Exp. Info.
^{155}Eu (105 keV)	0.499 ± 0.015	0.021 ± 0.039	Decay Corrected To:
^{154}Eu	0.120 ± 0.003	0.014 ± 0.028	5/5/2014
^{144}Ce (133 keV)	88.002 ± 2.711	0.016 ± 0.035	Measured: 11/17/2016
^{125}Sb	0.769 ± 0.033	-0.005 ± 0.044	$V_{aq,tot} = 0.80 \pm 0.02$
^{106}Rh	55.754 ± 1.937	0.023 ± 0.037	$V_{or,tot} = 8.00 \pm 0.08$
^{134}Cs	1.497 ± 0.064	-0.008 ± 0.043	$V_{aq,m} = 7.95 \pm 0.02$
^{137}Cs	9.035 ± 0.386	-0.000 ± 0.043	$V_{aq,m} = 0.79 \pm 0.16$

The alpha activity balance data is given in Table 3.11. The alpha spectroscopy results are presented with results from Experiment 7, where mass balance is shown for the three completed mega cycles. All results have been presented for ^{239}Pu and as if the entire pellet were processed for each of the mega cycles. This means all results were divided by the fraction of the pellet that each experiment worked with. This was done for easy comparison between results. The top half of Table 3.11 shows mass balance for the extraction portion of the mega cycle, and the bottom half shows the mass balance for the

back-extraction portion of the mega cycle. Both extraction and back-extraction for the mega cycle of Experiment 7 combined solutions in the same way as was described earlier in Figure 3.5.

Table 3.11: ^{239}Pu alpha measurements mass balance for three experiments. Values are presented in mg and as if the entire pellet were processed. Each round was completed in parallel, not in sequence.

Description – **All units in mg**	Round 1	Round 2	Round 3
Initial mass	0.175 ± 0.026	0.171 ± 0.025	0.172 ± 0.026
Total Extracted (in Organic)	0.108 ± 0.008	0.104 ± 0.007	0.106 ± 0.007
Total in waste for extraction (Droplets, Phase Boundaries)	0.061 ± 0.013	0.053 ± 0.013	0.054 ± 0.014
Total Mass After Extractions	0.169 ± 0.015	0.156 ± 0.015	0.160 ± 0.015
Final - Initial	-0.006 ± 0.030	-0.015 ± 0.030	-0.012 ± 0.030
Plutonium Mass in Product Solution	0.096 ± 0.008	0.096 ± 0.008	0.114 ± 0.009
Total Waste from Back Extraction (Droplets, Phase Boundaries)	0.016 ± 0.011	0.017 ± 0.011	0.014 ± 0.009
Final Mass in Back Extractions	0.111 ± 0.014	0.113 ± 0.013	0.128 ± 0.013
Final - Initial	0.003 ± 0.016	0.009 ± 0.015	0.022 ± 0.014

The row labeled "Total Mass after Extractions" is the sum total of the mass determined to be in the final combined organic solution (immediately after all extractions) with the mass determined to be lost from sample processing. Sample processing losses were due to liquid droplets falling from pipettes as well as system volume losses from leaving the interface of organic and aqueous unseparated[iv]. The mass of ^{239}Pu in the droplets and interfaces were determined by first determining the volume lost, and then multiplying this value with the mass density of ^{239}Pu of the phase at the point of loss. The first row

[iv]note: Experiment 7 did not use an "intermediary"

labeled “Final - Initial” is the difference between the initial mass of ^{239}Pu in the system and the total mass of ^{239}Pu after all extractions. This value should ideally be zero, and are acceptable as they are within one standard deviation. These values are within the error and consistent with zero with the exception of one measurement.

The second row labeled “Final - Initial” is the difference between the total extracted mass of ^{239}Pu in the combined organic phase (immediately after all extractions), and the row labeled “Final Mass in Back Extractions”. This later row is the sum of the mass in the ^{239}Pu in the product solution and the mass of ^{239}Pu in the estimated losses during back-extraction. These losses are the same as were accounted for previously in the extraction portion of the experiment. The difference between the mass of ^{239}Pu before back-extraction and after back-extraction is within 1 standard deviation for mega cycle 1 and 2. For mega cycle 3 is within two standard deviations.

3.2.2. DC Values

The combined DC results from the experiments are presented in Table 3.12. Values for radioactive species were determined with Experiments 6 and 7, and non radioactive species in Table 3.12 were determined with Experiments 4 and 5 using mass spectrometry. Results that were derived from mass spectrometry are distinguished by an asterisk. Values have been averaged over the different measurements for these values with the error provided as the standard deviation for the measurements.

These DC values apply to equilibrium concentrations of species between 4 M HNO_3 and 30 vol.% TBP diluted in kerosene with a uranium saturation of less than 0.1%. There is a wide range of values in Table 3.12 because different elements chemically interact differently in the system. The large values for uranium and plutonium are attributed to their affinity towards making neutral complexes with TBP. Americium’s most stable oxidation state is the trivalent, which is not as easily extracted.

Table 3.12: Average DC values determined from Experiments 4, 6 and 7. These DC values apply to equilibrium concentrations of species between 4 M HNO_3 and 30 vol.% TBP diluted in kerosene with a uranium saturation of less than 0.1%

Isotope	DC value
^{239,240}Pu*	16 ± 2
^{235,238}U*	37 ± 5
^{241}Am	0.048 ± 0.007
^{153}Eu*	0.108 ± 0.032
^{154}Eu	0.075 ± 0.014
^{155}Eu	0.081 ± 0.010
^{149,151,152,154}Sm*	0.097 ± 0.029
^{147}Pm*	0.090 ± 0.013
^{143,145,146,148,150}Nd*	0.079 ± 0.012
^{144}Ce	0.035 ± 0.007
^{137}Cs	$4.6E{-}5 \pm 4.8E{-}5$
^{134}Cs	$3.9E{-}4 \pm 3.0E{-}4$
^{125}Sb	0.002 ± 0.001
^{106}Rh (Ru)	0.028 ± 0.011
^{101,102,104}Ru*	0.209 ± 0.032
^{97,98,100}Mo	0.046 ± 0.019

The lanthanides (Eu-Ce), have a decreasing DC trend as the atomic number decreases. This is attributable to the lanthanides contraction, where as the lanthenide's atomic number increases, the ionic radii decreases, thereby increasing the charge density, and increasing preference towards neutral complexes. Cesium has a very low DC value because of its low charge density. It exists as monovalent ion in solution, and preferentially stays in the aqueous phase. Cesium also has a very low electronegativity and cannot attract negative ions easily.

Two very different values for ruthenium are shown in Table 3.12. The first listed was determined with the radioactive daughter ^{106}Rh from Experiments 6 and 7, and the sec-

ond was determined with three isotopes of stable ruthenium with mass spectrometry from Experiment 4. Both values are believed to to be accurate for the experiments that were conducted. The reason for the difference is because ruthenium has several odd and even oxidation states with similar chemical potentials. The stock solution processed for Experiment 4 was drawn from the closet solution several months before the stock solution processed for Experiments 6 and 7. It was noticed that the closet solution drawn for Experiments 6 and 7 had a much yellower tint than for Experiment 4. This is due to decomposition into oxides of nitrogen[64], which could potentially reduce the system as a whole. The fact that the system changed from Experiment 4 to Experiments 6 and 7 will be much more evident when plutonium extraction is discussed in the next section.

3.3. Decontamination Factors Results and Discussion

Uranium and plutonium recovery in the product solution after back-extraction for Experiments 4, 5 and 7 are shown in Table 3.13. Experiments 5 and 7 completed what was called a mega cycle, which was defined in section 3.1.4.

Table 3.13: ^{239}Pu recovery (in percent) for Experiments 4, 5, 6 and 7. Experiment 5 Round 1 and 2 were performed in series, while Experiment 7 Rounds 1, 2, and 3 were performed in parallel.

Description	Pu Recovery %	U Recovery %
Experiment 4	83.4 ± 9.5	11.2 ± 1.3
Experiment 5a Round 1 (Series)	99.7 ± 4.2	6.8 ± 0.3
Experiment 5a Round 2 (Series)	93.0 ± 4.6	6.6 ± 0.3
Overall Experiment 5a	92.7 ± 6.0	0.5 ± 0.0
Experiment 7 Round 1 (Parallel)	63.7 ± 12.2	
Experiment 7 Round 2 (Parallel)	66.1 ± 12.5	
Experiment 7 Round 3 (Parallel)	73.9 ± 13.2	

Experiment 4 had approximately 10% of the U in the TBP phase back-extracted with a single contact of a 0.024 M iron sulfamate in 0.75 M HNO_3 solution. Experiment 5a successfully recovered approximately 93% of the original plutonium with less than 1% of the original uranium remaining. Even though Experiment 4 utilized only a single extraction and back-extraction, a much larger fraction of uranium was in the product solution. This is due to the higher concentration of HNO_3 in the back-extraction solution[4]. The higher molar concentration of HNO_3 helped with mitigating uranium back-extraction, but hindered plutonium back-extraction in mega cycle 2 of Experiment 5a. This is because the ferrous ion is unstable with higher levels of nitric acid[48]. The half-life of the ferrous ion in the back-extraction solution of Experiment 5a was estimated to be approximately 4 days[v]. The effect is shown in the differences in Pu recovery between Round 1 and Round 2 of Experiment 5a. This effect is expected to be small for the FPs because of their strong preference for the aqueous phase (low DCs).

A major difference between Experiment 7 and Experiment 5a is the re-making of the iron sulfamate solution right before back-extraction. This reduces the time available for the oxidation of Fe(II) with HNO_2[vi]. Despite this modification, Experiment 7 had much lower recoveries of plutonium. It appears that Pu(IV) had been reduced to Pu(III) over the course of time. This could be through disproportionation, increased concentrations of oxides of nitrogen, or some other means. Although sodium nitrite was added to the system for Experiment 7 - to transfer plutonium to the tetravalent oxidation state - a large fraction of the plutonium remained in the Pu(III) oxidation state. Further experiments revealed that heating the solution in addition to adding sodium nitrite helps plutonium transition to Pu(IV). Further experiments also have similar values for DCs of the other elements, and therefore this change should not affect most elements.

[v] Estimation used extrapolation on tabulated data in [48]

[vi] See chemical equation R.2.9

DF results are presented in Table 3.14. This table organizes the elements based on their position in the periodic table to better see trends among the elements. Isotopes with asterisks indicate that mass spectrometry was used, and elements without an asterisk indicate that gamma spectrometry was used for analysis. Experiments 4 and 5a utilized mass spectrometry while Experiment 7 utilized gamma spectroscopy. The DF calculations utilized concentration ratios between contaminants that were normalized to the Pu concentration per Equation 2.5, with the initial solution being the stock solution and the final solution being the back-extracted Pu solution. Experiment 4's extraction/back-extraction as well as Experiment 5a's and 7 first mega cycle DF values are shown in Table 3.14. FPs of interest were selected based on our previous publication[5] with additions of Mo, Ru, Pd, Cd, and Ce. ^{237}Np and ^{241}Am were not considered due to their low forensic value in this case. ^{99}Tc was also not considered due to its low forensic value and difficulty of assaying the low-intensity photons produced by this nuclide. Round 2 of Experiment 5a is not shown because the data were below background for these samples, which was generally less than 1 ppb. The low DF values reported were expected due to the reasons described above: the extraction and back-extraction were performed without intermittent scrubbing, and the number of stages was low.

The common trend is that DF decreases from Experiment 4 to Experiment 5a. The major exception is U, which has a higher DF value. This is expected due to the change in HNO_3 concentration in the iron sulfamate solution, where higher concentrations of HNO_3 reduce the degree of U back-extraction, as mentioned above. The rest of the elements have lower DF values because of the four extraction and three back-extraction steps in mega cycle 1 of Experiment 5a compared to one extraction and one back extraction in Experiment 4. This is illustrated in Figure 3.7, where theoretical DFs as a function of extraction step and volume ratio for a product with a DC of 10 and a contaminant with a DC of 0.1 are shown. Higher numbers of contacts decrease DF because less and less

Table 3.14: Decontamination factors for Experiments 4,5a, and 7. Decontamination is with reference to ^{239}Pu. Isotopes with asterisks indicate that mass spectrometry was used, and elements without an asterisk indicate that gamma spectrometry was used for analysis. Experiments 4 and 5a utilized mass spectrometry while Experiment 7 utilized gamma spectroscopy.

Isotopes Used	Experiment 4	Experiment 5a	Experiment 7 (Average)
Heavy Metal			
$^{238}_{92}$U*	6.8 ± 0.5	15.1 ± 0.6	
Alkali Metals			
$^{85}_{37}$Rb*	32.0 ± 1.6	1.8 ± 0.3	
$^{134,137}_{55}$Cs $^{133}_{55}$Cs*	146 ± 8	11.9 ± 1.0	785 ±491
Alkaline Earth Metals			
$^{90}_{38}$Sr*	234 ± 13	38.3 ± 5.9	
$^{138}_{56}$Ba*	344 ±200	0.4 ± 50.0	
Transition Metals/Post Transition Metals			
$^{97,98,100}_{42}$Mo*	5.7 ± 0.8	1.9 ± 0.2	
$^{106}_{44}$Ru $^{101,102,104}_{44}$Ru*	59.2 ± 6.4	16.6 ± 2.5	8.2 ± 0.9
$^{110}_{46}$Pd*	65.0 ± 14.0	8.9 ± 1.2	
$^{111,112,114}_{48}$Cd*	48.2 ± 20.7	4.5 ± 1.7	
$^{117,118,119,122}_{50}$Sn*	57.3 ± 39.9	6.1 ± 5.2	
Lanthanides			
$^{144}_{58}$Ce $^{140,142}_{58}$Ce*	43.0 ± 16.0	11.5 ± 4.9	6.4 ± 2.3
$^{143}_{60}$Nd*	19.2 ± 2.1	5.9 ± 0.4	
$^{147}_{61}$Pm*	12.8 ± 1.9	3.9 ± 0.3	
$^{151}_{62}$Sm*	11.5 ± 1.5	3.6 ± 0.3	
$^{154,155}_{63}$Eu $^{153}_{63}$Eu*	8.4 ± 0.5	3.6 ± 0.3	3.2 ± 0.9

product is extracted with each step, while the contaminant extraction increases linearly with each step. Experiment 5a DF values decrease relative to experiment 4 DF values because of the same reason.

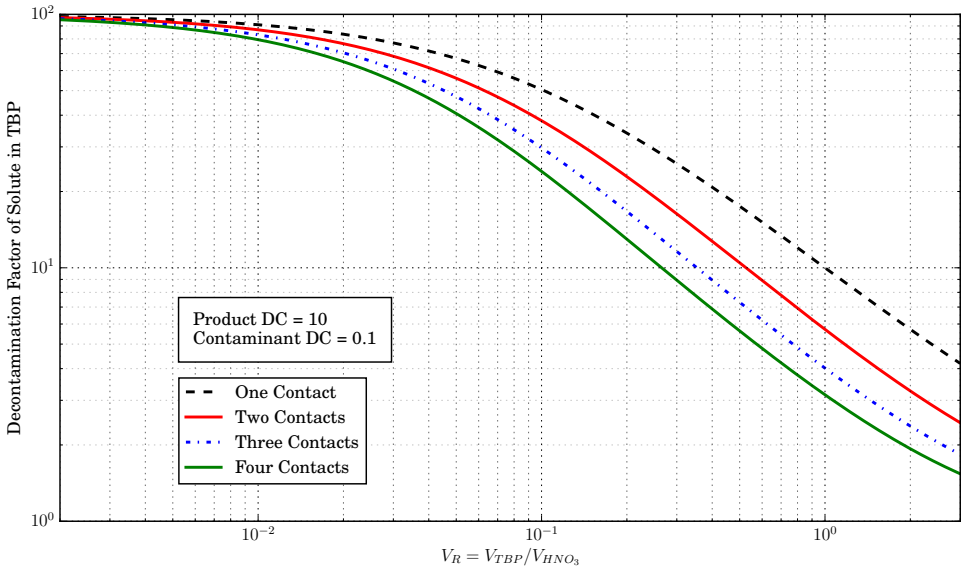

Figure 3.7: DFs as a function of volume ratios for the first to fourth contact in TBP.

Experiment 7 was limited in that only gamma and alpha measurements were available for analysis. A major difference between the two experiments which were analyzed by mass spectrometry and this experiment is the cesium. Ideally, both Experiments 5a and 7 should have similar DFs[vii], but here, the numbers are very significantly different. This large difference was the reason Experiment 6 was conducted.

As a reminder, Experiment 6 had a much larger value for V_R than for all the other experiments. Where most experiments utilized a V_R value near unity, Experiment 6 utilized a V_R value of 10. This means that there was 10 times more volume of organic than aqueous in a given extraction. This large difference in contact volumes is better suited to characterize elements which have a strong preference for a particular phase because more activity is extracted. Experiment 6 confirmed that the cesium DC value should be approximately

[vii]The DFs should not be exact because each experiment had slight differences in process, which will produce differences in final DF values

$3 \cdot 10^{-5}$. This is in agreement with Experiment 7, but not with Experiments 4 and 5a.

The discrepancy could be because of the following reason. If a very small amount of aqueous phase, approximately 6 μl, which is approximately 10% of a drop, contaminated the organic phase during the extraction step of Experiments 4 and 5a. This small amount of cross contamination would not affect other elemental DF or DC results significantly, because the other elements do not have as small of a DC value, but could and probably did change the cesium value by a large portion. Experiments 4 and 5 utilized a notably different experimental procedure than Experiments 6 and 7. The later procedure can be seen in Appendix D, and was specifically designed to ensure cross contamination was not an issue.

The error for experiment 7 was determined by taking a standard deviation of the triplicate experiments, which is a type of top-down uncertainty approach. This is contrasted with how experiments 4 and 5a calculated uncertainty, where errors were determined from a bottom-up approach of error propagation from instrument measurements. The bottom-up approach starts with the measured data and propagates the uncertainty in calculated results. A common problem for uncertainty measurements is what is called "dark uncertainty"[65] whereby measurements from a top-down approach, although they should have lower uncertainty estimates due to unaccounted bias[viii], tend to have a larger uncertainty than bottom up approaches. Although the measurements from experiment 7 are of different realizations of the same process, and might not qualify as top-down in the sense of measurements of the same sample, they do qualify to calculate estimates on the standard deviation of "reproducible" results, and could similarly be subject to larger errors than bottom-up error estimates. This is potentially a reason why experiment 7 errors are much larger than those from experiments 4 and 5a.

[viii] if bias were included then their uncertainty would be higher

3.4. Pellet Characterization

The previous results can be used to characterize the contents of the original neutron irradiated UO_2 uranium pellet. This will provide a very useful starting point for the forensic analysis because calculations will utilize these concentrations. The amount of uranium, plutonium, and fission products in the system should be determined for pellet characterization and further, forensic analysis.

The plutonium composition was taken from the mass spectrometry and alpha spectroscopy results. Uranium composition was determined from mass spectrometry results. The mass spectrometry results report an enrichment of 0.28 wt% ^{235}U, when the pellet started irradiation at 0.26 wt% and was expected to have a final post-irradiation enrichment of 0.22 wt%[66]. This large difference from the expected enrichment of the uranium fuel is assumed to come from contamination, which presumably occurred during the dissolution, and the determination thereof is described in section 3.4.1 below.

The next part of the fuel pellet that was characterized was the fission product concentration. It would be very difficult to precisely measure all the different fission products in the system. To estimate the total mass of fission products in the pellet, ^{137}Cs was used with its fission yield and an average fission product molar mass. This characterization is shown in section 3.4.2. The oxygen component of the pellet will be determined by subtracting the plutonium, uranium, and fission product masses from the original pellet. The oxygen component should represent around 12% of the total mass of the pellet.

3.4.1. Determination of U Contamination in Sample

Three reasons to believe that the closet solution has uranium contamination are as follows: first, the total mass of uranium determined with mass spectrometry is larger than would be expected for 12.9 mg of DUO_2, second, the enrichment of ^{235}U in the uranium should have been around 0.22%, when the mass spectrometry results report a value of

0.28%. Third, another student made measurements on another machine, with different calibration results and got an enrichment of 0.28% as well.

It should be first established that the enrichment estimates from mass spectrometry can be trusted, probably more than any other measurement taken. In order to defend this claim, the following is provided.

First, ^{235}U mass enrichment is defined as shown in Equation 3.6, where m is the mass of the subscripted species.

$$\epsilon_{235} = \frac{m_{235}}{m_{234} + m_{235} + m_{236} + m_{238}} \tag{3.6}$$

Although this definition is the most intuitive means for determining ^{235}U enrichment, mass spectrometry reports results in terms of concentrations, and therefore Equation 3.7 is provided, where c is the per unit mass or per unit volume concentration results that mass spectrometry provides. In the case of Equation 3.7, c is in units of mass per unit volume because it is multiplied by the volume, V to get to the same quantity as in Equation 3.6.

$$\epsilon_{235} = \frac{c_{235} \cdot V}{c_{234}V + c_{235}V + c_{236}V + c_{238}V} \tag{3.7}$$

The volume term can cancel, and we are left with enrichment solely as a function of concentration. This is important because the enrichment calculation will not vary with dilution or concentration of a solution, because either event affects all concentrations by the same amount. Volume independence is useful because if there were lost volume, or even mass of material, the enrichment calculation is not affected. This means errors in ^{235}U enrichment are only as good as how well the concentration can be determined.

To delve deeper, the means for determining the concentration of a solution is provided in Equation 3.8, where the detector registered counts per second for a given mass bin is given by CPS, and the conversion between CPS and concentration is provided in the

"Instrument Response" term.

$$c_i = \text{CPS} \cdot \text{Instrument Response}_i \tag{3.8}$$

Errors in the concentration term could derive from either of the terms in Equation 3.8. For the first term, the CPS could be low, and therefore statistics for estimated values would not be very good or there could be mass interferences that erroneously increase the number of counts a detector registers for a given mass bin. The solution for poor statistics is longer counting times, but uranium, the most abundant species in the pellet, provided enough counts so that statistical error was not an issue. Mass interferences for ^{235}U and ^{238}U, the most abundant isotopes for uranium, are ^{235}Np and ^{238}Pu. Both these interferences are probably in the solution in some capacity, but are in very low quantity, especially the ^{235}Np, which does not have an easy production path[ix]. Of the two, ^{238}Pu, has a direct production path in neutron irradiation (^{239}Pu(n,2n)^{238}Pu) [x], and probably is in higher abundance, which would decrease the ^{235}U enrichment, not increase it.

3.4.1.1. Hydride Formation

Another error that could affect the number of counts per second a detector receives is hydride formation. The following is a short discussion on why hydride formation is first, not occurring in any appreciable quantity, and second, because its not occurring in an appreciable quantity, why it does not change the ^{235}U enrichment measurement. The basic assumption behind the following is that hydride formation is a chemical phenomenon that has equal probability of occurring among all isotopes of uranium. If this is not the case, then hydride formation should be considered for uranium enrichment because its separa-

[ix] The only isotopes that decay to ^{235}Np are ^{239}Am and ^{235}Pu. Another production path is neutron capture on ^{234}Np. All isotopes of which are in very small quantity.

[x] there is another production path for ^{238}Pu for longer irradiations

tion factor would be approximately 1.3[xi], whereas centrifuges have separation factors of approximately 1.15[67].

Before contending for the above two points, it should be mentioned why hydride formation could be an issue. If uranium atoms are forming hydrides while being measured by ICP-MS, then the mass of some of the uranium atoms will be measured incorrectly. The hydrides containing ^{235}U will be measured in the 236 mass bin and the hydrides containing ^{238}U will be measured in the 239 bin. The issue lies in the fact that the 236 mass is still considered with the other uranium isotopes while the 239 mass is attributed to ^{239}Pu. There is a loss in the amount of ^{238}U in the system and therefore the enrichment of ^{235}U is erroneously high.

An approach for seeing why hydride formation is not the culprit in our ^{235}U enrichment discrepancy is to calculate what fraction of the uranium would have to hydride in order to get an enrichment change from 0.22% to 0.285%. To do this, we can write the measured ICP-MS enrichment, ϵ_m, as a function of the actual ^{235}U enrichment, ϵ_5, and the fraction of the uranium that underwent hydration, p, as given in Equation 3.9.

$$\epsilon_m = \frac{\epsilon_4 p + \epsilon_5(1-p)}{\epsilon_4 + \epsilon_5 + (\epsilon_6 + \epsilon_8)(1-p)} \tag{3.9}$$

where:

Actual quantities (all except ϵ_m) come from MCNP simulation[66]

$\epsilon_m = 0.00285$

$\epsilon_4 = 0.000009$

$\epsilon_5 = 0.00224$

$\epsilon_6 = 0.0001$

[xi] 0.285/0.22

$\epsilon_8 = 0.9976$

Note that ^{234}U mass contributes towards increasing the ^{235}U enrichment and its total is included in the denominator because both mass bins 234 and 235 are considered to be uranium. Similarly, the total contribution from ^{235}U is included in the denominator because 235 and 236 mass bins are considered to be uranium. For ^{236}U and ^{238}U the hydrides fitting into the mass bins 237 and 239 are not considered to be uranium and therefore the fraction that did not form a hydride is in the denominator. Solving for p in Equation 3.9 yields Equation 3.10

$$p = \frac{\epsilon_m - \epsilon_5}{\epsilon_m(\epsilon_6 + \epsilon_8) + \epsilon_4 - \epsilon_5} \tag{3.10}$$

The fraction of hydration that would need to occur in order for the enrichment measurement to shift from 0.22% to 0.285%, according to Equation 3.10 and the inputs given above, would be 99.6%. If 99% of the uranium hydrided and was measured in the wrong mass bin, then the majority of the sample would have been recognized as ^{239}Pu, which was not the case.

It might be tempting to state that hydride formation is a contributor for part of ^{235}U enrichment discrepancy. In order to show why this is probably not the case, Figure 3.8 is provided. Where the fraction of hydration, as calculated with Equation 3.10 is plotted against potential ϵ_m values. Figure 3.8 shows that the in order for any appreciable change in ^{235}U enrichment, a large fraction of the uranium would have to form hydrides.

3.4.1.2. Instrument Response Errors

Errors in the instrument response of Equation 3.8 are possible. First, the instrument response could have been calculated incorrectly. The instrument response could have shifted, or the samples measured were outside the scope of the calibration used to determine the instrument response. In response to incorrect calculation of instrument response, two sep-

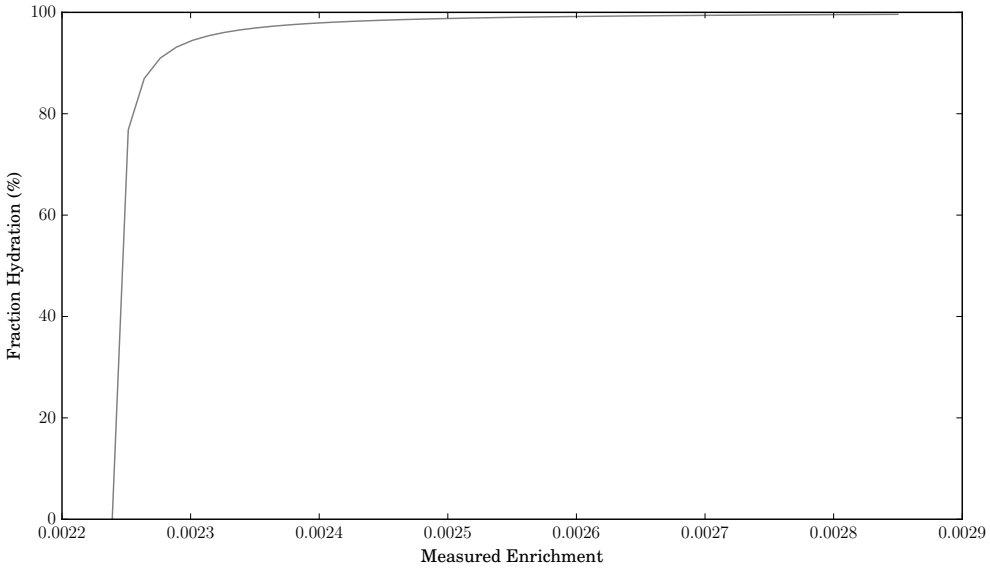

Figure 3.8: Fraction of hydration needed in order to have a measured ^{235}U enrichment given on the x-axis.

arate individuals determined concentration values for the uranium samples and arrived at very similar answers. In response to detector shift sources of error, Table 3.15 is provided for explanation.

Table 3.15: Measurements of Percent enrichment of ^{235}U in the pellet. Measurements are provided from Experiments 2, 5a, and 5b. The different experiments are distinguished by an exponent on the error term.

Enrichment Measurements		
0.271 ± 0.016^{5b}	0.287 ± 0.009^{5b}	0.281 ± 0.009^{5a}
0.284 ± 0.009^{5b}	0.288 ± 0.011^{5b}	0.280 ± 0.009^{5a}
0.288 ± 0.009^{5b}	0.288 ± 0.008^{5a}	0.283 ± 0.008^{5a}
0.284 ± 0.008^{5b}	0.285 ± 0.008^{5a}	0.280 ± 0.009^{5a}
0.285 ± 0.008^{5b}	0.280 ± 0.008^{5a}	0.275 ± 0.016^{5a}
0.290 ± 0.010^{5b}	0.279 ± 0.013^{5a}	0.285 ± 0.010^{2}

Table 3.15 shows 18 different measurements of ^{235}U enrichment from mass spectrometry. These results are from Experiments 2, 5a, and 5b. It is highly unlikely that the instrument response is responsible for a shift in enrichment reported by 0.06% in the final result (0.28% - 0.22% = 0.06%) for every single measurement taken. Also, these measurements were taken on separate days.

Also, all of these samples had largely different concentrations of uranium, and all of them produced the same result, an average of 0.283% with a standard deviation of 0.005% enrichment of ^{235}U. Further, another student measured the same sample, with a completely different machine and different calibration standards, and got a ^{235}U enrichment of 0.28%.

The errors in Table 3.15 were determined as described in Appendix B and were dependent on the standards error, the count time and the count rate. Because uranium was the most abundant species in the system, the count rate and counting time did not contribute appreciably towards the error in most cases. This means the error was mostly dictated by the error in the uranium standard used to determine concentrations. The reasoning behind this error estimation is described in Appendix B and was calculated at 2%.

3.4.1.3. Uranium Correction

The correction on ^{235}U enrichment has no bearing on DCs or DFs, it should be applied though, to the solutions used in the forensic methodology. The two solution compositions that will be used in the forensic methodology are the initial closet solution and a 4 times extracted 3 times back-extracted closet solution which contains chemically separated plutonium. The first solution correction is relatively straight-forward and is shown below. The product solution correction will correct the final uranium concentration based on the fraction of the original uranium that passed to the final solution. This is given in Equation 3.11

$$m_{\text{U,corrected,final}} = m_{\text{U,uncorrected,final}} - T \cdot \frac{m_{\text{U,uncorrected,final}}}{m_{\text{U,uncorrected,initial}}} \tag{3.11}$$

where:

$m_{\text{U,corrected,final}}$ = the corrected uranium mass for the product solution

$m_{\text{U,uncorrected,final}}$ = the uncorrected uranium mass for the product solution

T = total contamination in closet solution (mg)

$m_{\text{U,uncorrected,initial}}$ = the uncorrected uranium mass for the initial solution

The correction for the uranium content in the final solution given in Equation 3.11 will introduce a relatively large error in the uranium total amount (>15%), but will fix the enrichment level of uranium to a much more reasonable value so that the forensic analysis is not biased or affected before the start.

The initial uranium solution correction is as follows. If a small amount of uranium contamination, T, contaminated the closet solution, then the enrichment of uranium would need to be corrected for with Equation 3.12.

$$\frac{m_{\text{U}_5} - T \cdot \chi_5}{m_{\text{U}_4} + m_{\text{U}_5} + m_{\text{U}_6} + m_{\text{U}_8} - T} = \chi_5' \tag{3.12}$$

where:

χ_5 = ^{235}U enrichment (mass fraction) of contamination

χ_5' = ^{235}U enrichment of pellet (mass fraction)

m_{U_5} = measured mass in mg of ^{235}U in closet solution.

The enrichment of the contamination can be determined by solving for χ_5, shown in Equation 3.13.

$$\chi_5 = \frac{m_{\text{U}_5} - \chi_5' \left(m_{\text{U}_4} + m_{\text{U}_5} + m_{\text{U}_6} + m_{\text{U}_8} - T\right)}{T} \tag{3.13}$$

In order to determine the total contamination of uranium, T, Equation 3.14 was used, where 86% of the pellet mass is attributed to uranium because UO_2 fuel attributes about 88% of the fresh fuel mass to uranium, and in our irradiated sample, about 2% of the fuel mass is Pu. The 86% attribution of mass to uranium is verified by MCNP results[66].

$$T = m_{\text{MS}} - m_{\text{Macro}} \cdot 0.86 \tag{3.14}$$

where:

m_{MS} = Total mass of uranium in original closet solution determined by MS

m_{Macro} = Macroscopic mass of pellet.

Uranium mass spectrometry results for an initial closet solution are shown in Table 3.16. The calculations for determining the total initial amounts of each species in the closet solution are described in section 2.3.1. According to this measurement and Equation 3.13 and 3.14, the total uranium contamination would be 0.3 mg of 2.5% enriched uranium.

The above defense for why the author believes ^{235}U contamination exists is open to scrutiny and could very well be erroneous. There is also uncertainty as to where this contamination could have come from. If at one point the glovebox used for dissolution contained 2.5 wt.% enriched uranium (or another amount), then the a trace amount (0.3 mg) could have been left in the glovebox and been introduced into the sample. Another alternative is that while being processed at Oak Ridge in their glovebox, contamination could have been introduced that way. Whether through improper measurement, contamination, or some other reason, it very well agreed that the enrichment of 0.28 wt% of uranium is impossible given the initial conditions of the system. It is for this reason the forensic analysis as well as for the pellet characterization will use a more reasonable 0.22 wt% enrichment as determined in Swinney's work[66].

Table 3.16: Mass Spectrometry results for the initial closet solution.

Isotope	Sample (ng/ml)	Total ng per 0.5 ml aliquat of stock	Total mg if entire closet solution processed
^{234}U	$(4.89\pm0.50)\times10^{0}$	$(2.17\pm0.25)\times10^{0}$	$(2.00\pm0.24)\times10^{-4}$
^{235}U	$(7.89\pm0.19)\times10^{2}$	$(3.50\pm0.20)\times10^{2}$	$(3.23\pm0.23)\times10^{-2}$
^{236}U	$(3.94\pm0.32)\times10^{1}$	$(1.75\pm0.17)\times10^{1}$	$(1.61\pm0.17)\times10^{-3}$
^{237}Np	$(1.07\pm0.07)\times10^{1}$	$(4.74\pm0.42)\times10^{0}$	$(4.38\pm0.42)\times10^{-4}$
^{238}U	$(2.77\pm0.06)\times10^{5}$	$(1.23\pm0.07)\times10^{5}$	$(1.13\pm0.08)\times10^{1}$
^{239}Pu	$(4.33\pm0.12)\times10^{3}$	$(1.92\pm0.12)\times10^{3}$	$(1.77\pm0.13)\times10^{-1}$
^{240}Pu	$(3.62\pm0.11)\times10^{2}$	$(1.60\pm0.10)\times10^{2}$	$(1.48\pm0.11)\times10^{-2}$
^{241}Pu+^{241}Am	$(1.50\pm0.21)\times10^{2}$	$(6.64\pm0.98)\times10^{1}$	$(6.15\pm0.94)\times10^{-3}$
^{242}Pu	$(8.71\pm2.82)\times10^{0}$	$(3.86\pm1.26)\times10^{0}$	$(3.57\pm1.18)\times10^{-4}$
^{235}U Percentage	$(2.84\pm0.09)\times10^{-1}$	U Total	$(1.14\pm0.08)\times10^{1}$
^{239}Pu Percentage	$(8.93\pm0.35)\times10^{1}$	Pu Total	$(1.99\pm0.14)\times10^{-1}$

3.4.2. Fission Product Total Mass Estimate

The total mass of fission products was estimated with ^{137}Cs. ^{137}Cs was chosen because its production is mostly due to its fission yield and does not have many losses. Equation 3.15 was used for the calculation.

$$\text{Mass}_{FP} = \frac{2 \cdot \text{Mass}_{^{137}\text{Cs}}}{\gamma_{^{137}\text{Cs}}} \cdot \frac{M_{avg}}{M_{^{137}\text{Cs}}} = \text{Mass}_{^{137}\text{Cs}} \cdot F \tag{3.15}$$

where:

Mass_{FP} = Estimated mass of fission products

$\text{Mass}_{^{137}\text{Cs}}$ = Total mass of ^{137}Cs in the pellet

$\gamma_{^{137}\text{Cs}}$ = Cumulative fission yield for ^{137}Cs

M_{avg} = Yield weighted average Molar mass for fission products

$M_{^{137}Cs}$ = Molar mass of ^{137}Cs

F = Factor which converts ^{137}Cs to fission product mass (estimate)

Equation 3.15 has a factor of 2 because there are two fission products per each fission.

The yield weighted average mass number was determined with Equation 3.16, where i is summed over all mass numbers except those which end in a stable isotope of noble gases of xenon or krypton. Equation 3.16 is divided by a factor of 2 because the yields sum up to 2. The fission yields are shown in Figure 3.9[56]. The average mass for fission was determined by using the fraction of fissions from isotopes ^{235}U, ^{239}Pu, and ^{241}Pu. This means that Equation 3.16 was used for isotopes ^{235}U, ^{239}Pu, and ^{241}Pu and an average was determined by multiplying each by their corresponding fraction of fissions and summing the result.

$$M_{avg} = \frac{1}{2}\sum_{i}^{N} M_i \cdot \gamma_i \tag{3.16}$$

The conversion factor, F for the three main fission isotopes in the system, ^{235}U, ^{239}Pu, and ^{241}Pu, were determined to be 23.1, 21.9, and 22.1, respectively. The total mass of ^{137}Cs in the pellet as of 10/20/2014 was determined with mass spectrometry to be 0.00185 mg. If the factor for ^{239}Pu were used, the estimate for the total amount of fission products in the pellet would be 0.0404 mg. Errors in this estimate were not determined because this method provides a only an estimate for the total amount of fission products. MCNP results predicted that the mass of fission products in the pellet is closer to 0.0374 mg[66].

3.4.3. Pellet Composition

Given the estimates described in the previous sections, the pellet composition information is provided in Tables 3.17, 3.18 and 3.19. These masses will be the starting point for

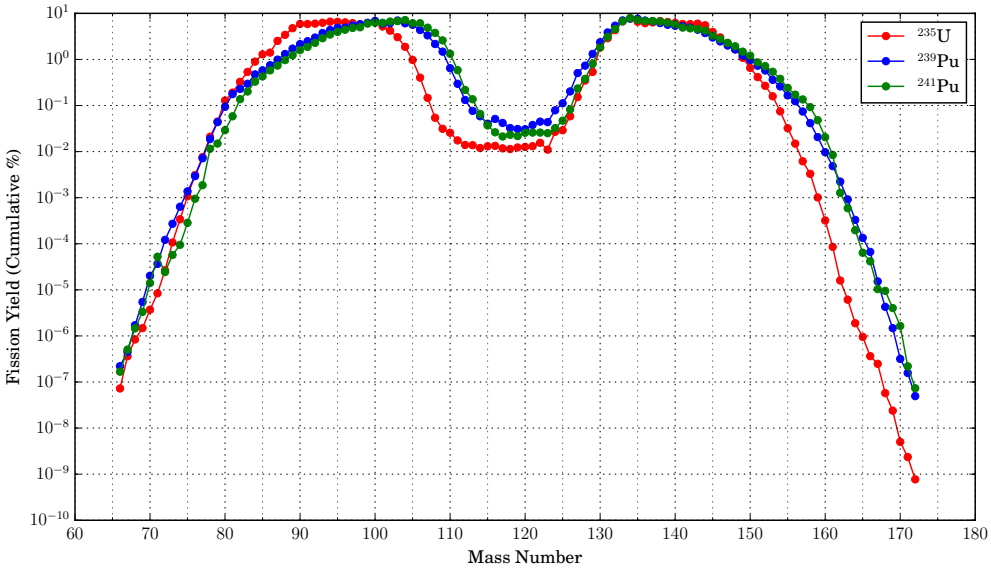

Figure 3.9: Reprinted JENDL cumulative fission yields versus mass number for thermal fissions for ^{235}U, ^{239}Pu, and ^{241}Pu[56].

the forensic analysis.

Table 3.17: Initial breakdown of pellet contents.

Component	Mass (mg)
Total Mass	12.90 ± 0.05
Total U	11.08 ± 0.79
Total Pu	0.199 ± 0.013
Total FP	0.040 ± 0.005
Total Oxygen	1.58 ± 0.79

Table 3.18: Plutonium Vector for pellet.

Weight Percent			
^{239}Pu	^{240}Pu	^{241}Pu	^{242}Pu
89.3 ± 3.5	7.46± 0.30	3.09 ± 0.43	0.180 ± 0.058

Table 3.19: Specifically determined initial amounts of fission products in pellet.

Component	Mass (mg)
$^{85}_{37}Rb$	(1.00±0.07)×10^{-4}
$^{133}_{55}Cs$	(1.94±0.13)×10^{-3}
$^{134}_{55}Cs$	(1.45±0.05)×10^{-5}
$^{137}_{55}Cs$	(1.85±0.09)×10^{-3}
$^{97}_{42}Mo$	(1.33±0.11)×10^{-3}
$^{98}_{42}Mo$	(1.88±0.16)×10^{-3}
$^{100}_{42}Mo$	(1.67±0.11)×10^{-3}
$^{106}_{44}Ru$	(2.58±0.09)×10^{-4}
$^{110}_{46}Pd$	(8.02±0.57)×10^{-5}
$^{111}_{48}Cd$	(5.32±0.38)×10^{-5}
$^{144}_{58}Ce$	(3.80±0.11)×10^{-4}
$^{140}_{58}Ce$	(1.76±0.15)×10^{-3}
$^{143}_{60}Nd$	(1.40±0.11)×10^{-3}
$^{151}_{62}Sm$	(1.09±0.08)×10^{-4}
$^{154}_{63}Eu$	(8.38±0.25)×10^{-6}
$^{153}_{63}Eu$	(1.44±0.12)×10^{-4}

3.5. DC-DF Relationship

The experiment that will be used in the forensic methodology is the 4 extraction 3 back extraction equal volume sequence. In section 2.1.1, the fraction of a particular species that transfers to the organic phase in a liquid-liquid contact between two immiscible phases was described using Equation 2.3. This assumed material equilibrium and conservation

of mass. If only a certain fraction of the organic phase were removed, then Equation 3.17 would represent the fraction of solute (mass) removed from the system.

$$f_{org} \cdot V_E = \frac{V_E}{(1 + DC_i^{-1} V_R^{-1})} \tag{3.17}$$

where:

$V_R = V_{org}/V_{aq}$

V_E = Ratio of organic phase removed to the total organic phase present

DC_i = The distribution coefficient for species i

Conversely, if a part of the aqueous phase were removed from a liquid-liquid partition, as is the case in back-extraction, then the fraction of species removed during the partition would be given by Equation 3.18.

$$f_{aq} \cdot V_{BE} = \frac{V_{BE}}{(1 + DC_i V_R)} \tag{3.18}$$

where:

V_{BE} = Ratio of aqueous phase removed over the total aqueous phase present

3.5.1. Derivation

Every liquid-liquid extraction removes a certain fraction of dissolved species. Equations 2.3, 3.17, and 3.18 show examples for fractions removed in scenarios of perfect and imperfect separation. For convenience the variable f will be used to denote when a fraction of mass is removed from a system with subscripts denoting the numeric instance of mass removal. For example, f_1 is the first mass fraction removed from the system. The

following also assumes that all mass fractions which are removed from the system are collected together in f_{tot} so that as the number of contacts increases the total mass removed from the system reaches unity.

The total amount collected from a system after two, three, and four extractions are given in Equations 3.19, 3.20, and 3.21.

$$f_{tot,2} = (1 - f_1) f_2 + f_1 = f_1 + f_2 - f_1 f_2 \tag{3.19}$$

$$\begin{aligned} f_{tot,3} =& (1 - f_1 - f_2 + f_1 f_2) f_3 + f_1 + f_2 - f_1 f_2 \\ =& f_1 + f_2 + f_3 - f_1 f_2 - f_1 f_3 - f_2 f_3 + f_1 f_2 f_3 \end{aligned} \tag{3.20}$$

$$\begin{aligned} f_{tot,4} =& (1 - f_1 - f_2 - f_3 + f_1 f_2 + f_1 f_3 + f_2 f_3 - f_1 f_2 f_3) f_4 + \\ & f_1 + f_2 + f_3 - f_1 f_2 - f_1 f_3 - f_2 f_3 + f_1 f_2 f_3 \\ =& \sum_{i=1}^{4} f_i - \sum_{i=1}^{3} \sum_{j=i+1}^{4} f_i f_j + f_1 f_2 f_3 + f_1 f_2 f_4 + f_1 f_3 f_4 + f_2 f_3 f_4 \\ & + f_1 f_2 f_3 f_4 \end{aligned} \tag{3.21}$$

If the fraction removed was the same at every step, these equations would simplify to Equations 3.22, 3.23, and 3.24.

$$f_{tot,2} = 2f - f^2 \tag{3.22}$$

$$f_{tot,3} = f^3 - 3f^2 + 3f \tag{3.23}$$

$$f_{tot,4} = -f^4 + 4f^3 - 6f^2 + 4f \tag{3.24}$$

The combined fraction after both 4 extractions and 3 back-extractions for a given species i is given in Equation 3.25.

$$f_{\text{combined},i} = f_{tot,4,\text{Extraction}} \cdot f_{tot,3,\text{Back-Extraction}} \tag{3.25}$$

The decontamination factor for species i is given in Equation 3.26.

$$DF_i = \frac{f_{\text{combined},Pu}}{f_{\text{combined},i}} \tag{3.26}$$

3.5.2. Implementation of DC-DF Relationship

The formulas in the previous section were used to calculate DF values from experimentally determined DC values. Both calculated and experimental results are shown in Table 3.20 for the first mega cycle of Experiment 7. Average DC values were used in the calculation as well as Equations 3.22 3.23 and 3.24, which assume that the same fraction of material is removed at each step.

Table 3.20: Experiment 7 comparison between DF values estimated from DCs and from experiment.

Element	DF From Experiment	DF Determined with DC values	$\frac{\text{DF}_{\text{DC}}}{\text{DF}_{\text{Experiment}}}$
Cs	$(2.89 \pm 0.47) \times 10^2$	$(4.22 \pm 0.18) \times 10^2$	1.46 ± 0.06
Ru	$(7.94 \pm 0.27) \times 10^0$	$(8.28 \pm 0.41) \times 10^0$	1.04 ± 0.05
Ce	$(5.19 \pm 1.03) \times 10^0$	$(5.12 \pm 0.20) \times 10^0$	0.985 ± 0.038
Eu	$(2.77 \pm 0.26) \times 10^0$	$(2.54 \pm 0.09) \times 10^0$	0.914 ± 0.033

Experiment 7 was corrected so that equal contact volumes and no volume losses could be simulated. Results are shown for a specific experiment because the formulas in the previous section reference specific volumes. This variation would be mitigated in with larger material throughput and therefore a single experiment was shown to display how well DC values can be used to determine DF values. The methodology in the following sections requires knowledge of the process used for purification, and therefore the process followed for the first round of Experiment 7 will be used for the forensic methodology. The code for these as well as for other calculations is shown in Appendix E.

4. ATTRIBUTION METHODOLOGY

Any venture into forensic analysis requires an understanding of how relevant phenomena affected the state of the current system. The phenomena are then tied to models which can predict either what will occur, or what has occurred. Forward methods are more easily understood in that a future state of a system is predicted based on current information and an understanding of the science of the system. Conversely, inverse methods attempt to predict the original state of a system, which is more difficult because there are a many scenarios that could lead to the system's current condition[9]. Nuclear forensic analysis utilizes both methods of deduction.

For example, forward models are used to determine estimates on neutron flux spectra - which can be used to calculate one-group neutron cross sections - which simplify the estimations of isotopic concentrations during neutron irradiation in a reactor. This information can be used for inverse model prediction. Unfortunately, without prior information about the history of a sample, distinctions between different forward models cannot be made, and therefore databases and iterations are necessary to determine which model best fits the data.

In the case for used nuclear fuel, the most important attributes to determine are the fuel burnup, initial uranium enrichment, reactor type, and age of the fuel. Fuel attribution is much easier with this information and can be confirmed with forward models. The calculations explained in the following sections will utilize one-group neutron cross section approximations to determine the above attributes of used fuel and are subject to the shortcomings of approximation. The physics behind used fuel isotopics are complex, and therefore error bars for estimations will not be provided.

The neutron irradiation experiment discussed in previous sections was modeled using

MCNP[66] code; with the irradiation history known, MCNP provided neutron flux spectra will be tested as the forward model and compared to experimental results. The neutron flux spectra is important for determining one-group neutron cross sections, which are one of the primary actors in equations for determining the aforementioned attributes of used fuel. Although most reactor systems have variance in the neutron flux across the core[68], only a set of one-group cross sections were used for the calculation because the pellet in question was not strictly power producing and is of low burnup[i]. It is also small, the variation in neutron spectrum across the pellet is small

Figure 4.1[66,69] shows the initial neutron flux spectrum for the irradiated pellet covered in Gd in the HFIR and the average flux in an FBR blanket. Comparison of these two flux spectra is important because the irradiated system was designed to resemble that of an FBR. The calculations that require one-group cross sections will use cross sections generated from the initial HFIR sample flux spectra, the Fast Breeder Reactor (FBR) blanket region, an AP1000, and a Pressurized Heavy Water Reactor (PHWR).

One-group cross sections were calculated for the mentioned spectra using ENDF/B-VII cross section data, and a python script utilizing a trapezoidal integration scheme. The iteration scheme had satisfactory agreement with cross sections generated from sources such as the Java-based Nuclear Information Software (JANIS) and the National Nuclear Data Center for the fission spectrum. The cross sections were calculated in a similar manner as the comprehensive multi-group nuclear cross section generation code NJOY[70], with the exception that Doppler broadening (for the temperature dependence) was not considered[71]. In essence, nuclear data in the U.S. Evaluated Nuclear Data Files (ENDF) format were processed via Equation 4.1,

[i]Variance in neutron flux at different regions in the core produce variance in isotopic composition but this effect is ignored in the present study.

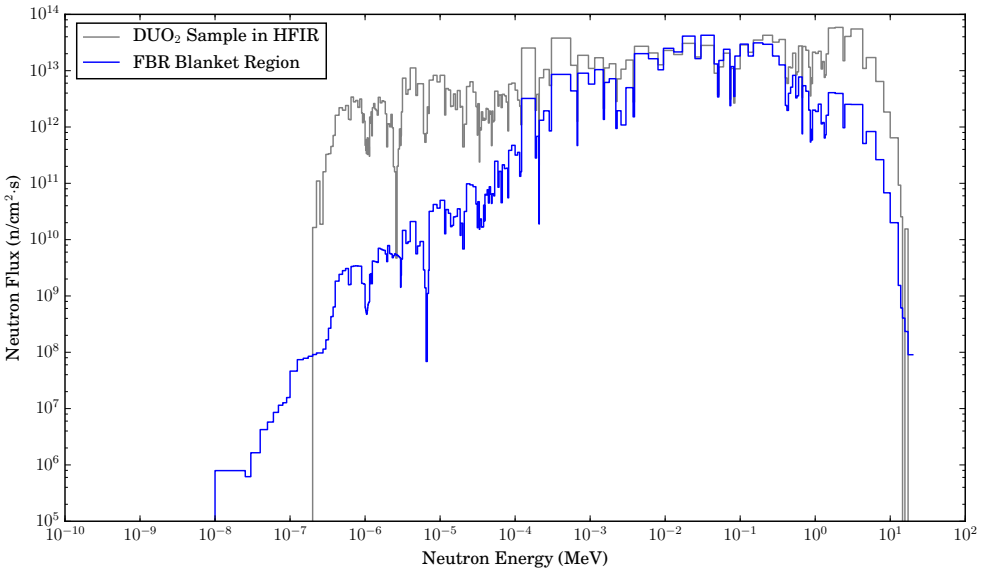

Figure 4.1: Comparison of the neutron flux in the sample to the spectrum in the blanket of an FBR[66]. Reprinted with permission from[69].

$$\sigma_{\text{one-group}} = \frac{\int_0^\infty \sigma(E)\phi(E)dE}{\int_0^\infty \phi(E)dE} \tag{4.1}$$

where $\sigma(E)$ is the neutron cross section and $\phi(E)$ is the energy-dependent scalar neutron flux in the DUO_2 pellet. The accuracy of single group cross sections is very important for the analysis described in the following sections. Because Doppler broadening was not incorporated into this analysis cross sections evaluated at temperatures near the operating temperature of the system were used (300 K).

Because the cross sections are calculated averages from average flux values in the region, spatial variances were not captured (ex. self-shielding). The sample size for this experiment ($R_{eff} \approx 0.07$ cm[ii]) was not of an appreciable size compared to the mean free path of a neutron in this energy range (~ 4 cm) so that this phenomena should not reflect

[ii] R_{eff} as defined as the radius as if the total volume was converted to a sphere

a major concern. In the case of larger samples with appreciable self-shielding, the group cross section could reflect this via multi-group disadvantage factors or a meshing of the geometry, which could be computationally expensive.

4.1. Algorithm Overview

This experiment utilized an irradiated 12.9 $\pm$ 0.1 mg of DUO_2 irradiated to a lower burnup (< 5 MWd/MTU) in a particular fast neutron environment. The specifics of irradiation history was known to some, but not initially to the author, and working through the procedures for the forensic analysis will give some grounding for the history of the sample. Working from this "blind" perspective helped by removing bias towards particular results or conclusions. Near the end of the project, more and more specifics of the sample were made known and results were verified.

The analytical attribution methodology followed a series of calculations as depicted in Figure 4.2. Each individual calculation will be discussed, but the flow chart depicts the order in which the used fuel attributes are determined. The following calculations will assume a point-wise irradiation. Fuel burnup is solved for first because it has minimal dependency on the neutron scalar flux and its energy dependence, whereas the rest of the calculations depend on one or both. In order to solve for the rest of the used fuel attributes, the calculations were performed over a wide range of potential normalized energy-dependent neutron scalar fluxes and the neutron energy spectrum that produces the most consistent fuel age indicators, which will be compared with results from MCNP.

The non-burnup indicators are dependent on the energy-dependent neutron scalar flux in the uranium sample. An issue with this dependency is the complexity surrounding the shape of the energy-dependent neutron scalar flux. It varies with temperature, geometry, fuel composition, and density of the materials in the system. These complexities cannot be ignored or simplified for precise answers, and various transport codes like MCNP[72] or

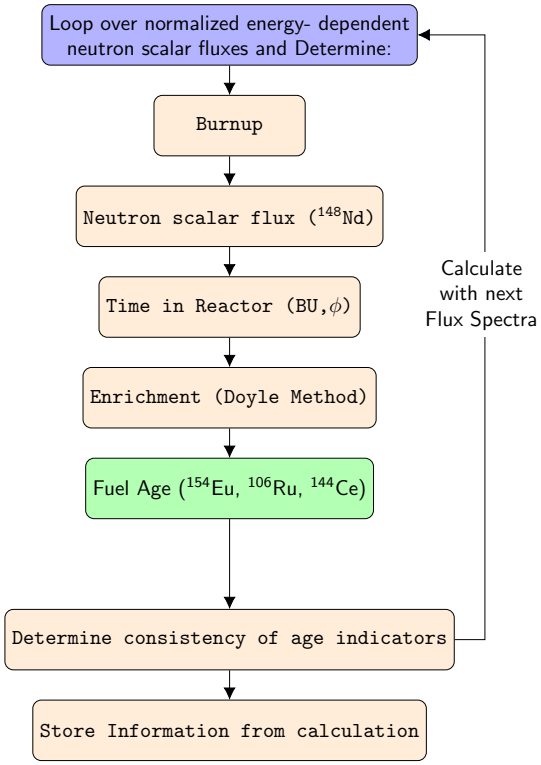

Figure 4.2: Flow chart for analytical calculations.

WIMS[73] can be used to resolve the scalar flux spectra. In the case at hand, several flux spectra from different reactor systems will be used.

Calculations will also assume that the magnitude of the neutron scalar flux is constant for an irradiation, when in reality it may not be. This assumption may be valid because lower burn-ups are more common for weapons-grade plutonium.

In short, the methodology assumes a normalized energy-dependent neutron scalar flux and uses this scalar flux to calculate the used fuel attributes. This is done by calculating one-group cross sections and using them in the equations shown in the following sections. Then, another normalized energy-dependent neutron scalar flux is assumed, which will provide another set of cross sections with the same calculations ensuing for the fuel pa-

rameters. This is done for several energy-dependent scalar fluxes and the most internally consistent set of results will be compared to what the sample actually underwent. The information about the specifics of the sample irradiation were not used to guide to arrive at the results, but results are compared to results from MCNP. This methodology provides an energy-dependent neutron scalar flux which would give an indication to what type of reactor the fuel was irradiated in.

4.2. Burnup

The first parameter in Figure 4.2 to determine is the fuel burnup. Fuel burnup is an operational parameter for the amount of energy produced per unit mass of the fissionable material, and is calculated with Equation 4.2,

$$\text{BU} = \frac{\text{Power [MW]} \cdot \text{days}}{\text{mass [tHM]}} \tag{4.2}$$

where:

$mass$ = the initial mass of heavy metal in the irradiated fuel in metric tons

Power = the thermal power released into the working fluid.

From an operational standpoint, an average of this fuel burnup for an entire fresh core is relatively straightforward to determine. Knowing the amount of fuel put into a system, the amount of energy produced can either be calculated with a specific heat calculation on the working fluid in the reactor system or with the amount of energy produced in the turbine coupled with efficiencies. With the operation time, the above parameters could be used to determine an average fuel burnup for a core.

Something a little more useful from a nuclear security perspective would be a knowledge of the fuel burnup for specific fuel assemblies and/or pins within an assembly. Although precise fuel burnup knowledge down to the pin level might be a little unrealistic,

computationally it is something to keep in mind that different parts of the core and or assembly at different heights could have a variation in burnup levels that will lead to different isotopics.

In forward analysis the overall power is usually known. Without this information, inverse models are required and Equation 4.2 can be modified to measure burnup through FPs via Equation 4.3[9]

$$\text{BU} = \left[\frac{N^B}{N_0^{HM}}\right] \cdot \frac{N_A E_R}{\gamma_B} \cdot \frac{1}{M_0^{HM}} \tag{4.3}$$

where:

N^B = the *atomic* concentration of a FP in the matrix of post-irradiated fuel

N_A = Avogadro's constant

E_R = the recoverable energy per fission

γ_B = the effective atomic cumulative fission product yield (usually ^{137}Cs or ^{148}Nd)

N_0^{HM} = the initial atomic concentration of heavy metal in the fuel matrix

M_0^{HM} = the initial heavy metal molar mass (units may vary).

^{238}U or ^{232} Th are sometimes used as a weight in Equation 4.3 because they typically are the most abundant heavy element in used fuel matrices, but are not necessary in this calculation. If the units of E_R are [MeV/fission] then if a conversion factor of 1.85E-24 [MWd/MeV][iii] is applied, dimensional analysis shows Equation 4.2 and Equation 4.3 to have the same units.

[iii] $1.85 \times 10^{-24} \left[\frac{MWd}{MeV}\right] = \frac{1.60218 \times 10^{-19} \text{ MJ}}{1 \text{ MeV}} \cdot \frac{1 \text{ day}}{3600 \cdot 24 \text{ s}}$

To precisely determine this parameter from a reactor physics point of view, the total number fissions from each fissionable isotope should be known along with respective recoverable energy per fission. This information is more difficult to acquire because the concentrations of fissionable material in a fissioning system (nuclear reactor) is constantly changing. Burnup will thus be determined with a fission product that builds into the fuel matrix linearly as a function of burnup such as ^{137}Cs or ^{148}Nd.

Although the fuel burnup units between the forward and inverse analysis are the same, Equation 4.3 has additional stipulations that need to be met before the two analyses produce the same numerical value. First N^B builds into the fuel matrix linearly and second and third, γ_B and E_R should be constant across all fissionable isotopes (and across all fission energies). All three stipulations are never exactly true, but they are reasonably true for some isotopes over others. The fission product yield can be modified to increase accuracy by considering different fission energies and/or different mass chains[74].

Depending on the original concentration and the build up of transuranics, the fissionable isotopes may be a combination of uranium, plutonium or TRU. With mass spectroscopy, the atomic concentrations for the end of irradiation fissionable isotopes can be determined by converting mass concentrations of the isotopes into atomic concentrations of the isotopes. N^B and N^{U238} would be determined in that manner.

The initial concentration of heavy metal can be determined via Equation 4.4

$$\left[\frac{N^{U238}}{N_0^{HM}}\right] = \frac{N^{U238}}{\frac{N^B}{\gamma_B} + \sum N^{HM,i}} \tag{4.4}$$

where $\sum N^{HM,i}$ is the post-irradiated atomic sum of heavy metal with the index i as the heavy metal isotope. This equation utilizes the fact that every production of a fission product comes from destruction of a fissionable isotope.

The last unknown from Equation 4.3, M_0^{HM}, requires an additional relationship. M_0^{HM}

is a combination of weight fraction of each heavy metal isotope at the start of irradiation and can be approximated by using the post-irradiation heavy metal concentrations. Otherwise an additional correlation for the initial heavy metal atomic concentration can be manipulated to solve for M_0^{HM}. This correlation is given in Equation 4.5[9].

$$\left[\frac{N_0^{HM}}{N^{U238}}\right] = \frac{\frac{\sum N^{HM,i}}{N^{U238}}}{1 - \frac{M_0^{HM}}{N_A E_R} BU} \tag{4.5}$$

Equation 4.5 divides the "weighted" atomic number density of heavy metal by the fraction of atoms that did not undergo fission. This should give an initial "weighted" atomic number density for heavy metal. The above relationships are combined in Equation 4.6 to give a relationship for the initial heavy metal atomic mass.

$$M_0^{HM} = \frac{N_A E_R}{BU}\left(1 - \left[\frac{N^{U238}}{N_0^{HM}}\right]\frac{\sum N^{HM,i}}{N^{U238}}\right) \tag{4.6}$$

Finally, mass fractions were converted to atomic fractions via Equation 4.7, where PPB refers to the mass concentration. The fraction of total burn-up from fission of fissionable isotope i was determined with Equation 4.8, where σ_f refers to the microscopic single group fission cross section. Note that these fractions are normalized such that $\sum f_i = 1$. This equation applies only to a single moment in time and would need to be integrated to determine the overall fission fraction for an isotope. The summation over index j corresponds to fissionable isotopes. A more complicated analysis for this could be attempted with ^{106}Ru because of its large discrepancy in fission yields between isotopes[75].The average fission product yield for mass chain i was determined with Equation 4.9 and the energy per fission was determined in a similar manner.

$$\frac{N^i}{N^{U238}} = \frac{\text{PPB}^i}{\text{PPB}^{U238}} \cdot \frac{M^{U238}}{M^i} \tag{4.7}$$

where:

PPB represents part per billion concentration with respect to the total sample

$$f_i = \frac{\sigma_{f,i} N_i}{\sum_{j=1}^{M} \sigma_j N_j} \tag{4.8}$$

$$\gamma_B = \sum f_i \gamma_B^i \tag{4.9}$$

The burn-up of the fuel was estimated by analyzing ^{137}Cs and ^{148}Nd concentrations. Both isotopes have been used to estimate fuel burn-up due to the fact that their fission yields are reasonably constant as a function of the neutron flux energy and fissionable isotope[75,76]. This is important for reasons described above.

It should be noted that two other indicators have been used to determine burn-up for fuel in both thermal and fast reactors, such as the ratio of ^{134}Cs to ^{137}Cs as well as the ratio of ^{154}Eu to ^{137}Cs[32,77], and both rely on the fact that ^{134}Cs and ^{154}Eu are proportional to the square of fluence while ^{137}Cs is directly proportional to the fluence. The added complexity of these analyses require more extensive forward analysis, as the production chains for ^{154}Eu and ^{134}Cs are more detailed[78,79].

Concentrations of ^{137}Cs and ^{148}Nd were determined with mass spectrometry and ^{137}Cs additionally was determined with gamma spectroscopy. The calculation using gamma spectroscopic results used a variation of the equations above with concentration replaced with atomic values.

4.3. Scalar Neutron Flux

The neutron scalar flux magnitude calculation will be completed with the typical burnup monitor ^{148}Nd[75,80].Thus monitor is known to build into the fuel matrix linearly as a function of burnup, and typically a fission yield is used in order to calculate an actual

value. In the case of ^{148}Nd there is a potential for a sizable amount of contribution from neutron capture in the 147 mass chain; therefore, an effective yield value would be necessary for this calculation, especially in thermal systems[74]. If burnup for the system were already known, say with ^{137}Cs, then the effective yield could be used to solve for neutron flux from a balance equation of ^{148}Nd. This is how this calculation was performed.

The buildup of ^{148}Nd undergoes a slightly different process from ^{137}Cs. The general assumption for both these fission products is that they linearly increase with burnup. ^{137}Cs builds into the fuel matrix mostly through direct fission, without much contribution from other mass chains, losses from its own mass chain, or decay of the final product. These assumptions are reasonable in that the longest lived precursor in the 137 mass chain has a half-life of 3.82 minutes with a negligible absorption cross section and the 136 mass chain does not contribute towards cesium because of very short half-lives (<1.39 min) and an end product with 0.1 b resonance integral cross section.

The 148 mass chain has minimal losses prior to ^{148}Nd, due to the fact that the longest lived precursor has a half-life of 2.27 minutes with a negligible absorption cross section. ^{148}Nd is stable, but has a tendency to be a very largest contributor towards the complicated ^{154}Eu production through neutron capture[79][iv]. Also, contributions from other mass chains can be sizable. Mass chain 147 contains ^{147}Nd, which has a large resonance integral cross section (630 b) and a half-life of 11 days, by default[v], this isotope also contributes towards ^{154}Eu production, and if ^{148}Nd were to be used as a burn-up indicator in a thermal reactor, an effective yield value is necessary[74].

A simplified version of the ^{147}Nd production rate differential equation is provided in Equation 4.10 to show production and loss operators. This simplified version assumes that the cumulative yield for the mass chain instantaneously arrives at ^{147}Nd. This assump-

[iv] the samarium isotopes, 149 through 152, all have large cross sections see reference for more details

[v] (n,γ) on ^{147}Nd goes to ^{148}Nd

tion partially based based on the combination of short half-lives of precursors and small absorption cross sections but is not perfect. For example, ^{147}Nd has a 13.4 minute half life and a non-negligible absorption cross section. Some consolation lies in the fact that the order of magnitude of neutron absorption cross sections between ^{147}Nd and ^{147}Pr are roughly the same, but the fact remains that Equation 4.10 has approximation error.

$$\frac{dN_7}{dt} = \gamma_7 \phi N_f \sigma_f - \phi N_7 \sigma_{a,7} - \lambda_7 N_7 \tag{4.10}$$

where:

^{147}Nd has been subscripted to 7

N = the atomic concentration

γ = the cumulative fission yield

ϕ = the neutron scalar flux (assumed constant)

λ = decay constant

The contribution of ^{147}Nd neutron absorption to ^{148}Nd can be determined by integrating the solution of Equation 4.10 from 0 to t and multiplying by $\sigma_{a7}\phi$. This is shown in Equation 4.11, where the number density of fissionable material is assumed constant and the initial amount of ^{147}Nd in the system is $N_{7,0}$. The number density of fissionable material in the system will change, but Equation 4.11 could still be used with time steps if $N_{7,0}$, N_f, γ_7 and σ_f were updated at each step.

$$\begin{aligned} N_{147\rightarrow148}(t) = & \frac{\sigma_{a,7}\phi}{\sigma_{a,7}\phi + \lambda_7} \cdot \gamma_7 \phi N_f \sigma_f \left[t - \frac{1}{\sigma_{a,7}\phi + \lambda_7} \left(1 - e^{-(\sigma_{a,7}\phi + \lambda)t} \right) \right] + \\ & \frac{N_{7,0}\sigma_{a,7}\phi}{\sigma_{a,7}\phi + \lambda_7} \left(1 - e^{-(\sigma_{a,7}\phi + \lambda_7)t} \right) \end{aligned} \tag{4.11}$$

The entirety of the contribution from ^{147}Nd is dependent on the absorption cross section. Also notice how this contribution grows "linearly" with time at longer times. Given a superposition argument, and assuming that the absorption cross section of ^{148}Nd is negligible, then summing the two "linear" contributions for ^{148}Nd would yield a linear function, which is what is expected for ^{148}Nd, especially for longer time periods.

Given a system that has a fast neutron spectrum with low burn-up, this contribution from ^{147}Nd can be ignored because of lower neutron cross sections in fast systems, but our flux spectrum has a non-negligible thermal portion and there are several studies indicating that the ^{147}Nd contribution should not be ignored, and its contribution has been described[78,81,82]. Further, to estimate reactor scalar flux, the solution to Equation 4.12 should be analyzed, where ^{148}Nd is subscripted as an 8.

$$\frac{dN_8}{dt} = \gamma_8 \phi N_f \sigma_f - \phi N_8 \sigma_{a,8} + \phi \sigma_{a,7} N_7 \tag{4.12}$$

The solution to Equation 4.12 is given in Equation 4.13, where the fission term, $\phi N_f \sigma_f$, has been set to F[82].

$$\begin{aligned} N_8(t) = &\left(\frac{F\gamma_8}{\sigma_{a,8}\phi} + \frac{F\gamma_7\sigma_{a,7}}{(\lambda_7 + \sigma_{a,7}\phi)\sigma_{a,8}} \right) \left[1 - e^{-\sigma_{a,8}\phi t}\right] + \\ &\frac{F\gamma_7\sigma_{a,7}\phi}{(\lambda_7 + \sigma_{a,7}\phi)(\lambda_7 + \sigma_{a,7}\phi - \sigma_{a,8}\phi)} \left(e^{-(\lambda_7 + \sigma_{a,7}\phi)t} - e^{-\sigma_{a,8}\phi t}\right)(1 - N_{7,0}) \\ &+ N_{8,0} e^{-\phi\sigma_{a,8}t} \end{aligned} \tag{4.13}$$

If small time steps were used with Equation 4.13, where time-dependent items are updated at each time step, then the only major approximations with this solution are the single energy group approximation as well as the single point approximation. Flux in Equation 4.13 could be numerically solved for our given input parameters. An easier

approach would be to assume $\sigma_{8,a}$ is zero and to solve for flux., This is a typical assumption for a linear burnup monitor. With this stipulation, the solution to Equation 4.12 is given in Equation 4.14.

$$\begin{aligned} N_8(t) =& Ft\left(\gamma_8 + \gamma_7\frac{\phi\sigma_{a,7}}{\phi\sigma_{a,7}+\lambda_7}\right) + \\ & \frac{\phi\sigma_{a,7}}{\phi\sigma_{a,7}+\lambda_7}\left(\gamma_7\frac{F}{\phi\sigma_{a,7}+\lambda_7} - N_{7,0}\right)\left(e^{-(\phi\sigma_{a,7}+\lambda_7)t} - 1\right) + N_{8,0} \end{aligned} \tag{4.14}$$

Taking the first two terms of the Taylor series expansion of the exponent, Equation 4.14 simplifies to Equation 4.15, which is valid only when $(\sigma_{a,7}\phi + \lambda_7)t < 0.1$ and $\sigma_{a,8} \approx 0$.

$$N_8(t) = (F\gamma_8 + N_{7,0}\phi\sigma_{a,7})t + N_{8,0} \tag{4.15}$$

When $N_{7,0} = N_{8,0} = 0$, Equation 4.15 resembles the form of the solution for ^{137}Cs at all time steps. If taking small time steps, $N_{7,0}$ would have to be set to $\gamma_7 Ft + N_{7,i-1}(1 - \phi\sigma_{a,7} + \lambda_7)t$. In this scenario, we assume we know the shape of the scalar flux, and F as a function of time. This would mean that ϕ and t_{end} are the only unknowns. To solve the system we would need another set of equations. Otherwise, if we ignore the time dependency of F and assume t is fairly large, so that $e^{-(\phi\sigma_{a,7}+\lambda_7)t} \approx 0$, then if we start at $t = 0$, with $N_{7,0} = N_{8,0} = 0$, Equation 4.14 turns into Equation 4.16.

$$\begin{aligned} N_8(t) &= Ft\left(\gamma_8 + \gamma_7\frac{\phi\sigma_{a,7}}{\phi\sigma_{a,7}+\lambda_7}\right) - \gamma_7 F\frac{\phi\sigma_{a,7}}{(\phi\sigma_{a,7}+\lambda_7)^2} \\ &= Ft\left(\gamma_8 + \gamma_7\frac{\phi\sigma_{a,7}}{\phi\sigma_{a,7}+\lambda_7} - \gamma_7\frac{\phi\sigma_{a,7}}{t(\phi\sigma_{a,7}+\lambda_7)^2}\right) \\ &\approx Ft\left(\gamma_8 + \gamma_7\frac{\phi\sigma_{a,7}}{\phi\sigma_{a,7}+\lambda_7}\right) \end{aligned} \tag{4.16}$$

If the expression in the parenthesis is seen as the effective yield for ^{148}Nd, γ_8^*, then this value can be related to burn-up though Equation 4.17. This can be plugged into Equation 4.18, which takes the effective yield from Equation 4.16 and solves for flux.

$$\gamma_8^* = \frac{N_8 N_A E_R}{\text{BU} N_0^{HM} M_0^{HM}} \tag{4.17}$$

$$\phi \approx \frac{\lambda_7}{\sigma_7 \left(\frac{\gamma_7}{\gamma_8^* - \gamma_8} - 1 \right)} \tag{4.18}$$

The assumptions and approximations behind arriving at Equations 4.17 and 4.18 are summarized below:

1. one-group approximation
2. System approximated as a point
3. ϕ is constant throughout the irradiation
4. The energy shape of ϕ is known
5. $\phi N_f \sigma_f$ is constant throughout the irradiation
6. $e^{-(\phi\sigma_{a,7}+\lambda_7)t} \approx 0$
7. $\frac{\phi\sigma_{a,7}}{t(\phi\sigma_{a,7}+\lambda_7)^2} << \frac{\phi\sigma_{a,7}}{\phi\sigma_{a,7}+\lambda_7}$
8. Continuous irradiation (otherwise ^{147}Nd would decay away with an 11 day half-life)

Numbers 3, 5 and 8 are the most problematic assumptions. As stated above a second equation could be used to mitigate number 5, and another scheme would be needed to determine reactor shutdowns.

4.4. Time in Reactor

Equation 4.2 shows how burn-up is typically calculated. Another means for determining this value would be to use the total mass defect for the fuel. The total mass defect, Δm is provided in Equation 4.19.

$$\Delta m = \left[\left(\begin{smallmatrix} \text{mass} \\ \text{of heavy} \\ \text{metal} \end{smallmatrix} \right)_{\text{initial}} - \left(\begin{smallmatrix} \text{mass} \\ \text{of heavy} \\ \text{metal} \end{smallmatrix} \right)_{\text{final}} - \left(\begin{smallmatrix} \text{mass} \\ \text{of fission} \\ \text{products} \end{smallmatrix} \right)_{\text{final}} - \left(\begin{smallmatrix} \text{total} \\ \text{\# of} \\ \text{fissions} \end{smallmatrix} \right) \left(\begin{smallmatrix} \text{mass} \\ \text{of a} \\ \text{neutron} \end{smallmatrix} \right) (\nu - 1) \right] \quad (4.19)$$

where:

All masses are in atomic mass units (amu)

ν = the average number of neutrons released per fission event

$\left(\begin{smallmatrix} \text{total} \\ \text{\# of} \\ \text{fissions} \end{smallmatrix} \right) = \int_0^t \Sigma_f \phi$

The total amount of energy released from fission events can be related to the mass defect[83] with the constant, C_1, of 931.494 MeV/amu. Further, if we assume a only a fraction of the energy is absorbed by the system, ϵ, and if we set C_2 = 5.39E23 MeV/MW·days, and C_3 =6.022E29 amu/ton, then the mass defect and burn-up can be related with Equation 4.20.

$$\text{BU} = \epsilon \cdot \frac{\Delta m \cdot \frac{C_1}{C_2}}{\text{tHM}_{\text{initial}}} \quad (4.20)$$

As a note:

$$C_3 = \frac{\left(\begin{smallmatrix} \text{amu mass} \\ \text{of heavy} \\ \text{metal} \end{smallmatrix} \right)_{\text{initial}}}{\text{tHM}_{\text{initial}}}$$

If the initial mass of heavy metal were known, the total number of fissions could be

determined with Equation 4.21.

$$\int_0^t \Sigma_f \phi = \frac{\left(\frac{\text{BU}C_2}{\epsilon \cdot C_1} - C_3\right) \text{tHM}_{\text{initial}} + \left(\begin{smallmatrix}\text{amu mass}\\ \text{of heavy}\\ \text{metal}\end{smallmatrix}\right)_{\text{final}} + \left(\begin{smallmatrix}\text{amu mass}\\ \text{of fission}\\ \text{products}\end{smallmatrix}\right)_{\text{final}}}{\left(\begin{smallmatrix}\text{amu mass}\\ \text{of a}\\ \text{neutron}\end{smallmatrix}\right)(1-\nu)} \tag{4.21}$$

Laboratory analysis of any interdicted material could potentially provide information on all the above parameters except the initial mass of HM, but a method for determining this parameter was presented in section 4.2.

If $\Sigma_f \phi$ is assumed to be constant as a function of time, then the time in the reactor t would be determined with Equation 4.22. It should be noted that $\Sigma_f \phi$ is not constant as a function of time because the number density of the fission products constantly decreases in a neutron field. In power reactors, to produce the same amount of power as a function of time, ϕ is increased as Σ_f decreases. In situations where weapons-grade plutonium is being produced, lower burn-ups are utilized, and Σ_f would not have had much time to decrease. Still, this is an assumption behind this calculation and introduces some error in the final result.

$$t = \frac{\left(\frac{\text{BU}C_2}{\epsilon \cdot C_1} - C_3\right) \text{tHM}_{\text{initial}} + \left(\begin{smallmatrix}\text{amu mass}\\ \text{of heavy}\\ \text{metal}\end{smallmatrix}\right)_{\text{final}} + \left(\begin{smallmatrix}\text{amu mass}\\ \text{of fission}\\ \text{products}\end{smallmatrix}\right)_{\text{final}}}{\Sigma_f \phi \left(\begin{smallmatrix}\text{amu mass}\\ \text{of a}\\ \text{neutron}\end{smallmatrix}\right)(1-\nu)} \tag{4.22}$$

4.5. Initial Enrichment

Given that only a single isotope undergoes fission in a system, the estimate for the initial enrichment of a sample would increase linearly with burn-up. Most systems have fissile material transmuted into the system through capture reactions. Due to this, multiple isotopes fission, and more complicated analysis is required. Even so, a series of conservation equations may be solved iteratively with the assumption that burnup, heavy metal compositions, and one-group cross sections are known. This methodology was presented

by Doyle[9], and will be used for this calculation.

Although more nuclides can be included, the analysis for initial enrichment will assume that only ^{235}U, ^{238}U, ^{239}Pu, ^{240}Pu, and ^{241}Pu fission. The one-group cross sections will be derived in the same way as described previously. This analysis assumes that ^{239}Pu is directly produced from ^{238}U (through neutron capture and two β^- decays) and that fissionable isotopes do not decay (or have very long half-lives). For long-lived samples this would pose a problem for ^{241}Pu, because of its short half life, and a correction would be needed. This analysis also assumes negligible mass defect effects during transmutation, which is reasonable.

From a balance of uranium atom density Equation 4.23 to Equation 4.27 show how the calculation is performed[9], where e_o is the initial enrichment, $\sigma_{f,X}$ is the one-group fission cross section for isotope X, and $\sigma_{a,X}$ is the one-group absorption cross section for isotope X. This solution assumes that all the higher actinides are built into the system from capture in ^{238}U.

$$\begin{aligned} e_0 =& \frac{N^{U238}(T)}{N_0^U}\left[\frac{N^{U235}(T)}{N^{U238}(T)} + \frac{N^{U236}(T)}{N^{U238}(T)}\right] \\ &+ \frac{M_0^U}{N_A E_R}\mathrm{BU}(T) - G^{238} - G^{239} - G^{240} - G^{241} \end{aligned} \tag{4.23}$$

Several of the terms in Equation 4.23 have been previously defined. The first bracketed term corresponds to the final enrichment with reference to initial heavy metal – where initial heavy metal mass is previously solved for. The second term adds to the final enrichment the enrichment contribution from burn-up, where burn-up was previously solved for. The second term includes fissions from ^{238}U, ^{239}Pu, ^{240}Pu, and ^{241}Pu. In order to account for this, the additional G terms are needed to subtract out their individual contributions. These equations are shown in Equation 4.24 to Equation 4.27. It should be noted that phys-

ically, the G terms are all positive, but due to the numerous simplifications associated with this solution and possibly errors in one-group cross section, some, especially the ^{240}Pu and ^{241}Pu terms – with small contribution of total fissions can sometimes be calculated to be negative. These negative G terms were disregarded, as they are non-physical.

$$G^{238} = \frac{\sigma_{f,U238}}{\sigma_{a,U238}} \left[1 - e_0 - \frac{N^{U238}(T)}{N_0^U} \right] \tag{4.24}$$

$$G^{239} = \frac{\sigma_{f,Pu239}}{\sigma_{a,Pu239}} \left[\frac{-N^{Pu239}}{N^{U238}(T)} \frac{N^{U238}(T)}{N_0^U} + G^{238} \frac{\sigma_{\gamma,U238}}{\sigma_{f,U238}} \right] \tag{4.25}$$

$$G^{240} = \frac{\sigma_{f,Pu240}}{\sigma_{a,Pu240}} \left[\frac{-N^{Pu240}}{N^{U238}(T)} \frac{N^{U238}(T)}{N_0^U} + G^{239} \frac{\sigma_{\gamma,Pu239}}{\sigma_{f,Pu239}} \right] \tag{4.26}$$

$$G^{241} = \frac{\sigma_{f,Pu241}}{\sigma_{a,Pu241}} \left[\frac{-N^{Pu241}}{N^{U238}(T)} \frac{N^{U238}(T)}{N_0^U} + G^{240} \frac{\sigma_{\gamma,Pu240}}{\sigma_{f,Pu240}} \right] \tag{4.27}$$

4.6. Reactor Type

Knowing the reactor type provides a tremendous advantage with the previous calculations. Ideally, if information about the reactor type and neutron flux profile were known initially, better estimates of one-group cross sections could be made, which contributes significantly towards accuracy of the previous calculations. One-group cross sections also lead to information about dominant reactions in the system, and provide better approximation on average fission yields, and average energy per fission. The calculations described previously start with the assumption of known flux energy spectra, and use that knowledge to calculate fission fractions, burn-up, fluence, and initial enrichment. The calculations resulting from this section merely authenticate this assumption. Rigorous analysis in this regard would ideally couple all the previously described calculations with a database of

flux spectra (or flux weighted single or two group cross sections) – wherein the best fit to the data provides the most likely solution. Understandably, error analysis in this regard is difficult, which is why only numerical results are presented whereas relative differences give indication of reactor types.

Some suggested reactor type monitors are: ^{109}Ag, $^{\mathbf{153}}\mathbf{Eu}$, ^{156}Gd, $^{\mathbf{143}}\mathbf{Nd}$, ^{240}Pu, $^{\mathbf{108}}\mathbf{Pd}$, $^{\mathbf{113}}\mathbf{Cd}$, $^{\mathbf{149}}\mathbf{Sm}$, ^{166}Er, ^{132}Ba, ^{98}Tc, $^{\mathbf{115}}\mathbf{In}$, ^{72}Ge, ^{115}Sn[9]. The bolded isotopes will be utilized in the following analysis. It should be noted that the accuracy of this calculation, like most in nuclear engineering, are strongly dependent on the accuracy of one-group cross sections and fission yield data. According to Doyle, it is best to use stable or long-lived isotopes to avoid having to correct for decay[9].

The effective yield for the previously bolded isotopes would need to be calculated with attention to the following isotopes capture cross sections: ^{153}Eu, ^{143}Pr, ^{108}Pd, ^{113}Cd, ^{149}Pm, ^{149}Sm, and ^{115}In. These isotopes are either long-lived or stable but some have very large capture cross sections. For example, ^{153}Eu, in term of mass spectrometry analysis is relatively straightforward to quantify, but the effective yield for this isotope requires some extra thought. As noted previously, ^{154}Eu is produced in the reactor in small quantities, primarily through absorption in ^{148}Nd, ^{150}Nd, and ^{145}Pr[79],[vi]. All three of these production chains pass through ^{153}Eu to produce ^{154}Eu. For the sake of reactor type selection, this complication and other similar complications will be ignored – as they are beyond the scope of this project.

As was previously shown, the number of a stable or long lived nuclide in a reactor as a function of time can be depicted with Equation 4.28[9],

$$N^X(T) = \sum_{i=1}^{I} \gamma_X^i \sigma_f^i \int_0^T \phi N^i(T) \tag{4.28}$$

[vi]Please see reference for more details, isotopes involved in the complex production chain have large absorption cross sections.

where i is summed over all fissile isotopes, γ_X^i is the effective yield for nuclide from the fission of isotope i, and all other terms have been previously defined. Equation 4.28 assumes that the cross section and yield are constant as a function of time. The first is generally linked to the flux, in that if the flux is constant, then the single group cross section is constant. The yield, especially for the isotopes listed, is definitely not a constant as a function of time, but will be assumed so unless the decay chains contain significant contribution from absorption.

It should be noted that assuming the yield is a constant as a function of time is a major assumption, which is why the following analysis will not provide quantitative results, but rather a soft comparison of a residual in a calculation. It should also be noted that some of the isotopes listed above decay, and correction for their decay will be taken into account with the time since removal calculation.

Given the relationship for burn-up given in Equation 4.29[9] a series of equations can be expressed where the concentration of fission products can be predicted via a matrix inverse solve and this is given in Equation 4.30[9], where the integral portion of Equation 4.28 is defined as $I_{N,i}$, and $N_A E_R / M_0^U N_0^U$ is defined as C. Every variable besides cross section in both arrays in Equation 4.30 are a function of time.

$$\text{BU}(T) = \sum_{i=1}^{I} \frac{N_A E_{R,i} \sigma_{f,i}}{M_0^U N_0^U} \int_0^T \phi N_i(t) \tag{4.29}$$

$$\begin{bmatrix} 1 & 1 & 1 & 1 & 1 \\ \gamma_1^5 & \gamma_1^8 & \gamma_1^9 & \gamma_1^0 & \gamma_1^1 \\ \gamma_2^5 & \gamma_2^8 & \gamma_2^9 & \gamma_2^0 & \gamma_2^1 \\ \gamma_3^5 & \gamma_3^8 & \gamma_3^9 & \gamma_3^0 & \gamma_3^1 \\ \gamma_4^5 & \gamma_4^8 & \gamma_4^9 & \gamma_4^0 & \gamma_4^1 \end{bmatrix} \begin{bmatrix} \sigma_f^{235} I_{N,235} \\ \sigma_f^{238} I_{N,238} \\ \sigma_f^{239} I_{N,239} \\ \sigma_f^{240} I_{N,240} \\ \sigma_f^{241} I_{N,241} \end{bmatrix} = \begin{bmatrix} \frac{\text{BU}}{C} \\ N^1 \\ N^2 \\ N^3 \\ N^4 \end{bmatrix} \tag{4.30}$$

It should be noted that the series of equations does not necessarily need to include the burn-up equation, and another equation could be provided with additional fission products, but including the burn-up equation usually decreases the condition number of the square matrix by a large margin which presents prevents ill-posed problems . The advantage of including the burn-up equation is that a single right hand side solution is correct, whereas the fission product equations are not correct due to different effective yields. The problem will be solved via both methods.

The reactor type should be determined by choosing the flux spectrum that yields the minimum residual, shown in Equation 4.31 [9], where the double brackets represent a vector norm.

$$\left\| \begin{bmatrix} 1 & 1 & 1 & 1 & 1 \\ \gamma_1^5 & \gamma_1^8 & \gamma_1^9 & \gamma_1^0 & \gamma_1^1 \\ \gamma_2^5 & \gamma_2^8 & \gamma_2^9 & \gamma_2^0 & \gamma_2^1 \\ \gamma_3^5 & \gamma_3^8 & \gamma_3^9 & \gamma_3^0 & \gamma_3^1 \\ \gamma_4^5 & \gamma_4^8 & \gamma_4^9 & \gamma_4^0 & \gamma_4^1 \end{bmatrix} \begin{bmatrix} \sigma_f^{235} I_{N,235} \\ \sigma_f^{238} I_{N,238} \\ \sigma_f^{239} I_{N,239} \\ \sigma_f^{240} I_{N,240} \\ \sigma_f^{241} I_{N,241} \end{bmatrix} - \begin{bmatrix} \frac{\mathrm{BU}}{C} \\ N^1 \\ N^2 \\ N^3 \\ N^4 \end{bmatrix} \right\| = R \tag{4.31}$$

4.7. Time Since Removal from Reactor

The fuel age will be determined with a simple decay calculation, but requires information from all of the above analyses as well as a Bateman [84] solver with readily changeable one-group cross sections. These are needed to estimate the expected value of a radioactive species in a fissioning system at a particular burnup with one-group cross sections. The radioactive species should have a high level of independence for its yield for different fission isotopes and be readily found in the fuel matrix, such as ^{90}Sr, ^{106}Ru, ^{125}Sb, ^{144}Ce, ^{134}Cs, ^{137}Cs, or ^{154}Eu.

The fuel age is easily determined if the concentration of a particular radioactive fission product is known at the end of irradiation time and time of measurement. Given that reactor burn-up is known, estimates on the concentration of fission product at the end of irradiation can be made with information about the reactor type by solving the Bateman equations for a particular isotope or coming up with another estimate for what the atomic concentration of the radionuclide should be at the end of irradiation. The fuel age would then utilize a form of the decay equation shown in Equation 5.6.

$$t_d = \frac{-1}{\lambda} ln \left(\frac{N_{\text{measured}}}{N_{\text{EOI}}} \right) \tag{4.32}$$

Long lived isotopes with small absorption cross sections are ideal for this calculation so as to make the end of irradiation estimate more accurate. ^{106}Ru and ^{137}Cs were used for this analysis (others can be used as well, for example ^{134}Cs).

The results for the nuclear forensics attribution calculations described in Section 4 are shown and discussed in this section. The difference between one-group cross sections can be significant even among reactor systems with the same type of neutron flux spectra. This can occur if one flux spectra has a dip in a certain energy region where a particular reaction has a peak and the other flux spectra does not. In order to show some differences, one-group cross sections were calculated with the cross sections and flux spectra shown in Figure 5.1 [5,13,69,85].

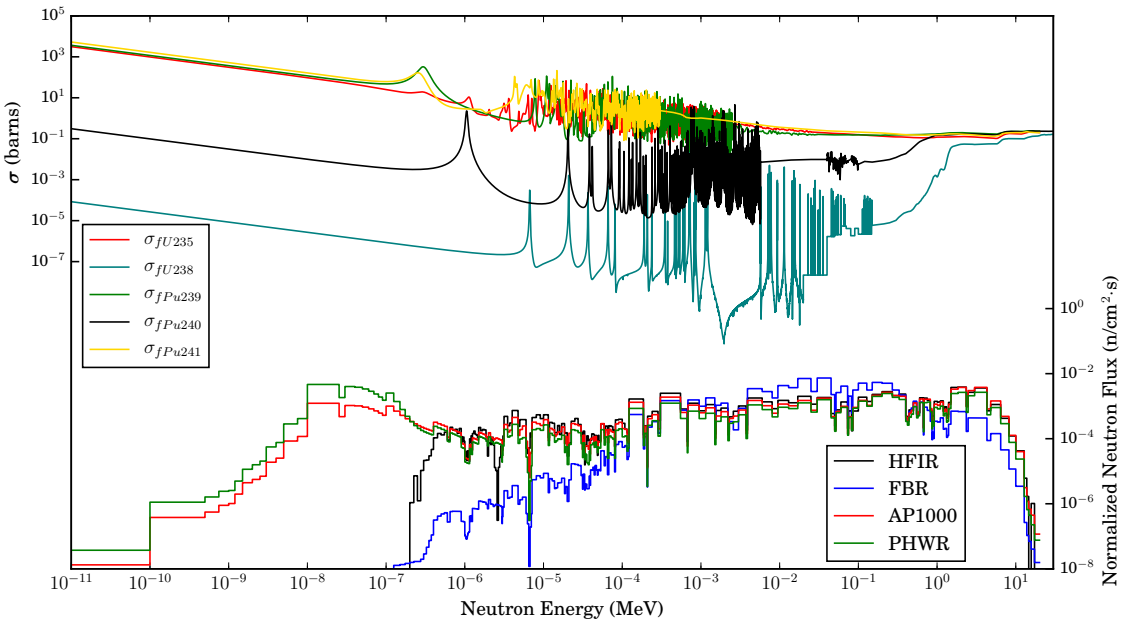

Figure 5.1: Fission cross sections plotted against neutron flux spectra. Cross section data used ENDF/B VII [13] and the fast neutron flux spectra are reprinted with permission from [69] and the thermal flux spectra are reprinted with permission from [85].

Figure 5.1[5,69,85] depicts the normalized flux spectra with its axis label on the right as a function of energy, and the cross section for important fissile and fissionable isotopes in barns are also depicted on the top portion of the graph as a function of energy with its y-axis label on the left. The four different spectra shown are the MCNP predicted initial spectra for the samples (HFIR)[66], an averaged FBR blanket spectra[5], an AP1000 spectra??, and a PHWR spectra[5].

Faster spectra pose a concern for producing weapons-grade plutonium as discussed in Section 1 with Table 1.1. The thermal spectra is shown for comparison. The one-group cross sections were calculated with Equation 4.1, and are shown in Table 5.1. It should be noted that the Equation 4.1 uses an energy-dependent flux spectra, and therefore the spectra shown in Figure 5.1 were modified to be per MeV. Integration used a trapezoidal rule.

Table 5.1: Microscopic fission cross section for major fissionable isotopes.

Isotope	HFIR Flux Spectrum	FBR Blanket Flux Spectrum	AP1000 Flux Spectrum	PHWR Flux Spectrum
^{235}U	11.65 b	3.64 b	54.88 b	149.63 b
^{238}U	0.10 b	0.02 b	0.11 b	0.07 b
^{239}Pu	16.81 b	2.69 b	112.74 b	242.32 b
^{240}Pu	0.61 b	0.21 b	0.60 b	0.45 b
^{241}Pu	27.10 b	4.24 b	124.70 b	301.74 b

From Figure 5.1 it can be seen why there is such a large variance in one-group cross section between the different spectra, even among similar systems. The PHWR one-group fission cross sections are double of the AP1000, both thermal systems. The reason for this is because of the larger thermal component of the PHWR. Among the two faster spectra there is a large spread as well, but is probably more due to the larger thermal component of

the HFIR. The HFIR is a thermal reactor, but this spectra was modified with a gadolinium shield so that part of the thermal neutron flux was absorbed. The thermal parts of each spectrum, coupled with large cross section resonances, led to sharp increases in cross section for the DU sample spectrum as opposed to the FBR system.

For ^{238}U the single group cross sections for the different reactor systems seem to be different than what is expected. ^{238}U has a threshold reaction, where neutrons under 2 MeV in energy have a low probability of causing fission. Table 5.1 shows that the thermal systems, along with the HFIR[i], have a larger calculated single group cross section than the FBR, which is a fast system. The reason why the FBR has a lower single group cross section for ^{238}U is because the neutron flux in the fission region is depressed due to scattering. This is shown in Figure 5.1, where the normalized neutron scalar flux in the regions above 2 MeV for the FBR are lower than for the other systems. A similar effect also explains why the same trend is seen for ^{240}Pu.

Despite their usefulness in speed, programs that utilize one-group cross sections for quick burnup calculations should utilize the proper neutron flux spectrum. The one-group cross section of the most abundant fissionable isotope in our system, ^{238}U, varied largely even among similar systems. Most of these variances are due to large increases in cross section in the fast (> 2 MeV) region of flux. ^{238}U and ^{240}Pu both have a threshold energy for fission, and therefore lead to major changes in their cross section in the fast region. This is shown in Figure 5.1.

One-group cross sections can be used to determine the fraction of fissions associated with each isotope for the four different spectra. This requires knowledge of fissionable isotope concentrations, which means the calculation is only useful at a given time, but will provide information on how much yields can vary across flux spectra, and at different times

[i]The energy region of interest for fission of ^{238}U is everything above 2 MeV and because the HFIR spectra was a thermal reactor with a gadolinium cover for absorption of thermal neutrons, the HFIR spectra in the fast regions resembles that of the thermal systems

of irradiation. The different flux spectra will be the ones used to determine the one-group cross sections in Table 5.1. Two different concentrations are used, the end of irradiation concentration determined experimentally and shown in Section 3, and hypothetical beginning of irradiation concentrations. Although the concentrations of the actinides used in this calculation change as a function of time, the shortest half-life among the actinides used has a 14 year half-life, which is for ^{241}Pu. The concentration of this isotope was small to begin with and therefore decay corrections were not applied. The equation used to calculate the fraction of fissions associated with each isotope was given in Equation 4.8

The fraction of fissions associated with each isotope is shown in Table 5.2. A large contributing factor for these numbers was the atomic density for each isotope, as the fission cross sections are all within two orders of magnitude. This means the fraction of fissions was mostly determined by the flux spectrum. An example calculation for the beginning of irradiation fraction of fissions is shown below for the AP1000, where the initial enrichment was used for the number densities and the cross sections from Table 5.1 are plugged in the last step so that other calculations can be checked[ii].

$$\begin{aligned}
f_{235} =& \frac{\sigma_{235} N_{235}}{\sigma_{235} N_{235} + \sigma_{238} N_{238}} \\
=& \frac{\sigma_{235} \frac{0.26}{235}}{\sigma_{235} \frac{0.26}{235} + \sigma_{238} \frac{99.74}{238}} \\
=& \frac{\sigma_{235}}{\sigma_{235} + \sigma_{238} \frac{99.74}{238} \frac{235}{0.26}} \\
=& \frac{\sigma_{235}}{\sigma_{235} + \sigma_{238} \cdot 379} \\
=& \frac{54.884}{54.884 + 0.106 \cdot 379} \\
=& 0.577
\end{aligned}$$

[ii]Note, the difference between 57.7 and the 59.61 are due to rounding and the slight difference between the use of number density and actual values. Values in Table 5.2 are unrounded

A previous section attempted to use ^{106}Ru to determine these fractions with a acceptable agreement. The ^{106}Ru calculation had numerous assumptions, and would need further refinement and computational backing before use in subsequent calculations, but its notable comparability using gamma sources and macroscopic mass measurements merits further investigation.

Table 5.2: Fraction of fissions associated with each isotope for end of life (top) and beginning of life (bottom)

Isotope	HFIR Flux Spectrum	FBR Blanket Flux Spectrum	AP1000 Flux Spectrum	PHWR Flux Spectrum
^{235}U	6.39	11.56	5.94	7.64
^{238}U	25.05	24.80	5.03	1.65
^{239}Pu	64.78	60.00	85.73	86.97
^{240}Pu	0.20	0.40	0.04	0.01
^{241}Pu	3.59	3.25	3.26	3.72
^{235}U	22.85	35.11	57.81	84.31
^{238}U	77.15	64.89	42.19	15.69

To be expected, the largest contributor of fissions in the system was ^{239}Pu which contributed approximately 65% of the total fissions at the end of irradiation with about 2% of the total mass of heavy metal. The high enrichment of ^{239}Pu in the fuel indicates a low burnup, which gives credence towards assuming a linear function for the plutonium isotopes to determine the integrated reaction rates to give an overall fission fraction for each isotope. Under this assumption, coupled with the assumptions already described for Equation 4.8, Equation 4.8, can be modified to estimate the total number of fissions from each element over the course of irradiation with Equation 5.1.

$$f_{i,\text{overall}} = \frac{\int_0^t \sigma_i N_i}{\sum_{i'=1}^{m} \int_0^t \sigma_{i'} N_{i'}} \tag{5.1}$$

With the assumption that the number density of the uranium isotopes remains relatively constant, the integral term of Equation 5.1 would be $\sigma_j N_j t$, where t is the time of irradiation. With the assumptions for the plutonium isotopes of a zero initial condition as well as a linear increase, the integral term of Equation 5.1 would be $\sigma_j \frac{N_j}{2} t$[iii]. This means all terms in Equation 5.1 have time included, which cancels. This means that this approximation is independent of irradiation time. The total fraction of fissions, calculated by the above described scheme is given in Table 5.3.

Table 5.3: Estimated overall fraction of fissions associated with each isotope for different flux spectra. Table5.2 shows BOI and EOI estimates for the fraction of fissions whereas this table shows an estimated total.

Isotope	HFIR Flux Spectrum	FBR Blanket Flux Spectrum	AP1000 Flux Spectrum	PHWR Flux Spectrum
^{235}U	9.73	16.95	10.71	13.99
^{238}U	38.11	36.38	9.07	3.02
^{239}Pu	49.28	44.00	77.26	79.58
^{240}Pu	0.15	0.29	0.03	0.01
^{241}Pu	2.73	2.38	2.94	3.40

With the assumptions:

- The scalar flux shape and magnitude are constant
- Plutonium production is linear as a function of time[iv]
- Initial plutonium content is zero

[iii] A t cancels here because the slope of the line would be $\frac{N_j}{t}$

[iv] Please see early portions of Figure 1.3

❖ The concentration of uranium in the system is constant through irradiation

The above is expanded to shed some light on the fraction of fissions associated with two different energy groups. This distinction is utilized because information is provided for yields among thermal and epithermal fissions[86]. The fraction of "thermal" and fast fissions for isotope i is calculated with Equation 5.2

$$f_{g,i} = \frac{\phi_g \sigma_{g,i} \int_0^t N_i}{\sum_{g'=1}^{G} \sum_{i'=1}^{m} \phi_{g'} \sigma_{g',i'} \int_0^t N_{i'}} \tag{5.2}$$

where:

g represents the energy group

$\phi_g = \int_{\Delta E} \phi(E) dE$ (fraction of flux in energy group)

$\sigma_{g,i} = \int_{\Delta E} \phi(E) \sigma(E)_i dE / \int_{\Delta E} \phi(E) dE$

$\sigma_{g,i} \phi_g = \int_{\Delta E} \phi(E) \sigma(E)_i dE$

Table 5.4 shows the calculated fraction of fissions with the same assumptions as above for the two different energy groups and using Equation 5.2. The cut off energy between "thermal" and epi-thermal regions was 1 keV, following with the National Nuclear Data Center's cut-off for fission spectrum integration. This means all energies below 1 keV were in the thermal group and all energies above 1 keV were in the epi-thermal group. For the fission spectrum, this table would have over 99.9% of the fissions occurring from fast fissions. With the slight "thermal" portion of our DUO_2 spectrum, we have sizable increase in fraction of fissions because of the drastic increase in cross section.

These fractions are used to determine average fission yields via Equation 4.9. This is important because ^{238}U and ^{239}Pu usually have different fission yields, even for isotopes like ^{137}Cs and ^{148}Nd[87]. The fission yields are shown shown in Table 5.5[86].

Using the information from Tables 5.5 and 5.4 the yield for ^{137}Cs and ^{148}Nd were calculated for the given flux spectra and shown in Table 5.6. Although these isotopes are considered to have constant fission yields across the fissioning isotopes, there is an 8% range between the different calculated results for ^{137}Cs.

The same calculation was done for the energy per fission for the fissile isotopes with results shown in Table 5.7. It should be noted that these values used fraction of fissions from Table 5.3 and energy per fission amounts that ranged from 201 MeV/fission for uranium to 210 MeV/fission for plutonium. The reason why values are closer to plutonium in most cases is because Table 5.3 reported that the fraction of fissions for plutonium was at least 50% for three out of the four flux spectra.

Table 5.4: Fraction of fissions associated with each isotope for different flux spectra and with different energies. Calculated with Equation 5.2

	HFIR		FBR Blanket		AP1000		PHWR	
	Flux Spectrum		Flux Spectrum		Flux Spectrum		Flux Spectrum	
Isotope	Thermal	Epi	Thermal	Epi	Thermal	Epi	Thermal	Epi
^{235}U	8.50	1.20	6.53	10.42	10.46	0.24	13.90	0.09
^{238}U	0.00	38.22	0.00	37.21	0.00	9.07	0.00	3.02
^{239}Pu	45.11	4.08	14.20	28.98	76.40	0.85	79.26	0.32
^{240}Pu	0.01	0.14	0.00	0.30	0.00	0.03	0.00	0.01
^{241}Pu	2.54	0.19	0.75	1.61	2.90	0.04	3.39	0.01

5.1. Fuel Burnup

The fuel burnup was calculated using ^{137}Cs and ^{148}Nd concentrations shown in Section 3 as well as the average yields and energy per fission shown above. Mass spectrometry was used to determine ^{137}Cs and the ^{148}Nd concentration. Gamma spectroscopy was also used to determine the ^{137}Cs concentration.

The burnup calculation results are shown in Table 5.8 with units of MWd/tHM. The

Table 5.5: Cumulative fission yields for ^{137}Cs and ^{148}Nd given in units of $\left[\frac{\text{Atoms}\times 100}{\text{Fission}}\right]$.

Fission Isotope	^{137}Cs Thermal (0.025 eV)	^{137}Cs Epi (500 keV)	^{148}Nd Thermal (0.025 eV)	^{148}Nd Epi (500 keV)
^{235}U	6.16	6.20	1.67	1.68
^{238}U	6.04	5.16	2.11	1.74
^{239}Pu	6.60	6.58	1.64	1.66
^{240}Pu	6.55	6.55	1.77	1.77
^{241}Pu	6.65	6.38	1.93	1.95

Table 5.6: Calculated cumulative fission yields for ^{137}Cs and ^{148}Nd with different flux spectra given in units of $\left[\frac{\text{Atoms}\times 100}{\text{Fission}}\right]$.

Isotope	HFIR Flux Spectrum	FBR Blanket Flux Spectrum	AP1000 Flux Spectrum	PHWR Flux Spectrum
^{137}Cs	6.01	5.99	6.43	6.50
^{148}Nd	1.69	1.70	1.66	1.66

Table 5.7: Energy per fission calculation using different flux spectra.

Isotope	HFIR Flux Spectrum	FBR Blanket Flux Spectrum	AP1000 Flux Spectrum	PHWR Flux Spectrum
E_R $\frac{\text{MeV}}{\text{Fission}}$	206.77	206.20	208.96	209.15

mass spectroscopy calculations assumed that natural levels of barium contamination could be derived from ^{136}Ba, which is shielded from fission production by stable ^{136}Xe, and had low contamination from ^{136}Ce. This calculation is only done for unprocessed dissolved samples. Solutions that had undergone any type of processing had large background barium which swamped out the signal of ^{137}Cs so that ^{133}Cs had to be used for decontamination factors.

The burnup calculation was shown with different spectra assumptions to show that

Table 5.8: Burnup as calculated from Cs and Nd with different flux spectra in units of MWd per metric ton of initial heavy metal.

Isotope	HFIR Flux Spectrum	FBR Blanket Flux Spectrum	AP1000 Flux Spectrum	PHWR Flux Spectrum
$^{137}Cs_{MS}$	$(4.64\pm0.35)\cdot10^3$	$(4.64\pm0.35)\cdot10^3$	$(4.39\pm0.33)\cdot10^3$	$(4.34\pm0.32)\cdot10^3$
$^{148}Nd_{MS}$	$(4.96\pm0.28)\cdot10^3$	$(4.93\pm0.28)\cdot10^3$	$(5.10\pm0.28)\cdot10^3$	$(5.11\pm0.29)\cdot10^3$
$^{137}Cs_{\gamma}$	$(4.62\pm0.46)\cdot10^3$	$(4.63\pm0.46)\cdot10^3$	$(4.37\pm0.43)\cdot10^3$	$(4.32\pm0.43)\cdot10^3$

even with different spectra, each estimate was within a standard deviation of another for the same isotopes, supporting the use of ^{137}Cs and ^{148}Nd as linear burnup indicators.

The ^{137}Cs amount determined with mass spectrometry was not decay-corrected, as only an estimated background ^{137}Ba was subtracted from the 137 mass bin. The rest, assuming similar instrument responses for the two isotopes, should be from ^{137}Cs, and its daughter. The gamma-measured ^{137}Cs was decay-corrected to the date of dissolution, and should have a lower estimate of burnup than the MS ^{137}Cs. The ^{148}Nd calculation did not utilize any correction, but should have accounted for ^{147}Nd and ^{147}Pm, which have sizable absorption cross sections, and contribute to the 148 mass chain. The cross sections and the corresponding flux spectra are shown in Figure 5.2[13,69]. This would explain why the burnup estimate from ^{137}Cs is slightly lower than that of ^{148}Nd.

To show how ^{147}Nd was built into the system during irradiation, Figure 5.3 is provided, which models two 24 day operational times separated by a 30 day period of decay. This figure shows that the dynamics of ^{147}Nd are rapidly changing due to its 11 day half-life. This isotope decays to ^{147}Pm, which has a 2 year half-life. Trying to account for contributions from these isotopes by rigorously mathematical schemes is possible – so that an effective fission yield for ^{148}Nd is obtained – but is much easier determined through industry codes like ORIGEN. As such, the next section will use an approximated estimate for an effective yield will be used to estimate the flux in the system.

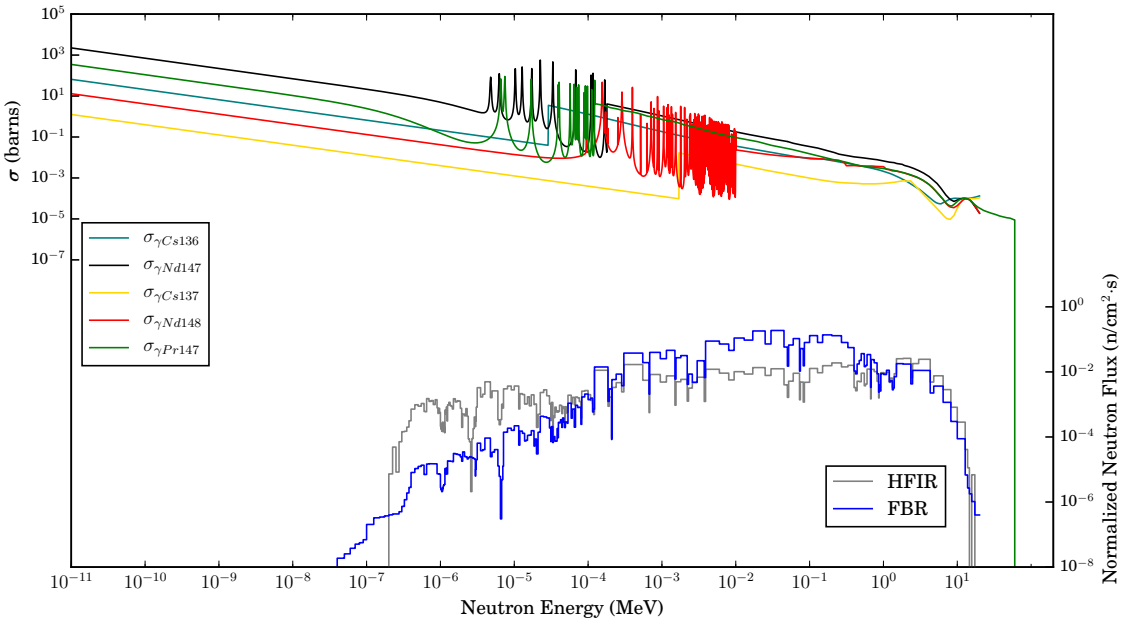

Figure 5.2: Absorption cross sections for ^{147}Nd, ^{147}Pm, ^{148}Nd and ^{137}Cs plotted against flux where the higher energies for ^{147}Pr drop to zero to show where the cross section has not been measured. Cross section data used ENDF/B VII[13] and flux spectra are reprinted with permission from[69].

5.2. Scalar Flux Determination

The following analysis utilized results from previous analyses. Due to the fact that burnup for both ^{137}Cs and ^{148}Nd were already calculated, the effective yield for ^{148}Nd can be calculated through a modified effective yield equation given in Equation 5.3. This can be plugged into the approximate flux equation and is shown in Equation 5.4.

$$\gamma_8^* = \gamma \cdot \frac{\mathrm{BU}_{Nd}}{\mathrm{BU}_{Cs}} \tag{5.3}$$

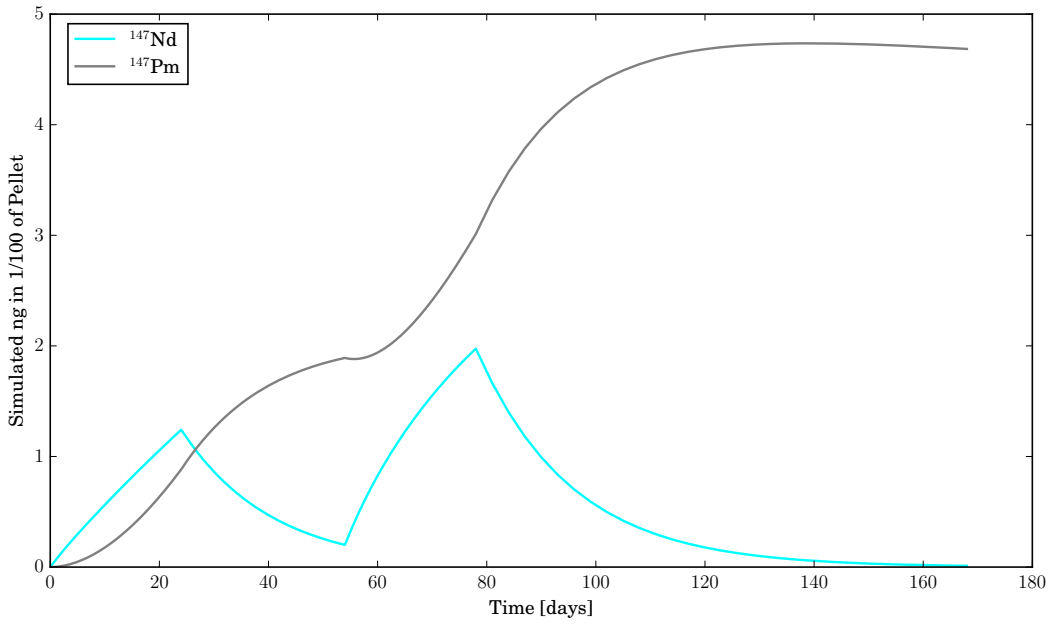

Figure 5.3: ^{147}Nd production as a function of time.

$$\phi \approx \frac{\lambda_{Nd147}}{\sigma_{a,Nd147}\left(\frac{\gamma_{Nd147}}{\gamma_{Nd148}\left(\frac{\mathrm{BU}_{Nd}}{\mathrm{BU}_{Cs}}-1\right)}-1\right)} \tag{5.4}$$

Most of the values used in this calculation have been shown previously. The microscopic absorption cross section and the yield for ^{147}Nd are shown in Table 5.9 for different flux spectra. The average yield and cross section were calculated in the same way as the last section, where the fraction of fission for each isotope was used to determine average yield values and the one-group cross section was determined over the entire energy range.

Results for the scalar flux calculation are shown in Table 5.10. The MCNP HFIR irradiation model had a *starting* flux magnitude of 1.73E15 n/cm^{2}s, which is not very close to any of the reactor type values. It was discovered after the fact that the sample's gadolinium sheath burned out during irradiation. This means that the sample would have

Table 5.9: Single group cross section for ^{147}Nd and ^{148}Nd as well as average percent yields for ^{147}Nd for the four reactor types.

	HFIR	FBR Blanket	AP1000	PHWR
Isotope	Flux Spectrum	Flux Spectrum	Flux Spectrum	Flux Spectrum
^{147}Nd	9.541 b	2.484 b	43.631 b	116.830 b
^{148}Nd	1.650 b	0.674 b	1.528 b	1.525 b
^{147}Nd	2.07%	2.07%	2.04%	2.05%

a flux value about double the initial, with a different spectrum. Given this, the results in Table 5.10 seem reasonable, because these calculations assumed a constant scalar flux. The scalar flux estimates assuming faster spectra are higher than the range of scalar flux values the sample actually saw. This is because the sample burned more than it would have if the spectra remained fast. The scalar flux estimates assuming thermal spectra are lower than the range of scalar flux values the sample saw, especially in the case of the PHWR, because to produce the same difference in burnup estimates between Cs and Nd, less flux is needed because of the higher absorption cross section in the thermal energy range.

Table 5.10: Scalar flux as calculated from Cs and Nd with different flux spectra in units of $n \cdot cm^{-2} \cdot s^{-1}$.

	HFIR	FBR Blanket	AP1000	PHWR
	Flux Spectrum	Flux Spectrum	Flux Spectrum	Flux Spectrum
$\phi \frac{n}{cm^2 s}$	4.6E+15	1.6E+16	2.5E+15	1.1E+15

5.3. Time in Reactor

The next calculation, time in the reactor, utilized equations given in section 4.4 as well as concentrations presented in Section 3. It should be noted that for the execution of Equation 4.22 required the mass of fission products in the sample. In Section 3, this number

was determined as described in Equation 3.15. In this section there were two differences in how Equation 3.15 was executed. First, noble gasses were included in the total mass of fission products, and second, an averaged F factor (see Equation 3.15) was used. This factor was averaged using the fraction of fissions associated with each fissionable isotope. The results of the calculation for time spent in the reactor are shown in Table 5.11, where previous calculated values, like burnup and scalar flux are used.

Table 5.11: Estimated time in reactor using four different flux spectra.

	HFIR Flux Spectrum	FBR Blanket Flux Spectrum	AP1000 Flux Spectrum	PHWR Flux Spectrum
T (days)	114.14	194.60	30.84	33.23

The sample was irradiated for 50 days. As a reminder, the calculations for each spectra are being done in parallel, but the results for each spectra are fed to the next part of the calculation for that same spectra. The results in Table 5.11 make sense in light of the changing flux spectra during irradiation. Less time in a thermal reactor is needed to reach the same concentrations of fission products and heavy metal in the system because of the higher cross section whereas a faster spectra would require more time.

5.4. Initial Enrichment

The initial enrichment calculation depends on the burnup, cross section, and heavy metal atomic concentrations as shown in Equations 4.23-4.27. The concentrations of heavy metal presented in Section 3 as well as burnup and cross section values calculated in previous sections in this section were used. The solution was iterative, and results are shown in Table 5.12.

Table 5.12 results were calculated with the modified uranium final enrichment. The

Table 5.12: Estimated initial enrichment given four different flux spectra.

	HFIR Flux Spectrum	FBR Blanket Flux Spectrum	AP1000 Flux Spectrum	PHWR Flux Spectrum
Enrichment (At.%)	0.43	0.43	0.29	0.22

actual start uranium enrichment was 0.28 wt%. This calculation relied both on on concentrations of the heavy metal in the system and on the one-group cross sections of the heavy metals.

The reason why the enrichment estimate is higher for faster systems can be seen by looking at Equation 4.25, where a shortened version of Equation 4.24 is substituted in for G^{238}, this is shown in Equation 5.5.

$$G^{239} = \frac{\sigma_{f,Pu239}}{\sigma_{a,Pu239}} \left[\frac{-N^{Pu239}}{N_0^U} + \Delta\epsilon_8 \cdot \frac{\sigma_{\gamma,U238}}{\sigma_{a,U238}} \right] \tag{5.5}$$

where:

$\Delta\epsilon_8$ = Estimated Fractional loss of ^{238}U

The term in the brackets is larger for thermal systems because the capture fraction is much higher in the thermal flux regions. This means that the burnup contribution from ^{239}Pu will be higher in a thermal system, which results in a lower estimate for the enrichment. Conversely, the opposite is true for fast neutron systems, where the fraction of radiative capture is lower, and therefore the burnup contribution for ^{239}Pu is estimated to be lower, which increases the enrichment estimate.

The fact that the PHWR system reports an enrichment about the same as what the sample ended at is indicative that this spectra probably did not produce the sample. The reason why the PHWR system estimate for enrichment is lower than the AP1000 estimate is more clearly explained with Figure 5.4[13,69,85], where the flux spectra are plotted against

the ratio of fission to absorption cross sections. Here it can be seen that the fission-to-absorption ratio is increasing near where the peak of flux is for both spectra. This is especially true for ^{239}Pu. With each flux spectra being normalized, it can be seen that a larger fraction of the PHWR has its flux in this region, which is why the PHWR has a larger estimate for the G^{239} term in Equation 5.5, and therefore a lower estimate for enrichment.

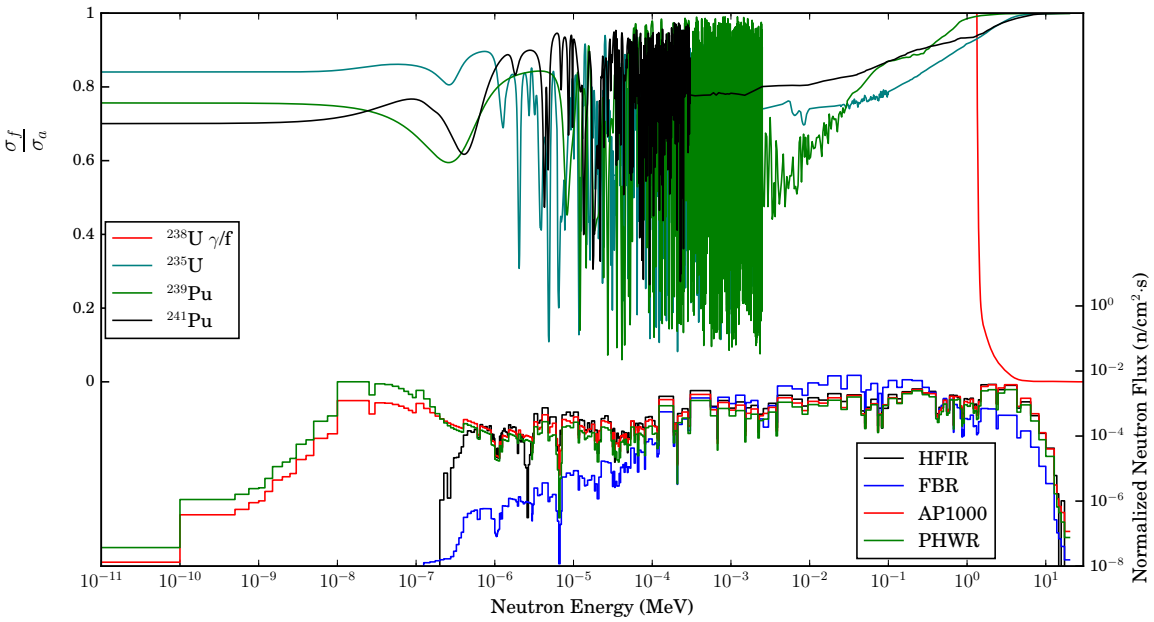

Figure 5.4: Fission over absorption cross sections plotted against flux spectra. Cross section data used ENDF/B VII[13] and the fast neutron flux spectra are reprinted with permission from[69] and the thermal flux spectra are reprinted with permission from[85].

5.5. Reactor Type

In section 4.6 Equation 4.31 describes the calculation for determining the residual with an assumed reactor flux spectra. Many different reactor spectra should be used in this analysis to solve for the residual, and the minimum residual would result the most likely

reactor candidate.

Experimentally determined values of N^1 to N^4 remain constant from spectra to spectra, whereas the cross sections, yields and burnup estimates change. This is because yields need to be averaged between thermal and fast fissions of each fissioning isotope and cross sections need to be averaged across spectra.

A normal and an effective yield was determined for the isotopes ^{108}Pd, ^{113}Cd, ^{137}Cs, ^{143}Nd, ^{148}Nd, ^{149}Sm, and ^{153}Eu. The effective yield was determined with Equation 5.6, where i refers to the isotope, and $i-1$ refers to the isotope minus a neutron. The reason why an effective yield was attempted was to alleviate concerns for contributions and losses due to radiative capture as well as to show the variation in results with different inputs. The methodology behind Equation 4.31 only requires 5 independent equations, and it was stated that the burnup information does not have to be one of them. Therefore, conditions where the burnup equation was not included were tested as well.

In order to utilize information from all available isotopes, the residual was calculated for each of the four conditions (effective yield, regular yield, burnup equation included, burnup equation not included) under all combinations and the standard deviation among results was determined. The results are shown in Table 5.13 in arbitrary units of millimoles for readability as the units in Equation 4.31 are in atoms.

$$\gamma_i^* = \gamma_i + \frac{\gamma_{i-1}\phi\sigma_{a,i-1}}{\phi\sigma_{a,i-1}+\lambda_{i-1}} - \frac{\gamma_i\phi\sigma_{a,i}}{\phi\sigma_{a,i}+\lambda_i} \tag{5.6}$$

The standard deviation is not shown in Table 5.13 because in the cases where burnup was included, it was not more than one percent. In the cases where it not was included, the standard deviation using the normal yield was around 25% and using an effective yield, it jumped up to around 50%. In all cases though, the thermal reactors had the smallest residual results. It seems that a thermal system is more likely to have produced the fission

Table 5.13: Calculated residual of reactor type calculation using four different flux spectra with four different sets of inputs.

R (millimoles)	HFIR Flux Spectrum	FBR Blanket Flux Spectrum	AP1000 Flux Spectrum	PHWR Flux Spectrum
γ with BU	13.136	13.632	8.107	7.489
γ^* with BU	13.148	13.641	8.115	7.497
γ w/o BU	0.653	0.680	0.311	0.270
γ^* w/o BU	0.805	0.754	0.425	0.382

product compositions seen in the sample.

The residual calculation utilizes measurements of several different fission products and in a scenario where a fission product measurement is inaccurate the entire average residual calculation will be larger. For example, if the ^{137}Cs content were multiplied by a factor of 5, then the residual calculation would show that the fast reactor systems have a smaller residual value (~ 0.8 compared to ~ 0.9 millimole, shown in Table 5.14). This leads to problems with the residual model in cases where erroneous isotope concentrations are measured. In order to help reduce the potential for error, it is advisable to have more than 4 isotopes included in the calculations. This way, residual calculations can be compared when certain isotopes are not included. For example, if ^{108}Pd, ^{113}Cd, ^{137}, ^{143}Nd, and ^{148}Nd were measured and used in a residual calculation, the residual could be calculated 5 different different times, each calculation excluding an isotope. If the 5 different residuals are roughly the same, then the calculations are in agreement, but if a single calculation has a drastically smaller residual than the other 4, then the isotope that was excluded for the calculation probably has error associated with it. The case where the ^{137}Cs concentration was increased by a factor of 5 is shown in Table 5.14, where each row has a particular isotope excluded in the residual calculation and each column represents a different reactor type.

Table 5.14 shows that the residual for when ^{137}Cs is excluded is drastically different than for the others and if it is excluded, the residual again reflects values as seen in Table 5.6. This provides some check for erroneous measurements.

Table 5.14: Calculated residual with ^{137}Cs concentration increased by a factor of 5. Each row shows the average residual when the isotope in the first column is not included in the calculation. Each column utilizes a different reactor type.

	HFIR	FBR Blanket	AP1000	PHWR
R (millimoles)	Flux Spectrum	Flux Spectrum	Flux Spectrum	Flux Spectrum
^{108}Pd	0.829	0.822	0.968	0.990
^{113}Cd	0.876	0.869	0.986	1.005
^{137}Cs	0.514	0.533	0.264	0.234
^{143}Nd	0.788	0.772	0.983	1.010
^{148}Nd	0.876	0.868	0.994	1.015
^{149}Sm	0.870	0.863	0.989	1.009
^{153}Eu	0.891	0.884	1.003	1.024
Average	0.803	0.799	0.879	0.893

5.6. Fuel Age

The Bateman solver used to estimate the fuel age was checked to see if the the concentrations of ^{137}Cs and ^{148}Nd increased linearly as a function of burnup. In order to do this, an independent calculation for burnup must be provided. Equation 5.7 was used for this purpose,

$$\text{BU} = \frac{\sum_{i=1}^{N} \int_0^t \phi \sigma_{f,i} N_i E_{R,i}}{\text{tHM}} \tag{5.7}$$

where:

i is summed over fissionable isotopes.

The production of ^{137}Cs and ^{148}Nd should follow what is described in Equation 5.8 below, which is modified from Equation 4.3 with unit conversions provided so that the units of the production are mg/MWd.

$$\frac{m_B}{BU \cdot m_{\text{HM}}} = \frac{\gamma_B}{E_R} \cdot \frac{M_B \times 10^3}{C \cdot N_A} \tag{5.8}$$

where:

m_B = mg mass of isotope B

BU = burnup in units of MWd/tHM

m_{HM} = mass of initial heavy metal in tons

γ_B = *effective* atomic yield fraction for isotope B

E_R = average energy per fission [MeV/fission]

C = Conversion Factor 1.85×10^{-24} [MWd/MeV]

M_B = molar mass for isotope B

Both sides of Equation 5.8 should give the same number. In order to determine this slope with the simulation data a zero intercept line is fit to the mass of both fission products to the burnup as determined with Equation 5.7. The results of these analyses are shown in Table 5.15, where the right hand of Equation 5.8 utilized an effective yield for ^{148}Nd. The ^{137}Cs number matches a rough estimate from Fig. 18.5 in the PANDA manual[75]. The plots of these two fission products as a function of burnup are shown in Figure 5.5 for the faster spectra and Figure 5.6 for the thermal spectra.

All systems were irradiated to twice the irradiation time estimated in Section 5.3. This was done so that end points could be chosen that were after the EOI defined in Section 5.3.

Table 5.15: Fission product production as calculated with Burnup, average yield, and the Bateman simulation for ^{137}Cs and ^{148}Nd using four different flux spectra.

	Slope $\frac{mg}{MWd}$	HFIR Flux Spectrum	FBR Blanket Flux Spectrum	AP1000 Flux Spectrum	PHWR Flux Spectrum
^{137}Cs	Simulation	38.1	37.2	38.1	37.9
	Burnup	35.5	35.5	37.6	38.0
	Yield	35.6	35.6	37.7	38.1
^{148}Nd	Simulation	11.3	10.2	12.2	12.4
	Burnup	11.5	11.5	12.2	12.3
	Yield	11.6	11.6	12.2	12.4

It should be noted that twice the irradiation time does not correlate to twice the burnup because burnup increased exponentially as a function of time due to the build-in of ^{239}Pu. This is shown in Figure 5.7.

Figure 5.5 would indicate that the faster systems, under the conditions of the high flux and longer irradiation times, would have very large burn-ups. These results could be erroneously high if the one-group cross sections were calculated high, but also the absurdly large burn-ups probably indicate that these two fast systems were probably not the systems where by most of the burnup occurred. Figure 5.6 shows much more reasonable burnup ranges for the sample.

Each set of calculated values, such as the burnup, scalar flux, and time in the reactor, were used as inputs in the Bateman solver. Each flux spectrum was used to determine one-group cross sections for the tracked isotopes as well as average yields for the fission products. ENDF/B-VII cross section libraries from MCNP6[88] and SERPENT[89] were used. Four different stopping points for the simulation were chosen, the first being the calculated time in reactor from Section 5.3, the second being the end burnup as calculated in Section 5.1, and the third and fourth being the concentrations of ^{137}Cs and ^{148}Nd. The second and third stopping points should be very close, as Table 5.15 indicates.

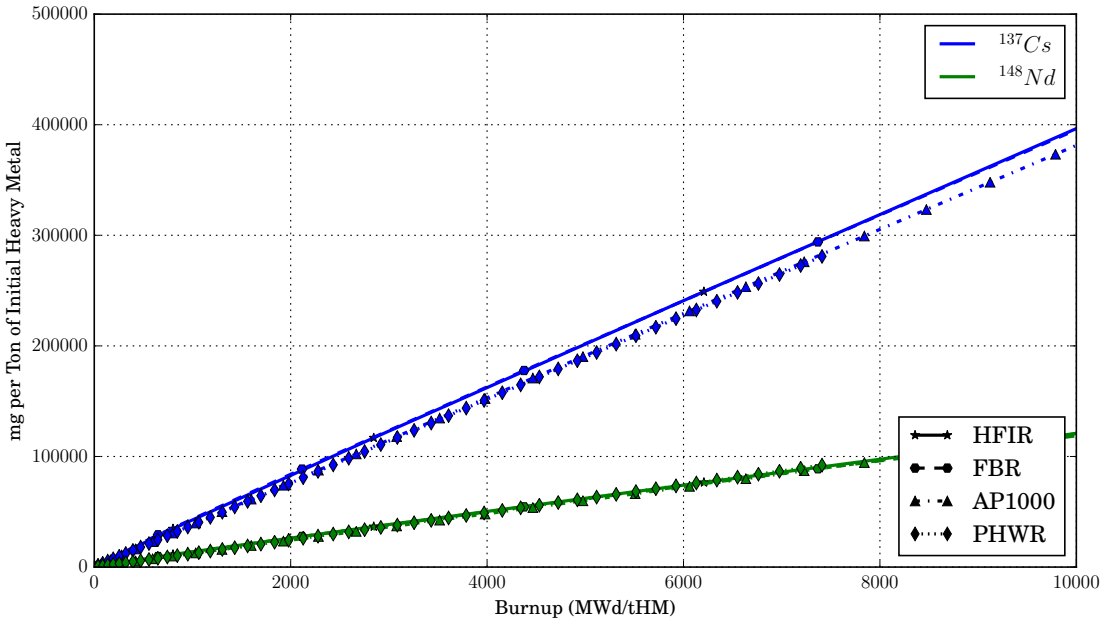

Figure 5.5: Mass of ^{137}Cs and ^{148}Nd as functions of burnup for the four different reactor systems.

The calculated concentrations of isotopes ^{235}U, ^{236}U, ^{238}U, ^{239}Pu, and ^{240}Pu were determined at the four stop points described above. These concentrations were then compared with the actual concentrations as determined with mass spectrometry and the ratio of simulated results over experimental results are shown in Tables 5.16–5.19, where the difference in the time estimated in Section 5.3 to the other stopping points is also shown. For example, in Table 5.16 to reach the endpoint for burnup, the system had to be irradiated for only 20% of the time estimated in Section 5.3 (-79%) to reach the burnup calculated in Section 5.1. The reason why the ΔT is different for each column is because the stop time was different for each column, as described in the previous paragraph. Each Δ was shown in reference to the time estimated in Section 5.3

The simulation over experiment results shown in Tables 5.16 and 5.17 show the ratios

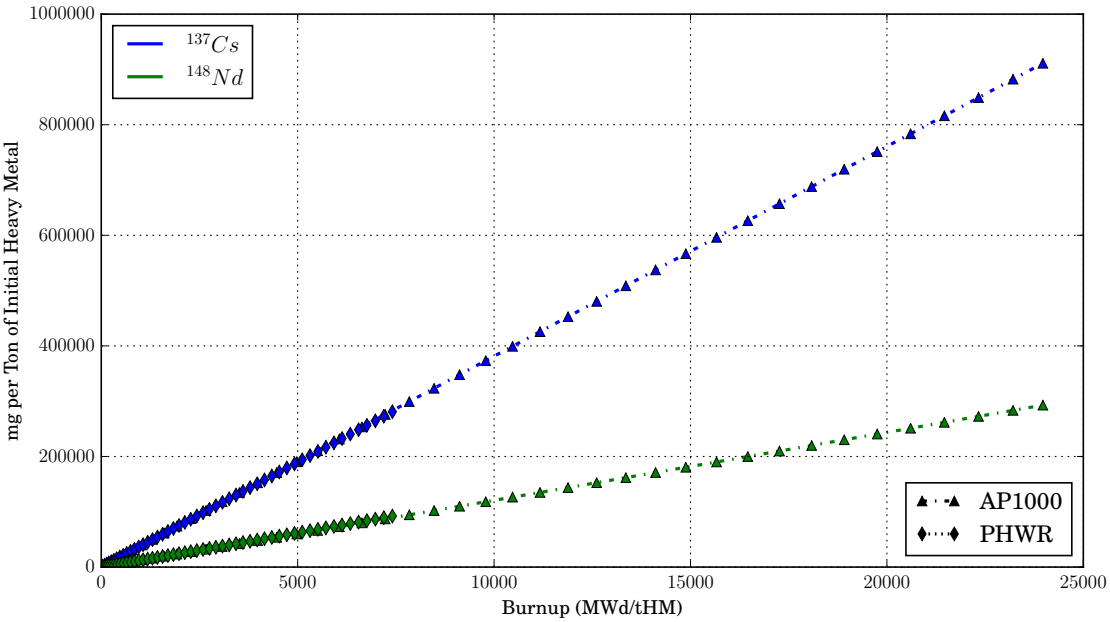

Figure 5.6: Mass of ^{137}Cs and ^{148}Nd as functions of burnup for the thermal reactor systems.

Table 5.16: Simulation over Experiment Ratios for the HFIR flux spectra assuming different stop times.

HFIR	EOI	Burnup	^{137}Cs Conc.	^{148}Nd Conc.
	ΔT = -0%	ΔT = -79%	ΔT = -81%	ΔT = -80%
^{235}U	0.8	1.6	1.7	1.7
^{236}U	6.4	1.9	1.8	1.8
^{238}U	0.7	1.0	1.0	1.0
^{239}Pu	9.0	3.0	2.8	2.9
^{240}Pu	5.1	1.7	1.6	1.6

for the faster systems. It can be seen that at every one of these stopping points, most of the ratios are very far from unity, meaning that these simulations using these flux spectra do not properly capture what happened during irradiation.

Tables 5.18 and 5.19 have values closer to unity. In all simulations a higher ^{236}U

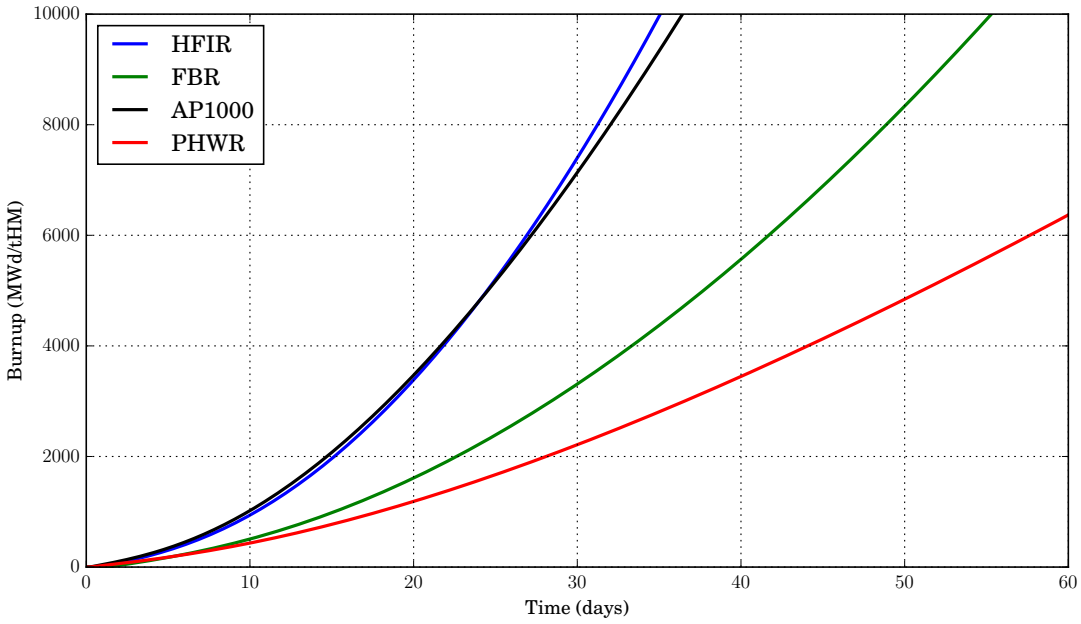

Figure 5.7: Burnup as a function of time for four different reactor systems

Table 5.17: Simulation over Experiment Ratios for the FBR flux spectra assuming different stop times.

FBR	EOI ΔT = -0%	Burnup ΔT = -81%	^{137}Cs Conc. ΔT = -83%	^{148}Nd Conc. ΔT = -82%
^{235}U	0.5	1.5	1.5	1.5
^{236}U	5.7	1.9	1.8	1.9
^{238}U	0.7	1.0	1.0	1.0
^{239}Pu	11.2	3.6	3.4	3.5
^{240}Pu	41.1	3.2	2.8	3.0

concentration is estimated than what was measured experimentally. This is probably due to the fact that gadolinium has a large resonance near where ^{235}U also has a resonance absorption around 2.5 eV. The plutonium production in the PHWR spectrum is much lower than in the sample. This could be due to the lower flux used for the PHWR system.

Table 5.18: Simulation over Experiment Ratios for the AP1000 flux spectra assuming different stop times.

AP1000	EOI ΔT = -0%	Burnup ΔT = -26%	^{137}Cs Conc. ΔT = -27%	^{148}Nd Conc. ΔT = -26%
^{235}U	0.8	0.9	0.9	0.9
^{236}U	1.5	1.2	1.2	1.2
^{238}U	1.0	1.0	1.0	1.0
^{239}Pu	0.9	0.7	0.7	0.8
^{240}Pu	1.7	1.1	1.1	1.2

Table 5.19: Simulation over Experiment Ratios for the PHWR flux spectra assuming different stop times.

PHWR	EOI ΔT = -0%	Burnup ΔT = 40%	^{137}Cs Conc. ΔT = 40%	^{148}Nd Conc. ΔT = 40%
^{235}U	0.6	0.5	0.5	0.5
^{236}U	1.0	1.3	1.3	1.3
^{238}U	1.0	1.0	1.0	1.0
^{239}Pu	0.3	0.3	0.3	0.3
^{240}Pu	0.5	0.8	0.8	0.8

The time since removal was determined with isotopes ^{106}Ru, ^{144}Ce, and ^{137}Cs at the four different stopping points. These results for the four spectra are shown in Tables 5.20–5.23. The average and standard deviation are displayed at the bottom of each table. The irradiation ended 6/1/2013 and the sample was dissolved 5/2/2014. This analysis should report a decay time of 335 days.

It should be noted that some of the averages in Tables 5.20–5.23 are unrealistic. This is indicative that the stopping time is probably not correct. For example, if a particular reactor was irradiated to the EOI stopping time had an estimated decay time of 17,000 days, then this point can be disregarded as reactors did not exist 47,000 years ago. In cases

where negative values are reported, the final calculated value of an isotope was *less* than what was measured experimentally and these points can also be disregarded.

Another interesting note for this calculation is the variation of ^{137}Cs estimations whereas the other two estimation isotopes (^{106}Ru and ^{144}Ce) do not have as much variation with different stopping time. This is due to the fact that ^{137}Cs is always linearly increasing in the fuel matrix as a function of time because of its low absorption cross section. The other two isotopes have non-negligible absorption cross sections and their concentration changes as a function of time less rapidly than ^{137}Cs. For longer irradiations, their concentrations can be steady state due to an equilibrium of production and loss.

Each system has a minimum percent standard deviation of the decay times and these values, which correspond to a stopping point, were chosen for the estimated decay time for each system. With this criteria, the estimates for the HFIR, FBR, AP1000, and the PHWR systems are 320, 322, 385, and 256 days, respectively.

Table 5.20: Decay time (days) estimates for the HFIR flux spectra assuming different stop times.

HFIR	EOI ΔT = -0%	Burnup ΔT = -79%	^{137}Cs Conc. ΔT = -81%	^{148}Nd Conc. ΔT = -80%
^{106}Ru	2116.1	533.9	462.9	499.0
^{144}Ce	1491.2	363.1	314.5	339.2
^{137}Cs	47675.2	2154.6	183.2	1184.5
Avg	17094.2	1017.2	320.2	674.2
STD	26485.8	988.7	140.0	449.1

5.7. Cumulative Forensic Results

The above analyses are combined in Table 5.24 below, where actual experimental values are depicted next to the calculated values. With these results, the AP1000 spectrum

Table 5.21: Decay time (days) estimates for the FBR flux spectra assuming different stop times.

FBR	EOI ΔT = -0%	Burnup ΔT = -81%	^{137}Cs Conc. ΔT = -83%	^{148}Nd Conc. ΔT = -82%
^{106}Ru	2027.3	499.8	426.0	463.6
^{144}Ce	1445.3	366.0	316.4	341.7
^{137}Cs	47251.1	2262.6	223.1	1260.9
Avg	16907.9	1042.8	321.8	688.7
STD	26279.6	1058.5	101.6	499.2

Table 5.22: Decay time (days) estimates for the AP1000 flux spectra assuming different stop times.

AP1000	EOI ΔT = -0%	Burnup ΔT = -26%	^{137}Cs Conc. ΔT = -27%	^{148}Nd Conc. ΔT = -26%
^{106}Ru	752.1	446.1	436.7	455.4
^{144}Ce	529.0	322.9	316.7	329.1
^{137}Cs	8774.1	386.1	131.7	638.1
Avg	3351.8	385.0	295.0	474.2
STD	4697.2	61.6	153.7	155.3

Table 5.23: Decay time (days) estimates for the PHWR flux spectra assuming different stop times.

PHWR	EOI ΔT = -0%	Burnup ΔT = 40%	^{137}Cs Conc. ΔT = 40%	^{148}Nd Conc. ΔT = 40%
^{106}Ru	82.0	397.3	397.3	397.3
^{144}Ce	119.3	312.4	312.4	312.4
^{137}Cs	-8087.1	58.4	58.4	58.4
Avg	-2628.6	256.0	256.0	256.0
STD	4727.2	176.3	176.3	176.3

was closest to the actual values for the initial enrichment and decay time and was second closest in determining irradiation time. Although the PHWR had a lower residual, the AP1000 seemed to produce closer results. The sample initially started in a thermal cut off HFIR type flux spectra, and near the end of irradiation most of the burnup in the sample was due to a thermal system which is why the thermal spectra seemed to produce the best results.

5.8. Average HFIR Flux Spectra

Due to the fact that the DUO_2 was subject to a changing flux spectra, the above analysis did not have HFIR calculated values that were the closest to the actual temporal irradiation conditions. To resolve this discrepancy, a temporal average flux spectra was suggested as an input for the forensic algorithm. Calculations utilized an average flux spectra, $\phi(E)_{\text{avg}}$, as determined with Equation 5.9.

$$\phi(E)_{\text{avg}} = \sum_{i=1}^{N} \phi(E)_i \cdot f_i \tag{5.9}$$

where:

i = the step of irradiation (for example $i = 1$ would be the step of irradiation starting at time = 0 days and ends at the time when $i = 2$ starts (for the MCNP simulation this would be 0.3 days))

f_i = the fraction that irradiation step i contributes towards the total flux spectra, where $\sum f_i = 1$

Equation 5.10 was used to determine the f_i values.

$$f_i = \left(\frac{m_{j,i} - m_{j,i-1}}{m_{\text{tot}}}\right) \cdot \frac{1}{2} + \left(\frac{m_{j,i+1} - m_{j,i}}{m_{\text{tot}}}\right) \cdot \frac{1}{2} \tag{5.10}$$

Table 5.24: Summary table for nuclear forensic analysis.

Attribute	HFIR Flux Spectrum	FBR Blanket Flux Spectrum	AP1000 Flux Spectrum	PHWR Flux Spectrum	Actual
BU $\left[\frac{\text{MWd}}{\text{tHM}}\right]$	$(4.64\pm0.35)\cdot10^3$	$(4.64\pm0.35)\cdot10^3$	$(4.39\pm0.33)\cdot10^3$	$(4.34\pm0.32)\cdot10^3$	$(4.36\pm0.28)\cdot10^3$ [66]
ϕ $\left[\frac{\text{n}}{\text{cm}^2\text{s}}\right]$	$4.61\cdot10^{15}$	$1.56\cdot10^{16}$	$2.55\cdot10^{15}$	$1.05\cdot10^{15}$	$1.73\cdot10^{15}$
T_{irr} (days)	114	195	31	33	50
ϵ_i (wt%)	0.428	0.425	0.291	0.216	0.28
R (mmol)	13.1	13.6	8.1	7.5	
T_{decay} (days)	$(3.20\pm1.40)\cdot10^2$	$(3.22\pm1.02)\cdot10^2$	$(3.85\pm0.62)\cdot10^2$	$(2.56\pm1.76)\cdot10^2$	$3.35\cdot10^2$

where:

Equation 5.10 reduces to $(0.5/m_{\text{tot}}) \cdot (m_{j,i+1} - m_{j,i-1})$ when i does not equal 1 or N (when $i = 1$, the first term in Equation 5.10 is used and when $i = N$ the second term is used)

$m_{j,i}$ refers to the mass of isotope j at the start of irradiation step i

Assuming an MCNP simulation were provided for the HFIR simulation[66], which would have masses of isotopes at different burn steps, the only thing left to determine for an average HFIR flux spectra would be the isotope used to determine the f values. Initial calculations for the forensic analysis used ^{137}Cs as the weighting isotope, but individual calculations where single group heavy metal cross sections were used (like the enrichment calculation) turned out to be very inaccurate. The reason for this is because the mass of ^{137}Cs was largely influenced during the irradiation where the DUO_2 pellet was in a more thermal spectra, due to an increased fission rate. This is shown in Swinney's work[66] where the mass of ^{137}Cs increased exponentially as a function of time. This is contrasted with ^{239}Pu, where its mass as a function of time was roughly linear. This means that the mass of ^{239}Pu in the pellet was more a function of the epithermal flux, which was relatively constant. If the average flux spectra as determined from ^{137}Cs were used to determine a single group cross section for ^{239}Pu, then the single group cross section for ^{239}Pu would be too high, because ^{137}Cs weights the flux spectra towards the thermal flux.

This is why two different average HFIR flux spectra were used. Equation 5.10 was used with ^{137}Cs to determine an average HFIR flux spectra for weighting fission products cross sections and Equation 5.10 was used with ^{239}Pu to determine an average HFIR flux spectra for weighting heavy metal cross sections. With this, the forensic analysis produces results that are the best of all the different reactors.

The two different average flux spectra are shown in Figure 5.8 and the results from the

forensic analysis using these flux spectra are shown in Table 5.25. If the results from this table are compared with Table 5.24, the values across the board are closer to actual values and the reactor residual is the smallest.

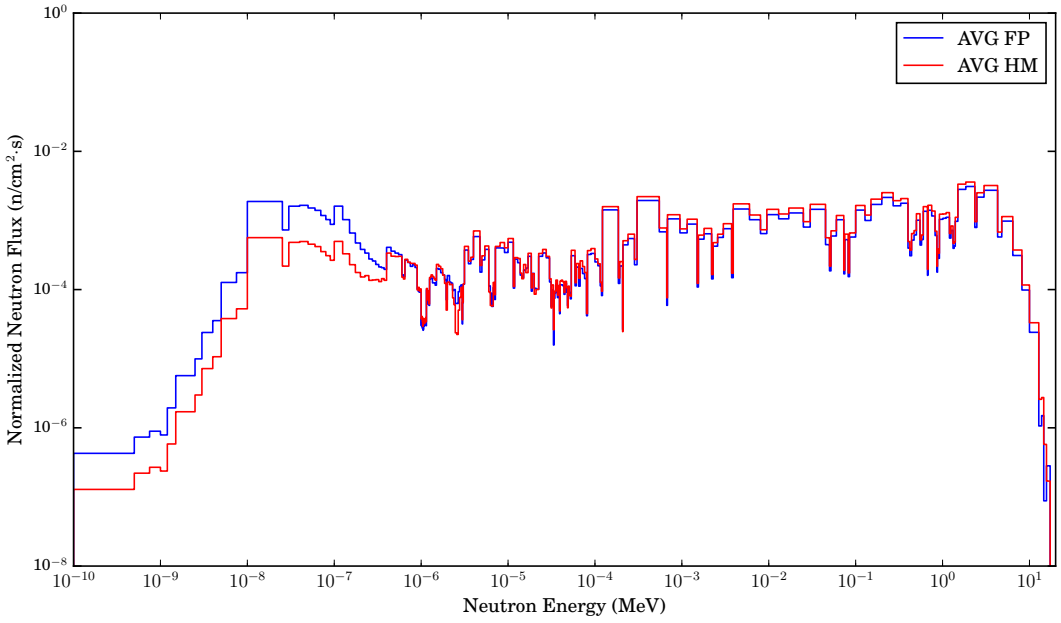

Figure 5.8: Two different average HFIR flux spectra. The fission product neutron average used ^{137}Cs and the heavy metal neutron flux average used ^{239}Pu.

5.9. Sensitivity Analysis

A basic sensitivity analysis is provided in this section. The ^{137}Cs input content was varied by $\pm$ 10% in 1% increments. All the forensic calculations were repeated at each concentration of ^{137}Cs. All the results presented in this section used the average HFIR flux spectra from section 5.8. When the values for the sensitivity parameters were known, they are highlighted in red color on the plots.

Table 5.25: Summary table for the average HFIR neutron flux analysis.

Attribute	HFIR Flux Spectrum	Actual
BU $\left[\frac{\text{MWd}}{\text{tHM}}\right]$	$(4.42\pm0.33)\cdot10^3$	$(4.36\pm0.28)\cdot10^3$ [66]
ϕ $\left[\frac{\text{n}}{\text{cm}^2\text{s}}\right]$	$1.62\cdot10^{15}$	$1.73\cdot10^{15}$
T_{irr} (days)	45	50
ϵ_i (wt%)	0.265	0.26
R (mmol)	4.4	
T_{decay} (days)	$(3.56\pm0.88)\cdot10^2$	$3.35\cdot10^2$

Figures 5.9 to 5.13 below show that when the ^{137}Cs concentration is varied, the results of each forensic calculation vary as well. ^{137}Cs was chosen for this analysis because all the calculations depend on this concentration. The initial enrichment calculations have plateaus because the convergence criteria was such that local minimum did not vary much with changing ^{137}Cs concentrations.

The time since removal from reactor calculation, shown in Figure 5.13, has sporadic behavior because the decay time was chosen based on the standard deviation of decay estimates from several isotopes given a particular irradiation time. There were four different stopping times chosen, and the jumping behavior is due to the fact that the standard deviations between two stopping times were similar.

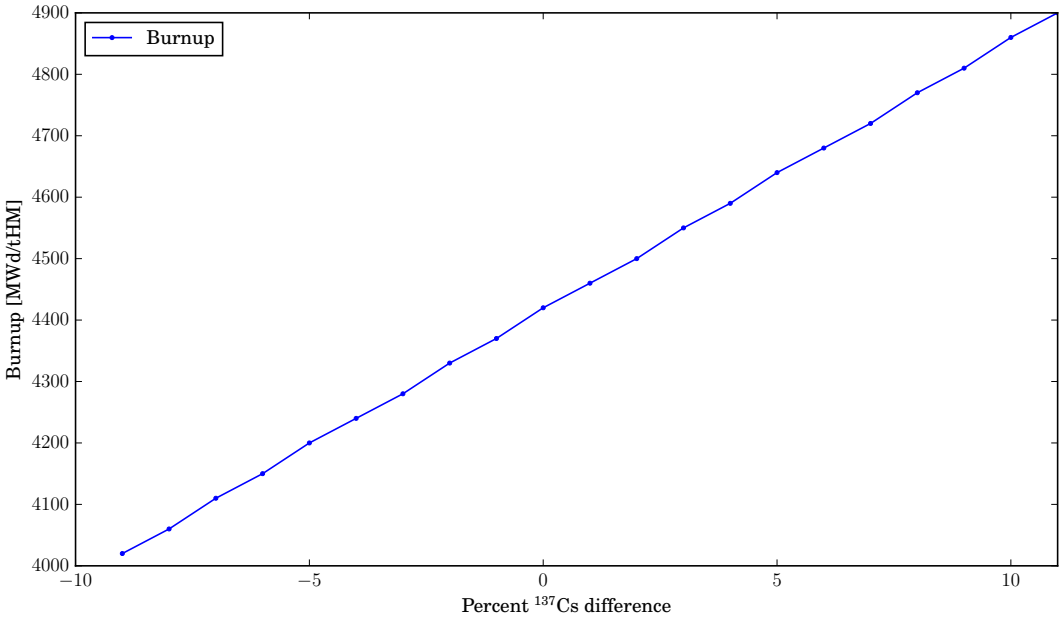

Figure 5.9: Burnup as a function of varied ^{137}Cs input.

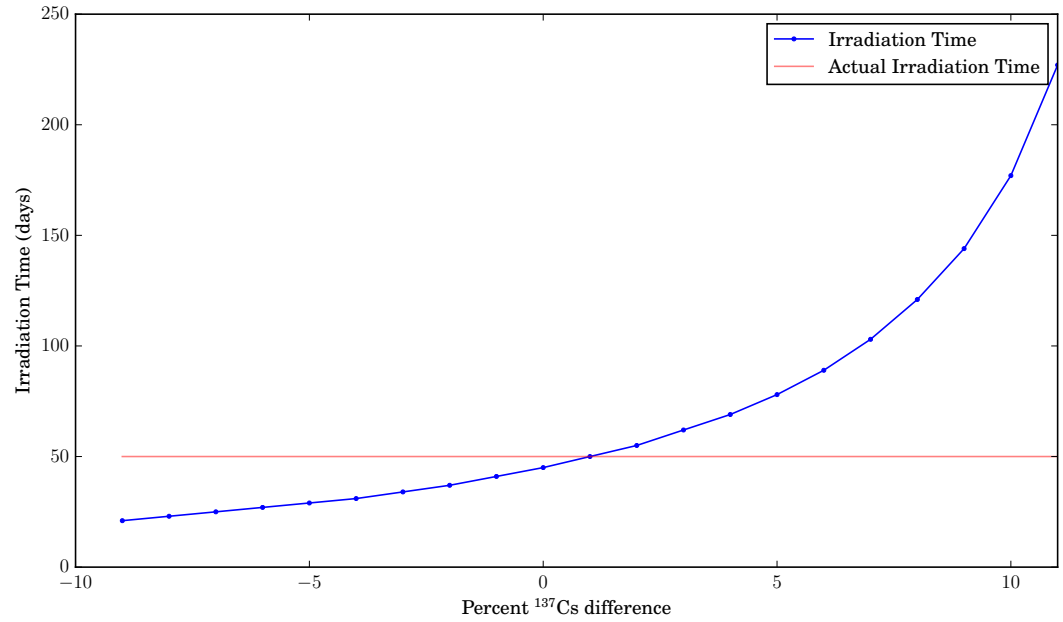

Figure 5.10: Irradiation time as a function of varied ^{137}Cs input.

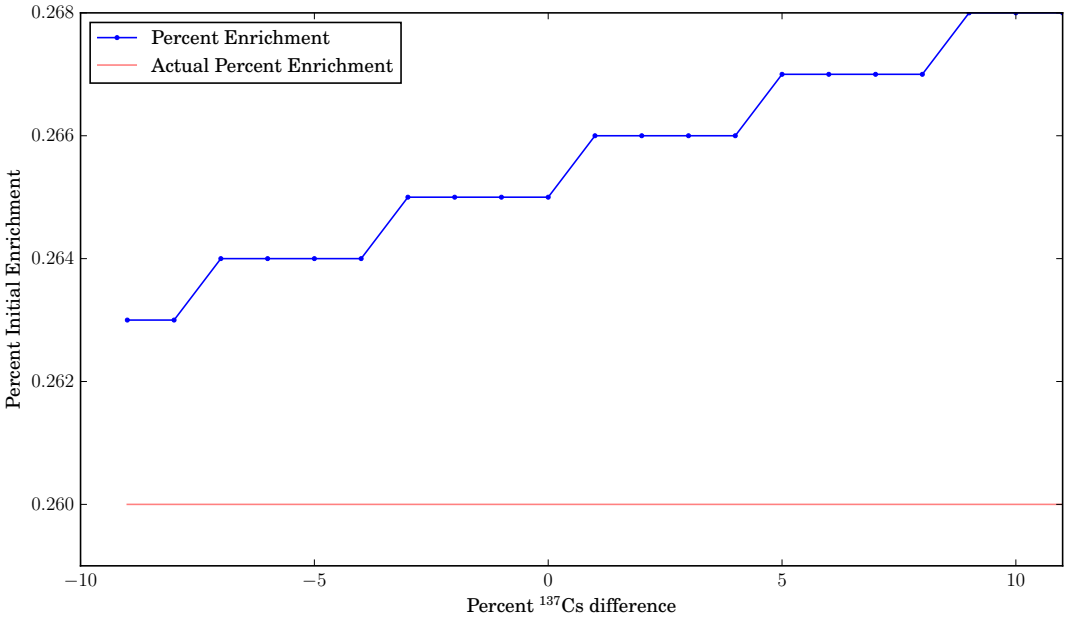

Figure 5.11: Enrichment as a function of varied ^{137}Cs input.

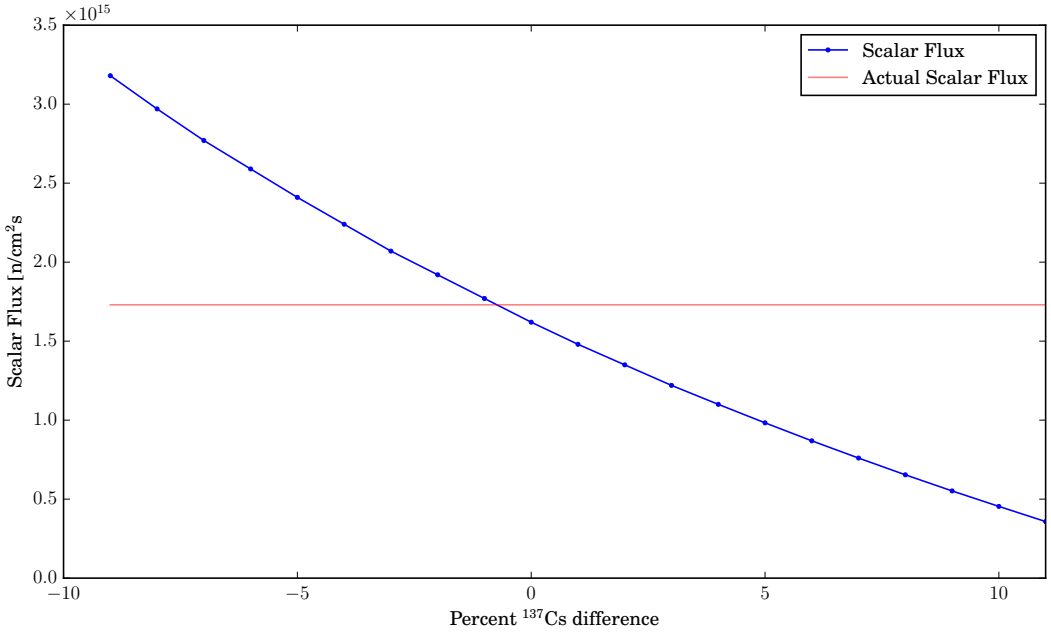

Figure 5.12: Scalar flux as a function of varied ^{137}Cs input.

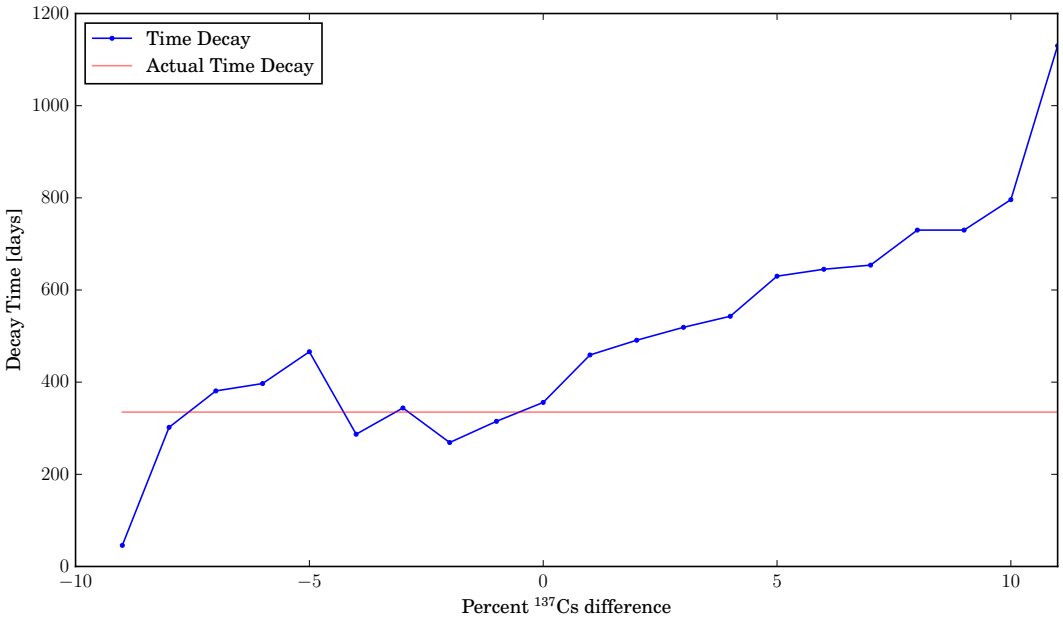

Figure 5.13: Decay time as a function of varied ^{137}Cs input.

6. CONCLUSIONS AND FUTURE WORK

6.1. Conclusions

Decontamination factors and distribution coefficients for a bench-top scale PUREX process for important forensics attribution elements (Cs, Eu, Rb, Sr, Nd, Pm, Sm, U, and Pu) were experimentally determined. The DFs were used in a developed forensics methodology to determine fuel burnup, reactor neutron scalar flux, irradiation time in reactor, initial enrichment, and fuel age associated with Pu production.

6.1.1. Experimental Conclusions on DFs and DCs

Seven different PUREX separation experiments were conducted each providing progression towards the final goal of determining elemental decontamination factors. The first 4 experiments were geared towards ensuring that plutonium made it to the product solution in the PUREX process. Later experiments were used to determine elemental DFs as well as DCs.

DFs for a mega cycle, with respect to Pu, for the elements U, Mo, Ru, Ce, Sm, Sr, Pm, Eu, Nd, Pd, and Cd were measured with mass spectrometry. DFs as well as DCs were determined with gamma spectroscopy for Cs, Ru, Ce, and Eu. In two sequential mega cycles, 93% of the Pu was recovered in a product solution with less than 1% of the original U.

Elements with very minimal extraction in these conditions, like Cs, with a distribution coefficient less than one part in a thousand had some variability in decontamination factors between experiments because a small amount of contamination from the aqueous phase causes a large difference in the amount of Cs that would be in the organic phase otherwise. A decontamination factor of 785 ± 491 was a achieved for Cs for a mega cycle, with the error coming from the standard deviation among different experiments. An experiment

under similar conditions achieved 93% of Pu recovered in a product solution with less than 1% of the original U.

In the course of these experiments, the pellet composition was also characterized. The final enrichment of the uranium was measured to be 0.28 wt.% ^{235}U, as compared to 0.22 wt.% for the actual sample. The plutonium isotopic analysis of the sample showed 89.3 wt.% of ^{239}Pu. The mass fraction of fission products was estimated to be 0.3%.

The mathematical correlation between DCs and DFs for a mega cycle was derived and used to compare with DFs calculated directly from initial and final PUREX sample solutions. The ratios of DFs for Cs, Ru, Ce, and Eu, from these two methods were calculated to be 1.5, 1.0, 0.99, and 0.91 respectively.

6.1.2. Forensic Conclusions

A forensic methodology was developed and tested with experimental results obtained from the investigations of an irradiated fuel sample. The irradiated sample saw both a fast and thermal neutron spectra during irradiation because the gadolinium burned out during the course of irradiation deviating from the plans. The reactor parameters determined from the developed forensics methodology were fuel burnup, scalar neutron flux, time of irradiation in reactor, initial ^{235}U enrichment, and time since removal from the reactor. The parameters were determined in the order listed because each calculation was built on top of each other.

Four different reactor spectra were utilized in the forensic methodology, two fast and two thermal reactors. These flux spectra were used to determine one-group cross sections to be fed into various calculations required for forensic methodology analysis. They were also used with the pellet concentrations to estimate the fraction of fissions associated with different fissionable elements. Averaged yields and energy per fission were calculated with the fraction of fission results.

Among the four reactor spectra, the AP1000 spectrum was closest to the actual values for the initial enrichment and decay time. The AP1000 was also the second closest in determining irradiation time. This indicates that the sample received the majority of its burnup while in a thermal spectra. The calculated parameters using the AP1000 flux spectrum estimated the sample to have a burnup of 4390 [MWd/tHM], a scalar flux of 2.55×10^{15} [n/cm^{2}s], 31 days of irradiation, an initial uranium enrichment of 0.29 wt.% ^{235}U, and 385 days between removal from reactor and the date 5/2/2014. However, since the experimental irradiation was done in HFIR this match with AP1000 was perplexing. Further investigations suggested the use of an average HFIR irradiation spectra instead of using HFIR spectra at the beginning of irradiation.

The forensics calculation using average HFIR spectra had calculated values closer than that of even the AP1000 because it was more representative of what the sample saw during irradiation. With the average HFIR spectra, the sample was estimated to have a burnup of 4420 [MWd/tHM], a scalar flux of 1.62×10^{15} [n/cm^{2}s], 45 days of irradiation, an initial uranium enrichment of 0.27 wt.% ^{235}U, and 356 days between removal from reactor and the date 5/2/2014. The initial scalar flux for the sample was estimated with MCNP as 1.73×10^{15} [n/cm^{2}s], there were 50 days of irradiation, the initial uranium enrichment was 0.28 wt.% ^{235}U, and there were actually 355 days between removal from the reactor and the date 5/2/2014.

6.2. Future Work

Future work that can be undertaken as a continuation of the research presented here are:

1. This methodology centers around DFs, and their usefulness in determining initial concentrations of certain isotopes in spent, unpurified, fuel. Error quantification based on sensitivity of the DFs on variable parameters such as concentration and

temperatures are areas of further investigations to define ranges of applicability.

2. Uncertainty in the attribution methodology was not pursued because of the added complexity of incorporating the uncertainty in the single group neutron reaction cross sections. More rigorous calculation in the forensic parameters would include uncertainty in the single group cross sections calculated.

3. DCs were used to calculate DFs given a chemical process. In order to expand the number of processes whereby a DF could be estimated (for our "important" elements), DCs over broad range of values should be determined.

4. Compare results of DFs that were calculated with DCs with measured DFs for a reprocessing plant.

5. The process described above determined DFs for one of the steps that would need to be taken in order to use Pu in a nuclear weapon. In order to use this methodology if interdicted material were processed further, DFs for other steps would need to be considered (e.g. converting to metal)

6. Determine DFs for particular reprocessing plants and estimate their variance. This approach would be much easier, but if a reprocessing plant changes their operating conditions, then DF values would change.

7. Incorporation of time dependence in forensic analysis would be useful in cases where a changing neutron flux is expected.

8. Flux spectra utilized MCNP generated neutron flux spectra for analysis. Attempts were made at fitting thermal, epithermal, and fast portions of these neutron spectra with poor success for the faster spectra. Better neutron flux fitting could occur with utilization of cross section weighting.

REFERENCES

[1] *Nuclear Forensics: A Capability at Risk (Abbreviated Version)*. Washington, DC: The National Academies Press, 2010.

[2] AAAS/APS, "Nuclear forensics: Role, state of the art and program needs," report, AAAS/APS, 2008.

[3] K. Mayer, M. Wallenius, and I. Ray, "Nuclear forensics–a methodology providing clues on the origin of illicitly trafficked nuclear materials," *Analyst*, vol. 130, no. 4, pp. 433–441, 2005.

[4] M. Benedict, H. Levi, and T. Pigford, "Nuclear chemical engineering," *Nucl. Sci. Eng.*, vol. 82, no. 4, 1982.

[5] S. S. Chirayath, J. M. Osborn, and T. M. Coles, "Trace fission product ratios for nuclear forensics attribution of weapons-grade plutonium from fast and thermal reactors," *Science & Global Security*, vol. 23, no. 1, pp. 48–67, 2015.

[6] M. R. Scott, *Nuclear forensics: attributing the source of spent fuel used in an RDD event*. Thesis, 2005.

[7] A. Glaser, "Isotopic signatures of weapon-grade plutonium from dedicated natural uranium-fueled production reactors and their relevance for nuclear forensic analysis," *Nuclear Science and Engineering*, vol. 163, no. 1, pp. 26–33, 2009.

[8] "International atomic energy agency." https://www.iaea.org/. Accessed: 2017-04-12.

[9] J. Doyle, *Nuclear Safeguards, Security and Nonproliferation: Achieving Security with Technology and Policy*. Elsevier, 2011.

[10] "The national museum of American history." http://americanhistory.si.edu/subs/history/timeline/different/nuclear_deterrence.html. Accessed: 2017-04-12.

[11] M. A. Levi, "Deterring nuclear terrorism," *Issues in Science and Technology*, vol. 20,

no. 3, pp. 70 – 73, 2004.

[12] "IAEA incident and trafficking database (ITDB)." https://www-ns.iaea.org/downloads/security/itdb-fact-sheet.pdf. Accessed: 2017-04-12.

[13] M. Chadwick, M. Herman, P. Obložinskỳ, M. E. Dunn, Y. Danon, A. Kahler, D. L. Smith, B. Pritychenko, G. Arbanas, R. Arcilla, *et al.*, "Endf/b-vii. 1 nuclear data for science and technology: Cross sections, covariances, fission product yields and decay data," *Nuclear Data Sheets*, vol. 112, no. 12, pp. 2887–2996, 2011.

[14] E. M. Baum, H. D. Knox, and T. R. Miller, *Nuclides and isotopes: chart of the nuclides*. KAPL, 2010.

[15] M. Wallenius, K. Lutzenkirchen, K. Mayer, I. Ray, L. A. de las Heras, M. Betti, O. Cromboom, M. Hild, B. Lynch, A. Nicholl, H. Ottmar, G. Rasmussen, A. Schubert, G. Tamborini, H. Thiele, W. Wagner, C. Walker, and E. Zuleger, "Nuclear forensic investigations with a focus on plutonium," *Journal of Alloys and Compounds*, vol. 444-445, no. SPEC. ISS., pp. 57 – 62, 2007.

[16] M. Wallenius, P. Peerani, and L. Koch, "Origin determination of plutonium material in nuclear forensics," *Journal of Radioanalytical and Nuclear Chemistry*, vol. 246, no. 2, pp. 317–321, 2000.

[17] T. B. Cochran, W. M. Arkin, and M. M. Hoenig, *Nuclear weapons databook*, vol. 1. Ballinger, 1984.

[18] J. C. Marka, "Explosive properties of reactor-grade plutonium," *Science and Global Security*, vol. 4, no. 1, pp. 111–128, 1993.

[19] M. Wallenius, P. Peerani, and L. Koch, "Origin determination of plutonium material in nuclear forensics," *Journal of Radioanalytical and Nuclear Chemistry*, vol. 246, no. 2, pp. 317–321, 2000.

[20] S. Chetal, V. Balasubramaniyan, P. Chellapandi, P. Mohanakrishnan, P. Puthiyavinayagam, C. Pillai, S. Raghupathy, T. Shanmugham, and C. S. Pillai, "The design of

the prototype fast breeder reactor," *Nuclear Engineering and Design*, vol. 236, no. 7, pp. 852–860, 2006.

[21] A. G. M. Ramana, "Weapon-grade plutonium production potential in the indian prototype fast breeder reactor," *Science Global Security, Princeton University*, 2007.

[22] A. E. Waltar, D. R. Todd, and P. V. Tsvetkov, *Fast spectrum reactors*. Springer, 2012.

[23] L. R. Morss, N. M. Edelstein, and J. Fuger, *The Chemistry of the Actinide and Transactinide Elements*. Dordrecht : Springer, [2010] 4th ed., 2010.

[24] M. F. Simpson and J. D. Law, "Nuclear fuel, reprocessing of," in *Nuclear Energy*, pp. 153–173, Springer, 2013.

[25] K. J. Moody, I. D. Hutcheon, and P. M. Grant, *Nuclear forensic analysis*. CRC Press, 2014.

[26] O. H. Zabunoglu and L. Özdemir, "Purex co-processing of spent lwr fuels: flow sheet," *Annals of Nuclear Energy*, vol. 32, no. 2, pp. 151–162, 2005.

[27] A. P. Colburn, "Simplified calculation of diffusional processes," *Industrial & Engineering Chemistry*, vol. 33, no. 4, pp. 459–467, 1941.

[28] T. K. Sherwood and R. L. Pigford, "Absorption and extraction," 1952.

[29] J. T. Long, *Engineering for nuclear fuel reprocessing*. American Nuclear Society, 1978.

[30] R. H. Perry and D. W. Green, *Perry's chemical engineers' handbook*. McGraw-Hill Professional, 1999.

[31] G. Nikolaou, "Determination of the origin of unknown nuclear material through an isotopic fingerprinting method," Tech. Rep. IAEA-TECDOC–1730, 2014.

[32] J. R. Phillips, B. K. Barnes, and T. R. Bement, "Correlation of the cesium-134/cesium-137 ratio to fast reactor burnup," *Nuclear Technology*, vol. 46, no. 1, pp. 21–29, 1979.

[33] A. G. Croff, "Origen2: a versatile computer code for calculating the nuclide compo-

sitions and characteristics of nuclear materials," *Nuclear Technology*, vol. 62, no. 3, pp. 335–352, 1983.

[34] W. S. Charlton, B. L. Fearey, C. W. Nakhleh, T. A. Parish, R. T. Perry, J. Poths, J. R. Quagliano, W. D. Stanbro, and W. B. Wilson, "Operator declaration verification technique for spent fuel at reprocessing facilities," *Nuclear Instruments and Methods in Physics Research Section B: Beam Interactions with Materials and Atoms*, vol. 168, no. 1, pp. 98–108, 2000.

[35] J. H. Rim, K. J. Kuhn, L. Tandon, N. Xu, D. R. Porterfield, C. G. Worley, M. R. Thomas, K. J. Spencer, F. E. Stanley, E. J. Lujan, *et al.*, "Determination of origin and intended use of plutonium metal using nuclear forensic techniques," *Forensic Science International*, vol. 273, pp. e1–e9, 2017.

[36] K. Mayer, M. Wallenius, M. Hedberg, and K. Lutzenkirchen, "Unveiling the history of seized plutonium through nuclear forensic investigations," *Radiochimica Acta*, vol. 97, no. 4-5, pp. 261 – 4, 2009//.

[37] B. Byerly, F. Stanley, K. Spencer, L. Colletti, K. Garduno, K. Kuhn, E. Lujan, A. Martinez, D. Porterfield, J. Rim, M. Schappert, M. Thomas, L. Townsend, N. Xu, and L. Tandon, "Forensic investigation of plutonium metal: a case study of crm 126," *Journal of Radioanalytical and Nuclear Chemistry*, vol. 310, no. 2, pp. 623 – 32, 2016/11/.

[38] K. J. Moody, "Determination of plutonium metal origins," Tech. Rep. 120253, Lawrence Livermore National Lab., CA (United States), 1995.

[39] E. C. Koeman, "A multi-analytical approach for developing nuclear forensic methods for source attribution using trinitite post-detonation material," *ProQuest Dissertations and Theses Global*, 2015.

[40] A. J. Fahey, C. J. Zeissler, D. E. Newbury, J. Davis, and R. M. Lindstrom, "Post-detonation nuclear debris for attribution," *Proceedings of the National Academy of*

Sciences of the United States of America, vol. 107, no. 47, pp. 20207 – 20212, 2010.

[41] D. D. Sood and S. K. Patil, "Chemistry of nuclear fuel reprocessing: Current status," *Journal of Radioanalytical and Nuclear Chemistry*, vol. 203, no. 2, pp. 547–573, 1996.

[42] J. J. Katz, L. R. Morss, N. Edelstein, and J. Fuger, *The Chemistry of the Actinide and Transactinide Elements (Volumes 1-5)*, vol. 1. Springer Science & Business Media, 2007.

[43] G. Best, H. McKay, and P. Woodgate, "Tri-n-butyl phosphate as an extracting solvent for inorganic nitrates-iii the plutonium nitrates," *Journal of Inorganic and Nuclear Chemistry*, vol. 4, no. 5-6, pp. 315–320, 1957.

[44] W. B. Lanham and A. T. Gresky, "Purex process laboratory development," *Oak Ridge National Laboratory*, vol. USAEC Report ORNL-717, 1950.

[45] A. J. Arker, "Terminal report on purex program in kapl separations pilot plant," *Knolls Atomic Power Laboratory*, 1954.

[46] D. O. Darby and J. M. Chandler, "Terminal report for the ornl pilot plant investigation of the purex process," *Oak Ridge National Laboratory*, vol. USAEC Report ORNL -1519, 1954.

[47] E. Irish and W. Reas, "The purex process–a solvent extraction reprocessing method for irradiated uranium," *Hanford Atomic Products Operation, Richland, Washington*.

[48] S. Stoller and R. Richards, "Reactor handbook, volume ii, fuel reprocessing," *Inter science Publishers, Inc., New York*, 1961.

[49] T. H. Siddall, W. E. Prout, S. G. Parker, U. S. A. E. Commission, L. Savannah River, E. I. d. P. d. Nemours, and Company, *Equilibrium distribution data for purex and similar extraction processes*. DP ; 53, E.I. du Pont de Nemours and Co., Explosives Dept., Atomic Energy Division, Technical Division, Savannah River Laboratory, 1957.

[50] D. Scargill, K. Alcock, J. Fletcher, E. Hesford, and H. McKay, "Tri-n-butyl phosphate as an extracting solvent for inorganic nitrates-ii yttrium and the lower lanthanide nitrates," *Journal of Inorganic and Nuclear Chemistry*, vol. 4, no. 5, pp. 304–314, 1957.

[51] K. Alcock, F. Bedford, W. Hardwick, and H. McKay, "Tri-n-butyl phosphate as an extracting solvent for inorganic nitrates-i: Zirconium nitrate," *Journal of Inorganic and Nuclear Chemistry*, vol. 4, no. 2, pp. 100–105, 1957.

[52] K. Alcock, G. Best, E. Hesford, and H. McKay, "Tri-n-butyl phosphate as an extracting solvent for inorganic nitrates-v: Further results for the tetra-and hexavalent actinide nitrates," *Journal of Inorganic and Nuclear Chemistry*, vol. 6, no. 4, pp. 328–333, 1958.

[53] E. Hesford, H. McKay, and D. Scargill, "Tri-n-butyl phosphate as an extracting solvent for inorganic nitratesiv thorium nitrate," *Journal of Inorganic and Nuclear Chemistry*, vol. 4, no. 5, pp. 321–325, 1957.

[54] G. Best, E. Hesford, and H. McKay, "Tri-n-butyl phosphate as an extracting agent for inorganic nitrates-vii: The trivalent actinide nitrates," *Journal of Inorganic and Nuclear Chemistry*, vol. 12, no. 1, pp. 136–140, 1959.

[55] E. Collins, D. Campbell, and L. Felker, "Measurement of achievable plutonium decontamination from gallium by means of purex solvent extraction," *ORNL/TM-1999/312, Oak Ridge National Laboratory*, 2000.

[56] K. Shibata, O. Iwamoto, T. Nakagawa, N. Iwamoto, A. Ichihara, S. Kunieda, S. Chiba, K. Furutaka, N. Otuka, T. Ohasawa, T. Murata, H. Matsunobu, A. Zukeran, S. Kamada, and J. Katakura, "Jendl-4.0: A new library for nuclear science and engineering," *Journal of Nuclear Science and Technology*, vol. 48, no. 1, pp. 1–30, 2011.

[57] K. D. Kok, *Nuclear engineering handbook*. Mechanical engineering series, Boca

Raton : CRC Press, [2009], 2009.

[58] Y. Enokida and I. Yamamoto, "Distribution coefficient correlations for nitric acid, u (vi) and pu (iv) in two-phase system with aqueous nitric acid and 30% tri-n-buthylphosphate solutions," *Journal of nuclear science and technology*, vol. 34, no. 7, pp. 700–707, 1997.

[59] K. Sawada, Y. Enokida, M. Kamiya, T. Koyama, and K. Aoki, "Distribution coefficients of u (vi), nitric acid and fp elements in extractions from concentrated aqueous solutions of nitrates by 30% tri-n-butylphosphate solution," *Journal of nuclear science and technology*, vol. 46, no. 1, pp. 83–89, 2009.

[60] N. Klueglein, F. Zeitvogel, Y.-D. Stierhof, M. Floetenmeyer, K. O. Konhauser, A. Kappler, and M. Obst, "Potential role of nitrite for abiotic fe (ii) oxidation and cell encrustation during nitrate reduction by denitrifying bacteria," *Applied and environmental microbiology*, vol. 80, no. 3, pp. 1051–1061, 2014.

[61] C. A. Colvin, "Reduction of plutonium (vi) to plutonium (iii) and (iv) by sodium nitrite," tech. rep., General Electric Co. Hanford Atomic Products Operation, Richland, Wash.; Hanford Site (HNF), Richland, WA (United States), 1963.

[62] J. Ryan and E. Wheelwright, "The recovery, purification, and concentration of plutonium by anion exchange in nitric acid," tech. rep., General Electric Co. Hanford Atomic Products Operation, Richland, Wash., 1959.

[63] G. F. Knoll, *Radiation detection and measurement*. John Wiley and Sons,New York, NY, 1979.

[64] P. May, "Nitric acid: The starting point for explosives and fertilisers," 2007.

[65] M. Thompson and S. L. Ellison, "Dark uncertainty," *Accrediation and quality assurance*, vol. 16, no. 10, p. 483, 2011.

[66] M. Swinney, *Experimental and Computational Assessment of Trace Nuclide Ratios in Weapons Grade Plutonium for Nuclear Forensics Analysis*. Thesis, 2015.

[67] C. F. III., "Lecture notes in special topics in radiochemistry," March 2016.

[68] J. D. Kim, C. S. Gil, J. T. Lee, and W. G. Hwang, "Development of a one-group cross section data base of the origen2 computer code for research reactor applications," 1992.

[69] M. W. Swinney, C. M. F. III, R. J. Ellis, and S. S. Chirayath, "Experimental and computational forensics characterization of weapons-grade plutonium produced in a fast reactor neutron environment," *Nuclear Technology*, vol. 197, no. 1, pp. 1–11, 2017.

[70] R. MacFarlane, R. Barrett, D. Muir, and R. Boicourt, "Njoy nuclear data processing system: user's manual," report, Los Alamos Scientific Lab., NM (USA), 1978.

[71] R. McFarlane, R. Barrett, D. Muir, and R. Boicourt, "The njoy nuclear data processing system: Users manual," *US Dept. of Energy Report LA-7854-M (ENDF-272)*, 1978.

[72] X. MCNP, "Monte carlo team, mcnp–a general purpose monte carlo n-particle transport code, version 5," tech. rep., LA-UR-03-1987, Los Alamos National Laboratory, April 2003. The MCNP5 code can be obtained from the Radiation Safety Information Computational Center (RSICC), PO Box 2008, Oak Ridge, TN, 37831-6362, 5.

[73] M. Roth, J. Macdougall, and P. Kemshell, "Winfrith improved multigroup scheme code system (wimsd5-b manual, nea-1507)," *Winfrith, Dorchester*, 1997.

[74] J. S. Kim, Y.-S. Jeon, S.-D. Park, B.-C. Song, S.-H. Han, and J.-G. Kim, "Dissolution and burnup determination of irradiated u-zr alloy nuclear fuel by chemical methods," *Nuclear Engineering and Technology*, vol. 38, no. 3, pp. 301–310, 2006.

[75] E. Reilly and K. Smith, "Passive nondestructive assay manual-panda," *Los Alamos, NM: Safeguards Science and Technology Group at LANL*, 1991.

[76] A. Nichols, M. Verpelli, and D. Aldama, "Handbook of nuclear data for safeguards,"

report, International Atomic Energy Agency, International Nuclear Data Committee, Vienna (Austria), 2007.

[77] D. Cobb, J. Phillips, G. Bosler, G. Eccleston, J. Halbig, C. Hatcher, and S. Hsue, "Nondestructive verification and assay systems for spent fuels," *Los Alamos Report LA-9041*, vol. 2, 1982.

[78] W. Maeck, W. Emel, J. Delmore, F. Duce, L. Dickerson, J. Keller, and R. Tromp, "Discrepancies and comments regarding 235 u and 239 pu thermal fission yields and the use of 148 nd as a burnup monitor," report, Idaho National Engineering Lab., Idaho Falls (USA), 1976.

[79] J. Phillips, J. Halbig, D. Lee, S. Beach, T. Bement, E. Dermendjiev, C. Hatcher, K. Kaieda, and E. Medina, "Application of nondestructive gamma-ray and neutron techniques for the safeguarding of irradiated fuel materials," report, Los Alamos Scientific Lab., NM (USA), 1980.

[80] N. Kocherov, M. Lammer, and O. Schwerer, "Handbook of nuclear data for safeguards," report, International Atomic Energy Agency, Vienna (Austria). International Nuclear Data Committee, 1997.

[81] J.-S. Kim, Y.-S. Jeon, K.-S. Park, B.-C. Song, S.-H. Han, and W.-H. Kim, "Burnup measurement of spent u_3 si/al fuel by chemical method using neodymium isotope monitors," *Nuclear Engineering and Technology*, vol. 33, no. 4, pp. 375–385, 2001.

[82] K. Suyama and H. Mochizuki, "Effect of neutron induced reactions of neodymium-147 and 148 on burnup evaluation," *Journal of nuclear science and technology*, vol. 42, no. 7, pp. 661–669, 2005.

[83] A. Einstein, "Does the inertia of a body depend upon its energy-content," *Ann Phys*, vol. 18, pp. 639–641, 1905.

[84] H. Bateman, "Partial differential equations of mathematical physics," *Partial Differential Equations of Mathematical Physics, by H. Bateman, Cambridge, UK: Cam-*

bridge University Press, 1932, 1932.

[85] J. M. Osborn, E. D. Kitcher, J. D. Burns, C. M. Folden III, and S. S. Chirayath, "Nuclear forensics methodology for reactor-type attribution of chemically separated plutonium," *Nuclear Technology*, vol. 201, pp. 1–10, 2018.

[86] J.-i. Katakura, "Jendl fp decay data file 2011 and fission yields data file 2011," *JAEA-Data/Code*, vol. 25, 2011.

[87] T. England and B. Rider, "Evaluation and compilation of fission product yields," *ENDF-349, LA-UR-94-3106, Los Alamos National Laboratory*, 1994.

[88] T. Goorley, M. James, T. Booth, F. Brown, J. Bull, L. Cox, J. Durkee, J. Elson, M. Fensin, R. Forster, *et al.*, "Initial mcnp6 release overview," *Nuclear Technology*, vol. 180, no. 3, pp. 298–315, 2012.

[89] J. Leppänen, M. Pusa, T. Viitanen, V. Valtavirta, and T. Kaltiaisenaho, "The serpent monte carlo code: Status, development and applications in 2013," *Annals of Nuclear Energy*, vol. 82, pp. 142–150, 2015.

APPENDIX A

SINGLE GROUP NEUTRON CROSS SECTIONS

The energy-dependent neutron scalar flux could alternatively be split into a magnitude and energy shape functions for the three different energy regions, as shown in Equation A.1, where ρ_1, ρ_2, and ρ_3 are functions in their respective energy regions and could be used to determine the fraction of flux in each energy region via integration because their energy integrated values will sum to unity $\left(\int \rho_1 + \int \rho_2 + \int \rho_3 = 1\right)$. An approach for assuming shapes for a thermal neutron flux in the three energy regions are listed in Appendix A where dependency on materials can be added by dividing by normalized cross sections in order to capture important resonances. In order to have varying percentages of flux in each region discontinuity would be allowed[i].

$$\phi(E) = \phi \int_0^\infty dE \begin{cases} \rho_1(E) & 0 < E \leq 1 \text{ eV} \\ \rho_2(E) & 1 \text{ eV} < E \leq 100 \text{ keV} \\ \rho_3(E) & 100 \text{ keV} < E \leq 20 \text{ MeV} \end{cases} \tag{A.1}$$

Selected integrations for cross section data. Modeled after Brookhaven

$$\phi_1 = \frac{E}{E_0^2} e^{-E/E_0} \tag{A.2}$$

$$\phi_2 = \frac{\sqrt{\frac{E}{E_f}}}{E_f} e^{-\frac{E}{E_f}} \tag{A.3}$$

[i]This method was not implemented in the current work, but a good amount of effort was put forth along these lines, preliminary results along with code are available upon request to the interested reader.

$$\sigma_{avg} = \begin{cases} \frac{2}{\sqrt{\pi}} \frac{\int_{E1}^{E2} \sigma(E)\phi_1(E)dE}{\int_{E1}^{E2} \phi_1(E)dE} & 1E-5 < E \leq 10 \text{ eV} \\ \int_{E1}^{E2} \frac{\sigma(E)}{E} dE & 0.5 \text{ eV} < E \leq 100 \text{ keV} \\ \frac{\int_{E1}^{E2} \sigma(E)\phi_2(E)dE}{\int_{E1}^{E2} \phi_2(E)dE} & 100 \text{ keV} < E \leq 10 \text{ MeV} \end{cases} \tag{A.4}$$

where:

$$E_0 = 0.0253$$

$$E_f = 1.35E6$$

The brookhaven site has a $\frac{2}{\sqrt{\pi}}$ term in the thermal region, this term will be ignored in calculations.

APPENDIX B

ERROR PROPAGATION

Error propagation for calculations assumed independence among variables and utilized general error propagation which is shown for the function, $u = u(x, y, z, ...)$, in Equation B.1.

$$\sigma_u = \sqrt{\left(\frac{\delta u}{\delta x}\sigma_x\right)^2 + \left(\frac{\delta u}{\delta y}\sigma_y\right)^2 + \left(\frac{\delta u}{\delta z}\sigma_z\right)^2 + ...} \tag{B.1}$$

Alpha and Gamma Error Propagation

Alpha error propagation utilized the same principles as for the gamma calculations. The major difference is that alpha absolute efficiency is constant as a function of energy. Below is an example calculation to determine activity of ^{137}Cs in an aqueous sample using count rates. The activity, A, of a gamma source is calculated with Equation B.2,

$$A[bq] = \frac{\text{CPS}_{\text{total}} - \text{CPS}_{\text{Background}}}{\epsilon_{abs} \cdot Y} = \frac{\text{CPS}_{\text{sample}}}{\epsilon_{abs} \cdot Y} \tag{B.2}$$

where CPS correspond to the number of counts per second registered for a particular photopeak, in the case of ^{137}Cs this would be 662 keV, ϵ_{abs} is the absolute detector efficiency at the energy of interest, and Y corresponds to the probability of emitting a photon at the energy of interest given a decay of the radionuclide.

The error in this calculation, σ_A, depends on the error of all the inputs. Using Equation B.1 above, this is given by Equation B.3. The Python package 'uncertainties' performs error propagation in this manner. Uncertainty propagation calculations for this entire project utilized both derivation and Python methods, with the majority utilizing the later to reduce potential for mistakes. Below is an example code for how python performs these operations. The output for the example code is (1.092+/-0.006)e+05, which is correct given the

inputs.

$$\sigma_A = \sqrt{\left(\frac{\sigma_{\text{CPS}}}{\epsilon \cdot Y}\right) + \left(\frac{\text{CPS} \cdot \sigma_\epsilon}{\epsilon^2 \cdot Y}\right) + \left(\frac{\text{CPS} \cdot \sigma_Y}{\epsilon \cdot Y^2}\right)} \tag{B.3}$$

Listing B.1: Sample of error propagation calculation using python

```
#!/usr/bin/env python3
from uncertainties import ufloat

CPS=ufloat(85.9915464,0.14819646)
e=ufloat(0.000925707944557,4.62854e-6)
Y=ufloat(0.851,0.002)

A=(CPS/(e*Y))

print(A)
```

The error for the absolute efficiency at a particular energy is a function of the calibration source's activity error, how long the calibration source was counted, how well the efficiency curve fits the calibration data, and on any geometric systematic errors. Because the source used for calibration was NIST traceable, and because the calibration source was counted such that the peak with the worst resolution was 0.36%, a 0.5% error was associated with this term across the all energies. This was appropriate because absolute activity was determined mostly for isotopes with energies above 122 keV[i].

Minimum Detectable Activity

Minimum detectable activity (MDA) became an issue for the gamma spectra where a small amount of activity was present in a given sample. The following was utilized to ensure all results for gamma measurements were above the MDA.

The following is adapted from Knoll[63], where equal count times are not assumed and the MDA is derived in terms of count rates and counting time instead of total number of

[i] ^{155}Eu is an exception

counts. The MDA was solved for in these terms because the output of the GENIE software provides peak area information in terms of count rate, and secondly, the background was counted for a much longer time than the samples. The below assumes all measured total counts are samples from Gaussian distributions. In the discussion it is stated that the count rates follow a Gaussian distribution as well. This assumes that time has no statistical variation[ii], and can be treated as a constant.

The net count rate from an unknown sample is given in Equation B.4.

$$\mathrm{CPS}_{\mathrm{sample}} = \mathrm{CPS}_{\mathrm{total}} - \mathrm{CPS}_{\mathrm{background}} \tag{B.4}$$

Where the count rate is the total number of counts divided by the time counted (N/T). The subscript, 'total' refers to the counting system when a sample is present with background, and the subscript 'background' refers to the system with no sample. The error for $\mathrm{CPS}_{\mathrm{sample}}$ is given in Equation B.5

$$\sigma^2_{\mathrm{CPS}_{\mathrm{sample}}} = \sigma^2_{\mathrm{CPS}_{\mathrm{total}}} + \sigma^2_{\mathrm{CPS}_{\mathrm{background}}} \tag{B.5}$$

In the next section it is proven that the error in a count rate, with respect to the count rate itself and the time counted, is equal to the square root of the count rate divided the time counted. Using this, Equation B.5 turns into Equation B.6, and further, using Equation B.4, we arrive at Equation B.7.

$$\sigma_{\mathrm{CPS}_{\mathrm{sample}}} = \sqrt{\frac{\mathrm{CPS}_{\mathrm{total}}}{T_{\mathrm{total}}} + \frac{\mathrm{CPS}_{\mathrm{background}}}{T_{\mathrm{background}}}} \tag{B.6}$$

$$= \sqrt{\frac{\mathrm{CPS}_{\mathrm{sample}}}{T_{\mathrm{total}}} + \mathrm{CPS}_{\mathrm{background}} \left[\frac{1}{T_{\mathrm{total}}} + \frac{1}{T_{\mathrm{background}}}\right]} \tag{B.7}$$

[ii]The counting time could have some systematic error, which is not quantified. Also the ratio of two Normal random variables is not Normal

where:

T_{total} is the time that the sample was counted (where both background and the sample contribute towards the total counts) and

$T_{\text{background}}$ is the time that background was counted.

If no activity is present, then the true mean value of $\text{CPS}_{\text{sample}}$ is zero. In order to have a false positive rate of 5% in this circumstance, the upper count rate limit should be set to $1.65\sigma_{\text{CPS}_{\text{sample}}}$ because 95% of the time a random sample from a standard normal will be less than 1.65σ. This threshold will be defined as CPS_L, and given in Equation B.8.

$$\begin{aligned} \text{CPS}_L =& 1.64\sigma_{\text{CPS}_{\text{sample}}} \\ =& 1.64\sqrt{\text{CPS}_{\text{background}}\left[\frac{1}{T_{\text{total}}}+\frac{1}{T_{\text{background}}}\right]} \end{aligned} \tag{B.8}$$

Next, if a minimium net count count rate, CPS_{min}, were defined as the net count rate corresponding to the minimium detectable activity whereby the false-negative probability is 5%, then the mean of this threshold net count rate should be 1.65σ away from CPS_L, this is shown in Equation B.9.

$$\text{CPS}_{\text{min}} = \text{CPS}_L + 1.64\sigma_{\text{CPS}_{\text{min}}} \tag{B.9}$$

Where $\sigma_{\text{CPS}_{\text{min}}}$ represents the standard deviation of the minimum net count rate. This was given in Equation B.7, where CPS_{min} is substituted for $\text{CPS}_{\text{sample}}$ and σ_{min} is substituted for σ_{sample}. Using Equation B.7, B.8, and B.9, the minimum count rate for which activity claimed has a 5% false positive and 5% false negative probability is given in Equation

B.10.

$$\mathrm{CPS}_{\mathrm{min}} = 1.64\left(\sqrt{\mathrm{CPS}_{\mathrm{background}}\left[\frac{1}{T_{\mathrm{total}}}+\frac{1}{T_{\mathrm{background}}}\right]}+\sqrt{\frac{\mathrm{CPS}_{\mathrm{min}}}{T_{\mathrm{total}}}+\mathrm{CPS}_{\mathrm{background}}\left[\frac{1}{T_{\mathrm{total}}}+\frac{1}{T_{\mathrm{background}}}\right]}\right) \tag{B.10}$$

In order to show that Equation B.10 follows the same derivation steps shown in Knoll[63], the assumption where $T_{\mathrm{total}} = T_{\mathrm{background}} = T$[iii] is applied and shown in Equation B.11 to be equivalent to what is in the text.

$$\begin{aligned}\mathrm{CPS}_{\mathrm{min}} &= 1.64\left(\sqrt{\mathrm{CPS}_{\mathrm{background}}\left[\frac{2}{T}\right]}+\sqrt{\frac{\mathrm{CPS}_{\mathrm{min}}}{T}+\mathrm{CPS}_{\mathrm{background}}\left[\frac{2}{T}\right]}\right)\\ &= \frac{1.64}{T}\left(\sqrt{2N_{\mathrm{background}}}+\sqrt{N_{\mathrm{min}}+2N_{\mathrm{background}}}\right)\end{aligned} \tag{B.11}$$

If we recall that the count rate is equivalent to the total number of counts divided by the total time, then multiplying both sides of Equation B.11 by time will yield the precurser to the "Currie equation", which is determined by solving for N_{min} and shown in Equation B.12.

$$N_{\mathrm{min}} = 4.65\sqrt{N_{\mathrm{background}}}+2.71 \tag{B.12}$$

It should be noted that this equation was used to estimate the counting time for the mass spectrometry samples by dividing by time and solving for time. The final form of the equation is a second order polynomial where the quadratic equation provides the solution.

[iii] for low activity samples equal allocation of time to the sample and background minimizes uncertainty in the net count rate[63]

The solution is shown in Equation B.13

$$T = \frac{B \pm \sqrt{B^2 - 4 \cdot C}}{2} \tag{B.13}$$

where:

$$B = \frac{5.42 \cdot \text{CPS}_{\text{min}} + 21.6 \text{CPS}_{\text{background}}}{\text{CPS}_{\text{min}}^2}$$

$$C = \frac{7.34}{\text{CPS}_{\text{min}}^2}.$$

Equation B.10 is not close formed, but can be iteratively solved for or approximated with Equation B.14.

$$\text{CPS}_{\text{min}} = \frac{2.71 + 3.29\sqrt{\text{CPS}_{\text{Background}} T_{\text{Total}} \left(1 + \frac{T_{\text{Total}}}{T_{\text{Background}}}\right)}}{T_{\text{Total}}} \tag{B.14}$$

A code for iteratively solving for CPS_{min} is shown below, and results show that the iterated solution is very close and always larger than the approximated solution. This means that the approximated solution is a conservative estimate on CPS_{min} because a larger count rate is needed in order to meet the requirements for detectable activity.

Listing B.2: Code

```
#Initialize
T_Background=48*3600
T_Total=6*3600
CPS_Total=0.0367
CPS_Background=0.031031

#Initial Guess for CPS_Min (usually pretty good)
CPS_Min=(2.71+3.29*np.sqrt(CPS_Background*T_Total*\
        (1+(T_Total/T_Background))))/T_Total
CPS_Initial=copy.copy(CPS_Min)
#While loop variables
i=0;tol=1E-8;Diff=1

#Loop through and find the MDA
A=CPS_Background*(1/T_Total+1/T_Background)
```

```
B=np.sqrt(A)
while Diff>tol:
    CPS_Min_New=1.64*(B+np.sqrt(CPS_Min/T_Total+A))
    Diff=abs(CPS_Min-CPS_Min_New)
    CPS_Min=copy.copy(CPS_Min_New)
    i=i+1

PercentDiff=(CPS_Initial-CPS_Min/CPS_Min)*100
```

To show that the approximated solution is very close and always larger than the actual solution, the algorithm below was iterated over reasonable counting times for the sample and background, and the percent difference between the approximated and actual solution are shown in Figure B.2. If a sample was counted for at least half an hour, then the difference between the solutions is less than 0.34%.

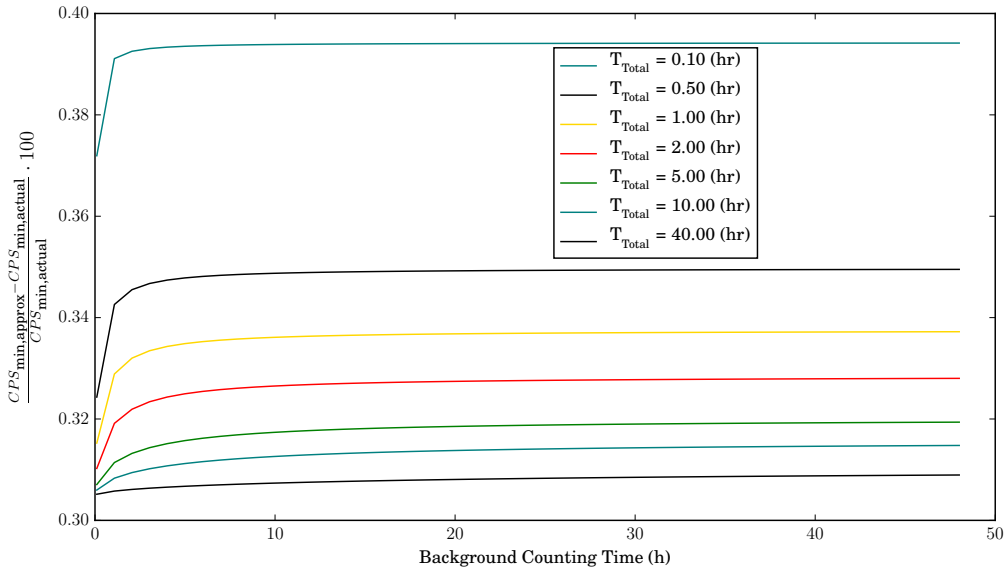

Figure B.1: Percent difference between approximated and actual solutions for CPS_{min} as a function of sample and background count time.

To show how increasing the count time decreases the MDA, Figure B.2 is provided

where $CPS_{Background}$ = 0.031. The value for CPS_{Total} was choosen because that was the count rate for background ^{137}Cs during the majority of the experiments, and had the largest count rate of background for the peaks we were trying to determine. This large background contamination made determining the DC and DF values for Cs difficult because the DC value for Cs was very low, and therefore not much was carried to the product solution.

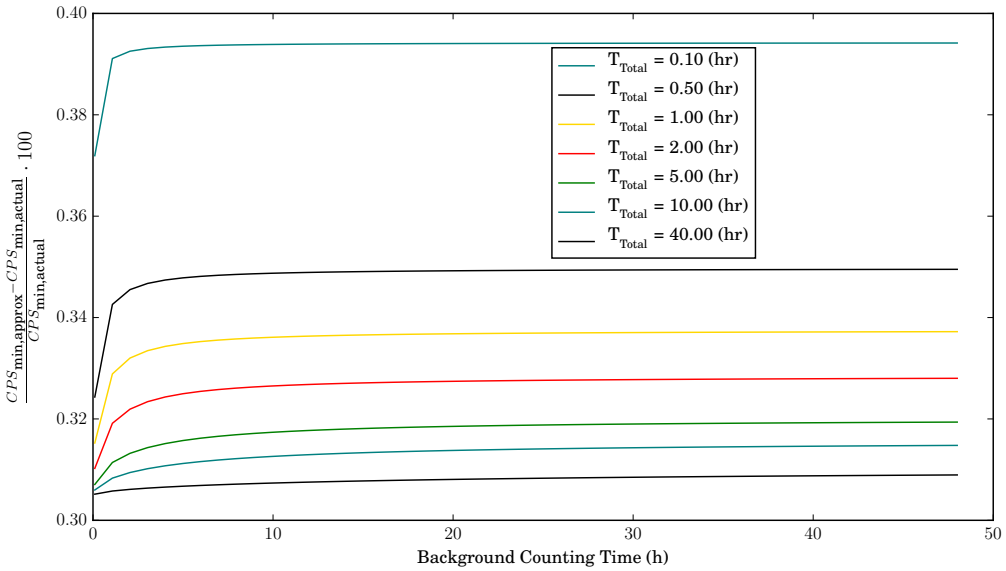

Figure B.2: The percent CPS_{Total} has to be above background for MDA calculations with CPS_{Total} = 0.035.

Figure B.2 shows that counting background much beyond 10 hours did not provide much benefit, and similiarlly counting the total sample for much longer than 10 hours also did not provide much benefit. These estimates on preferred counting times were provided based on the equations derived earlier in this section, where error was determined based on count rates and time counted. With the actual samples, it was discovered that the errors provided by the GENIE software were somewhat higher than what would be

expected based on peak fitted count rates and counting time alone. This was because the software subtracted the Compton continuum and errors are included in that process. Because background spectra did not have as much error associated due to subtracting the Compton continuum it was concluded that more counting time probably should be devoted to samples rather than background, because their peaks took a little longer to resolve, but because more sample spectra had to be measured, the background was counted for a much longer time than the samples.

Given that the errors for a given gamma peak are known from the GENIE software, the MDA was determined with the Equation B.15.

$$\text{MDA} = \frac{\text{CPS}_{\text{min}}}{f\epsilon} = \frac{1.64\sqrt{2}\sigma_{\text{CPS}_{\text{Background}}} + 1.64\sqrt{\sigma^2_{\text{CPS}_{\text{Total}}} + \sigma^2_{\text{CPS}_{\text{Background}}}}}{f\epsilon} \tag{B.15}$$

where:

f = radiation yield per disintegration

ϵ = absolute detection efficiency.

The value for CPS_{min} in Equation B.15 was determined based on the derivation above. The MDA for these experiments were determined for all the species, and results below the MDA were ommitted. Each measurement had a different value for the MDA based on corresponding errors, but the average for ^{137}Cs was on the order of 10^{-5} μCi.

Error Propagation through Volume Manipulations

All calculations which utilized volume in the chemistry experiments had standard percent errors applied. The errors ranged from 0.75% to 5% error depending on the pipette used and the volume pipetted.

Error Propagation for Mass Spectrometry

There were three main errors to determine for the mass spectrometry calculations. The first was the error in count rate reported by the detector, the second was the error in the standards used for determining the concentration of the solutions sent, and the third was the error in the enrichment calculations.

Count Rate Errors for Mass Spectrometry

The error in the count rate results were determined with the following. Five different counts were collected, divided by the time of collection, and their average was provided for analysis to A&M. To determine the error in this average count rate the following derivation is presented. An average of five different count rates is shown in Equation B.16.

$$\text{CPS}_{\text{avg}} = \frac{\text{CPS}_1 + \text{CPS}_2 + \text{CPS}_3 + \text{CPS}_4 + \text{CPS}_5}{5} \tag{B.16}$$

The count rate was presumably determined by dividing the total counts by the time of collection as shown in Equation B.17.

$$\text{CPS}_1 = \frac{\text{Counts in given time}}{\text{Time Counted}} \tag{B.17}$$

The error in this count rate, assuming the square root of the total amount of counts acts as an estimate of the standard deviation, is given in Equation B.18.

$$\sigma_{\text{Counts in given time}} = \sqrt{\text{Counts in given time}} \tag{B.18}$$

Assuming that there is no error in the count time, the count rate error for a single count rate is shown in Equation B.19.

$$\sigma_{\text{CPS}_1} = \frac{\sqrt{\text{Counts in given time}}}{\text{Time Counted}} \tag{B.19}$$

Because the count time and total counts were not provided a count time was estimated with B.13, the minimium detectable activity provided by the user and background counts. With the above a count time of 2 second was estimated. Although this might seem small, mass spectrometry measurements produce a large amount of counts in a small amount of time. With this assumption the total number of counts for a given count could be determined with Equation B.20.

$$\text{Counts in a given time} = CPS_1 \cdot \text{Time Counted} \tag{B.20}$$

Using Equation B.19 and B.20, the error for a single count rate is:

$$\sigma_{\text{CPS}_1} = \frac{\sqrt{CPS_1 \cdot \text{Time Counted}}}{\text{Time Counted}} = \sqrt{\frac{CPS_1}{\text{Time Counted}}} \tag{B.21}$$

With this as the error for a single count rate, the error of the average count rate can be determined with the error propagation formula shown in Equation B.1 operated on Equation B.16, which yields Equation B.22.

$$\sigma_{\text{CPS}_{\text{avg}}} = \frac{1}{5}\sqrt{\sigma^2_{\text{CPS}_1} + \sigma^2_{\text{CPS}_2} + \sigma^2_{\text{CPS}_3} + \sigma^2_{\text{CPS}_4} + \sigma^2_{\text{CPS}_5}} \tag{B.22}$$

Because the information about the individual count rates were not provided, it will be assumed that all five count rates were the same. If all the five count rates were the same, CPS_{same}, and counted for the same time, so that all the errors were the same ($\sigma_{\text{CPS}_{\text{same}}}$) then

Equation B.22 would reduce to,

$$\sigma_{\text{CPS}_{\text{avg}}} = \frac{\sqrt{5}}{5}\sigma_{\text{CPS}_{\text{same}}}. \tag{B.23}$$

Since the error for a single count rate is shown in Equation B.21 the error for the average count rate, with the information provided, could be presented in Equation B.24

$$\sigma_{\text{CPS}_{\text{avg}}} = \frac{\sqrt{5}}{5}\sqrt{\frac{CPS_{\text{same}}}{\text{Time Counted}}} \tag{B.24}$$

because there is an assumption that all the count rates are the exact same, the $\frac{\sqrt{5}}{5}$ term will be dropped so that the error in count rates for the mass spec were assumed to be.

$$\sigma_{\text{CPS}_{\text{avg}}} = \sqrt{\frac{CPS_{\text{same}}}{\text{Time Counted}}} \tag{B.25}$$

Errors in concentration of standards

Standards used for mass spectrometry usually ship with concentrations of 1000 $\pm$ 1 ppm. Most of the standards used for the experiment were on the order of 10 ppb. In order to reduce the higher concentration down to the 10 ppb range, a dilution was performed. If density changes are negligible then error propagation from the first concentration to the second would utilize $m_1v_1 = m_2v_2$. Regardless of the number of dilutions, the volume ratio between initial and final solutions would be $\frac{10^{-2}}{1000} = 10^{-5}$. Assuming a single dilution, and a final volume of 1 liter, the initial volume of standard would have to be 10 μl. Given the measurment certainty in measuring out these two volumes, an estimate on the uncertainty in the calibration standards can be determined. A 0.75% error will be assumed for the 1 liter measurement, and a 1.3% error will be assumed for the 10μl measurement.

Given this, the error in the volume ratio V_1/V_2 is given in Equation B.26.

$$\begin{aligned}\sigma_{V_1/V_2} =& \sqrt{\left(\frac{\sigma_{V_1}}{V_2}\right)^2 + \left(\frac{\sigma_{V_2} V_1}{V_2^2}\right)^2} \\ =& \sqrt{\left(\frac{0.00013}{1000}\right)^2 + \left(\frac{7.5 \cdot 0.01}{1000^2}\right)^2} \\ =& 1.5 \times 10^{-7}\end{aligned} \tag{B.26}$$

The concentration of the calibration standard after dilution is equal to the intital concentration multiplied by the volume ratio, and in the case of this example, was set at 0.01 ppm. The error in this value, given what has come before, is shown in Equation B.27.

$$\begin{aligned}\sigma_{m_2} =& \sqrt{\left(\sigma_{m_1} \cdot \frac{V_1}{V_2}\right)^2 + \left(m_1 \cdot \sigma_{V_1/V_2}\right)^2} \\ \sigma_{m_2} =& \sqrt{\left(1 \cdot 1 \times 10^{-5}\right)^2 + \left(1000 \cdot 1.5 \times 10^{-7}\right)^2} \\ =& 0.00015\end{aligned} \tag{B.27}$$

This is a 1.5% error. To be conservative, a 2% error will be assumed for all calibration standards.

To determine the error in the instrument response, which is the ratio of the concentration of the standard with its corresponding mass bin count rate, a counting time should be assumed for the standards. Because this quantity is unknown, its effect on the error in the instrument response will be explored. The instrument response for a particular isotope is given in Equation B.28

$$\text{Instrument Response} = \text{IR} = \frac{\text{ppb}_\text{i}}{\text{CPS}_\text{i}} \tag{B.28}$$

where:

i = isotope of interest

ppb = ng/gram of solution with isotope

The error for the instrument response is given as follows:

$$\sigma_{\text{Instrument Response}} = \sqrt{\left(\frac{\sigma_{\text{ppb}_\text{i}}}{\text{CPS}_\text{i}}\right)^2 + \left(\frac{\text{ppb}_\text{i}\sigma_{\text{CPS}_\text{i}}}{{\text{CPS}_\text{i}}^2}\right)^2} \tag{B.29}$$

Substituting the error terms, and noting that Err is the fraction of error for the concentration in the standard.

$$\begin{aligned}\sigma_{\text{Instrument Response}} &= \sqrt{\left(\frac{\text{ppb}_\text{i}\cdot\text{Err}}{\text{CPS}_\text{i}}\right)^2 + \left(\frac{\text{ppb}_\text{i}\sqrt{\frac{\text{CPS}_\text{i}}{\text{time}}}}{{\text{CPS}_\text{i}}^2}\right)^2} \\ &= \sqrt{{\text{IR}_\text{i}}^2\left(\text{Err}^2 + \frac{1}{\text{CPS}_\text{i}\cdot\text{time}_\text{i}}\right)} \\ &= \text{IR}_\text{i}\sqrt{\text{Err}^2 + \frac{1}{\text{CPS}_\text{i}\cdot\text{time}_\text{i}}}\end{aligned} \tag{B.30}$$

If the CPS are high then the error is mostly dictated by the error in the calibration standard. Figure B.3 shows that if the count rate is high, and if there is a reasonable counting time for a standard, then the error in the instrument response is very close to the error in the standard. A count time of 2 seconds was assumed for the standards. As a point of reference, the count rate was averaged over all samples that were sent for the initial mass spectrometry experiment, over all mass bins, and this number was on the order of 150,000. The instrument response was determined with standards which had a reasonable amount of the dissolved constituent and for the most provided enough counts so that the error in the instrument response was approximately equal to the error in the standard itself. There

were some exceptions, ^{234}U for example, and in these cases the lower count rate increased the error by a fair fraction.

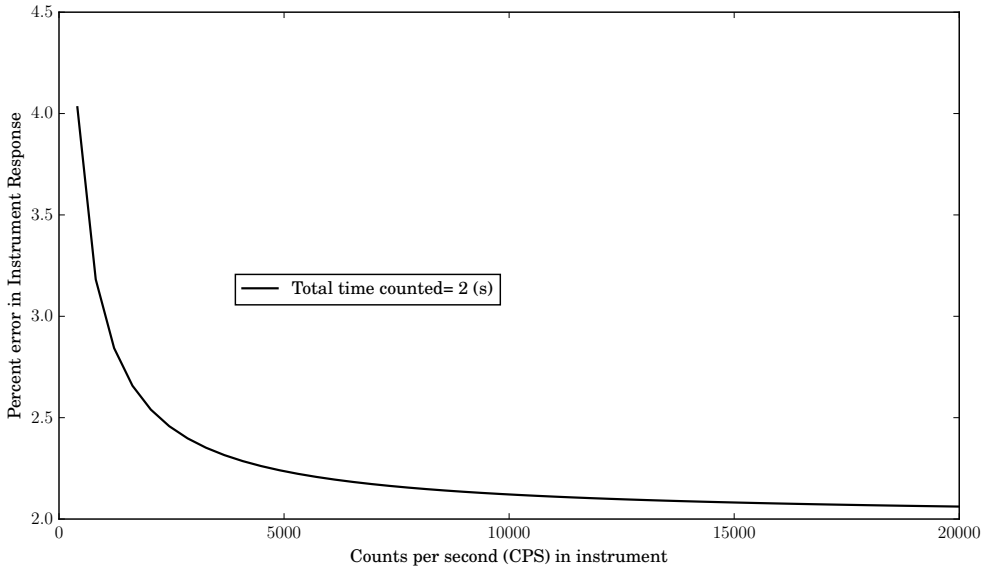

Figure B.3: The percent error in mass spectrometry instrument response with an assumed count time of 2 seconds as a function of count rate.

Error Propagation for Enrichment Calculation

The enrichment of uranium in the sample were determined with Equation B.31. ^{239}Pu enrichment was determined in a similar manner. Error was propagated in two steps for this calculation. The first step combined the all the concentrations and the second step divided the ^{235}U concentration by the total. This was for ease of calculation in excel, but neglects the covariance between the total uranium concentration and the ^{235}U concentration. The following proves that this two step error calculation has a slightly higher estimate of error than rigerous calculation at lower enrichments and always reports a larger error value at

any enrichment.

$$\epsilon_{235} = \frac{c_{235}}{c_{234} + c_{235} + c_{236} + c_{238}} \tag{B.31}$$

To rigorously calculate error, Equation B.32 should be used, where the isotope number has been shorted to the last digit.

$$\begin{aligned}
\sigma^2_{\epsilon_{235}} = &\left[\frac{c4 + c6 + c8}{(c4 + c5 + c6 + c8)^2}\right]^2 \sigma^2_{c5} + \left[\frac{-c5}{(c4 + c5 + c6 + c8)^2}\right]^2 \sigma^2_{c4} + \\
&\left[\frac{-c5}{(c4 + c5 + c6 + c8)^2}\right]^2 \sigma^2_{c6} + \left[\frac{-c5}{(c4 + c5 + c6 + c8)^2}\right]^2 \sigma^2_{c8} \\
=&\frac{1}{(c4 + c5 + c6 + c8)^4}\left[(c4 + c6 + c8)^2 \sigma^2_{c5} + c5^2 \cdot \left(\sigma^2_{c4} + \sigma^2_{c6} + \sigma^2_{c8}\right)\right] \\
\approx &\left(\frac{\sigma_{c5}}{c4 + c5 + c6 + c8}\right)^2 + \\
&\frac{1}{(c4 + c5 + c6 + c8)^4}\left[c5^2 \cdot \left(\sigma^2_{c4} + \sigma^2_{c6} + \sigma^2_{c8}\right)\right]
\end{aligned} \tag{B.32}$$

The last step is an approximation, where $(c4 + c6 + c8)^2/(c4 + c5 + c6 + c8)^2 \approx 1$. This is especially true at low enrichments of ^{235}U. To calculate error in two steps, first the error in the total concentration should be determined with Equation B.33.

$$\sigma_T = \sqrt{\sigma^2_{c4} + \sigma^2_{c5} + \sigma^2_{c6} + \sigma^2_{c8}} \tag{B.33}$$

Then the error in the enrichment was determined in second step via Equation B.34

$$\begin{aligned}
\sigma'^{2}_{\epsilon_{235}} &= \left(\frac{\sigma_{c5}}{T}\right)^2 + \left(\frac{c5\sigma_T}{T^2}\right)^2 \\
&= \left(\frac{\sigma_{c5}}{c4+c5+c6+c8}\right)^2 + \left(\frac{c5(\sqrt{\sigma_{c4}^2+\sigma_{c5}^2+\sigma_{c6}^2+\sigma_{c8}^2})}{(c4+c5+c6+c8)^2}\right)^2 \\
&= \left(\frac{\sigma_{c5}}{c4+c5+c6+c8}\right)^2 + \\
&\quad \frac{1}{(c4+c5+c6+c8)^4}\left[c5^2\cdot\left(\sigma_{c4}^2+\sigma_{c6}^2+\sigma_{c8}^2\right)+c5^2\cdot\sigma_{c5}^2\right]
\end{aligned} \tag{B.34}$$

If we compare the two means of determining error, the second means for determining it has an extra $\frac{c5^2\cdot\sigma_{c5}^2}{(c4+c5+c6+c8)^4}$ term, which shows that the second means of calculating the error would be slightly higher, but still acceptable. Figure B.4 shows a plot of the two means of calculating the error as a function of ^{235}U enrichment (keeping the percent error of ^{235}U constant around 2%). The point at where this approximation breaks down is around is around 1%, but the approximation always reports a larger error.

It should be noted that even though the percent error in the ^{235}U concentration was kept at a constant 2% error, the percent error in the enrichment of ^{235}U for the rigerous calculation dropped below 2%. Before calling foul on this calculation, the reader is asked to do the calculation themselves.

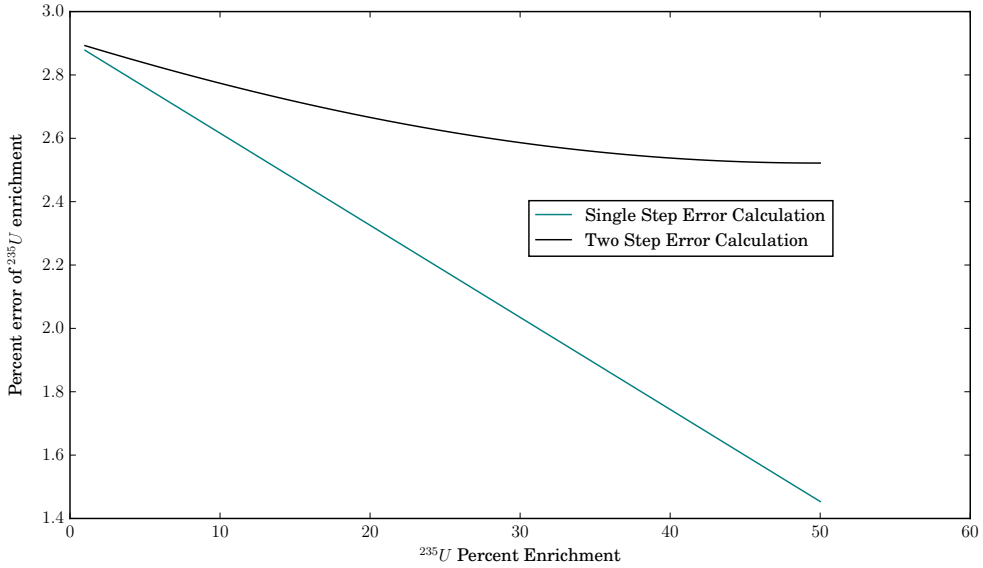

Figure B.4: Percent error in ^{235}U enrichment as a function of enrichment at two different means of calculation.

APPENDIX C

FEASIBILITY

A short feasibility study is presented here. In order to detect fission products from purified plutonium a minimum amount should be present for measurement. Through the course of PUREX fission products are preferentially removed from plutonium are less detectable. In this project the mass of plutonium in the sample was around 0.2 mg, where as the fission products were estimated at 0.04 mg. If all other constituents were removed then fission products would represent 20% of the total mass. If a general decontamination factor of 10^7 were applied across all fission products then the mass percentage of fission products after decontamination is calculated in Equation C.1[i].

$$\epsilon = \frac{m_{\text{FP,final}}}{m_{\text{FP,final}} + m_{\text{Pu,final}}}$$

$$\epsilon = \frac{\frac{m_{\text{FP,initial}}}{\text{DF}}}{\frac{m_{\text{FP,final}}}{\text{DF}} + m_{\text{Pu,final}}} \tag{C.1}$$

$$\epsilon = \frac{\frac{0.04}{10^7}}{\frac{0.04}{10^7} + 0.2} = 2 \times 10^{-8}$$

If 20 ppb were present of fission products in the final plutonium product, then it would be measurable by mass spectrometry. Dilution would probably add a minimum of reduction of concentration by a factor of 10^2-10^3, and therefore some solid form mass spectrometry should be pursued.

[i] assuming that plutonium has a 100% recovery and therefore $\text{DF} = \frac{C_{\text{FP,i}}}{C_{\text{FP,f}}} \cdot \frac{C_{\text{Pu,f}}}{C_{\text{Pu,i}}} \approx \frac{C_{\text{FP,i}}}{C_{\text{FP,f}}}$

APPENDIX D

LABORATORY NOTEBOOK EXCERPTS

The following pages contain some excerpts from the laboratory notebook for this experiment. Note that the page numbers for the notebook are provided as well as the page numbers for the overall document.

Thursday, 6 October 2016 8:30am - 11:00 am 1:30pm - 3:30pm

- Set up laboratory notebook
- Calculation To do calculation to determine the volumes needed for a final concentration of a particular volume, knowing the initial concentrations

$$V_2 = \frac{b_2 - \frac{M_1 b_1}{A}}{M_2 - \frac{M_1}{A}}$$
$$V_1 = \frac{b - BV_2}{A}$$

Where:

$$A = (1 - wt\%_1)\rho_1$$
$$B = (1 - wt\%_2)\rho_2$$
$$b_1 = (1 - wt\%_3)V_3\rho_3$$
$$b_2 = M_3V_3$$

With known Molarity and volume of a solution how much, and of what concentration do we need to combine with a second solution to get a final solution of known concentration and volume?

$$B = (1 - wt\%_3)V_3\rho_3 - (1 - wt\%_1)V_1\rho_1$$
$$A = M_3V_3 - M_1V_1$$
$$C = \frac{B}{A} = \frac{(1 - wt\%_2)\rho_2}{M_2}$$

Need iterative solution, choose:

$$M_2 = \frac{M_3V_3 - M_1V_1}{V_3 - V_1}$$
$$V_2 = V_3 - V_1$$

Use to determine molality $\rightarrow wt\%_2 \rightarrow \rho_2$. Then compare to C, iterate around the solution to find answer so that $C = \frac{(1-wt\%_2)\rho_2)}{M_2}$.

Friday, 7 October 2016
9:00am - 12:00 am
1:00pm - 4:00pm

1 Stock creation

☑ Program calculation for creation of stock - some results shown below

☑ Prepare shielding for transfer for closet solution

- Clean off and move leaded shielding in rad area to countertop next to fume-hood
- Add diaper paper on countertop, and on shielding incase of contamination
- Practice transfer

☑ -

0.149+/-0.011 ml of 15.43+/-0.06 M HNO_3 $\boxed{Stock\ HNO_3}$
+
1.91+/-0.08 ml of 0.0+/-0 M solution $\boxed{DI\ Water}$
=
2.048+/-0.026 ml of 1.12+/-0.08 M HNO_3 solution $\boxed{\rightarrow Stock}$ (glass container)

☑ -

Combine 0.500+/-0.005 ml of 15.43+/-0.06 M HNO_3 solution $\boxed{closet}$
+
2.048+/-0.026 ml of 1.12+/-0.08 M HNO_3 solution $\boxed{Stock}$
=
2.500+/-0.025 ml of 4.00+/-0.05 M HNO_3 solution. $\boxed{\rightarrow Stock}$

☑ Lock $\boxed{Stock}$ in glovebox

☑ Put Source back in rad closet

☑ Clean up contamination added to pipette tip from transfer (for some reason, the contamination was added to the inside of the pipette itself, the tips used don't have the block, but still, none of the solution should have traveled up the shaft

☑ Dispose of diaper paper laid down for transfer (where the glass bottle was set down which contained closet solution, there was contamination (the outside of the bottle of the closet solution is contaminated)

☑ Move shielding back to where it was

2 Preparation for Process 1

☑ Count calibration standard Eu-152 in HPGe 3 hours 22 minutes at furtherest position from detector (26 cm)

- Source 1577-22
- 497.0 nCi
- Assy Date: 15 Feb 12
- 1.00568g

☑ Create Eu-152 Excel Counting sheet template for standards

☑ Set up ROI (region of interest) file for Eu-152

☑ Start background count and done for the day

- Count lasted for 12 hours

Saturday, 8 October 2016
10:00am - 2:00 pm

1 Preparation for Process 1

☑ Finish background count, lasted 12 hours

☑ Remove 0.3 ml from $\boxed{Stock}$ transfer to $\boxed{1}$ for counting

- $\boxed{1}$ is a smaller tube, which will fit into a larger centrifuge tube for, well, centrifuging
- $\boxed{1}$ tube cannot fit into centrifuge tube with white push cap (pushes on outside of tube), white push cap is necessary when votex mixing, so a blue push cap (pushes on inside of tube), was put on for counting, these smaller tubes will have to have two caps following them around, I can't wait till the second cycle when the bigger tubes will be used
- Note for why smaller tubes are being used: when pipetting the smaller volume of 0.3 ml for aq/o phase separation it is much easier to have the smaller diameter tubes
- Stock was removed from glovebox, and after was put into the safe

☑ Count $\boxed{1}$ for 1 hour and 24 minutes

☑ Fix density calculation in code, was slightly wrong before, this means $\boxed{Stock}$ and $\boxed{1}$ are slightly different from what they should be, but within error

☑ Calculation for creation of Fe(II) solution (next page)

V_1 ml of $M_{1,Fe}$ Fe(II) in M_{1,HNO_3} HNO_3
+
V_2 ml of $M_{2,Fe}$ Fe(II) in M_{2,HNO_3} HNO_3
=
V_3 ml of $M_{3,Fe}$ Fe(II) in M_{3,HNO_3} HNO_3.

The knowns are:
$M_{1,Fe} = 2.302$, $\rho_1 = 1.418$, $M_{1,HNO_3} = 0$ (Fe Stock soltuion)
$M_{2,Fe} = 0$,$\rho_2 = \rho_{HNO_3}(M_{2,HNO_3})$
$V_3 = 4$ ml, $M_{3,Fe} = 0.024$, $M_{3,HNO_3} = 4$, $\rho_3 = \rho_{HNO_3}(4M)$

Mols of Fe(II) constant: $V_1 = \frac{M_{3,Fe}V_3}{M_{1,Fe}} = 0.042$
Mols of HNO_3 constant: $V_2 = \frac{V_3 M_{3,HNO_3}}{M_{2,HNO_3}}$
Mass Constant: $V_2 = \frac{V_3\rho_3 - V_1\rho_1}{\rho_2}$

Combine last two equations:$M_{2,HNO_3} - \frac{V_3 M_{3,HNO_3}\rho_2}{V_3\rho_3 - V_1\rho_1} = 0$

Solve iteratively (where M_{2,HNO_3} determines ρ_2) with first guess of: $M_{2,HNO_3} = \frac{M_{3,HNO_3}V_3}{V_2}$

Sunday, 9 October 2016
7:30 pm - 11:30 pm

1 Preparation for Process 1

☑ Prepare for multi contact extraction and back extraction exp

- Make solution of 30 vol.% TBP with kerosene
- Make 40 ml of solution 4.06 M HNO_3 solution,
- Transfer two smaller vials (one for TBP phase), one for Fe phase, with two different lids into glovebox (with a larger vial to hold them in the centrifuge)
- Transfer two smaller vials with centrifuge vials for centrifuging, keep one with water 0.3 ml, and TBP mix 0.32 ml $\boxed{Vial\ 1\ Budd}$, and the second with 1.2 ml of TBP mix and 1.25 ml water $\boxed{Vial\ 2\ Budd}$
- Transfer $\boxed{Stock}$ and $\boxed{1}$ to glovebox
- Transfer another vial to hold the Fe solution
- Make sure tweezers are in glovebox (they are) - to remove smaller vials from centrifuge tubes
- Transfer slightly contaminated pipette to glovebox
- All above vials that would contain solution were rinsed with whatever they would hold for approximately 3 minutes

☑ -

15+/-0.15 ml of TBP $\boxed{Stock\ TBP}$
+
35+/-0.35 ml of kerosene $\boxed{Stock\ kerosene}$
=
50+/-0.5 ml of 30 vol.% TBP. $\boxed{\rightarrow TBP}$

☑ -

10.579+/-0.011 ml of 15.35+/-0.13 M HNO_3 $\boxed{Stock\ HNO_3}$
+
30.355+/-0.030 ml of 0.0+/-0 M HNO_3 solution $\boxed{DI\ Water}$
=
39.94+/-0.14 ml of 4.07+/-0.04 M HNO_3 solution $\boxed{\rightarrow Fe\ Prep}$

Sunday, 9 October 2016 *7:30 pm - 11:30 pm*

To create an Fe solution for a back extraction, $\boxed{Fe\ Prep}$ should be combined in the following manner (Small portions created because this solution has a short half life with larger concentrations of HNO_3).

☐ -

0.0417+/-0.0018 ml of 2.302+/-0.009 M Fe(II) in 0.0+/-0 M HNO_3 $\boxed{Stock\ Fe(II)}$
+
3.941+/-0.027 ml of 0.0+/-0 M Fe(II) in 4.06+/-0.05 M HNO_3 solution $\boxed{Fe\ Prep}$
+
4.000+/-0.020 ml of 0.0240+/-0.0010 M Fe(II) in 4.00+/-0.05 M HNO_3 solution
$\boxed{\rightarrow Bk\ Ex\ Solution}$.

☑ Add Sodium Nitrite to $\boxed{1}$, it will sit overnight, but it doesn't have to

- Dropped $\boxed{1}$, solution probably contaminated blue lid (crap), centrifuged on 1000 rpm for 2 minutes

Monday, 7 November 2016

☐ -

~~Combine 2.500+/-0.025 ml of 4.00+/-0.05 M HNO_3 solution. *Stock Add*~~
~~+~~
~~0.700+/-0.028 ml of 4.00+/-0.05 M HNO_3 solution *Stock*~~
~~=~~
~~3.2+/-0.038 ml of 4.00+/-0.05 M HNO_3 solution. → *Stock*~~

- A problem...I am not sure how this happened, and I kind of don't want to bring it up, but I was able to get only, 400 μl out of *Stock*, I would expect to get 690 μl out of *Stock*..where did 290 μl go? Did it evaporate? Do we need to parafilm wrap it?
- As a precaution, I will parafilm wrap it

☑ Transfer 400 μl *Stock* to *Stock Add*

- Also switched caps (because aluminum foil cap was removed on *Stock* and I liked having it off)

☑ Transfer *closet* out of glovebox

☑ Transfer *closet* to rad closet

☑ Transfer 0.4 ml of *Stock Add* to 8

☑ Transfer 0.4 ml of *Stock Add* to 9

☑ Transfer 0.4 ml of *Stock Add* to 10

☑ Add scoop of sodium nitrite to 8

☑ Add scoop of sodium nitrite to 9

☑ Add scoop of sodium nitrite to 10

☑ Put 8, 9, and 10 into 15 ml centrifuge tubes

☑ Centrifuged 8, 9 and 10 to push all solution to botttom of vials

☑ Fixed shielding on detector

- Retake background and efficiency count

☐ Note when ^{137}Cs will be floating around lab

- T, Th 1-4 pm, and Wed 2-5, this week and next week
- Do not count during this time

☑ Background Count

Monday, 7 November 2016

☑ Eff Count

☐ Practice extraction with 400 μl while doing counts tonight

☑ Count 8

☑ Count 9

☐ Count 10

- Alarm didn't wake me up...didn't count 10

Tuesday, 8 November 2016

1 Cycle experiment, round 2, replicate of 3

☑ Count [10]

☑ Label vials, [8 *aq*], [8 *aq C*], [8 *or*], [8 *or C*] [9 *aq*], [9 *aq C*], [9 *or*], [9 *or C*] [10 *aq*], [10 *aq C*], [10 *or*], [10 *or C*] (smaller 2.5 ml tubes)

☑ Label vials [8 *mix*], [9 *mix*], [10 *mix*] (smaller 1 ml tubes from John Burns, have conical bottoms, makes more minute separations easier)

☑ Transfer [8], [9], and [10] into glovebox. With: [8 *aq*], [8 *aq C*], [8 *or*], [8 *or C*] [9 *aq*], [9 *aq C*], [9 *or*], [9 *or C*] [10 *aq*], [10 *aq C*], [10 *or*], [10 *or C*]. (3 clear push caps, and 9 blue push caps). Also with 6 15 ml centrifuge tubes, and [8 *mix*], [9 *mix*], [10 *mix*]

☑ Add 400 μl of [*TBP*] to [8], [9], and [10] each

☑ Vortex mix [8] for 15 minutes on pulse mode

☑ Vortex mix [9] for 15 minutes on pulse mode

☑ Vortex mix [10] for 15 minutes on pulse mode

- Switched to push caps for each of the above

☑ Centrifuge [8], [9], and [10] with [*Buddy*] on 3300 rpm, for 5 minutes

☑ During the vortex mixing and the centrifuge practice the transfer in the fumehood

- Was able to get about 395 ml of aqueous phase and 365 ml of organic phase

☑ Pipette with disposable pipette the aqueous phase first, then the organic (for all three vials), as much as so that there is no mixing. Then transferred the boundary to a smaller vial, centrifuged, and separated further. Counting solutions were also prepared of 250 μl of each of the solutions **Should have centrifuged final solutions before this**. A picture will be provided for the whole process for [8] on the following page, below are specific notes about what occured during the experiment.

- $\boxed{10}$ had to be centrifuged again with $\boxed{Buddy}$ (shock the phases too much so they mixed again - accidentally pipetted organic phase during aqueous phase first separation)
- $\boxed{9\ mix}$, $\boxed{10\ mix}$ had to be recentrifuged (accidentally dropped these two small(!) vials (no place to put them)
- $\boxed{8\ mix}$ Lost a drop while making 250 μl Aq sample
- $\boxed{9\ mix}$ Lost a drop while making 250 μl Aq sample
- $\boxed{10\ mix}$ Lost a drop while making 250 μl Aq sample

☐ Measure volumes of everything

☑ Transfer out $\boxed{8\ or\ C}$, $\boxed{8\ aq\ C}$, $\boxed{9\ or\ C}$, $\boxed{9\ aq\ C}$, $\boxed{10\ or\ C}$, $\boxed{10\ aq\ C}$, in 15 ml centrifuge tubes

☑ Radiac wash the above tubes, and store in fumehood behind lead - wait to count (Marianno has an experiment going on)

☑ Clean stuff in glovebox

☑ Start count $\boxed{10\ aq\ C}$ 4:00 pm

☑ Start count $\boxed{9\ aq\ C}$ 6:00 pm

☑ Start count $\boxed{8\ aq\ C}$ 8:00 pm

☑ Start count $\boxed{10\ or\ C}$ 10:00 pm - leave overnight

☑ Create graphic for experiment

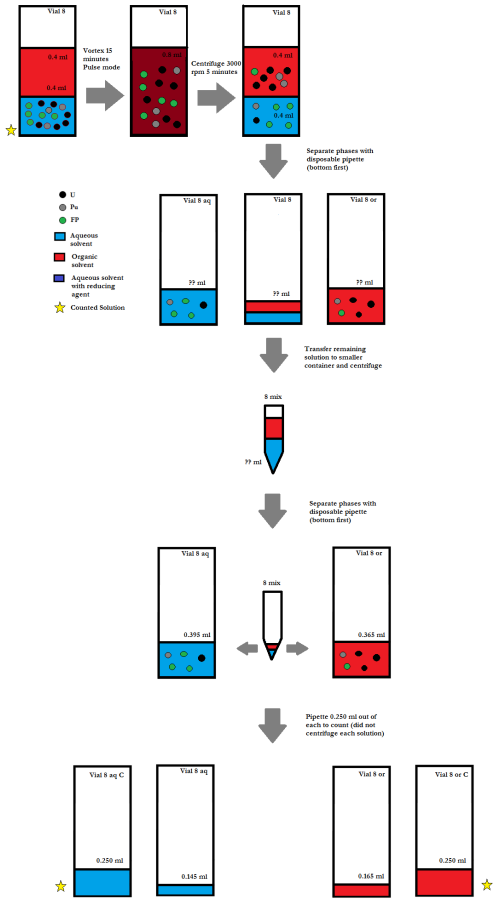

Extraction three times round 2 experimental setup

Wednesday, 16 November 2016

- ☑ Transfer in the glovebox a blue 2.5 ml vial (also hold smaller conical vials) holder - sorry Mary, it makes things much easier to have something to hold your vials
- ☑ Transfer smaller pipette tips into glovebox
- ☑ take out the trash in the glovebox

1 Cycle experiment, round 2, replicate of 3

- ☑ Finish count $\boxed{9\ or}$
- ☑ Begin count $\boxed{8\ or}$ (9:44 am)

2 Cycle experiment, round 2, replicate of 3, ALPHA preparation for extraction 1 (also Mass Spec preparation)

- ☑ Make alpha sample of stock, make 3 (Pipette Errors - assume 20 μl error 1%, 10 μl error 1.2%, 390 μl error 2%, 890 μl error 1%)

10+/-0.12 μl of $\boxed{Stock\ Add}$ (4 M HNO_3) [smaller pipette]
+
990+/-9.9 μl of DI water (leftover in glovebox)
=
1+/-9.9 ml of $\sim$ 0 M HNO_3 $\boxed{8, 9, 10\ Dilution}$

20+/-0.2 μl of $\boxed{8, 9, 10\ aq\ Dilution}$ dropped onto $\boxed{8\ Chip}$

~~20~~ 10?+/-0.2 μl of $\boxed{8, 9, 10\ aq\ Dilution}$ dropped onto $\boxed{9\ Chip}$

~~20~~ 10?+/-0.2 μl of $\boxed{8, 9, 10\ aq\ Dilution}$ dropped onto $\boxed{10\ Chip}$

- ☑ Make alpha sample of each aqueous
  - ☑ - $\boxed{8\ aq}$

10+/-0.12 μl of 8 *aq* (4 M HNO_3) [smaller pipette]
+
390+/-7.8 μl of DI water (leftover in glovebox)
=
0.4+/-0.0078 ml of $\sim$ 0 M HNO_3 8 *aq Dilution*

- 8 *aq* transfer contaminated gloves (had the blue push cap) and the vial accidentally fell

20+/-0.2 μl of 8 *aq Dilution* dropped onto 8 *aq Chip*

☑ - 9 *aq*

- 9 *aq* and 10 *aq* centrifuged, so no contamination on glovebox gloves like above

10+/-0.12 μl of 9 *aq* (4 M HNO_3) [smaller pipette]
+
390+/-7.8 μl of DI water (leftover in glovebox)
=
0.4+/-0.0078 ml of $\sim$ 0 M HNO_3 9 *aq Dilution*

20+/-0.2 μl of 9 *aq Dilution* dropped onto 9 *aq Chip*

☑ - 10 *aq*

10+/-0.12 μl of 10 *aq* (4 M HNO_3) [smaller pipette]
+
390+/-7.8 μl of DI water (leftover in glovebox)
=
0.4+/-0.0078 ml of $\sim$ 0 M HNO_3 10 *aq Dilution*

20+/-0.2 μl of 10 *aq Dilution* dropped onto 10 *aq Chip*

☑ Make alpha sample of each organic phase

☑ - 8 *or*

10+/-0.12 μl of 8 *or* (30% TBP) [smaller pipette]
+
890+/-8.9 μl of 30% TBP (leftover in glovebox)
=
0.9+/-0.0089 ml of 30% TBP 8 *or Dilution*

20+/-0.2 μl of 8 *or Dilution* dropped onto 8 *or Chip*

- **Spilled some organic on inner ring?? of** 8 *or Chip*, **question because hard to see in glovebox**

☑ - 9 *or*

10+/-0.12 μl of 9 *or* (30% TBP) [smaller pipette]
+
890+/-8.9 μl of 30% TBP (leftover in glovebox)
=
0.9+/-0.0089 ml of 30% TBP 9 *or Dilution*

10+/-0.12 μl of 9 *or Dilution* dropped onto 9 *or Chip*

- **Changed volume on chip because** 8 *or Chip* **potentially spilled over the inner ring**

☑ - 10 *or*

10+/-0.12 μl of 10 *or* (30% TBP) [smaller pipette]
+
890+/-8.9 μl of 30% TBP (leftover in glovebox)
=
0.9+/-0.0089 ml of 30% TBP 10 *or Dilution*

10+/-0.12 μl of 10 *or Dilution* dropped onto 10 *or Chip*

- **Changed volume on chip because** 8 *or Chip* **potentially spilled over the inner ring**

☑ **Note: Centrifuged all dilution vials before making alpha samples, which means that first all dilutions were made, then all alpha samples were made**

☑ The above 7 alpha samples take up space in the glovebox, and I didn't want to disturb the samples (moving them screws them up) so I let them dry overnight

3 Process Experiment (continuation from cycle experiment)

☑ Combine all aqueous phases together (done with disposable pipetets)

- ☑ 8 *aq C* + 8 *mix* → 8 *aq* (take all of first and add to second)
- ☑ 9 *aq C* + 9 *mix* → 9 *aq*
- ☑ 10 *aq C* + 10 *mix* → 10 *aq*

Thursday, 17 November 2016

1 Cycle experiment, round 2, replicate of 3, ALPHA preparation for extraction 1 (also Mass Spec preparation)

Note all alpha counts were done on the 9mm height setting on the pips detector.

- ☑ Start Count $\boxed{10\ or\ Chip}$ (10:52 am)
- ☑ End Count $\boxed{10\ or\ Chip}$ Run time 7.54 hrs
- ☑ Start count $\boxed{10\ aq\ Chip}$ (6:29 pm)

2 Experiment to double check ^{137}Cs using combined aqueous series 5 and 6, 56

In order to capture the D-value for ^{137}Cs, an experiment was proposed. Our problem with measuring ^{137}Cs is that its D-value and activity are so low that we aren't getting good statistics for its answer, and the answer we are getting is not the answer we want, we are getting something around 10^{-5}, and the answer is more probably around 0.01.

It was proposed to take an old series (series 5 or 6), and perform an extraction with a larger volume of organic, so that more ^{137}Cs could be extracted, and therefore better statistics on all the calculations. Some notes are copied down from hand calculations for the experiment.

- $\boxed{5\ aq}$ has 461 μl, 4.47 μCi, $\sim$ 3.6% dead time
- $\boxed{6\ aq}$ has 469 μl, 4.40 μCi, $\sim$ 3.6% dead time, this vial is also a little milky, meaning there is a small amount of organic in there
- Both above vials should were in fumehood
- Some evaporation happened in $\boxed{Stock}$, I know this because the activity density changed from $\boxed{Stock}$ and $\boxed{Stock\ add}$.
- If we take 800 μl total (after mixing $\boxed{5\ aq}$ and $\boxed{6\ aq}$), then we could expect $\sim$ 8.87 μl (about 200 cps), of ^{137}Cs with $\sim$ 6% dead time

- If we want 3 cps in the final organic (about an hour of count time) and if I assume the D-value is 0.01 (which Dr. Chirayath insists), (3/200 $\sim$ 1.5% of the counts)

$$\begin{aligned}\% =& \frac{1}{1+\frac{V_a}{V_o}\frac{1}{D}} \\ =& \frac{1}{1+\frac{1}{2}\frac{1}{0.01}} = 0.019\end{aligned}$$

This means if we double the volume of the organic, then we should get a decent count rate so as to count ^{137}Cs and get good statistics with an hour count. This is IF the D-value is 0.01, as Dr. Chirayath insists.

- Dr. Burns came by and said, instead of 2x the organic volume, should do 10x, to make sure we get all the counts!
- Okay! Sounds good! We will for sure get the right answer now! We also rederived the D-value equation

With conservation of mass, and using values from the two phases,

$$\% \text{ Extracted} = \frac{[\frac{CPS}{V_m}]_o \cdot V_{co}}{[\frac{CPS}{V_m}]_o \cdot V_{co} + [\frac{CPS}{V_m}]_a \cdot V_{ca}}$$

$$\begin{aligned}\frac{1}{\% \text{ Extracted}} =& \frac{[\frac{CPS}{V_m}]_o \cdot V_{co} + [\frac{CPS}{V_m}]_a \cdot V_{ca}}{[\frac{CPS}{V_m}]_o \cdot V_{co}} \\ =& 1 + \frac{[\frac{CPS}{V_m}]_a \cdot V_{ca}}{[\frac{CPS}{V_m}]_o \cdot V_{co}} \\ =& 1 + \frac{1}{D} \cdot \frac{V_{ca}}{V_{co}}\end{aligned}$$

$$\frac{1}{\frac{V_{ca}}{V_{co}}\left(\frac{1}{\% \text{ Extracted}} - 1\right)} = D$$

Where V_m is the measured volume for the count, V_{co} is the volume of the organic contact and V_{ao} is the volume of the aqueous contact.

- ☑ Combine $\boxed{5\ aq}$ and $\boxed{6\ aq}$ into $\boxed{5\ aq}$
- ☑ Take 800 μl out of $\boxed{5\ aq}$ and transfer into a 15 ml vial labeded $\boxed{56}$ (for some reason it was really difficult to get a precise volume - had to do many times)
- ☑ Start count $\boxed{56}$ at 26 cm

3 Cycle experiment, round 2, replicate of 3

☑ Finish count $\boxed{8\ or}$ ($\sim$ 9:45 am) about this time another count was started - vial 56, described above

☑ Analyzed last two organics, put into excel sheet

- All samples of organic, after mixing organic parts together, redrawing 250 μl and recounting, increased in activity. This could support the conclusion that some aqueous passed to the main organic, and when the 250 μl was first drawn, was on the bottom of the vial. When the 250 μl was second drawn, it had time to dissolve into the TBP, because HNO_3 is slightly soluble in TBP (Nuclear Chemical Engeineering pg 160)

4 Process Experiment (continuation from cycle experiment)

☑ Measure volumes of all aqueous phases, $\boxed{8\ aq}$ $\boxed{9\ aq}$, $\boxed{10\ aq}$

Volumes for combined aqueous phases

Series	Aqueous (8,9, or 10)
8	397 +/- 7.94
9	~~386~~ 389 +/- 7.78 (after centrifuge)
10	395 +/- 7.9

Second Contact...

☑ Label vials, $\boxed{8\ aqII}$, $\boxed{8\ aqII\ C}$, $\boxed{8\ orII}$, $\boxed{8\ orII\ C}$ $\boxed{9\ aqII}$, $\boxed{9\ aqII\ C}$, $\boxed{9\ orII}$, $\boxed{9\ orII\ C}$ $\boxed{10\ aqII}$, $\boxed{10\ aqII\ C}$, $\boxed{10\ orII}$, $\boxed{10\ orII\ C}$ (smaller 2.5 ml tubes)

- Will reuse $\boxed{8\ mix}$, $\boxed{9\ mix}$, $\boxed{10\ mix}$ (smaller 1 ml tubes from John Burns, have conical bottoms, makes more minute separations easier)

☑ Transfer: $\boxed{8\ aqII}$, $\boxed{8\ aqII\ C}$, $\boxed{8\ orII}$, $\boxed{8\ orII\ C}$ $\boxed{9\ aqII}$, $\boxed{9\ aqII\ C}$, $\boxed{9\ orII}$, $\boxed{9\ orII\ C}$ $\boxed{10\ aqII}$, $\boxed{10\ aqII\ C}$, $\boxed{10\ orII}$, $\boxed{10\ orII\ C}$. (3 clear push caps, and 6 blue push caps 6 red push caps). Also with 6 15 ml centrifuge tubes

☑ Add 397 μl of $\boxed{TBP}$ to $\boxed{8\ aq}$

☑ Add 389 μl of $\boxed{TBP}$ to $\boxed{9\ aq}$

☑ Add 396 μl of $\boxed{TBP}$ to $\boxed{10\ aq}$

Thursday, 17 November 2016

☑ Vortex mix $\boxed{8\ aq}$ for 15 minutes on pulse mode

☑ Centrifuge $\boxed{8\ aq}$ with $\boxed{Buddy}$ at 3,300 rpm for 10 minutes

- Decieded after this to wait, and centrifuge them all together

☑ Vortex mix $\boxed{9\ aq}$ for 15 minutes on pulse mode

☑ Vortex mix $\boxed{10\ aq}$ for 15 minutes on pulse mode

☑ Centrifuge $\boxed{8\ aq}$, $\boxed{9\ aq}$, and $\boxed{10\ aq}$ with $\boxed{Buddy}$ on 3300 rpm, for 5 minutes

☐ ~~During the vortex mixing and the centrifuge practice the transfer in the fumehood~~
Prayed instead

☑ Pipette with disposable pipette the organic phase first, then the aqueous (for all three vials), as much as so that there is no mixing. Then transferred the boundary to a smaller vial, let sit. Prepare counting solutions of 250 μl of each of the solutions A picture will be provided for the whole process for $\boxed{8\ aq}$ on the following page , below are specific notes about what occured during the experiment.

- $\boxed{8\ aq}$ was 248 μl pipetted to $\boxed{8\ aqII\ C}$ instead of 250 μl?

☐ ~~Measure volumes of everything~~

☑ Transfer out $\boxed{8\ orII\ C}$, $\boxed{8\ aqII\ C}$, $\boxed{9\ orII\ C}$, $\boxed{9\ aqII\ C}$, $\boxed{10\ orII\ C}$, $\boxed{10\ aqII\ C}$, in 15 ml centrifuge tubes

☑ Radiac wash the above tubes, and store in fumehood behind lead - wait to count

☑ Clean stuff in glovebox

☑ Start count $\boxed{9\ orII\ C}$ at 0 cm 4:06 pm

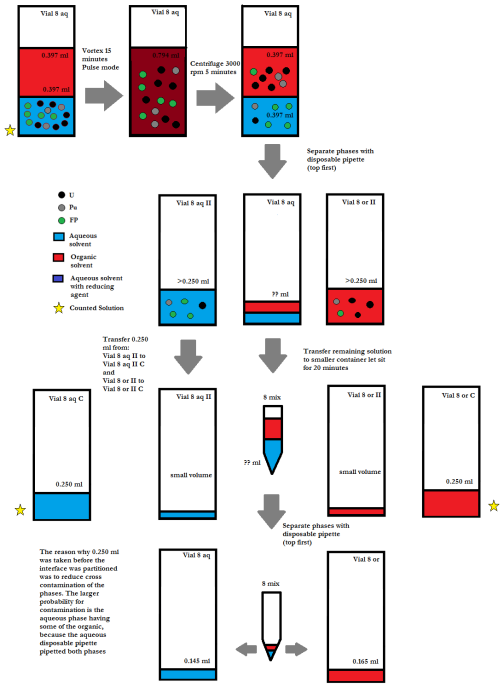

Extraction three times round 2 extraction 2

APPENDIX E

CODE REPOSITORY

This appendix was intentionally put at the end of the document because miscellaneous codes for various calculations are reproduced.

Chemistry Calculattions

Listing E.1: Chemistry calculation examples defined functions following in the next listing

```
#!/usr/bin/env python3

#################################################################
#################### Import packages ############################
#################################################################

import os.path
import pandas as pd
import numpy as np
import matplotlib.pyplot as plt
import datetime
from uncertainties import ufloat
from uncertainties.umath import *
from uncertainties import unumpy as unp
import re
import time
start_time = time.time()

import Functions as fun


#################################################################
## Calculate molar mass and concentrations of Fe(II) sulfamate #
#################################################################

#########################################################
############          Given              ##############
#########################################################

WtConcentration=ufloat(40.26,0.05)
density=ufloat(1.418,0.005)


#########################################################
############ Calculate grams per mol of ###############
############    a chemical formula      ###############
```

```
#######################################################

#Make sure your chemical form has no repeats
#And no parentheses
ChemicalFormula='FeH_4N_2O_6S_2'
ChemicalFormulaError=[0,0,0,0,0,0,0] #+/- error in integers of
                                     #chemical formula
ChemicalFormula=ChemicalFormula+"    "
List=fun.ChemList(ChemicalFormula)

#Enter Modifications:
#1. Each element should be a single item in the list
#2. Format: zaid atomfraction+/-error zaid atomfraction+/-error
#   or    : zaid atomfraction error zaid atomfraction
# For no modifications set = ['']
Modifications=['']

df = pd.read_csv('../Data/AtomicWeights.csv')


ModMass,ModSymbols,AtomFractions=fun.FormatMods(Modifications,df)
MolarMass=fun.DetermineMolarMass(List,df,
                                 ModSymbols,ModMass,
                                 AtomFractions,
                                     ChemicalFormulaError)


#######################################################
############### Molality and Molarity #################
#######################################################

m=fun.WttoMolality(MolarMass,WtConcentration)
M=fun.ConvertMolDenGiven(False,m,MolarMass,density)

#######################################################
################ Print Out Answer #####################
#######################################################

print("Molarity  : "+str(M))
print("Molality  : "+str(m))
print("WtConcentr: "+str(WtConcentration))
print("Molar Mass: "+str(MolarMass))
print("Density   : "+str(density))


#######################################################################
# To create the Fe(II) solution at a particular
# concentration of nitric acid and Fe(II) of a
# particular volume
#######################################################
```

```
V3=ufloat(4,0.02)
N=100
Range=0.1

#Fe(II)
MF1=ufloat(2.302,0.009)
MF2=ufloat(0,0)
MF3=ufloat(0.024,0.001)
V1=(MF3*V3)/MF1
gramsOmolF=ufloat(248.022,0.017)
p1=ufloat(1.418,0.005)

##### HNO3
gramsOmolN=ufloat(63.0130,0.0012)
Temperature=ufloat(24.8,3)
dfDen=pd.read_csv('../Data/Nitric_Acid.csv')
MN1=ufloat(0,0)
MN3=ufloat(4,0.05)
mN3=fun.ConvertMol(True,MN3,gramsOmolN,dfDen,Temperature)
WtN3=fun.GetWt(mN3,gramsOmolN)
p3=fun.GetDensity(Temperature,WtN3,dfDen)

#### Calculation

C=(V3*MN3)/(V3*p3-V1*p1)

MN2=(MN3*V3)/(V3-V1) # A Guess
MN2Range=np.linspace(MN2-MN2*Range,MN2+MN2*Range,N)

Compare=[]
for MN2i in MN2Range:
    mN2i=fun.ConvertMol(True,MN2i,gramsOmolN,dfDen,Temperature)
    WtN2i=fun.GetWt(mN2i,gramsOmolN)
    p2i=fun.GetDensity(Temperature,WtN2i,dfDen)
    Compare.append(abs(MN2i-C*p2i))
    if Compare[-1]==0:
        break
MN2=MN2Range[Compare.index(min(Compare))]
mN2=fun.ConvertMol(True,MN2,gramsOmolN,dfDen,Temperature)
WtN2=fun.GetWt(mN2,gramsOmolN)
p2=fun.GetDensity(Temperature,WtN2,dfDen)

V2=(V3*p3-V1*p1)/p2

print("Combine "+str(V1)+" ml of "+str(MF1)+\
      " M Fe(II) in "+str(MN1)+" M HNO_3 solution with "+str(V2)+\
      " ml of "+str(MF2)+" M Fe(II) in "+str(MN2)+" M HNO_3
         solution, to get "+str(V3)+" ml of "+\
      str(MF3)+" M Fe(II) in "+str(MN3)+" M HNO_3 solution")
```

```
#######################################################
# Known initial Molarities, and volumes
# Calculate final molarity and volume and density
#######################################################

Temperature=ufloat(24.8,3)
gramsOmol=ufloat(63.0130,0.0012)
dfDen=pd.read_csv('../Data/Nitric_Acid.csv')

PipettError=0.001 #Depends on volume preparing

#M1=ufloat(15.43,0.06)
M1=ufloat(4,0.13)
m1=fun.ConvertMol(True,M1,gramsOmol,dfDen,Temperature)

M2=ufloat(0,0)
m2=ufloat(0,0)

Vol1=ufloat(0.01,0.0003)
Vol2=ufloat(0.39,0.0039)

WtConcentration1=fun.GetWt(m1,gramsOmol)
WtConcentration2=fun.GetWt(m2,gramsOmol)

p1=fun.GetDensity(Temperature,WtConcentration1,dfDen)
p2=fun.GetDensity(Temperature,WtConcentration2,dfDen)


#Check calculation
m3,p3,Vol3,Wt,M3=fun.NewConcentration(m1,m2,gramsOmol,
                                      Temperature,dfDen,
                                      Vol1,Vol2)

print("Combine "+str(Vol1)+" ml of "+str(M1)+\
      " M solution with "+str(Vol2)+\
      " ml of "+str(M2)+" M solution, to get "+str(Vol3)+" ml of "
         +\
      str(M3)+" M solution")
print("The final density is "+str(p3))
print("The initial density is "+str(p1))


#######################################################
# With known Molarity and volume of a solution
# how much, and of what concentration
# do we need to combine with a second solution
# to get a final solution of known concentration
# and volume
#######################################################
N=100
Range=0.1
```

```
Temperature=ufloat(24.8,3)
gramsOmol=ufloat(63.0130,0.0012)
dfDen=pd.read_csv('../Data/Nitric_Acid.csv')

#M1=ufloat(15.43,0.06)
M1=ufloat(4,0.13)
m1=fun.ConvertMol(True,M1,gramsOmol,dfDen,Temperature)
#m1=ufloat(35.5,0.5)
Vol1=ufloat(0.01,0.0003)
#M2=ufloat(0,0)
#m2=ufloat(0,0)

M3=ufloat(2,0.02)
m3=fun.ConvertMol(True,M3,gramsOmol,dfDen,Temperature)
Vol3=ufloat(1,0.025)

WtConcentration1=fun.GetWt(m1,gramsOmol)
#WtConcentration2=fun.GetWt(m2,gramsOmol)
WtConcentration3=fun.GetWt(m3,gramsOmol)

p1=fun.GetDensity(Temperature,WtConcentration1,dfDen)
p3=fun.GetDensity(Temperature,WtConcentration3,dfDen)

A=M3*Vol3-M1*Vol1
B=(1-WtConcentration3)*Vol3*p3-(1-WtConcentration1)*Vol1*p1
C=B/A

M2Guess=(M3*Vol3-M1*Vol1)/(Vol3-Vol1)
M2Range=np.linspace(M2Guess-M2Guess*Range,M2Guess+M2Guess*Range,N)
Compare=[]

for M2i in M2Range:
    m2i=fun.ConvertMol(True,M2i,gramsOmol,dfDen,Temperature)
    Wt2i=fun.GetWt(m2i,gramsOmol)
    p2i=fun.GetDensity(Temperature,Wt2i,dfDen)
    Compare.append(abs(C-((1-Wt2i)*p2i)/M2i))
    V2i=A/M2i
    if Compare==0:
        break

M2=M2Range[Compare.index(min(Compare))]
m2=fun.ConvertMol(True,M2,gramsOmol,dfDen,Temperature)
Wt2=fun.GetWt(m2,gramsOmol)
p2=fun.GetDensity(Temperature,Wt2,dfDen)
V2=A/M2


#Check if we are correct
mc3,pc3,Vc3,Wtc3,Mc3=fun.NewConcentration(m1,m2,gramsOmol,
                                          Temperature,dfDen,
```

```
                                                    Vol1,V2)
#print(M2Guess,M2i,min(M2Range),max(M2Range))
#print(M3,Vol3)
#print(Mc3,Vc3)

#Print out answer
print("Combine "+str(Vol1)+" ml of "+str(M1)+\
      " M solution with "+str(V2)+\
      " ml of "+str(M2)+" M solution, to get "+str(Vol3)+" ml of "
         +\
      str(M3)+" M solution")

#########################################################
# What volumes to you need to get final solution of
# x concentration and y molarity
# You know the initial molarities, the final volume
# and molarity
#########################################################

Temperature=ufloat(24.8,3)
gramsOmol=ufloat(63.0130,0.0012)
dfDen=pd.read_csv('../Data/Nitric_Acid.csv')

PipettError=0.001 #Depends on volume preparing

#M1=ufloat(15.43,0.06)
M1=ufloat(15.35,0.13)
m1=fun.ConvertMol(True,M1,gramsOmol,dfDen,Temperature)

M2=ufloat(0,0)
m2=ufloat(0,0)

#M3=ufloat(1.14,0.08)
#M3=ufloat(4.06,0) #For Fe(II) pre solution
M3=ufloat(4,0)
m3=fun.ConvertMol(True,M3,gramsOmol,dfDen,Temperature)
#Vol3=ufloat(2.048,0.026)
#Vol3=ufloat(40,0)
Vol3=ufloat(10,0)

WtConcentration1=fun.GetWt(m1,gramsOmol)
WtConcentration2=fun.GetWt(m2,gramsOmol)
WtConcentration3=fun.GetWt(m3,gramsOmol)

p1=fun.GetDensity(Temperature,WtConcentration1,dfDen)
p2=fun.GetDensity(Temperature,WtConcentration2,dfDen)
p3=fun.GetDensity(Temperature,WtConcentration3,dfDen)

A=(1-WtConcentration1)*p1
B=(1-WtConcentration2)*p2
b1=(1-WtConcentration3)*Vol3*p3
```

```
b2=M3*Vol3

C1=M2-M1/A
C2=b2-(M1*b1)/A
Vol2=C2/C1
Vol1=(b1-B*Vol2)/A

Vol1=ufloat(Vol1.nominal_value,Vol1.nominal_value*PipettError)
Vol2=ufloat(Vol2.nominal_value,Vol2.nominal_value*PipettError)

#Check calculation
#print(M3,Vol3)

m3,p3,Vol3,Wt,M3=fun.NewConcentration(m1,m2,gramsOmol,
                                      Temperature,dfDen,
                                      Vol1,Vol2)

#print(M3,Vol3)

print("Combine "+str(Vol1)+" ml of "+str(M1)+\
      " M solution with "+str(Vol2)+\
      " ml of "+str(M2)+" M solution, to get "+str(Vol3)+" ml of "
         +\
      str(M3)+" M solution")


#################################################################
## Calculate molar mass and concentrations of HNO3 stock #
#################################################################

#########################################################
############          Given              ##############
#########################################################

WtConcentration=ufloat(69,0.5)

#########################################################
############ Calculate grams per mol of ###############
############    a chemical formula      ###############
#########################################################

#Make sure your chemical form has no repeats
#And no parentheses
ChemicalFormula='HNO_3'
ChemicalFormulaError=[0,0,0,0,0,0,0] #+/- error in integers of
                                     #chemical formula
ChemicalFormula=ChemicalFormula+"    "
List=fun.ChemList(ChemicalFormula)

#Enter Modifications:
#1. Each element should be a single item in the list
```

```
#2. Format: zaid atomfraction+/-error zaid atomfraction+/-error
#   or    : zaid atomfraction error zaid atomfraction
# For no modifications set = ['']
Modifications=['']

df = pd.read_csv('../Data/AtomicWeights.csv')


ModMass,ModSymbols,AtomFractions=fun.FormatMods(Modifications,df)
MolarMass=fun.DetermineMolarMass(List,df,
                                 ModSymbols,ModMass,
                                 AtomFractions,
                                     ChemicalFormulaError)

#########################################################
############### Molality and Molarity ###################
#########################################################

m=fun.WttoMolality(MolarMass,WtConcentration)

#Density in grams per cc or grams per ml
dfDen=pd.read_csv('../Data/Nitric_Acid.csv')
Temperature=ufloat(24.8,3) #Same degrees as dfDen!!!

M=fun.ConvertMol(False,m,MolarMass,dfDen,Temperature)

#########################################################
#################### Density ############################
#########################################################

density=fun.GetDensity(Temperature,WtConcentration,dfDen)

#########################################################
################ Print Out Answer ######################
#########################################################

print("Molarity  : "+str(M))
print("Molality  : "+str(m))
print("WtConcentr: "+str(WtConcentration))
print("Molar Mass: "+str(MolarMass))
print("Density   : "+str(density))
print("pH        : "+str(-log(M,10)))
```

Listing E.2: Functions for chemistry calculations.

```
#!/usr/bin/env python3

"""
FractionAM converts atom fractions to mass fractions
```

```
and mass fractions to atom fractions. Input is a
single string with MCNP style fractions.
"""

__author__      =  "Paul Mendoza"
__copyright__   =  "Copyright 2016, Planet Earth"
__credits__     = ["Sunil Chirayath",
                   "Charles Folden",
                   "Jeremy Conlin"]
__license__     =  "GPL"
__version__     =  "1.0.1"
__maintainer__  =  "Paul Mendoza"
__email__       =  "paul.m.mendoza@gmail.com"
__status__      =  "Production"

#####################################################################
#################### Import packages ################################
#####################################################################

import os.path
import pandas as pd
import numpy as np
import matplotlib.pyplot as plt
import datetime
from uncertainties import ufloat
from uncertainties.umath import *
from uncertainties import unumpy as unp
import re

#####################################################################
######################### Functions #################################
#####################################################################

def ReturnUfloat(string):
    """
    string has format   238.023249814(23)
            or format   [15.99903-15.99977]
            or format   235.04+/-0.0000019

    Returns a uncertain number so python can do calculations
    """
    if "(" in string:
        Number=str(string.split('(')[0])
        LastErrorNumber=str(string.split("(")[1].replace(")",""))
        NumberOfZeros=len(Number.split(".")[1])-len(
            LastErrorNumber)
        Error="0."
        for i in range(0,NumberOfZeros):
            Error=Error+"0"
        Error=Error+LastErrorNumber
    elif "[" in string:
```

```
        FirstNum=float(string.split('-')[0].replace("[",''))
        SecondNum=float(string.split('-')[1].replace(']',''))
        Number=str((FirstNum+SecondNum)/2)
        Error=str(float(Number)-FirstNum)
    elif "+/-" in string:
        Number=string.split("+/-")[0]
        Error=string.split("+/-")[1]

    return(ufloat(float(Number),float(Error)))

def FindAtomicMass(df,proton,Isotope):
    """
    This function will take in a dataset 'df' look through the
    'df.Protons' column and find the column that matches with
    'proton'. If the row that contains 'proton' also contains
    'Isotope' in the 'df.Isotope' column, then the value stored
    in 'df.Relative_Atomic_Mass' is reported for that row.
    Because the proton numbering scheme can have a format
    '10' for hydrogen and '10' for neon (following MCNP ZAID
    naming conventions) if we don't find a value with the whole
    string of 'proton' then the program looks through the first
    element of string and tries to match that 'proton[0]'
    If no matches are found, and error is thrown out.

    df = dataset with columns 'Protons' 'Isotopes' and
    'Relative_Atomic_Mass'. Dataset created with pandas

    proton = string with proton number (follow MCNP zaid format)

    Isotope = string with isotope number (just put the atomic mass
    do not follow MCNP format - different for few cases)
    """
    #print(df)
    for i in range(0,len(df.Protons)):
        dfPro=str(df.Protons[i])
        if proton==dfPro:
            dfIso=str(df.Isotope[i])
            if Isotope==dfIso:
                Mass=df.Relative_Atomic_Mass[i]
                break
    try:
        Mass
    except NameError:
        for i in range(0,len(df.Protons)):
            dfPro=str(df.Protons[i])
            if proton[0]==dfPro:
                dfIso=str(df.Isotope[i])
                if Isotope==dfIso:
                    Mass=df.Relative_Atomic_Mass[i]
                    break
    try:
```

```
            Mass
        except NameError:
            print("Could not find atomic mass for proton = "\
                  +proton+" and for Isotope = "+Isotope)
    Mass=ReturnUfloat(Mass)
    return(Mass)

def CheckInParen(i,ChemicalFormula):
    """
    i = index inside the string 'ChemicalFormula
    ChemicalFormula = string that could potentially have ()

    Please note, this code is not complete
    """
    NumberOpenParen=ChemicalFormula.count("(")
    NumberCloseParen=ChemicalFormula.count(")")
    if NumberOpenParen != NumberCloseParen:
        print("Unbalanced parentheses in chemical formula")
        quit()
    if NumberOpenParen==0:
        return(1,False)

    print("Hello")
    Mul=4
    Test=True
    return(Mul,Test)

def ChemList(ChemicalFormula):
    """
    This function will take in a string for a
    chemical formula.

    Please modify your formula to fit the following rules

    1. No repeats of elements (sum up all the same time element)
    2. To enter a subscript use "_", for example He_3 indicates
       three helium atoms.
    3. Use captical letters for the first letter of an element.
       If there are multiple letters for an elemental symbol,
       then use lowercase for the second letter (program does
       not interpret three symbol elements)
    4. If there are more than 999 of a single atom in your
       chemical
       formula, you will have to write your own code. Or modify
       this one.
    """
    i=0
    List=[]
    while (i <len(ChemicalFormula)-1):
        start=i
        #print("The beginning i index = "+str(i))
```

```
        if re.search('[A-Z]',ChemicalFormula[i]):                #
           Capital letter?
            if re.search('[a-z]',ChemicalFormula[i+1]):          #
               Followed by lowercase?
                if re.search('_',ChemicalFormula[i+2]):          #
                   Followed by more than 1?
                    if re.search('[0-9]',ChemicalFormula[i+5]): #
                       Hundreds check
                        List=np.append(List,ChemicalFormula[i:i
                            +6])
                        #print(ChemicalFormula[i:i+6])
                        i=i+6
                    elif re.search('[0-9]',ChemicalFormula[i+4]):
                       #tens check
                        List=np.append(List,ChemicalFormula[i:i
                            +5])
                        #print(ChemicalFormula[i:i+5])
                        i=i+5
                    else:                                        #
                       If not hundres or tens, then ones
                        List=np.append(List,ChemicalFormula[i:i
                            +4])
                        #print(ChemicalFormula[i:i+4])
                        i=i+4
                else:                                            #
                   If not more than one, print
                    List=np.append(List,ChemicalFormula[i:i+2])
                    #print(ChemicalFormula[i:i+2])
                    i=i+2
            elif re.search('_',ChemicalFormula[i+1]):            #
               If only single symbol, then do same as above
                if re.search('[0-9]',ChemicalFormula[i+4]):      #
                   hundreds
                    List=np.append(List,ChemicalFormula[i:i+5])
                    #print(ChemicalFormula[i:i+5])
                    i=i+5
                elif re.search('[0-9]',ChemicalFormula[i+3]):    #
                   tens
                    List=np.append(List,ChemicalFormula[i:i+4])
                    #print(ChemicalFormula[i:i+4])
                    i=i+4
                else:                                            #
                   ones
                    List=np.append(List,ChemicalFormula[i:i+3])
                    #print(ChemicalFormula[i:i+3])
                    i=i+3
            else:
                List=np.append(List,ChemicalFormula[i])
                #print(ChemicalFormula[i])
                i=i+1
        if start==i: #If we didn't find anything useful
```

```
            i=i+1
        #print("The end i index = "+str(i))
    return(List)

def StringToMass(string):
    """
    This function takes in a string of the form
    zaid fraction error zaid fraction error ...
    will read a file called 'AtomicWeights.csv'
    and find the atomic weight with error of the zaids
    and store those value in a list called Mass
    """
    ListOfString=string.split()

    if not len(ListOfString)%3==0:
        print("Check string variable missing fraction or error")
        quit()

    #Initialize fractions and zaid
    Zaid=0*np.arange(0,int(len(ListOfString)/3))

    #Gather fraction data and zaid data
    for i in range(0,int(len(ListOfString)/3)):
        Zaid[i]=int(ListOfString[i*3])


    df = pd.read_csv('../Data/AtomicWeights.csv')
    #Gather Mass Data
    for i in range(0,len(Zaid)):
        sZaid=str(Zaid[i])
        if len(sZaid)==4:
            proton=sZaid[0:2]
            if sZaid[2]=="0":
                Isotope=sZaid[3]
            else:
                Isotope=sZaid[2:4]
        elif len(sZaid)==5:
            proton=sZaid[0:2]
            if sZaid[2]=="0":
                Isotope=sZaid[3:5]
            if sZaid[3]=="0":
                Isotope=sZaid[4:5]
            if sZaid[2]!="0" and sZaid[3]!="0":
                Isotope=sZaid[2:5]
        elif len(sZaid)==6:
            proton=sZaid[0:3]
            Isotope=sZaid[3:6]
        else:
            print("Length of zaid is not 4 5 or 6 err")
            quit()
        try:
```

```
            Mass=np.append(Mass,FindAtomicMass(df,proton,Isotope))
        except NameError:
            Mass=FindAtomicMass(df,proton,Isotope)

    return(Mass,Zaid)

def StringToMass2(string):
    """
    This function takes in a string of the form
    zaid fraction error zaid fraction error ...
    will read a file called 'AtomicWeights.csv'
    and find the atomic weight with error of the zaids
    and store those value in a list called Mass
    """
    ListOfString=string.split()

    if not len(ListOfString)%3==0:
        print("Check string variable missing fraction or error")
        quit()

    #Initialize fractions and zaid
    Zaid=0*np.arange(0,int(len(ListOfString)/3))

    #Gather fraction data and zaid data
    for i in range(0,int(len(ListOfString)/3)):
        Zaid[i]=int(ListOfString[i*3])
        floatednumber=ufloat(float(ListOfString[i*3+1]),
                             float(ListOfString[i*3+2]))
        try:
            AtomFractions=np.append(AtomFractions,floatednumber)
        except NameError:
            AtomFractions=floatednumber

    df = pd.read_csv('../Data/AtomicWeights.csv')
    #Gather Mass Data
    for i in range(0,len(Zaid)):
        sZaid=str(Zaid[i])
        if len(sZaid)==4:
            proton=sZaid[0:2]
            if sZaid[2]=="0":
                Isotope=sZaid[3]
            else:
                Isotope=sZaid[2:4]
        elif len(sZaid)==5:
            proton=sZaid[0:2]
            if sZaid[2]=="0":
                Isotope=sZaid[3:5]
            if sZaid[3]=="0":
                Isotope=sZaid[4:5]
            if sZaid[2]!="0" and sZaid[3]!="0":
                Isotope=sZaid[2:5]
```

```
295         elif len(sZaid)==6:
                proton=sZaid[0:3]
                Isotope=sZaid[3:6]
            else:
                print("Length of zaid is not 4 5 or 6 err")
300             quit()
            try:
                Mass=np.append(Mass,FindAtomicMass(df,proton,Isotope))
                protons=np.append(protons,proton)
            except NameError:
305             Mass=FindAtomicMass(df,proton,Isotope)
                protons=proton

    return(Mass,protons,AtomFractions)

310 def ConvertFractions(string,Mass,MasstoAtom,Zaid):
    """
    This function will convert, with error, the mass or atom
       fraction
    to the other (mass to atom or atom to mass). It will use the
       masses
    provided in Mass, and the fractions provided in string. If its
        mass to Atom then
315 MasstoAtom=True, otherwise set False
    """

    ListOfString=string.split()
    Total=ufloat(0.,0)
320
    for i in range(0,len(Zaid)):

        Fraction=ufloat(float(ListOfString[i*3+1]),float(
           ListOfString[i*3+2]))
        if MasstoAtom: #Calculate total Atoms
325         Total=Total+Fraction/Mass[i]
        else: #Calculate total Mass
            Total=Total+Fraction*Mass[i]

    stringCalculated=''
330 for i in range(0,len(Zaid)):

        Fraction=ufloat(float(ListOfString[i*3+1]),float(
           ListOfString[i*3+2]))
        if MasstoAtom:
            #Calculate atom fractions
335         FractionCalculated=(Fraction/Mass[i])/Total
        else:
            #Calculate mass fractions
            FractionCalculated=(Fraction*Mass[i])/Total

340     stringCalculated=stringCalculated+\
```

```
                            str(Zaid[i])+' '+\
                            str(FractionCalculated)+' '

    return(stringCalculated)

def FindSymbol(NumofProtons,df):
    """
    This function will find the element symbol, based on number of
    protons.
    """
    for i in range(0,len(df.Protons)):
        if str(df.Protons[i])==NumofProtons:
            Symbol=df.Symbol[i]
            break

    try:
        Symbol
    except NameError:
        print("Could not find Symbol for Modfication zaid")
        quit()

    return(Symbol)

def FormatMods(Modifications,df):
    """
    This functions formats modifications

    """
    if(Modifications[0]==''):
        ModMass=''
        ModSymbols=''
        ModAFrac=''
        return(ModMass,ModSymbols,ModAFrac)
    for i in range(0,len(Modifications)):
        Modifications[i]=Modifications[i].replace('+/-',' ')

        Mass,protons,AtomFractions=StringToMass2(Modifications[i])
        Mass=" ".join(str(i) for i in Mass)
        protons=" ".join(str(i) for i in protons)
        LAtomFractions=" ".join(str(i) for i in AtomFractions)
        try:
            ModMass=np.append(ModMass,Mass)
            Modprotons=np.append(Modprotons,protons)
            ModAFrac=np.append(ModAFrac,LAtomFractions)
        except NameError:
            ModMass=[Mass]
            Modprotons=[protons]
            ModAFrac=[LAtomFractions]

```

```
    for i in range(0,len(Modifications)):
        proton=Modprotons[i].split(" ")[0]
        symbol=FindSymbol(proton,df)
        try:
            ModSymbols=np.append(ModSymbols,symbol)
        except NameError:
            ModSymbols=symbol

    return(ModMass,ModSymbols,ModAFrac)

def DetermineMolarMass(List,df,ModSymbols,
                       ModMass,AtomFractions,
                       ChemicalFormulaError):
    """
    this function determines the molar mass of a chemical formula
    with error:
    List is a list of the chemical formula
    df is a dataframe with atomic mass information
    ModSymbols are the modificaiton symbols (if using different
       Dudes
    AtomFractions are the atom fractions of the different dudes
    ChemicalFormulaError is the error in the number of each atom
       in the
    chemical formula, for example UO_2 could have a chemical
       formula
    ChemicalFormulaError=[0,0.001], meaning that a very small
       amount of
    the time, we have UO_3...this isn't the best way of doing this
       ...
    """
    MolarMass=ufloat(0,0)
    for i in range(0,len(List)):
        Symbol=List[i].split("_")[0]
        try:
            Multiplier=List[i].split("_")[1]
        except IndexError:
            Multiplier=1
        Multiplier=ufloat(Multiplier,ChemicalFormulaError[i])
        for j in range(0,len(df.Symbol)):
            if Symbol==str(df.Symbol[j]):
                ModifyElement=False
                for k in range(0,len(ModSymbols)):
                    if ModSymbols[k]==Symbol: #We are modifying
                        ModifyElement=True
                        Masses=ModMass[k].split(" ")
                        AFractions=AtomFractions[k].split(" ")
                        IndividualMolarMass=0
                        for l in range(0,len(Masses)):
                            IndividualMolarMass=
                               IndividualMolarMass+\
                                    ReturnUfloat(Masses[l])*\
```

```
                                        ReturnUfloat(AFractions[l])
                if not ModifyElement:
                    IndividualMolarMass=ReturnUfloat(
                                            df.
                                                Standard_Atomic_Weight
                                                [j]
                                                    )
                # print(Symbol+" "+
                #       str(IndividualMolarMass)
                #      )
                MolarMass=MolarMass+IndividualMolarMass*Multiplier
                break
    return(MolarMass)

def FindRange(List,Item):
    """
    This function returns a range...yup
    """
    for i in range(0,len(List)-1):
        if List[i] == Item:
            Range=[List[i]]
            break
        elif List[i+1] == Item:
            Range=[List[i+1]]
            break
        elif List[i] <= Item <= List[i+1]:
            Range=[List[i],List[i+1]]
            break
    return(Range)

def FindInTable(List1,List2,ItemMatchWithList2):
    """
    This function needs two lists that are the same
    length. and with data that corresponds to each other
    searches through list2 to find the item,
    then reports that same value from list1
    """
    for i in range(0,len(List2)):
        if(ItemMatchWithList2==List2[i]):
            return(List1[i])

def InterpolateDensity(dfDen,Temp,TRange,Conc,CRange):
    """
    This function interpolates stuff...don't ask me how
    """
    Concentrations=dfDen['Concentration_Percent_Weight']

    for i in range(0,len(TRange)):
        t=dfDen[str(int(TRange[i]))+'řC']
        for j in range(0,len(CRange)):
            C=CRange[j]
```

```
            D=FindInTable(t,Concentrations,C)
            try:
                Densities=np.append(Densities,D)
            except NameError:
                Densities=[D]

    if len(Densities)==4:
        Q11=((TRange[1]-Temp)*(CRange[1]-Conc))/\
            ((TRange[1]-TRange[0])*(CRange[1]-CRange[0]))
        Q21=((Temp-TRange[0])*(CRange[1]-Conc))/\
            ((TRange[1]-TRange[0])*(CRange[1]-CRange[0]))
        Q12=((TRange[1]-Temp)*(Conc-CRange[0]))/\
            ((TRange[1]-TRange[0])*(CRange[1]-CRange[0]))
        Q22=((Temp-TRange[0])*(Conc-CRange[0]))/\
            ((TRange[1]-TRange[0])*(CRange[1]-CRange[0]))

        density=Q11*Densities[0]+Q12*Densities[1]+\
                Q21*Densities[2]+Q22*Densities[3]

    if len(Densities)==1:
        density=Densities[0]

    if len(Densities)==2:
        if len(TRange)==2:
            density=((Temp-TRange[0])*(Densities[1]-Densities[0]))
                /\
                    (TRange[1]-TRange[0])+Densities[0]
        if len(CRange)==2:
            density=((Conc-CRange[0])*(Densities[1]-Densities[0]))
                /\
                    (CRange[1]-CRange[0])+Densities[0]

    #print(density)
    #print(Temp)
    #print(Conc)
    return(density)

def GetDensity(Temperature,WtConcentration,dfDen):
    """
    This function gets you density, don't ask me how
    """
    MinTemp=Temperature.nominal_value-Temperature.std_dev
    MaxTemp=Temperature.nominal_value+Temperature.std_dev
    ActTemp=Temperature.nominal_value
    MinWtCon=WtConcentration.nominal_value-WtConcentration.std_dev
    MaxWtCon=WtConcentration.nominal_value+WtConcentration.std_dev
    ActWtCon=WtConcentration.nominal_value

    Columns=list(dfDen.columns.values)
```

```
    #Find all the temperatures
    for i in range(0,len(Columns)):
        if ('řC' in Columns[i]):
            Temp=float(Columns[i].split("řC")[0])
            try:
                TempsAva=np.append(TempsAva,Temp)
            except NameError:
                TempsAva=Temp

    #Find the temperatures you fit between
    MinTempRange=FindRange(TempsAva,MinTemp)
    MaxTempRange=FindRange(TempsAva,MaxTemp)
    ActTempRange=FindRange(TempsAva,Temperature.nominal_value)

    #Find all the concentrations
    for i in range(0,len(dfDen.Concentration_Percent_Weight)):
        StrCon=float(dfDen.Concentration_Percent_Weight[i])
        try:
            Concentration=np.append(Concentration,StrCon)
        except NameError:
            Concentration=StrCon

    #Find concentrations you fit between
    MinConRange=FindRange(Concentration,MinWtCon)
    MaxConRange=FindRange(Concentration,MaxWtCon)
    ActConRange=FindRange(Concentration,
                          WtConcentration.nominal_value)

    density=InterpolateDensity(dfDen,
                               MinTemp,
                               MinTempRange,
                               MinWtCon,
                               MinConRange)


    density=np.append(density,InterpolateDensity(dfDen,
                                                 MinTemp,
                                                 MinTempRange,
                                                 MaxWtCon,
                                                 MaxConRange))

    density=np.append(density,InterpolateDensity(dfDen,
                                                 MaxTemp,
                                                 MaxTempRange,
                                                 MinWtCon,
                                                 MinConRange))

    density=np.append(density,InterpolateDensity(dfDen,
                                                 MaxTemp,
                                                 MaxTempRange,
                                                 MaxWtCon,
```

```
                                                    MaxConRange))

    densityactual=InterpolateDensity(dfDen,ActTemp,ActTempRange,
                                     ActWtCon,ActConRange)

    #densityN=(max(density)+min(density))/2
    densityEL=densityactual-min(density)
    densityEH=max(density)-densityactual
    density=ufloat(densityactual,max([densityEL,densityEH]))
    return(density)

def ConvertMol(MolarityToMolality,First,
               gramsOmol,dfDen,Temperature):
    """
    This function will convert molality to molarity
    and viceversa
    """
    #First either equals Molarity or Molality
    #Second either equals Molarity or Molality
    if not MolarityToMolality:
        if First==0:
            WtConcentration=ufloat(0,0)
        else:
            WtConcentration=100/(1000/(First*gramsOmol)+1)
    else:
        if First==0:
            WtConcentration=ufloat(0,0)
        else:
            dif=1
            WtConcentration=ufloat(30,0.1) #A Guess
            while( abs(dif)>0.001):
                OldWt=WtConcentration
                density=GetDensity(Temperature,OldWt,dfDen)
                WtConcentration=(100*gramsOmol*First)/(1000*
                    density)
                dif=(WtConcentration-OldWt)/WtConcentration

    density=GetDensity(Temperature,WtConcentration,dfDen)

    ################################################
    ################## Calculation ##################
    ################################################

    if MolarityToMolality:
        #(mols/kg)
        #dif=1
        #while (abs(dif)>0.001):
            #NewSecond=1/(density/First-gramsOmol*0.001)
            #WtConcentration=100/(1000/(NewSecond*gramsOmol)+1)
            #density=GetDensity(Temperature,WtConcentration,dfDen)
```

```
            #Second=1/(density/First-gramsOmol*0.001)
            #dif=Second-NewSecond
        if First==0:
            Second=0
        else:
            Second=1/(density/First-gramsOmol*0.001)
    else:
        if First==0:
            Second=0
        else:
        #(mols/L)
            Second=density/(1/First+gramsOmol*0.001)

    return(Second)

def NewConcentration(m1,m2,gramsOmol,
                     Temperature,dfDen,
                     Vol1,Vol2):
    """
    This function calculates a new concentration when
    two volumes of the same substance are added together
    same temperature, assuming that both solutions
    have had time to cool
    """
    if m1==0:
        WtConcentration1=ufloat(0,0)
    else:
        WtConcentration1=100/(1000/(m1*gramsOmol)+1)
    if m2==0:
        WtConcentration2=ufloat(0,0)
    else:
        WtConcentration2=100/(1000/(m2*gramsOmol)+1)


    p1=GetDensity(Temperature,WtConcentration1,dfDen)
    p2=GetDensity(Temperature,WtConcentration2,dfDen)

    molsV1=(m1*gramsOmol*p1*Vol1)/(1000*gramsOmol+m1*(gramsOmol
        **2))
    molsV2=(m2*gramsOmol*p2*Vol2)/(1000*gramsOmol+m2*(gramsOmol
        **2))

    #kgSol1=(1000*p1*Vol1)/(1000+m1*gramsOmol)/1000
    #kgSol2=(1000*p2*Vol2)/(1000+m2*gramsOmol)/1000

    kgSol1=(1-WtConcentration1/100)*(p1*Vol1)/(1000)
    kgSol2=(1-WtConcentration2/100)*(p2*Vol2)/(1000)

    Totmols=molsV1+molsV2
    Totkg=kgSol1+kgSol2
```

```
    m3=Totmols/Totkg
    WtConcentration3=100/(1000/(m3*gramsOmol)+1)
    #Assuming its had time to cool down
    p3=GetDensity(Temperature,WtConcentration3,dfDen)
    Vol3=(p1*Vol1+p2*Vol2)/p3

    Molarity=ConvertMol(False,m3,gramsOmol,dfDen,Temperature)

    return(m3,p3,Vol3,WtConcentration3,Molarity)

def GetWt(m,gramsOmol):
    if(m==0):
        WtConcentration=ufloat(0,0)
    else:
        WtConcentration=100/(1000/(m*gramsOmol)+1)

    return(WtConcentration)

def WttoMolality(gramsOmol,wt):
    """
    wt needs to be in percent (40.26 not 0.4026)
    """
    m=1000/(gramsOmol*(100/wt-1))
    return(m)

def ConvertMolDenGiven(MolarityToMolality,First,
                       gramsOmol,density):
    """
    This function will convert molality to molarity
    and viceversa
    """
    #First either equals Molarity or Molality
    #Second either equals Molarity or Molality
    if not MolarityToMolality:
        if First==0:
            WtConcentration=ufloat(0,0)
        else:
            WtConcentration=100/(1000/(First*gramsOmol)+1)
    else:
        if First==0:
            WtConcentration=ufloat(0,0)
        else:
            WtConcentration=(100*gramsOmol*First)/(1000*density)


    ##################################################
    ################## Calculation ###################
    ##################################################

    if MolarityToMolality:
        if First==0:
```

```
            Second=0
        else:
            Second=1/(density/First-gramsOmol*0.001)
    else:
        if First==0:
            Second=0
        else:
        #(mols/L)
            Second=density/(1/First+gramsOmol*0.001)

    return(Second)
```

Gamma Data processing

Listing E.3: Processes a directory of GENIE pdf outputs to pull peak information and store in separate csv files

```
#!/usr/bin/env python3
"""
Make sure quantified_Act_Energy.txt
and quantified_GENIE_Energy.txt are updated with
most recent energies contained in: ../Gamma_Template.xlsx
"""
import Functions as Fun
import re
import datetime

MaxPeakError=88   #Error (percent) for counts per second
distance="26 cm"  #Distance away from detector
err=0.005         #Percent error of Calibration standard
#Directory="../Process_1_Mess_Up/Gamma"  #Make sure files are "PDF
    " not "pdf"
#Directory="../Calibration/Gamma"
#Directory="../Cycle_x_3/Gamma/26cm"
#Directory="../Background/Gamma"
#Directory="../Cycle_x_3_round_2/Gamma/26cm"
#Directory="../Cycle_x_3_round_2/Gamma/0cm"
#Directory="../56_Round/Gamma"
#Directory="../Calibration/Gamma"
#Directory="../Cycle_x_3_round_2_extraction_2/Gamma/26cm"
#Directory="../Cycle_x_3_round_2_extraction_4/Gamma/0cm"
#Directory="../Cycle_x_3_Back_Extraction/Gamma/0cm"
#Directory="../Cycle_x_3_Back_Extraction/Gamma/0cm/Back_Ex_III"
Directory="../Cycle_x_3_Back_Extraction/Gamma/26cm"

#Get Constants for efficiency curve
C4,C3,C2,C1=Fun.GetConstants(distance)

#Get PDF filenames to analyze
```

```
Filelist=Fun.GetPDFFiles(Directory)
#Or just do one file, instead of a whole directory
#Filelist=["../Calibration/Gamma/Mendoza_Oct7_2016_26cm_BK.PDF"]

#Get Most recent background CPS, Err(P) and the date
#Excel files must be made (so make PDF, and run this program
#on the directory (hopefully you have precompiled versions,
#Else if you are using Pauls programs here for the first time,
#try putting the template in the directory...maybe it will work
#Put in a date from the background Excel files,
#Look at file names, not at dates printed in files
#                     YYYY,MM,DD
BKDate=datetime.date(2016,11,8)     #Second exp
#BKDate=datetime.date(2016,10,24)  #First exp
#BKDate=datetime.date(2016,10,7)     #Mess up experiment
BKdf=Fun.GetRecentBackgroundData(BKDate)

#Make data frame of Background information


#Loop through files in directory and make datasets for each
for filein in Filelist:
    #Save to excel sheet
    fileout=re.sub('\.PDF','',filein)+".xlsx"
    #Get the information from the PDF files
    df,Date=Fun.Gen_Data_Frame(filein,MaxPeakError)
    #Add Efficiency to each energy for the dataset
    df=Fun.GetEff(C4,C3,C2,C1,df)
    #Drop Energies not quantified and make sure each quantified
        energy has a row
    df=Fun.DropEnergies(df,Date)
    #Add the real Efficiency to each energy for the data set
    df=Fun.GetRealEff(C4,C3,C2,C1,df,err)

    #Add Most Recent Background Count Data
    df,BK_Names=Fun.AddBackground(df,BKdf)

    #In Case we misordered along the way
    df=df[['Energy',Date,'Err(P)','Eff',
    'Real_Eff','Real_Err',BK_Names[0],BK_Names[1]]]
    #Save dataset to a excel file
    df.to_excel(fileout)
    #print(df)
```

Listing E.4: Perform gamma calculations for activity of specified species uses output of the above code

```
#!/usr/bin/env python3
```

```
import Functions as Fun
from openpyxl import load_workbook

Directory="../Cycle_x_3/Gamma/26cm"
#Directory="../Background/Gamma/"
#Directory="../Cycle_x_3_round_2/Gamma/26cm"
#Directory="../56_Round/Gamma"
#Directory="../Process_1_Mess_Up/Gamma"
#Directory="../Cycle_x_3_round_2_extraction_2/Gamma/26cm"
#Directory="../Cycle_x_3_round_2_extraction_4/Gamma/0cm"
#Directory="../Cycle_x_3_Back_Extraction/Gamma/0cm"
#Directory="../Cycle_x_3_Back_Extraction/Gamma/0cm/Back_Ex_III"
Directory="../Cycle_x_3_Back_Extraction/Gamma/26cm"

#Get excel filenames that need adding to:
Filelist=Fun.GetExcelFiles(Directory)
#Or just do one file, instead of a whole directory
#Filelist=["../Calibration/Gamma/Mendoza_Oct7_2016_26cm_BK.PDF"]

#Open Template workbook
wb_from=load_workbook('../Gamma_Template.xlsx',data_only=False)
#wb_from=load_workbook('../Gamma_Template_0cm_Geo_Corr.xlsx',
    data_only=False)
ws_from=wb_from.active

#Loop through files we want to modify
for filein in Filelist:
   wb_to=load_workbook(filein)
   ws_to=wb_to.active
   for i in range(1,33):
      for j in range(10,66):
         ws_to.cell(row=i,column=j).value = ws_from.cell(row=i,
            column=j).value
         from_style=ws_from.cell(row=i,column=j).style
         from_style=True
         ws_to.cell(row=i,column=j).style=ws_from.cell(row=i,
            column=j).style
   wb_to.save(filein)
   print(filein)
```

Listing E.5: Function repository for above two codes

```
#!/usr/bin/env python3

import copy
import PyPDF2 #Package to get information out of PDF
import pandas as pd #Work with dataframes
import numpy as np #Numpy...classic
import os
```

```
import datetime
from openpyxl import load_workbook

def GetConstants(distance):
    """
    This function gets constants from John Burn's eff
    Excel sheet
    """
    CalFile=pd.ExcelFile("../Calibration/Eff_cal_summary_Eu-152.
        xlsm")
    df=CalFile.parse("Summary")
    C4=df.ix[distance][0]
    C3=df.ix[distance][1]
    C2=df.ix[distance][2]
    C1=df.ix[distance][3]
    return(C4,C3,C2,C1)

def GetEff(C4,C3,C2,C1,df):
    """
    This function calculates the efficiency
    and adds it to the dataframe df
    """
    Eff=[]
    #Loop through all Energy values in dataframe
    for E in df['Energy'].values: #Values!!!
        LE=np.log(E)
        Eff.append(np.exp(C4*(LE)**3+C3*(LE)**2+C2*LE+C1))
    #Turn efficiency into a data frame
    df2=pd.DataFrame(Eff,columns=['Eff'])
    #Concat the efficiency to original dataframe (need same index
        values)
    df = pd.concat([df, df2], axis=1, join_axes=[df.index])
    return(df)

def GetPDFFiles(directory):
    """
    This function gathers all files
    ending with ".PDF" in a certain directory
    Note...NOT ".pdf" capitalization matters!
    """
    Filelist=[]
    for file in os.listdir(directory):
        if ".PDF" in file:
            Filelist.append(directory+"/"+file)
    return(Filelist)

def GetExcelFiles(directory):
    """
    This function gathers all files
    ending with ".PDF" in a certain directory
    Note...NOT ".pdf" capitalization matters!
```

```
    """
    Filelist=[]
    for file in os.listdir(directory):
        if ".xlsx" in file:
            Filelist.append(directory+"/"+file)
    return(Filelist)

def MonthInteger(Month):
    """
    Assign a integer value to a date
    """
    if("Jan" in Month):
        Int=1
    if("Feb" in Month):
        Int=2
    if("Mar" in Month):
        Int=3
    if("Apr" in Month):
        Int=4
    if("May" in Month):
        Int=5
    if("Jun" in Month):
        Int=6
    if("Jul" in Month):
        Int=7
    if("Aug" in Month):
        Int=8
    if("Sep" in Month):
        Int=9
    if("Oct" in Month):
        Int=10
    if("Nov" in Month):
        Int=11
    if("Dec" in Month):
        Int=12
    try:
        Int
    except UnboundLocalError:
        print("Look at your month definition: "+Month+" does not"\
        " match any months (check background files months names)")
        quit()
    return(Int)

def GetRecentBackgroundData(BKDate):
    """
    Get recent background data
    """
    directory="../Background/Gamma"
    Filelist=[]
    for file in os.listdir(directory):
        if ".xlsx" in file and "~" not in file:
```

```
            Filelist.append(directory+"/"+file)
    dates=[]
    for File in Filelist:
        File=File.split("/")[-1]
        Date=File.split("_")[1]
        Year=File.split("_")[2]
        Month=''.join([i for i in Date if not i.isdigit()])
        Day=Date.strip(Month)
        MonthInt=MonthInteger(Month)
        date=datetime.date(int(Year),MonthInt,int(Day))
        dates.append(date)
    #RecentDate=max(dates)
    RecentDate=BKDate
    for i in range(0,len(dates)):
        if dates[i]==RecentDate:
            index=i
    try:
        index
    except UnboundLocalError:
        print("Look BKDate definition, I don't think you put in a
            proper" \
        "date")
        quit()

    wb_from=load_workbook(Filelist[index])
    ws_from=wb_from.active
    CPS=[]
    ERR=[]
    for i in range(2,33): #Rows
        CPS.append(ws_from.cell(row=i,column=3).value)
        ERR.append(ws_from.cell(row=i,column=4).value)
    Date=RecentDate.strftime('%m_%d_%y')

    BKdf1=pd.DataFrame(CPS,columns=['BK_CPS_'+Date])
    BKdf2=pd.DataFrame(ERR,columns=['ERR_BK_P'])
    #Concat the efficiency to original dataframe (need same index
        values)
    BKdf = pd.concat([BKdf1, BKdf2], axis=1, join_axes=[BKdf1.index
        ])

    return(BKdf)

def AddBackground(df,BKdf):
    BK_Names=BKdf.columns.values
    CPS=BKdf[BK_Names[0]].values
    ERR=BKdf[BK_Names[1]].values
    df2=pd.DataFrame(CPS,columns=[BK_Names[0]],index=df.index.
        values)
    df3=pd.DataFrame(ERR,columns=[BK_Names[1]],index=df.index.
        values)
    df=pd.concat([df,df2,df3],axis=1,join_axes=[df.index])
```

```
    return(df,BK_Names)

def Gen_Data_Frame(FileIn,MaxPeakError):
    """
    This function saves to a data frame
    the data found in 'FileIn' (Energy, CPS, Error)
    Error must be less than 'MaxPeakError'
    """
    #Open the file
    pdfFile=open(FileIn,'rb')
    #Store file in something that can read PDFs
    pdfReader=PyPDF2.PdfFileReader(pdfFile)
    #Create Dataframe
    df=pd.DataFrame([],columns=['Energy','CPS','Err(P)'])
    #Setup Index for dataframe
    index=0
    #Loop through pages in PDF
    for pageNum in range(pdfReader.numPages):
        #Get data from a particular page
        PageObj=pdfReader.getPage(pageNum)
        #Get the text from a particular page
        Pagetext=PageObj.extractText()
        #text into a list, based on new lines (save list in s)
        PageList=[s.strip() for s in Pagetext.splitlines()]
        #Loop through lines on a page
        for line in range(0,len(PageList)):
            lineList=PageList[line].split()
            if(lineList[0]=='Dead'):
                DeadTime=float(lineList[2])
            if(lineList[0]=='Acquisition'):
                if(lineList[1]=='Start:'):
                    Date=lineList[2]
                    df.columns=['Energy',Date,'Err(P)']
            #Print all the lines
            #print(lineList)
            #If we are looking at a peak,
            if(lineList[0].isnumeric()):
                #Perror=float(lineList[-1])/(1-DeadTime/100)
                if not "*" in lineList[-1]:
                    Perror=float(lineList[-1]) #GENIE already does
                        deadtime corr
                #If the error is acceptable, print
                if(Perror>0 and Perror<MaxPeakError and not "*" in
                    lineList[-1]):
                    E=float(lineList[1])
                    #CPS=float(lineList[6])/(1-DeadTime/100)
                    CPS=float(lineList[6]) #GENIE already does deadtime
                        corr
                    #Make data frame, and concatenate to old dataframe
                    data={'Energy' : [E],
                          Date : [CPS],
```

```
                    'Err(P)' : [Perror]}
                df2=pd.DataFrame(data,columns=['Energy',Date,'Err(P
                    )'],index=[index])
                index=index+1
                frames=[df,df2]
                df=pd.concat(frames)
                #print(lineList[1]+","+lineList[6]+","+lineList[7])
    return(df,Date)

def find_nearest(array,value,number):
    """
    This function will find the nth 'number' nearest
    to a number from an array.
    """
    arraycopy=copy.copy(array)
    for i in range(0,number-1):
        #arraycopy.remove(array[(np.abs(array-value)).argmin()])
        index=np.argwhere(arraycopy==arraycopy[(np.abs(arraycopy-
            value)).argmin()])
        arraycopy=np.delete(arraycopy,index)
    inx=(np.abs(arraycopy-value)).argmin()
    return arraycopy[inx]

def DropEnergies(df,Date):
    """
    Drops energies
    """
    #Open files with quantified GENIE energies and store
    with open('quantified_GENIE_Energy.txt') as f:
        content=f.readlines()
    GENIEEnergies=[]
    for i in content:
        i=float(i.replace("\n",""))
        GENIEEnergies.append(i)
    Error=1
    #Loop through all Energy values in dataframe
    #Drop peaks we haven't quantified yet
    for E in df['Energy'].values:
        In=False
        El1=find_nearest(GENIEEnergies,E,1)
        if abs(El1-E)<Error:
            In=True
        if not In:
            df=df[df.Energy != E]
    #Loop through all Values in quantified space, and
    #Make sure the data frame has a space for it
    for E in GENIEEnergies:
        In=False
        El1=find_nearest(df['Energy'].values,E,1)
        if abs(El1-E)<Error:
            In=True
```

```
        if not In:
            print("Missing Energy "+str(E))
            #Make data frame, and concatenate to old dataframe
            data={'Energy' : [E],
                Date : [0.0],
                'Err(P)' : [0.0]}
            df2=pd.DataFrame(data,columns=['Energy',Date,'Err(P)'],
                index=[max(df.index.values)+1])
            frames=[df,df2]
            df=pd.concat(frames)
    df=df.sort_values(by=['Energy'],ascending=[True])
    return(df)

def GetRealEff(C4,C3,C2,C1,df,err):
    """
    This function calculates the efficiency
    and adds it to the dataframe df
    """
    #Open files with actual energies that we have quantified and
        store
    with open('quantified_Act_Energy.txt') as f:
        content=f.readlines()
    ActEnergies=[]
    for i in content:
        i=float(i.replace("\n",""))
        ActEnergies.append(i)

    Eff=[]
    Err=[]
    #Loop through all Energy values in dataframe
    for E in df['Energy'].values: #Values!!!
        El1=find_nearest(ActEnergies,E,1)
        LE=np.log(El1)
        Eff.append(np.exp(C4*(LE)**3+C3*(LE)**2+C2*LE+C1))
        Err.append(Eff[-1]*err)
    #Turn efficiency into a data frame
    df2=pd.DataFrame(Eff,columns=['Real_Eff'],index=df.index.values
        )
    df3=pd.DataFrame(Err,columns=['Real_Err'],index=df.index.values
        )
    #Concat the efficiency to original dataframe (need same index
        values)
    df = pd.concat([df, df2,df3], axis=1, join_axes=[df.index])
    return(df)
```

Alpha Data Processing

Listing E.6: Function repository for above two codes

```
#!/usr/bin/env python3

#Will do some calculations on an excel file
#Useful for when lazy and not wanting to error prop by hand

from openpyxl import load_workbook
from uncertainties import ufloat

l39=ufloat(9.11012E-13,1.13357E-15);M39=ufloat
    (239.0521636,0.0000019)
l40=ufloat(3.34774E-12,3.57174E-15);M40=ufloat
    (240.0538138,0.0000019)
l41=ufloat(5.07733E-11,7.04206E-13);M41=ufloat
    (241.0568293,0.0000019)

Na=6.0221409E+23

P39=ufloat(0.923744651,0.006454028)
P40=ufloat(0.076255349,0.000526567)

P39=(P39/M39)/((P39/M39)+(P40/M40))
P40=(P40/M40)/((P39/M39)+(P40/M40))

Eff=ufloat(0.20492577,0.003694195)  #First Eff
#Eff=ufloat(0.22971492,0.007156969)  #Second Eff


def va(ws,row,column):
   return(ws.cell(row=row,column=column).value)
def setws(ws,row,column,Value):
   ws.cell(row=row,column=column).value=Value
   return(ws)
def v(Value):
   return(Value.nominal_value)
def s(Value):
   return(Value.std_dev)

#Open workbook
File='../Cycle_x_3_round_2/Alpha_Results.xlsx'
File='../Process_1_Mess_Up/Alpha_Results.xlsx'
wb=load_workbook(File,data_only=False)
ws=wb.active

#Set some column headers
PM=va(ws,1,6)
Headers=['CPSPu',PM,'CPSAm',PM,'g239/ul (Dilution Corrected)',
      PM,'g240/ul (Dilution Corrected)',PM,
      'g241/ul (Dilution Corrected)',PM,'To Stock = 2500 ul (total
          volume of dilution) x 10 (1/10th of pellet)']
for i in range(9,9+len(Headers)):
   ws=setws(ws,1,i,Headers[i-9])
```

```
#Loop through rows we want to modify
for i in range(2,33):  #Rows
   if va(ws,i,1) is not None:  #If we have input the data
      CPSPu=ufloat(va(ws,i,2)/va(ws,i,4),(va(ws,i,2)**0.5)/va(ws,i
          ,4))
      CPSAm=ufloat(va(ws,i,3)/va(ws,i,4),(va(ws,i,3)**0.5)/va(ws,i
          ,4))
      DF=ufloat(va(ws,i,7),va(ws,i,8))
      Vol=ufloat(va(ws,i,5),va(ws,i,6))
      ws=setws(ws,i,9,v(CPSPu))  #Set nominal value
      ws=setws(ws,i,10,s(CPSPu)) #Set STD Value
      ws=setws(ws,i,11,v(CPSAm))
      ws=setws(ws,i,12,s(CPSAm))
      g39=((CPSPu*M39)/(Eff*Na*(l39+l40*(1/P39-1))))*(DF/Vol)
      g40=((CPSPu*M40)/(Eff*Na*(l40+l39*(1/P40-1))))*(DF/Vol)
      g41=((CPSAm*M41)/(Eff*Na*l41))*(DF/Vol)
      ws=setws(ws,i,13,v(g39))
      ws=setws(ws,i,14,s(g39))
      ws=setws(ws,i,15,v(g40))
      ws=setws(ws,i,16,s(g40))
      ws=setws(ws,i,17,v(g41))
      ws=setws(ws,i,18,s(g41))


wb.save(File)
```

Corrected $f_{\text{combined},i}$ Values

Listing E.7: Code to correct final fractions to equal volume amounts

```
#!/usr/bin/env python3

"""
For the Vial 90G determine concentration of a particular
species as if equal volume
ratios were used
The experiment had 4 extractions and three back extractions
#  V_Rex  = V_organic/V_aqueous  (For Extraction)
#  V_Rbex = V_organic/V_aqueous  (For BackExtraction)
#  V_E    = V_organic_removed/V_organic_total (For Extraction)
#  V_BE   = V_aqueous_removed/V_aqueous_total (For BackExtraction)
#  D      = Concentration_in_organic/Concentation_in_aqueous
#  DB     = Set D value for Back-extraction (if different than for
#           extraction) - This program searches for D values
#           not DB values
#  ft     = Total Fraction of species in product solution (
   calculated)
```

```
#  ft_act = Total Fraction of species in product solution (looking
    for)
#  ft_Corrected = corrected value with equal volume ratios
#  fo     = Fraction removed into organic in a single extraction
#  ot     = Total Fraction removed into organic in a all 4
   extractions
#  at     = Total Fraction removed into aqueous phase (used for
   back
#           extraction
#  fa     = Fraction removed into aqueous in a single back-
   extraction
"""

################################################################
############################## Packages ########################
################################################################

from uncertainties import ufloat
import numpy as np

################################################################
########################### Conditions #########################
################################################################

#Fraction Looking for after 4 extractions and 3 back-extractions
ft_act=0.915984
ft_act=0.97
#Number of slices in the search space
N=10
#Initial Search Space for D
D=np.logspace(-5,3,N)
#Conditions for the experiment
V_E    = 0.5/0.7 # Organic Removed/ Organic Total  (extraction)
V_Rex  = 0.7/0.5 # V organic / V aqueous (extraction)
V_BE   = 2.0/2.2 # Aqueous removed / aqueous total (back-
   extraction)
V_Rbex = 2.0/2.2 # V organic / V aqueous (back-extraction)
DB     = 0.262       # If you want a different back-extraction
   Value
# Change to something other than 0

e=0.00001 # Point of converence

################################################################
########################### Functions ##########################
################################################################

def near_idx(array, value):
    """
    Find index in 'array' which is closest to 'value'
    """
```

```
    n = [abs(i-value) for i in array]
    idx = n.index(min(n))
    return(idx)

def Calc_ft(V_E,D,V_Rex,V_BE,V_Rbex,DB=0):
    """
    Calclate the expected fraction of species
    in the product solution with 4 extractions and 3 back-
       extractions
    """
    #Fraction Extracted into Organic Per Organic Extraction
    fo=(V_E)/(1+1/(D*V_Rex))
    #Total Fraction Extracted into Oranic with 4 extractions
    ot=-(fo**4)+4*(fo**3)-6*(fo**2)+4*fo
    #Change D value if we have a different one for back-extraction
    if not DB==0:
        D=DB
    #Fraction back-extracted into aqueous per back-extraction
    fa=(V_BE)/(1+D*V_Rbex)
    #Total fraction back-extracted
    at=fa**3-3*(fa**2)+3*fa
    #Total fraction in product solution
    ft=ot*at
    return(ft)

def Closest_D_ft(V_E,D,V_Rex,V_BE,V_Rbex,ft_act,DB=0):
    """

    """
    #Calculate ft for all the D values
    ft_list=[]

    for d in D:
        ft_list.append(Calc_ft(V_E,d,V_Rex,V_BE,V_Rbex,DB))
    #Find Index of closest D Value
    Idx=near_idx(ft_list,ft_act)
    #Save the closest D value
    D=D[Idx]
    Closest_ft=ft_list[Idx]
    Err=abs(Closest_ft-ft_act)/ft_act

    return(D,Closest_ft,Err)

############################################################
######################### Calculation ######################
############################################################


Err=100;Counter=0
#Find the D that corresponds to the final fraction
while Err>e:
```

```
    D_Mid,Closest_ft,Err=Closest_D_ft(V_E,D,V_Rex,V_BE,V_Rbex,
        ft_act,DB)
    D=np.linspace(D_Mid*(0.5),D_Mid*1.5,N)
    Counter=Counter+1
    if Counter>1000:
        print("Did Not Converge")
        break

#Calculate the fraction if equal volume ratios were used
V_E    = 1 # Organic Removed/ Organic Total  (extraction)
V_Rex  = 1 # V organic / V aqueous (extraction)
V_BE   = 1 # Aqueous removed / aqueous total (back-extraction)
V_Rbex = 1 # V organic / V aqueous (back-extraction)
D      = D_Mid

ft_Corrected=Calc_ft(V_E,D,V_Rex,V_BE,V_Rbex,DB)

print("Iterations",Counter)
print("Measured ft value ",ft_act)
print("Closest ft fit",Closest_ft)
print("Corrected ft value ",ft_Corrected)
print("Extraction D value ",D)
print("Back-extraction D Value ",DB)
```

Code for forensic analysis is extensive and is avaiable upon request.

APPENDIX F

ACTIVITY BALANCE TABLES

Table F.1: Vial 8 Extraction I Activity Balance

Vial 8 Extraction I	A_{initial}	$A_{\text{final,aq,m}}$	$A_{\text{final,or,m}}$
^{155}Eu (105 keV)	0.321 ± 0.010	0.187 ± 0.006	0.0158 ± 0.0005
^{154}Eu	0.067 ± 0.001	0.039 ± 0.001	0.0024 ± 0.0001
^{144}Ce (133 keV)	52.336 ± 0.948	31.424 ± 0.574	1.2032 ± 0.0220
^{125}Sb	0.398 ± 0.006	0.240 ± 0.005	0.0037 ± 0.0001
^{106}Rh	33.494 ± 0.517	17.294 ± 0.297	1.8754 ± 0.0292
^{134}Cs	0.760 ± 0.006	0.465 ± 0.005	0.0035 ± 0.0002
^{137}Cs	4.674 ± 0.026	2.841 ± 0.016	0.0234 ± 0.0002
Activity Units $[\mu Ci]$	$A_{\text{final,tot}}$	$\frac{A_{\text{initial}} - A_{\text{final,tot}}}{A_{\text{initial}}}$	Exp. Info.
^{155}Eu (105 keV)	0.325 ± 0.012	-0.010 ± 0.050	Decay Corrected To:
^{154}Eu	0.067 ± 0.002	-0.004 ± 0.037	5/5/2014
^{144}Ce (133 keV)	52.204 ± 1.453	0.003 ± 0.033	Measured: 11/08/2016
^{125}Sb	0.390 ± 0.012	0.020 ± 0.033	$V_{aq,tot} = 0.40 \pm 0.00$
^{106}Rh	30.671 ± 0.784	0.084 ± 0.027	$V_{or,tot} = 0.40 \pm 0.00$
^{134}Cs	0.750 ± 0.019	0.013 ± 0.026	$V_{aq,m} = 0.25 \pm 0.01$
^{137}Cs	4.583 ± 0.105	0.019 ± 0.023	$V_{aq,m} = 0.25 \pm 0.01$

Table F.2: Vial 9 Extraction I Activity Balance

Vial 9 Extraction I	A_{initial}	$A_{\text{final,aq,m}}$	$A_{\text{final,or,m}}$
^{155}Eu (105 keV)	0.316 ± 0.011	0.189 ± 0.007	0.0241 ± 0.0006
^{154}Eu	0.065 ± 0.001	0.037 ± 0.001	0.0038 ± 0.0000
^{144}Ce (133 keV)	51.777 ± 0.943	29.747 ± 0.541	1.6763 ± 0.0302
^{125}Sb	0.404 ± 0.008	0.239 ± 0.005	0.0013 ± 0.0001
^{106}Rh	32.958 ± 0.522	16.126 ± 0.270	1.8644 ± 0.0275
^{134}Cs	0.759 ± 0.008	0.445 ± 0.005	0.0000 ± 0.0000
^{137}Cs	4.599 ± 0.026	2.740 ± 0.016	0.0001 ± 0.0000
Activity Units $[\mu Ci]$	$A_{\text{final,tot}}$	$\frac{A_{\text{initial}} - A_{\text{final,tot}}}{A_{\text{initial}}}$	Exp. Info.
^{155}Eu (105 keV)	0.341 ± 0.013	-0.080 ± 0.056	Decay Corrected To:
^{154}Eu	0.065 ± 0.002	0.005 ± 0.037	5/5/2014
^{144}Ce (133 keV)	50.277 ± 1.374	0.029 ± 0.032	Measured: 11/08/2016
^{125}Sb	0.384 ± 0.011	0.047 ± 0.034	$V_{aq,tot} = 0.40 \pm 0.00$
^{106}Rh	28.785 ± 0.726	0.127 ± 0.026	$V_{or,tot} = 0.40 \pm 0.00$
^{134}Cs	0.711 ± 0.018	0.063 ± 0.025	$V_{aq,m} = 0.25 \pm 0.01$
^{137}Cs	4.385 ± 0.101	0.047 ± 0.023	$V_{aq,m} = 0.25 \pm 0.01$

Table F.3: Vial 10 Extraction I Activity Balance

Vial 10 Extraction I	A_{initial}	$A_{\text{final,aq,m}}$	$A_{\text{final,or,m}}$
^{155}Eu (105 keV)	0.321 ± 0.009	0.191 ± 0.006	0.0117 ± 0.0003
^{154}Eu	0.068 ± 0.001	0.038 ± 0.001	0.0017 ± 0.0000
^{144}Ce (133 keV)	52.209 ± 0.943	30.977 ± 0.564	0.7750 ± 0.0140
^{125}Sb	0.413 ± 0.005	0.245 ± 0.003	0.0007 ± 0.0001
^{106}Rh	34.032 ± 0.508	17.234 ± 0.282	0.9646 ± 0.0145
^{134}Cs	0.768 ± 0.004	0.474 ± 0.005	0.0001 ± 0.0000
^{137}Cs	4.636 ± 0.026	2.819 ± 0.016	0.0001 ± 0.0000
Activity Units $[\mu Ci]$	$A_{\text{final,tot}}$	$\frac{A_{\text{initial}} - A_{\text{final,tot}}}{A_{\text{initial}}}$	Exp. Info.
^{155}Eu (105 keV)	0.325 ± 0.012	-0.011 ± 0.047	Decay Corrected To:
^{154}Eu	0.063 ± 0.002	0.069 ± 0.030	5/5/2014
^{144}Ce (133 keV)	50.803 ± 1.430	0.027 ± 0.033	Measured: 11/08/2016
^{125}Sb	0.393 ± 0.010	0.048 ± 0.027	$V_{aq,tot} = 0.40 \pm 0.00$
^{106}Rh	29.117 ± 0.765	0.144 ± 0.026	$V_{or,tot} = 0.40 \pm 0.00$
^{134}Cs	0.758 ± 0.019	0.014 ± 0.025	$V_{aq,m} = 0.25 \pm 0.01$
^{137}Cs	4.510 ± 0.104	0.027 ± 0.023	$V_{aq,m} = 0.25 \pm 0.01$

Table F.4: Vial 8 Extraction II Activity Balance

Vial 8 Extraction II	A_{initial}	$A_{\text{final,aq,m}}$	$A_{\text{final,or,m}}$
^{155}Eu (105 keV)	0.278 ± 0.012	0.141 ± 0.004	0.0397 ± 0.0010
^{154}Eu	0.059 ± 0.002	0.032 ± 0.001	0.0059 ± 0.0001
^{144}Ce (133 keV)	46.661 ± 1.610	26.088 ± 0.472	3.3910 ± 0.0613
^{125}Sb	0.357 ± 0.013	0.227 ± 0.003	0.0010 ± 0.0001
^{106}Rh	25.680 ± 0.871	16.220 ± 0.250	1.3133 ± 0.0218
^{134}Cs	0.691 ± 0.022	0.487 ± 0.003	0.0001 ± 0.0000
^{137}Cs	4.219 ± 0.126	2.857 ± 0.016	0.0006 ± 0.0000
Activity Units $[\mu Ci]$	$A_{\text{final,tot}}$	$\frac{A_{\text{initial}} - A_{\text{final,tot}}}{A_{\text{initial}}}$	Exp. Info.
^{155}Eu (105 keV)	0.278 ± 0.009	0.000 ± 0.055	Decay Corrected To:
^{154}Eu	0.058 ± 0.002	0.004 ± 0.049	5/5/2014
^{144}Ce (133 keV)	44.784 ± 1.354	0.040 ± 0.044	Measured: 11/08/2016
^{125}Sb	0.342 ± 0.011	0.042 ± 0.047	$V_{aq,tot} = 0.37 \pm 0.01$
^{106}Rh	26.500 ± 0.806	-0.032 ± 0.047	$V_{or,tot} = 0.42 \pm 0.00$
^{134}Cs	0.729 ± 0.022	-0.055 ± 0.046	$V_{aq,m} = 0.25 \pm 0.00$
^{137}Cs	4.278 ± 0.127	-0.014 ± 0.043	$V_{aq,m} = 0.25 \pm 0.01$

Table F.5: Vial 9 Extraction II Activity Balance

Vial 9 Extraction II	A_{initial}	$A_{\text{final,aq,m}}$	$A_{\text{final,or,m}}$
^{155}Eu (105 keV)	0.277 ± 0.013	0.131 ± 0.004	0.0466 ± 0.0011
^{154}Eu	0.054 ± 0.002	0.032 ± 0.000	0.0071 ± 0.0000
^{144}Ce (133 keV)	43.350 ± 1.490	25.188 ± 0.455	4.0898 ± 0.0737
^{125}Sb	0.347 ± 0.012	0.243 ± 0.002	0.0009 ± 0.0000
^{106}Rh	23.601 ± 0.791	15.758 ± 0.236	1.3180 ± 0.0209
^{134}Cs	0.645 ± 0.020	0.473 ± 0.002	0.0000 ± 0.0000
^{137}Cs	3.977 ± 0.119	2.857 ± 0.016	0.0001 ± 0.0000
Activity Units $[\mu Ci]$	$A_{\text{final,tot}}$	$\frac{A_{\text{initial}} - A_{\text{final,tot}}}{A_{\text{initial}}}$	Exp. Info.
^{155}Eu (105 keV)	0.267 ± 0.008	0.037 ± 0.054	Decay Corrected To:
^{154}Eu	0.058 ± 0.001	-0.077 ± 0.049	5/5/2014
^{144}Ce (133 keV)	43.350 ± 1.274	0.000 ± 0.045	Measured: 11/08/2016
^{125}Sb	0.354 ± 0.011	-0.019 ± 0.048	$V_{aq,tot} = 0.36 \pm 0.01$
^{106}Rh	25.060 ± 0.755	-0.062 ± 0.048	$V_{or,tot} = 0.42 \pm 0.00$
^{134}Cs	0.687 ± 0.020	-0.064 ± 0.046	$V_{aq,m} = 0.25 \pm 0.01$
^{137}Cs	4.147 ± 0.124	-0.043 ± 0.044	$V_{aq,m} = 0.25 \pm 0.01$

Table F.6: Vial 10 Extraction II Activity Balance

Vial 10 Extraction II	A_{initial}	$A_{\text{final,aq,m}}$	$A_{\text{final,or,m}}$
^{155}Eu (105 keV)	0.218 ± 0.010	0.154 ± 0.004	0.0256 ± 0.0007
^{154}Eu	0.043 ± 0.002	0.036 ± 0.000	0.0038 ± 0.0001
^{144}Ce (133 keV)	34.800 ± 1.351	27.622 ± 0.498	1.9943 ± 0.0362
^{125}Sb	0.273 ± 0.010	0.252 ± 0.002	0.0008 ± 0.0002
^{106}Rh	19.610 ± 0.736	17.009 ± 0.254	1.0528 ± 0.0185
^{134}Cs	0.526 ± 0.019	0.478 ± 0.002	0.0000 ± 0.0000
^{137}Cs	3.134 ± 0.110	2.922 ± 0.016	0.0001 ± 0.0000
Activity Units $[\mu Ci]$	$A_{\text{final,tot}}$	$\frac{A_{\text{initial}} - A_{\text{final,tot}}}{A_{\text{initial}}}$	Exp. Info.
^{155}Eu (105 keV)	0.224 ± 0.008	-0.025 ± 0.060	Decay Corrected To:
^{154}Eu	0.048 ± 0.001	-0.120 ± 0.056	5/5/2014
^{144}Ce (133 keV)	34.800 ± 1.208	0.000 ± 0.052	Measured: 11/08/2016
^{125}Sb	0.282 ± 0.010	-0.032 ± 0.053	$V_{aq,tot} = 0.28 \pm 0.01$
^{106}Rh	21.070 ± 0.718	-0.074 ± 0.054	$V_{or,tot} = 0.51 \pm 0.01$
^{134}Cs	0.531 ± 0.019	-0.009 ± 0.051	$V_{aq,m} = 0.25 \pm 0.01$
^{137}Cs	3.249 ± 0.114	-0.037 ± 0.052	$V_{aq,m} = 0.25 \pm 0.01$

Table F.7: Vial 8 Extraction III Activity Balance

Vial 8 Extraction III	A_{initial}	$A_{\text{final,aq,m}}$	$A_{\text{final,or,m}}$
^{155}Eu (105 keV)	0.041 ± 0.002	0.122 ± 0.004	0.0400 ± 0.0010
^{154}Eu	0.009 ± 0.000	0.028 ± 0.000	0.0061 ± 0.0001
^{144}Ce (133 keV)	7.657 ± 0.309	24.449 ± 0.445	4.0489 ± 0.0730
^{125}Sb	0.067 ± 0.003	0.248 ± 0.004	0.0005 ± 0.0001
^{106}Rh	4.760 ± 0.187	16.150 ± 0.263	0.7242 ± 0.0126
^{134}Cs	0.143 ± 0.005	0.486 ± 0.004	0.0000 ± 0.0000
^{137}Cs	0.839 ± 0.031	2.959 ± 0.017	0.0001 ± 0.0000
Activity Units $[\mu Ci]$	$A_{\text{final,tot}}$	$\frac{A_{\text{initial}} - A_{\text{final,tot}}}{A_{\text{initial}}}$	Exp. Info.
^{155}Eu (105 keV)	0.137 ± 0.005	-2.310 ± 0.201	Decay Corrected To:
^{154}Eu	0.024 ± 0.001	-1.480 ± 0.127	5/5/2014
^{144}Ce (133 keV)	17.374 ± 0.576	-1.269 ± 0.118	Measured: 11/22/2016
^{125}Sb	0.073 ± 0.003	-0.101 ± 0.065	$V_{aq,tot} = 0.07 \pm 0.00$
^{106}Rh	6.536 ± 0.230	-0.373 ± 0.072	$V_{or,tot} = 0.63 \pm 0.02$
^{134}Cs	0.141 ± 0.006	0.010 ± 0.056	$V_{aq,m} = 0.25 \pm 0.01$
^{137}Cs	0.862 ± 0.037	-0.027 ± 0.058	$V_{aq,m} = 0.25 \pm 0.01$

Table F.8: Vial 9 Extraction III Activity Balance

Vial 9 Extraction III	A_{initial}	$A_{\text{final,aq,m}}$	$A_{\text{final,or,m}}$
^{155}Eu (105 keV)	0.184 ± 0.008	0.109 ± 0.004	0.0447 ± 0.0011
^{154}Eu	0.045 ± 0.002	0.026 ± 0.001	0.0068 ± 0.0000
^{144}Ce (133 keV)	35.566 ± 1.434	22.602 ± 0.411	4.7419 ± 0.0855
^{125}Sb	0.343 ± 0.013	0.249 ± 0.005	0.0004 ± 0.0000
^{106}Rh	22.251 ± 0.869	15.653 ± 0.250	0.7318 ± 0.0130
^{134}Cs	0.668 ± 0.024	0.492 ± 0.005	0.0000 ± 0.0000
^{137}Cs	4.034 ± 0.147	2.936 ± 0.017	0.0001 ± 0.0000
Activity Units $[\mu Ci]$	$A_{\text{final,tot}}$	$\frac{A_{\text{initial}} - A_{\text{final,tot}}}{A_{\text{initial}}}$	Exp. Info.
^{155}Eu (105 keV)	0.219 ± 0.010	-0.186 ± 0.075	Decay Corrected To:
^{154}Eu	0.046 ± 0.002	-0.029 ± 0.057	5/5/2014
^{144}Ce (133 keV)	38.780 ± 1.507	-0.090 ± 0.061	Measured: 11/21/2016
^{125}Sb	0.353 ± 0.016	-0.029 ± 0.061	$V_{aq,tot} = 0.35 \pm 0.01$
^{106}Rh	23.162 ± 1.003	-0.041 ± 0.061	$V_{or,tot} = 0.36 \pm 0.01$
^{134}Cs	0.695 ± 0.030	-0.041 ± 0.059	$V_{aq,m} = 0.25 \pm 0.01$
^{137}Cs	4.146 ± 0.177	-0.028 ± 0.058	$V_{aq,m} = 0.25 \pm 0.01$

Table F.9: Vial 10 Extraction III Activity Balance

Vial 10 Extraction III	A_{initial}	$A_{\text{final,aq,m}}$	$A_{\text{final,or,m}}$
^{155}Eu (105 keV)	0.223 ± 0.010	0.115 ± 0.003	0.0217 ± 0.0005
^{154}Eu	0.052 ± 0.002	0.027 ± 0.000	0.0033 ± 0.0000
^{144}Ce (133 keV)	39.996 ± 1.612	21.298 ± 0.385	2.0001 ± 0.0361
^{125}Sb	0.365 ± 0.013	0.203 ± 0.002	0.0005 ± 0.0001
^{106}Rh	24.629 ± 0.961	13.350 ± 0.206	0.6697 ± 0.0108
^{134}Cs	0.692 ± 0.025	0.396 ± 0.002	0.0000 ± 0.0000
^{137}Cs	4.231 ± 0.154	2.385 ± 0.013	0.0001 ± 0.0000
Activity Units $[\mu Ci]$	$A_{\text{final,tot}}$	$\frac{A_{\text{initial}} - A_{\text{final,tot}}}{A_{\text{initial}}}$	Exp. Info.
^{155}Eu (105 keV)	0.247 ± 0.011	-0.108 ± 0.070	Decay Corrected To:
^{154}Eu	0.055 ± 0.002	-0.049 ± 0.058	5/5/2014
^{144}Ce (133 keV)	42.170 ± 1.786	-0.054 ± 0.062	Measured: 11/23/2016
^{125}Sb	0.368 ± 0.016	-0.010 ± 0.058	$V_{aq,tot} = 0.36 \pm 0.01$
^{106}Rh	25.376 ± 1.092	-0.030 ± 0.060	$V_{or,tot} = 0.36 \pm 0.01$
^{134}Cs	0.718 ± 0.031	-0.037 ± 0.058	$V_{aq,m} = 0.20 \pm 0.01$
^{137}Cs	4.317 ± 0.185	-0.020 ± 0.057	$V_{aq,m} = 0.20 \pm 0.01$

Table F.10: Vial 8 Extraction IV Activity Balance

Vial 8 Extraction IV	A_{initial}	$A_{\text{final,aq,m}}$	$A_{\text{final,or,m}}$
^{155}Eu (105 keV)	0.154 ± 0.009	0.097 ± 0.004	0.0336 ± 0.0008
^{154}Eu	0.035 ± 0.002	0.025 ± 0.001	0.0052 ± 0.0000
^{144}Ce (133 keV)	30.806 ± 1.422	22.274 ± 0.406	3.8028 ± 0.0686
^{125}Sb	0.312 ± 0.014	0.255 ± 0.004	0.0003 ± 0.0000
^{106}Rh	20.350 ± 0.925	15.850 ± 0.250	0.5529 ± 0.0086
^{134}Cs	0.612 ± 0.027	0.494 ± 0.005	0.0000 ± 0.0000
^{137}Cs	3.728 ± 0.160	3.001 ± 0.017	0.0001 ± 0.0000
Activity Units $[\mu Ci]$	$A_{\text{final,tot}}$	$\frac{A_{\text{initial}} - A_{\text{final,tot}}}{A_{\text{initial}}}$	Exp. Info.
^{155}Eu (105 keV)	0.165 ± 0.008	-0.072 ± 0.078	Decay Corrected To:
^{154}Eu	0.038 ± 0.002	-0.070 ± 0.067	5/5/2014
^{144}Ce (133 keV)	32.896 ± 1.315	-0.068 ± 0.065	Measured: 12/07/2016
^{125}Sb	0.321 ± 0.015	-0.029 ± 0.066	$V_{aq,tot} = 0.32 \pm 0.01$
^{106}Rh	20.673 ± 0.905	-0.016 ± 0.064	$V_{or,tot} = 0.32 \pm 0.01$
^{134}Cs	0.623 ± 0.027	-0.017 ± 0.062	$V_{aq,m} = 0.25 \pm 0.01$
^{137}Cs	3.782 ± 0.162	-0.014 ± 0.061	$V_{aq,m} = 0.25 \pm 0.01$

Table F.11: Vial 9 Extraction IV Activity Balance

Vial 9 Extraction IV	A_{initial}	$A_{\text{final,aq,m}}$	$A_{\text{final,or,m}}$
^{155}Eu (105 keV)	0.140 ± 0.008	0.085 ± 0.004	0.0383 ± 0.0009
^{154}Eu	0.033 ± 0.002	0.021 ± 0.001	0.0059 ± 0.0000
^{144}Ce (133 keV)	28.931 ± 1.336	19.641 ± 0.358	4.7284 ± 0.0852
^{125}Sb	0.319 ± 0.015	0.252 ± 0.004	0.0004 ± 0.0000
^{106}Rh	20.036 ± 0.908	15.088 ± 0.246	0.5905 ± 0.0093
^{134}Cs	0.630 ± 0.027	0.488 ± 0.005	0.0000 ± 0.0000
^{137}Cs	3.758 ± 0.161	2.941 ± 0.017	0.0001 ± 0.0000
Activity Units $[\mu Ci]$	$A_{\text{final,tot}}$	$\frac{A_{\text{initial}} - A_{\text{final,tot}}}{A_{\text{initial}}}$	Exp. Info.
^{155}Eu (105 keV)	0.158 ± 0.007	-0.132 ± 0.084	Decay Corrected To:
^{154}Eu	0.034 ± 0.001	-0.043 ± 0.068	5/5/2014
^{144}Ce (133 keV)	31.193 ± 1.194	-0.078 ± 0.065	Measured: 12/07/2016
^{125}Sb	0.322 ± 0.015	-0.011 ± 0.066	$V_{aq,tot} = 0.32 \pm 0.01$
^{106}Rh	20.069 ± 0.878	-0.002 ± 0.063	$V_{or,tot} = 0.32 \pm 0.01$
^{134}Cs	0.624 ± 0.027	0.009 ± 0.061	$V_{aq,m} = 0.25 \pm 0.01$
^{137}Cs	3.764 ± 0.161	-0.002 ± 0.061	$V_{aq,m} = 0.25 \pm 0.01$

Table F.12: Vial 10 Extraction IV Activity Balance

Vial 10 Extraction IV	A_{initial}	$A_{\text{final,aq,m}}$	$A_{\text{final,or,m}}$
^{155}Eu (105 keV)	0.177 ± 0.009	0.130 ± 0.003	0.0218 ± 0.0005
^{154}Eu	0.041 ± 0.002	0.031 ± 0.000	0.0034 ± 0.0000
^{144}Ce (133 keV)	32.799 ± 1.513	25.566 ± 0.461	2.2176 ± 0.0400
^{125}Sb	0.313 ± 0.014	0.254 ± 0.002	0.0004 ± 0.0000
^{106}Rh	20.559 ± 0.928	16.469 ± 0.245	0.6324 ± 0.0102
^{134}Cs	0.610 ± 0.026	0.496 ± 0.002	0.0000 ± 0.0000
^{137}Cs	3.673 ± 0.157	3.047 ± 0.017	0.0001 ± 0.0000
Activity Units $[\mu Ci]$	$A_{\text{final,tot}}$	$\frac{A_{\text{initial}} - A_{\text{final,tot}}}{A_{\text{initial}}}$	Exp. Info.
^{155}Eu (105 keV)	0.187 ± 0.008	-0.058 ± 0.072	Decay Corrected To:
^{154}Eu	0.042 ± 0.002	-0.009 ± 0.060	5/5/2014
^{144}Ce (133 keV)	34.230 ± 1.457	-0.044 ± 0.066	Measured: 12/07/2016
^{125}Sb	0.313 ± 0.013	-0.002 ± 0.062	$V_{aq,tot} = 0.31 \pm 0.01$
^{106}Rh	21.069 ± 0.913	-0.025 ± 0.064	$V_{or,tot} = 0.31 \pm 0.01$
^{134}Cs	0.611 ± 0.026	-0.001 ± 0.061	$V_{aq,m} = 0.25 \pm 0.01$
^{137}Cs	3.754 ± 0.161	-0.022 ± 0.062	$V_{aq,m} = 0.25 \pm 0.01$

Table F.13: Vial 8 Back Extraction I Activity Balance

Vial 8 Back Extraction	A_{initial}	$A_{\text{final,aq,m}}$	$A_{\text{final,or,m}}$
^{155}Eu (105 keV)	0.132 ± 0.003	0.066 ± 0.002	0.0055 ± 0.0001
^{154}Eu	0.021 ± 0.000	0.010 ± 0.000	0.0008 ± 0.0000
^{144}Ce (133 keV)	12.689 ± 0.229	6.653 ± 0.120	0.1607 ± 0.0029
^{125}Sb	0.003 ± 0.000	0.001 ± 0.000	0.0002 ± 0.0000
^{106}Rh	4.618 ± 0.073	1.946 ± 0.031	0.3298 ± 0.0053
^{134}Cs	0.002 ± 0.000	0.001 ± 0.000	0.0000 ± 0.0000
^{137}Cs	0.014 ± 0.000	0.008 ± 0.000	0.0000 ± 0.0000
Activity Units $[\mu Ci]$	$A_{\text{final,tot}}$	$\frac{A_{\text{initial}} - A_{\text{final,tot}}}{A_{\text{initial}}}$	Exp. Info.
^{155}Eu (105 keV)	0.128 ± 0.006	0.035 ± 0.050	Decay Corrected To:
^{154}Eu	0.019 ± 0.001	0.087 ± 0.037	5/5/2014
^{144}Ce (133 keV)	12.100 ± 0.545	0.046 ± 0.046	Measured: 12/15/2016
^{125}Sb	0.002 ± 0.000	0.359 ± 0.054	$V_{aq,tot} = 0.89 \pm 0.03$
^{106}Rh	4.041 ± 0.159	0.125 ± 0.037	$V_{or,tot} = 0.89 \pm 0.03$
^{134}Cs	0.002 ± 0.000	0.065 ± 0.121	$V_{aq,m} = 0.50 \pm 0.01$
^{137}Cs	0.014 ± 0.001	0.029 ± 0.042	$V_{aq,m} = 0.50 \pm 0.01$

Table F.14: Vial 9 Back Extraction I Activity Balance

Vial 9 Back Extraction	A_{initial}	$A_{\text{final,aq,m}}$	$A_{\text{final,or,m}}$
^{155}Eu (105 keV)	0.163 ± 0.004	0.078 ± 0.002	0.0065 ± 0.0002
^{154}Eu	0.025 ± 0.000	0.012 ± 0.000	0.0009 ± 0.0000
^{144}Ce (133 keV)	16.065 ± 0.290	8.185 ± 0.148	0.2027 ± 0.0037
^{125}Sb	0.003 ± 0.000	0.002 ± 0.000	0.0002 ± 0.0000
^{106}Rh	4.772 ± 0.076	2.134 ± 0.035	0.3652 ± 0.0057
^{134}Cs	0.000 ± 0.000	0.000 ± 0.000	0.0003 ± 0.0001
^{137}Cs	0.000 ± 0.000	0.000 ± 0.000	0.0000 ± 0.0000
Activity Units $[\mu Ci]$	$A_{\text{final,tot}}$	$\frac{A_{\text{initial}} - A_{\text{final,tot}}}{A_{\text{initial}}}$	Exp. Info.
^{155}Eu (105 keV)	0.155 ± 0.007	0.054 ± 0.049	Decay Corrected To:
^{154}Eu	0.024 ± 0.001	0.017 ± 0.040	5/5/2014
^{144}Ce (133 keV)	15.299 ± 0.688	0.048 ± 0.046	Measured: 12/15/2016
^{125}Sb	0.003 ± 0.000	-0.004 ± 0.130	$V_{aq,tot} = 0.91 \pm 0.03$
^{106}Rh	4.559 ± 0.180	0.045 ± 0.041	$V_{or,tot} = 0.91 \pm 0.03$
^{134}Cs	0.001 ± 0.000	-19.091 ± 12.416	$V_{aq,m} = 0.50 \pm 0.01$
^{137}Cs	0.000 ± 0.000	-0.019 ± 0.127	$V_{aq,m} = 0.50 \pm 0.01$

Table F.15: Vial 10 Back Extraction I Activity Balance

Vial 10 Back Extraction	A_{initial}	$A_{\text{final,aq,m}}$	$A_{\text{final,or,m}}$
^{155}Eu (105 keV)	0.092 ± 0.002	0.047 ± 0.001	0.0035 ± 0.0001
^{154}Eu	0.014 ± 0.000	0.008 ± 0.000	0.0005 ± 0.0000
^{144}Ce (133 keV)	7.829 ± 0.141	4.281 ± 0.077	0.0932 ± 0.0017
^{125}Sb	0.003 ± 0.000	0.001 ± 0.000	0.0001 ± 0.0000
^{106}Rh	4.644 ± 0.070	2.002 ± 0.032	0.2715 ± 0.0041
^{134}Cs	0.001 ± 0.000	0.000 ± 0.000	0.0000 ± 0.0000
^{137}Cs	0.005 ± 0.000	0.003 ± 0.000	0.0000 ± 0.0000
Activity Units $[\mu Ci]$	$A_{\text{final,tot}}$	$\frac{A_{\text{initial}} - A_{\text{final,tot}}}{A_{\text{initial}}}$	Exp. Info.
^{155}Eu (105 keV)	0.088 ± 0.004	0.048 ± 0.049	Decay Corrected To:
^{154}Eu	0.014 ± 0.001	0.029 ± 0.040	5/5/2014
^{144}Ce (133 keV)	7.551 ± 0.341	0.036 ± 0.047	Measured: 12/15/2016
^{125}Sb	0.002 ± 0.000	0.284 ± 0.069	$V_{aq,tot} = 0.86 \pm 0.03$
^{106}Rh	3.924 ± 0.158	0.155 ± 0.036	$V_{or,tot} = 0.86 \pm 0.03$
^{134}Cs	0.001 ± 0.000	0.188 ± 0.082	$V_{aq,m} = 0.50 \pm 0.01$
^{137}Cs	0.004 ± 0.000	0.047 ± 0.042	$V_{aq,m} = 0.50 \pm 0.01$

Table F.16: Vial 8 Back Extraction II Activity Balance

Vial 8 Back Extraction	A_{initial}	$A_{\text{final,aq,m}}$	$A_{\text{final,or,m}}$
^{155}Eu (105 keV)	0.008 ± 0.000	0.005 ± 0.000	0.0004 ± 0.0000
^{154}Eu	0.001 ± 0.000	0.001 ± 0.000	0.0001 ± 0.0000
^{144}Ce (133 keV)	0.244 ± 0.011	0.155 ± 0.003	0.0032 ± 0.0002
^{125}Sb	0.000 ± 0.000	0.000 ± 0.000	0.0000 ± 0.0000
^{106}Rh	0.501 ± 0.023	0.210 ± 0.003	0.1161 ± 0.0020
^{134}Cs	0.000 ± 0.000	0.000 ± 0.000	0.0004 ± 0.0003
^{137}Cs	0.000 ± 0.000	0.000 ± 0.000	0.0000 ± 0.0000

Activity Units $[\mu Ci]$	$A_{\text{final,tot}}$	$\frac{A_{\text{initial}} - A_{\text{final,tot}}}{A_{\text{initial}}}$	Exp. Info.
^{155}Eu (105 keV)	0.008 ± 0.000	0.025 ± 0.066	Decay Corrected To:
^{154}Eu	0.001 ± 0.000	-0.089 ± 0.065	5/5/2014
^{144}Ce (133 keV)	0.240 ± 0.011	0.016 ± 0.064	Measured: 12/16/2016
^{125}Sb	0.000 ± 0.000	0.278 ± 0.155	$V_{aq,tot} = 0.76 \pm 0.02$
^{106}Rh	0.496 ± 0.017	0.011 ± 0.056	$V_{or,tot} = 0.76 \pm 0.02$
^{134}Cs	0.001 ± 0.000	$-7.026821194267 \pm 4.626024.247$	$V_{aq,m} = 0.50 \pm 0.01$
^{137}Cs	0.000 ± 0.000	$-0.155892.052 \pm 87.656.022$	$V_{aq,m} = 0.50 \pm 0.01$

Table F.17: Vial 9 Back Extraction II Activity Balance

Vial 9 Back Extraction	A_{initial}	$A_{\text{final,aq,m}}$	$A_{\text{final,or,m}}$
^{155}Eu (105 keV)	0.010 ± 0.000	0.006 ± 0.000	0.0004 ± 0.0000
^{154}Eu	0.001 ± 0.000	0.001 ± 0.000	0.0001 ± 0.0000
^{144}Ce (133 keV)	0.310 ± 0.014	0.195 ± 0.004	0.0043 ± 0.0001
^{125}Sb	0.000 ± 0.000	0.000 ± 0.000	0.0001 ± 0.0000
^{106}Rh	0.559 ± 0.025	0.234 ± 0.004	0.1233 ± 0.0021
^{134}Cs	0.000 ± 0.000	0.000 ± 0.000	0.0000 ± 0.0000
^{137}Cs	0.000 ± 0.000	0.000 ± 0.000	0.0000 ± 0.0000
Activity Units $[\mu Ci]$	$A_{\text{final,tot}}$	$\frac{A_{\text{initial}} - A_{\text{final,tot}}}{A_{\text{initial}}}$	Exp. Info.
^{155}Eu (105 keV)	0.010 ± 0.000	0.026 ± 0.066	Decay Corrected To:
^{154}Eu	0.002 ± 0.000	-0.063 ± 0.064	5/5/2014
^{144}Ce (133 keV)	0.306 ± 0.014	0.015 ± 0.064	Measured: 12/16/2016
^{125}Sb	0.000 ± 0.000	0.325 ± 0.136	$V_{aq,tot} = 0.77 \pm 0.02$
^{106}Rh	0.547 ± 0.018	0.021 ± 0.055	$V_{or,tot} = 0.77 \pm 0.02$
^{134}Cs	0.000 ± 0.000	0.904 ± 0.035	$V_{aq,m} = 0.50 \pm 0.01$
^{137}Cs	0.000 ± 0.000	-6.335 ± 60.087	$V_{aq,m} = 0.50 \pm 0.01$

Table F.18: Vial 10 Back Extraction II Activity Balance

Vial 10 Back Extraction	A_{initial}	$A_{\text{final,aq,m}}$	$A_{\text{final,or,m}}$
^{155}Eu (105 keV)	0.005 ± 0.000	0.003 ± 0.000	0.0003 ± 0.0000
^{154}Eu	0.001 ± 0.000	0.001 ± 0.000	0.0000 ± 0.0000
^{144}Ce (133 keV)	0.144 ± 0.007	0.094 ± 0.002	0.0019 ± 0.0003
^{125}Sb	0.000 ± 0.000	0.000 ± 0.000	0.0000 ± 0.0000
^{106}Rh	0.418 ± 0.019	0.190 ± 0.003	0.0874 ± 0.0015
^{134}Cs	0.000 ± 0.000	0.000 ± 0.000	0.0000 ± 0.0000
^{137}Cs	0.000 ± 0.000	0.000 ± 0.000	0.0000 ± 0.0000
Activity Units $[\mu Ci]$	$A_{\text{final,tot}}$	$\frac{A_{\text{initial}} - A_{\text{final,tot}}}{A_{\text{initial}}}$	Exp. Info.
^{155}Eu (105 keV)	0.006 ± 0.000	-0.030 ± 0.070	Decay Corrected To:
^{154}Eu	0.001 ± 0.000	-0.076 ± 0.064	5/5/2014
^{144}Ce (133 keV)	0.147 ± 0.007	-0.027 ± 0.067	Measured: 12/17/2016
^{125}Sb	0.000 ± 0.000	-0.261 ± 0.228	$V_{aq,tot} = 0.77 \pm 0.02$
^{106}Rh	0.427 ± 0.015	-0.021 ± 0.058	$V_{or,tot} = 0.77 \pm 0.02$
^{134}Cs	0.000 ± 0.000	-0.281 ± 0.352	$V_{aq,m} = 0.50 \pm 0.01$
^{137}Cs	0.000 ± 0.000	1.000 ± 0.000	$V_{aq,m} = 0.50 \pm 0.01$

Table F.19: Vial 8 Back Extraction III Activity Balance

Vial 8 Back Extraction	A_{initial}	$A_{\text{final,aq,m}}$	$A_{\text{final,or,m}}$
^{155}Eu (105 keV)	0.000 ± 0.000	0.000 ± 0.002	0.0000 ± 0.0000
^{154}Eu	0.000 ± 0.000	0.000 ± 0.000	0.0000 ± 0.0000
^{144}Ce (133 keV)	0.004 ± 0.000	0.002 ± 0.115	0.0004 ± 0.0002
^{125}Sb	0.000 ± 0.000	0.000 ± 0.000	0.0000 ± 0.0000
^{106}Rh	0.143 ± 0.007	0.040 ± 0.030	0.0531 ± 0.0010
^{134}Cs	0.001 ± 0.000	0.000 ± 0.000	0.0000 ± 0.0000
^{137}Cs	0.000 ± 0.000	0.000 ± 0.000	0.0000 ± 0.0000
Activity Units $[\mu Ci]$	$A_{\text{final,tot}}$	$\frac{A_{\text{initial}} - A_{\text{final,tot}}}{A_{\text{initial}}}$	Exp. Info.
^{155}Eu (105 keV)	0.000 ± 0.002	0.000 ± 5.056	Decay Corrected To:
^{154}Eu	0.000 ± 0.000	0.000 ± 1.230	5/5/2014
^{144}Ce (133 keV)	0.004 ± 0.177	0.000 ± 45.052	Measured: 12/18/2016
^{125}Sb	0.000 ± 0.000	-0.472 ± 0.960	$V_{aq,tot} = 0.62 \pm 0.02$
^{106}Rh	0.143 ± 0.047	0.000 ± 0.328	$V_{or,tot} = 0.62 \pm 0.02$
^{134}Cs	0.001 ± 0.000	0.000 ± 0.662	$V_{aq,m} = 0.40 \pm 0.01$
^{137}Cs	0.000 ± 0.000	-29.503 ± 669.136	$V_{aq,m} = 0.40 \pm 0.01$

Table F.20: Vial 9 Back Extraction III Activity Balance

Vial 9 Back Extraction	A_{initial}	$A_{\text{final,aq,m}}$	$A_{\text{final,or,m}}$
^{155}Eu (105 keV)	0.001 ± 0.000	0.000 ± 0.002	0.0000 ± 0.0000
^{154}Eu	0.000 ± 0.000	0.000 ± 0.000	0.0000 ± 0.0000
^{144}Ce (133 keV)	0.005 ± 0.000	0.003 ± 0.146	0.0001 ± 0.0001
^{125}Sb	0.000 ± 0.000	0.000 ± 0.000	0.0000 ± 0.0000
^{106}Rh	0.153 ± 0.007	0.045 ± 0.036	0.0537 ± 0.0008
^{134}Cs	0.000 ± 0.000	0.000 ± 0.000	0.0000 ± 0.0000
^{137}Cs	0.000 ± 0.000	0.000 ± 0.000	0.0000 ± 0.0000
Activity Units $[\mu Ci]$	$A_{\text{final,tot}}$	$\frac{A_{\text{initial}} - A_{\text{final,tot}}}{A_{\text{initial}}}$	Exp. Info.
^{155}Eu (105 keV)	0.001 ± 0.003	0.000 ± 5.319	Decay Corrected To:
^{154}Eu	0.000 ± 0.000	0.000 ± 1.873	5/5/2014
^{144}Ce (133 keV)	0.005 ± 0.226	-0.000 ± 42.654	Measured: 12/19/2016
^{125}Sb	0.000 ± 0.000	-0.000 ± 3.059	$V_{aq,tot} = 0.62 \pm 0.02$
^{106}Rh	0.153 ± 0.056	0.000 ± 0.367	$V_{or,tot} = 0.62 \pm 0.02$
^{134}Cs	0.000 ± 0.000	0.000 ± 0.268	$V_{aq,m} = 0.40 \pm 0.01$
^{137}Cs	0.000 ± 0.000	-1.125 ± 4.929	$V_{aq,m} = 0.40 \pm 0.01$

Table F.21: Vial 10 Back Extraction III Activity Balance

Vial 10 Back Extraction	A_{initial}	$A_{\text{final,aq,m}}$	$A_{\text{final,or,m}}$
^{155}Eu (105 keV)	0.000 ± 0.000	0.000 ± 0.001	0.0000 ± 0.0000
^{154}Eu	0.000 ± 0.000	0.000 ± 0.000	0.0000 ± 0.0000
^{144}Ce (133 keV)	0.002 ± 0.000	0.001 ± 0.075	0.0001 ± 0.0001
^{125}Sb	0.000 ± 0.000	0.000 ± 0.000	0.0000 ± 0.0000
^{106}Rh	0.109 ± 0.005	0.034 ± 0.030	0.0361 ± 0.0006
^{134}Cs	0.000 ± 0.000	0.000 ± 0.000	0.0000 ± 0.0000
^{137}Cs	0.000 ± 0.000	0.000 ± 0.000	0.0000 ± 0.0000

Activity Units $[\mu Ci]$	$A_{\text{final,tot}}$	$\frac{A_{\text{initial}} - A_{\text{final,tot}}}{A_{\text{initial}}}$	Exp. Info.
^{155}Eu (105 keV)	0.000 ± 0.002	0.000 ± 5.425	Decay Corrected To:
^{154}Eu	0.000 ± 0.000	0.000 ± 1.750	5/5/2014
^{144}Ce (133 keV)	0.002 ± 0.117	-0.000 ± 48.635	Measured: 12/19/2016
^{125}Sb	0.000 ± 0.000	-0.802 ± 1.216	$V_{aq,tot} = 0.62 \pm 0.02$
^{106}Rh	0.109 ± 0.047	0.000 ± 0.438	$V_{or,tot} = 0.62 \pm 0.02$
^{134}Cs	0.000 ± 0.000	-3.517 ± 6.552	$V_{aq,m} = 0.40 \pm 0.01$
^{137}Cs	0.000 ± 0.158	-0.000 ± 14.931	$V_{aq,m} = 0.40 \pm 0.01$

Table F.22: Vial 56 Extraction II Activity Balance

Vial 56 Extraction II	A_{initial}	$A_{\text{final,aq,m}}$	$A_{\text{final,or,m}}$
^{155}Eu (105 keV)	0.227 ± 0.011	0.111 ± 0.003	0.1214 ± 0.0031
^{154}Eu	0.054 ± 0.002	0.028 ± 0.000	0.0297 ± 0.0002
^{144}Ce (133 keV)	48.224 ± 2.223	27.853 ± 0.503	21.4778 ± 0.3876
^{125}Sb	0.664 ± 0.029	0.653 ± 0.005	0.0028 ± 0.0007
^{106}Rh	37.097 ± 1.665	31.341 ± 0.457	5.4976 ± 0.0910
^{134}Cs	1.309 ± 0.056	1.294 ± 0.004	0.0008 ± 0.0001
^{137}Cs	7.903 ± 0.338	7.784 ± 0.043	0.0026 ± 0.0002
Activity Units $[\mu Ci]$	$A_{\text{final,tot}}$	$\frac{A_{\text{initial}} - A_{\text{final,tot}}}{A_{\text{initial}}}$	Exp. Info.
^{155}Eu (105 keV)	0.234 ± 0.008	-0.028 ± 0.063	Decay Corrected To:
^{154}Eu	0.058 ± 0.002	-0.072 ± 0.057	5/5/2014
^{144}Ce (133 keV)	49.686 ± 1.633	-0.030 ± 0.058	Measured: 11/20/2016
^{125}Sb	0.660 ± 0.028	0.005 ± 0.060	$V_{aq,tot} = 0.70 \pm 0.02$
^{106}Rh	37.104 ± 1.438	-0.000 ± 0.059	$V_{or,tot} = 7.00 \pm 0.21$
^{134}Cs	1.304 ± 0.055	0.004 ± 0.060	$V_{aq,m} = 6.95 \pm 0.02$
^{137}Cs	7.843 ± 0.335	0.008 ± 0.060	$V_{aq,m} = 0.69 \pm 0.21$

Table F.23: Vial 56 Extraction III Activity Balance

Vial 56 Extraction III	A_{initial}	$A_{\text{final,aq,m}}$	$A_{\text{final,or,m}}$
^{155}Eu (105 keV)	0.111 ± 0.005	0.049 ± 0.003	0.0517 ± 0.0013
^{154}Eu	0.028 ± 0.001	0.013 ± 0.000	0.0127 ± 0.0001
^{144}Ce (133 keV)	27.853 ± 1.057	14.851 ± 0.274	11.0563 ± 0.1994
^{125}Sb	0.653 ± 0.023	0.617 ± 0.005	0.0016 ± 0.0003
^{106}Rh	31.341 ± 1.157	27.295 ± 0.411	2.5249 ± 0.0413
^{134}Cs	1.294 ± 0.045	1.231 ± 0.007	0.0006 ± 0.0000
^{137}Cs	7.784 ± 0.274	7.446 ± 0.041	0.0019 ± 0.0002
Activity Units $[\mu Ci]$	$A_{\text{final,tot}}$	$\frac{A_{\text{initial}} - A_{\text{final,tot}}}{A_{\text{initial}}}$	Exp. Info.
^{155}Eu (105 keV)	0.103 ± 0.005	0.065 ± 0.059	Decay Corrected To:
^{154}Eu	0.027 ± 0.001	0.034 ± 0.050	5/5/2014
^{144}Ce (133 keV)	26.731 ± 0.886	0.040 ± 0.048	Measured: 11/28/2016
^{125}Sb	0.653 ± 0.028	-0.001 ± 0.056	$V_{aq,tot} = 0.57 \pm 0.02$
^{106}Rh	31.331 ± 1.302	0.000 ± 0.056	$V_{or,tot} = 5.72 \pm 0.17$
^{134}Cs	1.300 ± 0.056	-0.005 ± 0.056	$V_{aq,m} = 5.72 \pm 0.02$
^{137}Cs	7.860 ± 0.336	-0.010 ± 0.056	$V_{aq,m} = 0.54 \pm 0.17$

Table F.24: Vial 5 Extraction 1 Activity Balance

Vial 5 Extraction 1	A_{initial}	$A_{\text{final,aq,m}}$	$A_{\text{final,or,m}}$
^{155}Eu (105 keV)	0.381 ± 0.010	0.332 ± 0.009	0.0165 ± 0.0016
^{154}Eu	0.079 ± 0.001	0.070 ± 0.001	0.0038 ± 0.0002
^{144}Ce (133 keV)	61.975 ± 1.118	56.096 ± 1.012	1.1889 ± 0.0263
^{125}Sb	0.485 ± 0.004	0.432 ± 0.004	0.0019 ± 0.0013
^{106}Rh	38.965 ± 0.573	32.763 ± 0.485	1.3900 ± 0.0353
^{134}Cs	0.913 ± 0.004	0.838 ± 0.004	0.0006 ± 0.0002
^{137}Cs	5.528 ± 0.031	5.118 ± 0.028	0.0164 ± 0.0003
Activity Units $[\mu Ci]$	$A_{\text{final,tot}}$	$\frac{A_{\text{initial}} - A_{\text{final,tot}}}{A_{\text{initial}}}$	Exp. Info.
^{155}Eu (105 keV)	0.379 ± 0.012	0.004 ± 0.041	Decay Corrected To:
^{154}Eu	0.080 ± 0.002	-0.017 ± 0.024	5/5/2014
^{144}Ce (133 keV)	62.224 ± 1.749	-0.004 ± 0.034	Measured: 10/21/2016
^{125}Sb	0.471 ± 0.011	0.030 ± 0.025	$V_{aq,tot} = 0.50 \pm 0.01$
^{106}Rh	37.151 ± 0.954	0.047 ± 0.028	$V_{or,tot} = 0.50 \pm 0.01$
^{134}Cs	0.910 ± 0.021	0.004 ± 0.023	$V_{aq,m} = 0.43 \pm 0.01$
^{137}Cs	5.570 ± 0.128	-0.008 ± 0.024	$V_{aq,m} = 0.46 \pm 0.01$

Table F.25: Vial 6 Extraction 1 Activity Balance

Vial 6 Extraction 1	A_{initial}	$A_{\text{final,aq,m}}$	$A_{\text{final,or,m}}$
^{155}Eu (105 keV)	0.380 ± 0.010	0.349 ± 0.012	0.0264 ± 0.0024
^{154}Eu	0.079 ± 0.001	0.070 ± 0.001	0.0059 ± 0.0003
^{144}Ce (133 keV)	62.277 ± 1.123	55.015 ± 1.000	2.2698 ± 0.0496
^{125}Sb	0.469 ± 0.004	0.431 ± 0.008	0.0079 ± 0.0011
^{106}Rh	39.011 ± 0.575	32.298 ± 0.520	1.9599 ± 0.0447
^{134}Cs	0.919 ± 0.004	0.833 ± 0.009	0.0170 ± 0.0010
^{137}Cs	5.566 ± 0.031	5.043 ± 0.029	0.1108 ± 0.0010
Activity Units $[\mu Ci]$	$A_{\text{final,tot}}$	$\frac{A_{\text{initial}} - A_{\text{final,tot}}}{A_{\text{initial}}}$	Exp. Info.
^{155}Eu (105 keV)	0.403 ± 0.015	-0.059 ± 0.049	Decay Corrected To:
^{154}Eu	0.081 ± 0.002	-0.027 ± 0.030	5/5/2014
^{144}Ce (133 keV)	61.291 ± 1.692	0.016 ± 0.032	Measured: 10/23/2016
^{125}Sb	0.469 ± 0.013	0.000 ± 0.030	$V_{aq,tot} = 0.50 \pm 0.01$
^{106}Rh	36.712 ± 0.952	0.059 ± 0.028	$V_{or,tot} = 0.50 \pm 0.01$
^{134}Cs	0.908 ± 0.022	0.012 ± 0.024	$V_{aq,m} = 0.43 \pm 0.01$
^{137}Cs	5.506 ± 0.124	0.011 ± 0.023	$V_{aq,m} = 0.47 \pm 0.01$

APPENDIX G

BATEMAN EQUATION SOLUTION METHOD

The production of an isotope is dictated by production and loss

$$\frac{dn_i}{dt} = -\lambda_i^{eff} n_i + \sum_{j=1}^{N} b_{j\to i}^{eff} \lambda_j^{eff} n_j$$

where,

$$\lambda_i^{eff} = \lambda_i + \phi \sum_{j=1}^{N} \sigma_{i\to j}$$

and

$$b_{j\to i}^{eff} = \frac{b_{j\to i}\lambda_j + \sigma_{j\to i}\phi}{\lambda_j^{eff}}.$$

For a system of isotopes, this can be reduced to:

$$\frac{d\vec{n}}{dt} = \boldsymbol{A}\vec{n}(t),$$

where $\boldsymbol{A}$ is a matrix whose diagonal elements are $[-\lambda_1^{eff}, -\lambda_2^{eff}, ..., -\lambda_N^{eff}]$, all off diagonal elements are $b_{j\to i}^{eff}\lambda_j^{eff}$ (i for the diagonal, and j is for the off diagonal position) and $\vec{n}(t) = [n_1, n_2, ..., n_N]$.

The solution to this system is obvious

$$\vec{n} = e^{\boldsymbol{A}t}\vec{n}_0$$

Determing $e^{\boldsymbol{A}t}\vec{n}_0$ will be done 3 different ways,

Matrix Exponential

Analytic Solution, unstable with large N.

$$\vec{n}(t) = e^{\boldsymbol{A}t}\vec{n}_0 \approx \left[\sum_{m=0}^{\infty} \frac{1}{m!}\boldsymbol{A}^m t^m\right]\vec{n}_0$$

Backward Euler

Unstable for large Δt, but can take time steps.

$$\begin{aligned}\frac{d\vec{n}}{dt} \approx \frac{\vec{n}(\Delta t) - \vec{n}_0}{\Delta t} \approx &\boldsymbol{A}\vec{n}(\Delta t) \\ \vec{n}(\Delta t) \approx &(\boldsymbol{I} - \boldsymbol{A}\Delta t)^{-1}\vec{n}_0\end{aligned}$$

Rational Approximation

$$\vec{n}(t) = e^{\boldsymbol{A}t}\vec{n}_0 \approx -2\Re\sum_{k=1}^{N/2} c_k(z_k\boldsymbol{I} - \boldsymbol{A}t)^{-1}\vec{n}_0$$

The $\Re$ symbol means taking the real part of the solution. Further,

$$c_k = \frac{i}{N}e^{z_k}w_k$$

where z_k and w_k are both scalers defined as

$$\begin{aligned}z_k =&\phi(\theta_k) \\ w_k =&\phi'(\theta_k)\end{aligned}$$

with

$$\phi(\theta) = N[0.1309 - 0.1194\theta^2 + 0.2500i\theta]$$

or

$$\phi(\theta) = 2.246N\,[1 - sin(1.1721 - 0.3443i\theta]$$

or

$$\phi(\theta) = N[0.5071\theta cot(0.6407\theta) - 0.6122 + 0.2645i\theta]$$

or

$$\phi(\theta) = \text{Best Possible}$$

and

$$\theta_k = \pm\frac{\pi}{N}\,(1 + 2k) \quad \text{k from 0 to N-1},$$

where N doesn't have to go much higher than 10 to have low errors (for the best Rational Approximation). Also both plus and minus terms were written here, but the first equation in this solution method only uses the positive terms. This is because using the negative β's yields the same real part as the positive β's, with opposite complex parts (the complex cancels). Thats why the $\sum$ only goes to $N/2$ and the solution is multiplied by 2.